

**The Dynamic Characterisation of ESR Prosthetic  
Running Feet: An investigation of the key  
parameters affecting their performance.**

James Richard Hawkins

---

A thesis submitted in partial fulfilment of the requirements of  
Bournemouth University for the degree of Doctor of Philosophy

---

January 2015



**This copy of the thesis has been supplied on condition that anyone who consults it is understood to recognise that its copyright rests with its author and due acknowledgement must always be made of the use of any material contained in, or derived from, this thesis.**

# ABSTRACT

**Author:** James Richard Hawkins

**Title:** The Dynamic Characterisation of ESR Prosthetic Running Feet: An investigation of the key parameters affecting their performance.

Prosthetic running feet (referred to as Energy Storing & Returning (ESR) or Running Specific Prostheses (RSP) but better known as ‘blades’) take the form of a carbon fibre leaf spring with a deflecting keel component. Available literature on the subject of their dynamic response is limited but suggests that the amputee with running foot can be considered to act in accordance with Simple Harmonic Motion, but this does not appear to be reflected by the prescription processes currently employed by manufacturers. The research question is asked: ‘Is the current method of prescribing prosthetic ESR running feet appropriate and are there additional factors that should be taken into consideration?’

This thesis aims to first understand the static mechanical characteristics of a single model of prosthetic foot; the Flex Run from Ossur (Reykjavik, Iceland). Previous works carried out (that aim to define the energy return efficiency of the devices but results vary from 63% - 100%) are examined and replicated using a series of fabricated jig fixtures, and the disparity in efficiency results is explained. The running action of an amputee is measured using a wearable measurement system that is developed as well as high-speed video capture. The measured action is then replicated in the laboratory using a rig capable of reproducing the dynamic response of the foot. This rig is subsequently used to manipulate the variables of Simple Harmonic Motion and evaluate the suitability of this assumption to model the running action of an amputee.

The research concludes by using the gathered learning to create a tool capable of mathematically replicating the response of a prosthetic foot, and the application of such a tool is discussed.

It is found during the course of the research that the available Flex Run feet possess an energy return efficiency of >99% and a variable stiffness along the length of the deflecting keel. As a contribution to knowledge, it was also found that during amputee running the ground contact point (and therefore effective stiffness) of the prosthetic changes significantly from foot strike through to toe-off and the profile of this change is defined. As such the principle of a spring-mass system cannot be applied in such a simplistic manner as previously suggested. Furthermore the relationship between amputee mass, stance length, foot deflection and response timing is defined for the first time. It was also discovered that the passive nature of the prosthetic device (and therefore fixed response) has the potential of limiting the top speed of running of an amputee and as such the current prescription method falls some way short of expectations. Methods of improving the prescription process are discussed and further work is suggested to improve the function of these prosthetic devices and therefore the user experience of the amputee athlete.

# LIST OF CONTENTS

<b>COPYRIGHT STATEMENT</b> .....	2
<b>ABSTRACT</b> .....	3
<b>LIST OF CONTENTS</b> .....	4
<b>ACKNOWLEDGEMENTS</b> .....	12
<b>DECLARATION</b> .....	13
<b>ABBREVIATIONS</b> .....	14
<b>CHAPTER 1: INTRODUCTION &amp; LITERATURE REVIEW</b>	
<b>1.1 Project Scope</b> .....	15
<b>1.2 Introduction</b> .....	15
<b>1.3 Research Objectives</b> .....	20
<b>1.4 Publications</b> .....	21
1.4.1 Journal Publications .....	21
1.4.2 Conference Publications .....	21
<b>1.5 Literature Review</b> .....	22
1.5.1 Characterisation of Papers .....	23
1.5.2 Walking/Running Dynamics Papers .....	24
1.5.3 Prosthetics Comparative & Review Papers .....	28
1.5.4 Prosthetics Prescription Papers .....	32
1.5.5 Prosthetics Dynamics Papers inc. Measurement .....	35
<b>1.6 Conclusions on the Literature Review</b> .....	40
<b>CHAPTER 2: RESEARCH METHODOLOGY &amp; PLAN</b>	
<b>2.1 Research Questions</b> .....	44
2.1.1 Sub-question 1 .....	44
2.1.2 Sub-question 2 .....	45
2.1.3 Sub-question 3 .....	45
2.1.4 Sub-question 4 .....	45

<b>2.2</b>	<b>Research Methodology</b> .....	46
2.2.1	Qualitative vs. Quantitative Research .....	46
2.2.2	Design of Experiments Methodology .....	48
<b>2.3</b>	<b>Chapter Summary</b> .....	49
2.3.1	(Chapter 3): Static Characterisation .....	49
2.3.2	(Chapter 4): Dynamic Characterisation .....	49
2.3.3	(Chapter 5): Bringing Running into the Laboratory ..	50
2.3.4	(Chapter 6): Changing SHM Variables on the Rig ....	50
2.3.5	(Chapter 7): Amputee Testing & the Effect of Speed Variation .....	50
2.3.6	(Chapter 8): Characterisation of Foot Categories .....	50
2.3.7	(Chapter 9): Can the Action of a Foot be Modelled Mathematically? .....	51

### **CHAPTER 3: STATIC CHARACTERISATION**

<b>3.1</b>	<b>Introduction &amp; Chapter Objectives</b> .....	52
<b>3.2</b>	<b>Mounting Methods for Static Testing</b> .....	53
3.2.1	Mounting Methods Shown in Existing Published Papers	53
3.2.2	Mounting Strategy Analysis .....	55
3.2.3	Conclusions on Foot Mounting Methods .....	59
3.2.4	Reproducing Previous Static Rating Test Methods ..	61
3.2.4.1	Theory .....	61
3.2.4.2	Method .....	62
3.2.4.3	Results .....	65
3.2.4.5	Conclusions .....	68
<b>3.3</b>	<b>Development of Mounting Fixtures</b> .....	70
<b>3.4</b>	<b>Static Characterisation of a Single Foot</b> .....	74
3.4.1	Theory .....	74
3.4.2	Method .....	74
3.4.3	Results .....	75
3.4.4	Conclusions .....	76
<b>3.5</b>	<b>Chapter Conclusions</b> .....	77

## CHAPTER 4: DYNAMIC CHARACTERISATION

<b>4.1</b>	<b>Introduction &amp; Chapter Objectives</b> .....	78
<b>4.2</b>	<b>Development of a Wearable Sensing System</b> .....	80
4.2.1	Scope & Objective .....	80
4.2.2	Design .....	81
<b>4.3</b>	<b>Overview of Methodology</b> .....	84
<b>4.4</b>	<b>Results</b> .....	85
4.4.1	Foot Deflection .....	85
4.4.2	Ground Contact Position .....	86
<b>4.5</b>	<b>Amputee Testing Conclusions</b> .....	91
4.5.1	Summary .....	91
4.5.2	Further Work .....	92
<b>4.6</b>	<b>Spring Rate Calibration</b> .....	93
4.6.1	Method .....	93
4.6.2	Results .....	94
<b>4.7</b>	<b>Single Condition Calibration</b> .....	96
4.7.1	Method .....	96
4.7.2	Results .....	98
<b>4.8</b>	<b>Dynamic Spring Rate Testing</b> .....	100
4.8.1	Method .....	100
4.8.2	Results .....	103
4.8.3	Conclusions .....	104
<b>4.9</b>	<b>Power Calculations</b> .....	105
<b>4.10</b>	<b>Chapter Conclusions</b> .....	107

<b>CHAPTER 5: BRINGING RUNNING INTO THE LABORATORY</b>	
<b>5.1 Introduction &amp; Chapter Objectives</b> .....	109
<b>5.2 Rig Specification</b> .....	112
<b>5.3 Rig Design</b> .....	115
5.3.1 Basic Design .....	115
5.3.2 Mounting of the Foot .....	117
5.3.3 Instrumentation .....	121
<b>5.4 Rig Validation</b> .....	122
5.4.1 Introduction .....	122
5.4.2 Ground Contact Point .....	124
5.4.3 Method .....	126
5.4.4 Results .....	128
<b>5.5 Characterisation of Rig Efficiency</b> .....	136
<b>5.6 Chapter Conclusions</b> .....	137
<b>CHAPTER 6: INVESTIGATING SHM VARIABLES</b>	
<b>6.1 Introduction &amp; Chapter Objectives</b> .....	139
<b>6.2 Exploring the Principles of SHM</b> .....	140
6.2.1 The Effect of Mass Variation .....	140
6.2.1.1 Method .....	140
6.2.1.2 Results .....	142
6.2.2 The Effect of Stiffness Variation .....	146
6.2.2.1 Method .....	146
6.2.2.2 Results .....	147
6.2.3 Variation Conclusions .....	149
6.2.4 The Effect of Displacement Amplitude Variation .....	151
6.2.4.1 Method .....	151
6.2.4.2 Results .....	152
<b>6.3 Chapter Conclusions</b> .....	156

## **CHAPTER 7: THE EFFECT OF SPEED VARIATION**

<b>7.1</b>	<b>Introduction &amp; Chapter Objectives</b> .....	160
<b>7.2</b>	<b>Velocity Testing (Part 1)</b> .....	161
7.2.1	Method .....	161
7.2.2	Results .....	162
7.2.3	Conclusions .....	163
<b>7.3</b>	<b>Velocity Testing (Part 2)</b> .....	165
7.3.1	Method .....	165
7.3.2	Foot Deflection .....	170
7.3.2.1	Results .....	170
7.3.2.2	Deflection Conclusions .....	173
7.3.3	Ground Contact Progression .....	174
7.3.3.1	Stance Length Results .....	174
7.3.3.2	Ground Contact Progression Results .....	177
7.3.4	Foot Stiffness Progression .....	182
7.3.4.1	Method .....	183
7.3.4.2	Results .....	184
7.3.5	Data Validity Check .....	187
<b>7.4</b>	<b>Chapter Conclusions</b> .....	188

## **CHAPTER 8: CHARACTERISATION OF FOOT CATEGORIES**

<b>8.1</b>	<b>Introduction &amp; Chapter Objectives</b> .....	191
<b>8.2</b>	<b>Category Testing</b> .....	194
8.2.1	Defining a Datum .....	194
8.2.2	Method .....	198
8.2.3	Results .....	199
<b>8.3</b>	<b>Chapter Conclusions</b> .....	202

<b>CHAPTER 9: MATHEMATICAL MODELLING OF A FOOT</b>		
<b>9.1</b>	<b>Introduction &amp; Chapter Objectives</b> .....	203
<b>9.2</b>	<b>Theory</b> .....	204
<b>9.3</b>	<b>Contributing Factors</b> .....	206
9.3.1	$\Delta$ GCP .....	206
	9.3.1.1 Foot Strike Position Simulation .....	207
	9.3.1.2 Conclusions .....	212
9.3.2	Foot Stiffness .....	214
	9.3.2.1 Defining the True Spring Rate of the Foot ....	215
	9.3.2.2 Conclusions .....	220
9.3.3	Calculating Response Time .....	221
	9.3.3.1 Method .....	223
	9.3.3.2 Assumption of a Single Foot Stiffness .....	225
<b>9.4</b>	<b>Chapter Conclusions</b> .....	230
 <b>CHAPTER 10: DISCUSSION &amp; CONCLUSIONS</b>		
<b>10.1</b>	<b>Discussion</b> .....	233
10.1.1	What are the mechanical characteristics of a prosthetic running foot? .....	233
10.1.2	Is the claim that a foot mimics Simple Harmonic Motion legitimate? .....	235
10.1.3	Can the action of a prosthetic running foot be modelled mathematically? .....	236
10.1.4	Can the prescription of feet be changed such that the user experience for active amputees is improved? ..	237
10.1.5	Primary Research Question .....	239
10.1.6	Contribution to Knowledge .....	240
<b>10.2</b>	<b>Conclusion</b> .....	242
<b>10.3</b>	<b>Further Work</b> .....	244
10.3.1	Improve Understanding of the Amputee ‘System’ ...	244
10.3.2	Investigate the Suitability of Including a Modification Factor .....	245

10.3.3 Increase Sample Sizes of Feet Tested for Category Characterisation .....	245
10.3.4 Designing the Next Generation of Prosthetic Running Foot .....	246
<b>REFERENCES</b> .....	247
<b>APPENDICES</b> .....	257
<b>A1 FOOT INSTRUMENTATION</b>	
A1.1 Displacement Sensor .....	257
A1.2 Ground-Force Sensors .....	259
A1.3 Resistive Force Signal Conditioner .....	260
A1.4 Analogue Data Logger .....	261
A1.5 Battery Pack .....	262
A1.6 Equipment Setup .....	263
A1.6.1 Displacement Sensor .....	263
A1.6.2 Ground Force Sensors.....	264
<b>A2 RIG FABRICATION</b>	
A2.1 Framework .....	266
A2.2 Carriage & Linear Motion Apparatus .....	267
A2.3 Securing the Mass .....	268
<b>A3 RIG INSTRUMENTATION</b>	
A3.1 Processing Hardware .....	271
A3.2 Ground Reaction Force Load Cell .....	273
A3.3 Excitement Force Load Cell .....	276
A3.4 Linear Resistive Transducer .....	279
A3.5 Displacement of Foot .....	282
A3.6 Data Logger .....	282
<b>A4 RIG EFFICIENCY</b>	
A4.1 Method 1: Hysteresis Curves .....	284
A4.2 Method 2: Input Energy vs. Stored Energy .....	288
A4.3 Method 3: Carriage Amplitude Decay .....	292
A4.4 Rig Efficiency Conclusions .....	296

<b>A5</b>	<b>VIDEO-BASED MEASUREMENT ACCURACY &amp; REPEATABILITY</b>	
A5.1	Stance length intra-rater reliability investigation .....	300
A5.2	Deflection sensor vs. frame rate timing methods .....	301
<b>A6</b>	<b>FURTHER DOCUMENTATION</b>	
A6.1	ISPO Journal Publication Abstract .....	303
A6.2	Ethical Approval Documentation .....	305

## ACKNOWLEDGEMENTS

As this project developed it gathered supporters, sources and reliable aids who are sympathetic to the purpose, without whom it would not be possible to complete as presented here. As such, the author would like to sincerely thank these individuals and organisations for their significant assistance, patience and understanding.

Firstly, and most directly, the three supervisors for their guidance and trusting approach, and in particular Dr Philip Sewell for his efforts in focussing not just the author's mind but also the other supervisors' tangential brilliance.

This work, as it concerns the application of prosthetic feet, inevitably required amputee volunteers. Sincerest thanks must go to John L., Mark A. and Mark F. for their invaluable feedback and particularly to John L. and Mark F. for their patience in foot testing, running laps of sports facilities whilst being scrutinised.

Throughout the course of the past 36 months, whenever testing has been required equipment has been sourced. The author has received exceptional support from two specific organisations; Ossur UK for their assistance in understanding their specific prosthetic devices and the supply of a multitude of feet and foot coverings to allow repeatable test work to be conducted, and MSR Electronics GmbH for the supply of their flagship data logger. Thanks must also go to Dr Jan Walter Schroeder and Richard Hawkins Esq. for the design of the electronic circuits used in the various signal amplifiers and conditioner case as detailed in this report.

And finally thank you to the University of Bournemouth and the staff of the Graduate School for appreciating the value of such work and for funding not only the position under the Studentship scheme, but also for the ongoing funding opportunities that have been available.

## **AUTHOR'S DECLARATION**

The author declares that the work presented herein is entirely original. Where figures or quotes are used that are the property of a third party they are referenced within the body of the work.

## **ABBREVIATIONS**

**IAAF** - International Association of Athletics Federations

**ESR** - Energy Storing and Returning

**NHS** - National Health Service

**AK** - Above Knee (amputation)

**BK** - Below Knee (amputation)

**SACH** - Solid Ankle Cushioned Heel (prosthetic device)

**FDM** - Fused Deposition Modelling

**RSP** – Running Specific Prosthesis

**ESR** – Energy Storing & Returning

**GCP** – Ground Contact Point

**GCT** – Ground Contact Time

**SHM** – Simple Harmonic Motion

# CHAPTER 1: INTRODUCTION & LITERATURE REVIEW

## 1.1 Project Scope

The work detailed herein was conducted in order to further knowledge in the area of the dynamic response and use of prosthetic running feet. Within this remit is the static characterisation and testing of ESR devices but moreover the examination of the first-order dynamic performance and characteristics of the foot and amputee athlete. It is concerned with the dynamics of a foot in as much as can be appreciated (or 'felt') by the user and therefore secondary, tertiary, etc. orders or modes of vibration are ignored. Whilst a more complex dynamic performance of a composite structure (such as an ESR foot) exists and is acknowledged by the author, the literature studied shows that a more detailed and fundamental understanding of first-order performance could directly benefit the amputee athlete.

## 1.2 Introduction

Since the commercial introduction of the ESR (Energy Storing and Returning) prosthetic foot in 1985 (Michael, 1987) prosthetists and amputees have been able to choose ever-more specific and potentially suitable feet for any given application. The principle of an ESR foot is that it captures energy that would otherwise be dissipated when the runner lands (beginning at the moment of foot strike until mid-stance), and returns this energy (from mid-stance until toe-off) therefore propelling the runner forward (figure 1.1).

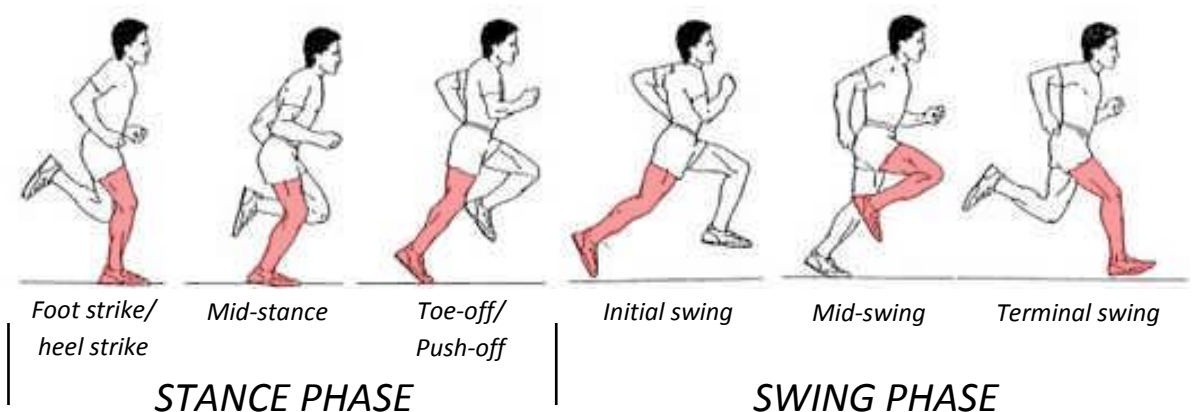


**Figure 1.1:** The running gait cycle at maximum velocity (adapted from <http://www.oandplibrary.org>)

The remit of purely restoring basic function to the amputee dissolved in lieu of greater and greater performance enhancements culminating in the development of the first specialised prosthetic sprint foot, the Flex Run (figure 1.2) in 1996 (Lechler, 2005). However as the complexity and specific nature of the feet increases, so does the importance of effective prescription, although as Hafner (2005, p.8) notes, *'There is currently little compelling scientific evidence to guide the clinical prescription of prosthetic foot-ankle systems.'*



**Figure 1.2:** Typical ESR running-specific foot (Ossur Flex Run)

The advent of the specialist sprinting foot has enabled adaptive athletes to run faster than ever before. Indeed 2012 was a landmark year in prosthetic sprinting with Oscar Pistorius, a bi-lateral trans-tibial amputee, competing in the able-bodied summer Olympic Games in the individual 400m race and alongside his South African colleagues in the 4 x 400m relay.

The journey to the Olympic Games for an amputee using ESR feet was not without controversy and in 2008 Pistorius was banned from IAAF (the International Association of Athletics Federations; the governing body in world athletics) competition. Dr Peter Brüggemann, Professor of Biomechanics at the Cologne Sports University, was charged with investigating the performance of Pistorius's feet. Following the testing he commented that:

*"(Pistorius) has considerable advantages over athletes without prosthetic limbs who were tested by us. It was more than just a few percentage points. I did not expect it to be so clear."* (Die Welt newspaper, December 2007).

Noroozi et al. (2012a) suggest a comparison can be made between an amputee runner and a basic spring - mass system, relying on spring stiffness and exhibiting natural damping and hysteresis behaviour and further:

*'If [the] bending mode could be synchronised with the cyclic excitation force generated by the body, the mass/body can exhibit a bouncing behaviour'. (Noroozi et al. 2012b, p.40).*

The suggestion of a resonance-based principle of operation is supported by other publications (Lehmann, 1993a, b) and Noroozi et al. (2012b) embellish the subject with the modal analysis of two prosthetic devices to understand the conditions affecting their harmonic frequencies.

Despite this work the prevalence of research in this field over the past two decades is limited. Indeed according to Nolan:

*'Only one study measuring the dynamic hysteresis has been found. This showed a Cheetah foot (Ossur, Reykjavik, Iceland) to have 63% energy efficiency'. (Nolan, 2008, p.126).*

Nolan also reports that using basic energy calculations:

*'the human foot has been calculated to have an energy efficiency of 241% during running at  $2.8m s^{-1}$ '. (Nolan, 2008, P.127).*

This is due to the positive work that can be achieved with musculature that is absent in an amputee subject. The disparity in these published energy return efficiency figures would suggest a distinct advantage for able-bodied athletes. However if able-bodied

Discipline	Able-bodied world record (a)	Assistive world record (b)	% of time =(b)/(a) x 100
400m	<b>43.18s</b> (Michael Johnson)	<b>45.07s</b> (Oscar Pistorius)	95.8%
200m	<b>19.19s</b> (Usain Bolt)	<b>20.66s</b> (Alan Oliveira)	92.9%
100m	<b>9.58s</b> (Usain Bolt)	<b>10.85s</b> (Jonnie Peacock)	88.3%

**Table 1.1:** Comparison of current world record sprinting times of able-bodied and amputee athletes.

and assistive world record times are compared for various disciplines (table 1.1) it would suggest that there is a more complex picture emerging; the equation is not as simple as these basic efficiency numbers would suggest.

If the 241% **(c)** efficiency of the human foot is combined with the reported 63% **(d)** efficiency of the ESR prosthetic device it would suggest an advantage of 383% in favour of the able-bodied athlete exists ( $100/(\mathbf{d}) \times (\mathbf{c})$ ). If this is a genuine advantage in energy return with a natural foot - ankle system, how can an amputee be remotely competitive and why are the time discrepancies so small in high-level sprinting? What can explain the progressively tightening times of able-bodied athletes vs. their amputee colleagues as the event distance increases? When examining the times for the 100metre sprint for both the able-bodied and amputee world records it can be seen that the able-bodied record is 88.3% of the amputee time. This figure increases to 95.8% for the 400m discipline. It can be seen that as the distance of the run increases, the able-bodied and amputee times become progressively close.

This phenomenon is compounded when one considers the pool of athletes that the assistive sports have to draw from when compared with its able-bodied counterpart. There appear to be no solid statistics published to suggest the numbers of amputees in the UK but the estimate from the Limbloss Information Centre (2015) is circa 62,000. According to the NHS (2015) *'Approximately 5-6,000 major limb amputations are carried out in the UK every year'* but this figure includes lower and upper limb operations. The general proportion of upper:lower limb amputations has been suggested as 20:80 by the Limbless Association (2012) but no figures are published to confirm these numbers. However the NHS (2015) go on to suggest that *'the most common reason for amputation is a loss of blood supply to the affected limb (critical ischaemia), which accounts for 70% of lower limb amputations.'* Such conditions are most likely to occur in the less active population and the elderly, and the NHS (2015) conclude that *'More than half of all amputations are performed in people aged 70 or over'*. Following this thread and assuming some validity to the numbers available it could be suggested that there are some 24 - 34,000 lower limb amputees under the age of 70 in the UK today.

To progress this further and obtain more accurate numbers is not a trivial task as, according to the NHS and the Limbless Association, data only exists for those considered 'live' amputees; this means those who are registered on the NHS database which essentially originates from those who undergo an NHS procedure. However if further work were to be done, additional factors exist that should be taken into account and would again diminish the numbers of those available to represent Great Britain & Northern Ireland in the assistive sports. For example the proportions of AK: BK (Above Knee: Below Knee) amputees that exist (all current adaptive world sprinting records have been set by BK amputees), the aging amputee population as well as the proportion of the general population who are not only young enough but athletically gifted enough to compete on an international stage, regardless of disability.

However working with the data that is available it would not be unreasonable to suggest that the total number of amputees in the UK who are of an age to take part in competitive sports (circa. 20 – 35 years) does not exceed perhaps ten thousand. According to the Office of National Statistics (2011) and the 2011 UK Census the estimated UK population for the same age group is approximately thirteen million.

Very crudely put, for every Paralympic sprinter hopeful that exists in the UK there are around 1,300 in the able-bodied community of the equivalent age and at least an equal athletic ability. This information leaves no questions answered but does suggest that this is an area worthy of further study. Given the diminutive nature of the trans-tibial (BK) amputee population and the apparent disadvantage that any runner has when using a prosthetic foot, what allows adaptive athletes to be remotely competitive? Perhaps the prosthetic devices themselves provide an advantage over able-bodied athletes that has yet to be understood. If so, what research has been done to help understand the dynamics of a runner using an ESR foot and how are these feet prescribed? Given that a prosthetic running foot is a passive device, how does the prescription process make allowances for different running styles, speeds and weights of amputees? A literature review was conducted in order to identify what research has been conducted in the field of ESR prosthetic dynamics and where significant areas of study remain.

### **1.3 Research Objectives**

A research question was defined as stated below:

***'Is the current method of prescribing prosthetic ESR running feet appropriate and are there additional factors that should be taken into consideration?'***

Justification for this question is provided in the proceeding chapters following the Literature Review. The objectives of this study were:

- **To define the mechanical characteristics of a specific prosthetic running foot including spring rate and energy return efficiency**
- **To measure, understand and explain the action of a prosthetic running foot when in use across a range of running velocities**
- **To replicate the action of an amputee runner in a laboratory environment and manipulate variables to demonstrate the application of Simple Harmonic Motion**
- **To define what limitations a prosthetic foot imposes on running performance**
- **To suggest an alternative and improved method of running foot prescription based on the work conducted.**

## **1.4 Publications**

### **1.4.1 Journal Publications**

#### **Written, awaiting submission:**

Hawkins, J., Schroeder, J.W., Sewell, P., Noroozi, S., Dupac, M. Development of a wearable sensor system for dynamically mapping the behaviour of a prosthetic running leg.

#### **Planned / in progress:**

Hawkins J., Sewell, P., Noroozi, S., Dupac, M., 2015 Spring Rate Variations of a Prosthetic Running Foot: A Quantitative Investigation.

Hawkins J., Sewell, P., Noroozi, S., Dupac, M., 2015. Limitation Mechanisms of a Prosthetic Running Foot With Regard to Velocity, Cadence and Stance Length.

Hawkins J., Sewell P., Noroozi, S., Dupac, M., LaCompte, C., 2015. Techniques for Effective Characterisation of Prosthetic Feet in a Laboratory Environment: Controlling Boundary Conditions.

Hawkins J., Sewell P., Noroozi, S., Dupac, M., LaCompte, C., 2015. Techniques for Effective Characterisation of Prosthetic Feet in a Laboratory Environment: Friction and Hysteresis Sensitivity.

Hawkins J., Sewell P., Noroozi, S., Dupac, M., LaCompte, C., 2016. Prosthetic Running Foot Prescription: An Investigation into the Required Parameters.

### **1.4.2 Conference Publications**

Sewell, P., Hawkins, J. 2015. An Investigation of the Ground Contact Point and Sagittal Plane Displacement of Energy Storage and Return (ESR) Composite Lower-Limb Prosthetic Feet during Running. ISPO 2015

## 1.5 Literature Review

The papers published in the field of lower limb prosthetics are varied in their nature and scope. In 'Perspectives on How and Why Feet are Prescribed' Stark comments:

*'Modern prosthetic practice includes a growing array of foot designs that offer a wide spectrum of functions, indications, and costs.'* (Stark 2005, p.18).

Further:

*'this constant innovation requires a greater knowledge of physiologic foot function and more descriptive terminology when recommending feet to patients.'* Stark (2005, p.18).

Indeed it is clear that there are a wide variety of feet available, each with their increasingly specific and appropriate application. When considering the available literature it is important to remember the remit of this piece of work; specifically that is the function and dynamic characterisation of ESR prosthetic feet. The aim of this section is to understand the areas of knowledge that already exist in this field and importantly identify the gaps in this knowledge. What potential is there for expansion, what can be learned from previous investigations and what research methods should be adopted.

The review was carried out by searching a variety of published databases as well as using a central repository and reference managing tool for controlling the papers. In this case Mendeley (Mendeley Ltd.) was chosen. The primary sources for papers were online databases Elsevier.com, Scimedirect.com and MEDLINE/PubMed (<http://www.ncbi.nlm.nih.gov/pubmed>). Articles were limited to those published in, or translated into the English language and keywords used for searching included, but were not limited to, such words as 'prosthetic', 'feet', 'foot', 'artificial', 'prescription', 'energy', 'composite', 'dynamics' and combinations thereof. Papers were mainly selected for review if their primary research questions were regarding the function of ESR prosthetic feet or their prescription process.

## 1.5.1 Characterisation of Papers

This review is intended to give the reader an understanding of the research that has been carried out in the field of ESR prosthetic feet to date and identifies any areas of information deficit. Papers were divided into four distinct categories as defined in the following four sections:

Walking/Running Dynamics Papers (section 1.5.2)

Prosthetic Comparative & Review Papers (section 1.5.3)

Prosthetic Prescription Papers (section 1.5.4)

Prosthetic Dynamics Papers inc. Measurement (section 1.5.5)

## 1.5.2 Walking/Running Dynamics Papers

*This category includes papers that describe the action & mechanism of walking and running for both able-bodied and amputee athletes. There are many theories concerning the most efficient gait styles or how different variables affect bipedal locomotion (for example stride length, strike rate and ground reaction force). Running has also been compared with mechanical models such as a spring – mass system.*

---

It has been generally accepted that as animals (including humans) run they bounce over the ground, effectively using legs as musculoskeletal springs. This action can be considered as storing and returning elastic energy (Cavagna et al., 1964, 1977). Farley et al. (1996) comment:

*‘all of the elements of the musculoskeletal system are integrated in such a way that the overall system behaves like a single linear spring during running.’  
(Farley et al., 1996, p.185).*

Seyfarth et al. (2002, p.649) continue by suggesting *‘Mechanically self-stabilized running requires a spring-like leg operation’*. This is by contrast to the action of bipedal walking which was described in the seventeenth century as the action of vaulting over stiff legs (Borelli 1685) and has developed into the ‘inverted pendulum’ model (Alexander 1976). Subsequently the concept of a spring-mass model to describe walking has been suggested and according to Geyer et al. (2006, p.2861) *‘not stiff but compliant legs are essential to obtain basic walking mechanics’*.

The action of a runner has successfully long been compared with a spring-mass system and has been shown to accurately predict running mechanics (Alexander 1992; Blickhan 1989; Blickhan et al. 1993; Cavagna et al. 1988; Dalleau et al. 1998; Farley et al. 1991, 1993; He et al. 1991; Ito et al. 1983; McGeer 1990; McMahon et al. 1990; Seyfarth et al. 2003; Thompson et al. 1989). A graphical representation of this concept is shown in figure 1.3.

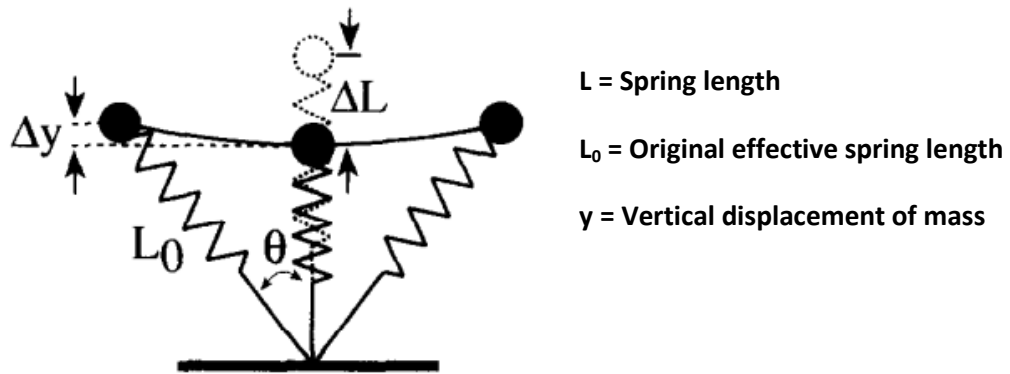


**Figure 1.3:** Illustration of a typical spring-mass system as proposed valid to represent human running (Farley et al. 1996).

The change in spring length represents the amplitude of compression of the effective leg spring and the change in ‘y’ value demonstrates the vertical oscillation of the centre of mass of the runner. This model has been the basis of further research under various running conditions investigating ground reaction forces, foot strike conditions, leg stiffness predictions, gait efficiency and fatigue (Bobbert et al. 1992; Dutto et al. 2002; Farley et al. 1996; Geyer et al. 2002; Gottschall et al. 2005; Gunther et al. 2002; Keller et al. 1996; Kerdok et al. 2002; Morin et al. 2006). Furthermore the accuracy of such an approach has been investigated by Bullimore et al. (2007) who suggested the majority of running parameters could be predicted to within 10% of the measured values.

Additional research has been conducted to investigate if a rigid body assumption is valid for running and progressively complex models have been constructed that employ a multitude of mass, spring and damper elements (Clark et al. 2014; Liu and Nigg, 2000; Ly et al., 2010; Nigg and Liu, 1999; Nikooyan and Zadpoor, 2011; Zadpoor and Nikooyan, 2010). However as the model becomes more complex it can be seen that the case becomes more specific to an individual and less suitable for predicting the action of a broad spectrum of runners. Clarke et al. (2014, p.2037) suggest ‘*the relatively specific objective of the multi-mass models has limited the breadth of their application*’ and conclude:

*‘two mechanical phenomena, acting in parallel, are sufficient to explain running ground reaction forces: (1) the collision of the lower limb with the running*

*surface, and (2) the motion of the remainder of the body's mass throughout the stance phase.'* (Clark et al. 2014, p.2037).

In a study to understand how runners affect a faster running velocity Weyand et al. (2000) found that stride frequency, stride length and contact length were all increased for faster runners.

*'We conclude that human runners reach faster top speeds not by repositioning their limbs more rapidly in the air but by applying greater support forces to the ground.'* (Weyand et al. 2000, p. 1998).

Subsequently Weyand et al. (2010) expand on this research concluding that:

*'a limit to spring running speed is imposed not by the maximum forces that can be applied to the ground but rather by the maximum rates at which the limbs can apply the forces required.'*

In support of these conclusions Keller et al. (1996) found that *'(Ground reaction force) increased linearly during walking and running from 1.2 BW (Body Weight) to approximately 2.5 BW at 6.0 ms<sup>-1</sup>'* (Keller et al. 1996, p.253) suggesting that as running speed increases so too does the ground reaction force exerted by the athlete. It would be logical to suggest that this increase in ground reaction force is accompanied by increased effective leg stiffness, but Farley et al. (1996) report the contrary:

*'Biomechanical studies have shown that as animals run faster, the body's spring system is adjusted to bounce off the ground in less time by increasing the angle swept by the leg spring during the ground contact phase rather than by increasing the stiffness of the leg spring'* (Farley et al. 1996, p.181).

And further:

*'The stiffness of the leg spring remains nearly the same at all speeds in a variety of animals including running humans, hopping kangaroos and trotting horses'* (Farley et al. 1996, p.181).

In order to affect a change in leg stiffness there is some disagreement in published literature. Bobbert (1992, p.223) observed *'spring-like behaviour of pre-activated knee flexor and knee extensor muscles'* suggesting the knee is responsible for a change in effective leg stiffness and Arampatzis et al comment:

*'Running velocity influences the leg spring stiffness, the effective vertical spring stiffness and the spring stiffness at the knee joint. The spring stiffness at the ankle joint showed no statistical difference ( $p < 0.05$ ) for the five velocities.'*  
(Arampatzis et al. 1999, p.1349).

However contrary to this Farley et al (1999, p.267) conclude that *'the primary mechanism for leg stiffness adjustment is the adjustment of ankle stiffness'*

Regardless of which part of the leg anatomy is responsible for the alteration of effective spring stiffness, the available literature suggests that running can be equated to a spring – mass system with the musculature of the entire system combining to effectively form a spring. In order to run faster, the athlete is capable of stiffening this spring and exerting positive work to the ground plane thus affecting a larger ground reaction force. This additional energy allows an increased stride length with the contact length and stride frequency naturally lengthening at higher running velocities. No evidence of a decreased swing time (as running speed increases) could be found in the literature.

Furthermore, following research into the stiffness of the running surface substrate Kerdok et al. suggest:

*'a reduction in metabolic cost occurs as the elastic rebound provided by a more compliant surface replaces that otherwise provided by a runner's leg.'* (Kerdok et al. 2002, p.474).

This suggests that if an artificial spring were included into a leg (as in the case of a prosthetic running foot) the resulting elastic rebound could result in a reduction of metabolic cost.

### 1.5.3 Prosthetic Comparative & Review Papers

*This category includes papers that compare different styles of feet and/or review feet and relevant literature. To date there have been many research projects that serve to pitch one style or model of foot against another. Often the merit of each of the feet is discussed and a testing regime defined in order to scientifically test their effectiveness or suitability. Commonly (and usefully) this involves the comparison of a SACH (Solid Ankle Cushioned Heel – figure 1.4) foot with some version of an ESR foot for both walking and running.*



**Figure 1.4:** Typical SACH (Solid Ankle Cushioned Heel) foot for low activity (Blatchfords)

Contrary to expectation for a style of foot that has been renowned for improving running performance, the majority of the comparison work relating to ESR feet that is evident in the literature is primarily concerned with basic ambulation and self-selected walking speeds (Collins et al. 2005; Fey et al. 2011; Mattes et al. 1999; Thomas et al. 2000; Yack et al. 1999). Torburn et al. (1990, P.370) noted that in their investigation '*Gait analysis was done during self-selected free and fast-paced walking over a 10 meter level walkway*' and in perhaps the most relevant and thorough comparison of the ESR style of foot with a SACH foot, Lehmann et al. (1993a, P.853) wrote that in their testing '*...a range of walking speeds was selected (ie, 73, 90, 107, and 120m/min)*'. This is perhaps a function of the relatively recent development of ESR feet but also suggests the limited amount of scientific research that has been undertaken in this field. In his review of the literature from 2005 Hafner writes:

*'Given that more than 20 years of scientific research has examined the effect of prosthetic feet on amputee gait, [the]limited evidence to support prescription or use of prosthetic feet appears to fall short of expectations'. (Hafner 2005, P.5)*

To compound this apparent shortage of relevant papers, those that are available and comment on the comparative dynamic function of ESR prosthetic feet (such as the Flex Run vs. SACH foot) most commonly do so with a heel component fitted, meaning that the only energy absorption that can take place in assisting plantorflexion (the action of standing on tip-toes) occurs from mid-stance through to when the toe is fully loaded (see figure 1.1 for a diagram explaining the running cycle). Therefore a large proportion of energy (resulting from heel strike) is dissipated in the heel component which is not present in modern running prostheses.

Additionally Lehmann et al. suggest:

*'The timing of the release of the stored energy during unloading relates directly to the natural frequency of the prosthetic limb' (Lehmann et al. 1993a, P.859)*

and also note:

*'To effectively use the energy released during unloading, it must be timely to assist in propulsion of the body, as in a pogo stick.' (Lehmann et al. 1993a, P.859)*

This suggested link between the harmonic of the foot under load and the stance-phase timing of the amputee is the subject of discussion in the first paper from 1993 by Lehman et al. whereby some dynamic testing of these feet was undertaken.

*'In order to determine if the release of stored energy due to compression of the foot occurred timely to assist with propulsion during walking, the natural frequency of oscillation was assessed.' (Lehman et al. 1993a, P.855)*

However this testing demonstrated a natural harmonic frequency grossly higher than that demanded when walking and efficiency calculations performed on amputee subjects confirmed that no advantage was yielded from the use of an ESR foot.

*'There was no significant difference in metabolic rate or efficiency while using either prosthesis at any given walking speed' (Lehmann et al., 1993a, P.855).*

Energy calculations performed by others also confirmed that no performance increase could be found when using an ESR foot when walking. Upon comparing an array of ESR prosthetic devices with a SACH foot, Torburn et al. (1990, P.369) noted that *'There were no clinically significant advantages of any of the feet tested'* and:

*'The results of this pilot study suggest there are no advantages of the dynamic elastic response feet for the amputee who is limited to level walking. Further investigation is needed' (Torburn et al. 1990, P.383).*

It is clear from the literature that the various authors believe there to be a more in-depth dynamic function of the feet that has yet to be understood fully. Lehman et al. suggest:

*'It may be possible to exploit energy storage and release within the prosthetic limb, but the time from compression to release should be more closely related to the timing of the gait cycle. This approach may serve as the basis for future research in the development of more effective prosthetic foot designs'. (Lehman et al. 1993a, P.860)*

Hafner et al. write:

*'Future research must concentrate not on analyzing which devices work, but on analyzing why the devices that do work are successful for the particular amputee'. (Hafner et al. 2002, P.6)*

Additionally Hansen et al. (2004b) comment on the changing boundary conditions that exist throughout the stance phase of the gait cycle; this is to say the changing contact

area and load shift throughout the foot. All feet in this study were fitted with a heel component but this provides a further variable to measure when considering the dynamic function of ESR feet. Does the boundary condition of an ESR foot change dramatically and should this exhibit a dynamically significant effect?

#### 1.5.4 Prosthetic Prescription Papers

*These are papers that discuss foot prescription, be it the effectiveness of various prescription processes or simply commenting on how feet are prescribed. Such publications include the manufacturers' documentation and advice to the prosthetists for effective fitment of their specific feet. These papers are particularly useful for understanding the current processes employed by healthcare professionals.*

---

With the exception of the various manufacturers' fitting manuals that describe the clinical advised prescription procedure for their respective feet, only two papers were found that have any mention of ESR feet and are solely concerned with the topic of prescription. These are separate to the papers mentioned elsewhere in this report that touch upon the prescription process as part of a larger discussion around their dynamics, etc.

In a paper by Stark (2005), 'Perspectives on How and Why Feet are Prescribed', there is almost no mention of ESR feet and despite the various sections of the report detailing the important parameters to consider, running-specific devices do not feature. An important observation that is made however is:

*'[This] constant innovation requires a greater knowledge of physiologic foot function and more descriptive terminology when recommending feet to patients.'* (Stark 2005, P.18)

A nod to the specificity of modern feet for the patient and their desired level of activity. A more comprehensive and relevant review is provided by Lechler et al. (2008) and describes the considerations when specifying an ESR foot for running. Despite being a journal authored by the employees of Ossur Ltd. and is arguably biased towards their products and interests, it does cite some useful papers that are also included in this review of the literature. Some conclusive statements are made which seem to simplify the area somewhat, such as:

*'The appropriate stiffness selection can reduce the metabolic cost when the driving frequency matches the resonance frequency of ambulation.'* (Lechler et al. 2008, P.231)

However this is taken from Lehmann et al. (1993a,b) and in this specific paper it is more of a hypothesis than a conclusion. One piece of information that does not appear elsewhere is:

*'for the 100m sprint, the category is selected by weight according to the manufacturer's chart; for the 400-m sprint, one category lower is selected; and for long jump, two categories up are selected'* (Lechler et al. 2008, P.231)

Another acknowledgement of the importance of matching the driving frequency with natural system harmonics is:

*'During acceleration the change in cadence would require a continuous adaption of the prosthetic device to the resonance frequency of ambulation'* (Lechler et al. 2008, P.231).

These statements would suggest that Ossur as a prosthetic devices manufacturer have found a more direct correlation between running efficiency and system harmonics than were merely suggested by Lehmann et al. (1993a,b) and other authors since, but these findings are not in the public domain.

If the literature available from Ossur is examined there appears to be some confusion regarding the intended use of their ESR prosthetic feet. The most commonplace model of foot is the Flex-Run and according to the 2014 products catalogue (Ossur, 2014) the foot is suitable for *'high impact activities such as recreational jogging, trail running, distance running and triathlons'*. Meanwhile the Ossur website suggests the foot is suitable for *'activities involving running, track and field, sprinting, and long-distance running.'* (Ossur.com, 2014). Feet are offered in a range of stiffness values, divided into specified 'categories' and are prescribed according to the mass of an amputee with little or no consideration for their specific ability or desired activity as demonstrated by the stiffness prescription guide from Ossur (table1.2).

WEIGHT KG	37-44	45-52	53-59	60-68	69-77	78-88	89-100	101-116	117-130
WEIGHT LBS	81-96	97-115	116-130	131-150	151-170	171-194	195-220	221-256	257-287
High to Extreme Impact Level	1	2	3	4	5	6	7	8	9

**Table 1.2:** Flex Run stiffness prescription guide (Source: Ossur.com)

Weight (lbs)	Impact Level		Weight (kg)
	Low (New)	Moderate (Experienced)	
100-115	1	1	44-52
116-130	1	2	53-59
131-150	2	3	60-68
151-170	3	4	69-77
171-195	4	5	78-88
196-220	5	6	89-100
221-255	6	7	101-116
256-285	7	8	117-130
286-325	8	9	131-147
326-365	9		148-166

**Table 1.3:** Nitro stiffness prescription guide (Source: Freedom-innovations.com)

User	User Weight										kg lbs
	44-52 100-115	53-59 116-130	60-68 131-150	69-77 151-170	78-88 171-195	89-100 196-220	101-116 221-255	117-130 256-285	131-147 286-325	148-166 326-365	
Jogger	1	2	3	4	5	6	7	8	9	9	Foot spring set
Runner	2	3	4	5	6	7	8	9	9		

**Table 1.4:** Blade XT stiffness prescription guide (Source: Endolite.co.uk)

This practice is consistent with other manufacturers of ESR prosthetic feet. Freedom Innovations (Freedom Innovations LLC, California, USA) provide a chart to guide the prosthetist (table 1.3) which features a shift of one category based on the experience of the athlete and Endolite (Chas A Blatchford & Sons Ltd, Basingstoke, UK) suggest a shift of a single category based on a subjective measure of being a ‘jogger’ or ‘runner’ (table 1.4). It is not clear if the stiffness categories are comparable with one another across these different manufacturers and there are no tangible units associated with the various categories.

### 1.5.5 Prosthetic Dynamics Papers inc. Measurement

*Particularly key to this project, these are papers that attempt to describe the dynamic action of various feet from a fundamentally mechanical point of view. Some choose to evaluate the feet when fitted to an amputee, whilst others isolate the foot and treat the amputee and foot as a simple mechanical system. Also included is a summary of those methods used to measure and record the variables of running, whether with or without a prosthetic device.*

---

Numerous research projects are available that are concerned with the development of adaptive, active and bionic foot/ankle designs (Au et al. 2008; Hansen et al. 2004a; Herr et al. 2002; Holgate et al. 2008; Michael et al. 1990; Tokuda et al. 2006; Versluys et al. 2009) but these are almost solely concerned with improving the performance of prosthetics for walking activities. No compelling work was found in the area of active running prosthetics and as such this section deals with the papers that form the vast majority of research in this area; passive ESR running feet.

The most recent work that has been published on the topic of the dynamic function of ESR prosthetic feet is that of Noroozi et al. (2012a,b, 2014) in a series of three papers. Through various means including FEA prediction, mathematical modelling and rig testing the authors have demonstrated the link that exists between impulse timing and the energy return from a prosthetic foot.

*'The mathematical and experimental results demonstrates that if the impact frequency due to self-selected running frequency is synchronised with the natural bending modes of vibration, the ESR foot responds like a trampoline, resulting in higher take-off speed and higher potential energy storage in the system' (Noroozi et al. 2012a, P.113).*

Throughout the course of this work exists the comparison of an amputee and prosthetic ESR foot to a spring - mass system. This approach assumes the body of the amputee to be a rigid mass. In addition to a natural flexibility the human body also exhibits an infinitely variable nature of musculature control, but crucially in making this

assumption it allows the removal of variables that would otherwise complicate the equation.

Noroozi et al. (2012a,b, 2014) are not the first authors of papers to make this same assumption. Able-bodied running has been effectively compared with spring-mass models many times (McGowan et al., 2012, Blickhan, R., 1993, 1989, Alexander, R. M. 1992). During their defence of Oscar Pistorius prior to the 2012 Olympic games Weyand et al. (2009, p.903) state that:

*'passive, elastic prostheses are designed to provide the spring-like function that human lower limbs do during the stance phase of each stride'.*

However the application of such a model in amputee running is relatively recent. Wilson notes *'there have been no published studies to date that have used a spring-mass model to evaluate amputee biomechanics'* (Wilson et al. 2009, p.218).

Noroozi et al. (2012a,b, 2014) have extended knowledge in this area through theoretical development, simulation and physical testing utilising modern prosthetic devices. However, this research has been focused heavily on the development of the fundamental science behind the dynamics of the foot, while little discussion has been made to date on the effect this will have on their prescription.

A repetitive theme in the papers that have been published over the last 20 years is that of synchronisation. Synchronisation of the natural resonance of the prosthetic with that of some measurable of running and suggestions are made that this will enhance performance. Lechler et al. suggest:

*'The appropriate stiffness selection can reduce the metabolic cost when the driving frequency matches the resonance frequency of ambulation'* (Lechler et al. 2008, P231)

This view is shared by Lehmann et al. (1993a,b) and Noroozi et al. (2012a,b, 2014) although it has yet to be conclusively demonstrated.

A further theme that establishes itself is that of the inconsistency in measurement techniques to compare various feet. Geil (2001) conducted work focused on the

hysteresis and efficiency of energy return of a variety of ESR feet and did so using a dynamic hydraulic testing machine and describes how *'Two Teflon sheets (DuPont, Wilmington, DE) were placed between the table and the foot to minimize friction during foot loading and deformation'* (Geil 2001, P.71). The resulting hysteresis loops are therefore more likely to have occurred as a result of the friction in the slippage system under load than from the damping properties of the spring itself. Such a technique would also potentially result in the changing boundary condition of the ground contact point as the foot deflects, which is not mentioned. This effect is discussed by Dyer who mentions that:

*'an assessment of energy return technology when loaded under dynamic conditions demonstrates changes in mechanical stiffness due to bending and effective blade length variation during motion'. (Dyer 2013, P.116)*

Other investigations have taken place using similar techniques but none have exactly replicated this same methodology. Repeating such an investigation in an accurate manner would be impractical given that the friction co-efficient ( $\mu$ ) between the toe and test machine would need to be precisely replicated.

Buckley (2000, P.358) summarises that *'The findings in the present study, indicate that 100% of the energy absorbed by the (Sprint-Flex or Cheetah) prosthesis was returned'*; a direct contradiction of the work carried out by Geil (2001) who defined the efficiency of a Flex Foot prosthesis as 75%. Czerniecki et al. (1991) propose a value of 84% for the same model of foot whereas Bruggemann et al. suggest:

*'The material behaviour of the carbon keels of the dedicated prosthesis provided a hysteresis of less than 10 per cent, indicating a high per cent of energy return.'* (Bruggemann et al. 2008. P.227)

Wilson et al. mention this lack of parity in measurement techniques.

*'...there is often difficulty linking the quantitative results to clinically relevant findings. This difficulty is compounded by the inconsistency in measurement approaches limiting the ability for comparison between studies'* (Wilson et al. 2009, P.219)

All of the measurement approaches mentioned previously concern the isolation of a prosthetic device and subsequent analysis using laboratory equipment. However numerous research studies are available that observe human running and record specific variables. The technique chosen should reflect the parameters demanded by the research.

Visual referencing systems can be used to record the positioning (in two- or three-dimensional space) of reflective markers placed at specific locations on a participant and the resulting video interrogated to understand the relative movement of these markers (Hillery et al. 1997; Pasparakis & Darras 2009; Lehmann et al., 1993a,b; Strike & Hillery, 2000; Palermo et al. 2014; Riener et al. 2001; Torburn et al. 1990; Wilson et al., 2009). This process has been used to analyse running gait, joint kinematics, powers, torques, moments and velocities, but assumes an effective calibration and secure application of the markers. Video data is typically captured at 120Hz (Vicon, Oxford Metrics Inc.) to allow improved resolution if compared with regular video cameras. Choosing a lower frame rate will result in a poorer resolution and as summarised by Keogh (2011, p.239) (when commenting on the Oscar Pistorius athletics defence case prior to the 2012 Olympic games) *'the use of 30Hz video footage by Grabowski et al (2010) is insufficient'*.

Ground force reaction, stance- and swing-phase timing and stride length can be evaluated using force plates that can be mounted in the floor of a controlled test area or on the bed of a specialist treadmill (Riener et al. 2001; Hillery et al. 1997; Pasparakis & Darras 2009).

Further to these and often in consort, Electromyography (EMG) can be used to monitor the activity of musculature of the participant being observed (Fey et al. 2010; Pasparakis & Darras 2009; Perry & Shanfield 1993). This involves the insertion of probes into the relevant muscles and can be used to determine the timing and relative intensity of muscle activation although is not suitable for the definition of absolute values.

On occasion researchers have chosen to develop additional measurement techniques and instrumentation which are specific to the task being undertaken. Examples of this

are foot switches attached to the feet of athletes for determining stride cadence (Perry & Shanfield 1993), or a series of gyroscopes and accelerometers to measure angular velocity of body segments and accelerations of various skeletal positions (Liu et al. 2009). These somewhat custom techniques have the distinct advantage of allowing freedom from a gait laboratory environment that could prove restrictive to the activity in question.

It should also be noted that for each of these measurement techniques there must also exist the relevant hardware and software for the recording (at a suitable frequency), storing and analysis of the data gathered. This could take the form of a standalone data logger or computer with specialist software.

## 1.6 Conclusions on the Literature Review

It is clear from the papers reviewed that limited work has been conducted in this area and there is a lack of parity on the topic of the dynamics of ESR prosthetic feet. Partly this could be because those papers that are available are spread over more than two decades and designs/styles of feet have changed somewhat in this time. However it is more likely that this has occurred due to a basic lack of research conducted on the subject. The fundamentally small group of individuals that benefit from such ESR running feet means that their commercial value is limited and hence the funding for research is also limited.

More concerning, there appears to be little or no scientific literature surrounding the reasons for selecting a foot, or rather foot *category* for a specific amputee. In their study of running biomechanics, Wilson et al. (2009, P.221) comment '*The exact stiffness categorization was somewhat arbitrary*'. Hafner (2005, P.8) goes further to say '*limitations in the research studies conducted to date preclude the direct application of scientific evidence to clinical decision making*.' In other words the prescription process used in the designation of prosthetic ESR feet is unscientific. Strike & Hillery (2000, P.606) comment that '*Change and development in prosthetic design appears to have been carried out on a trial and error basis*' and Hafner (2005, P.8) mentions that '*There is currently little compelling scientific evidence to guide the clinical prescription of prosthetic foot-ankle systems*.'

It is clear and often recommended in the literature that more work should be conducted in the area of dynamic characterisation of ESR feet, particularly surrounding the prescription process with logic and reason. Much of the literature concerning the dynamic properties of such devices suggests a strong link between the natural harmonic frequency of the prosthetic and some manner of running frequency/driving frequency. Whether or not this link is fully understood in the private domain, it is not reflected in the recommendation of one stiffness category over another for a specific patient. No consideration is currently evident with regards to running style, distance, speed, cadence, height or type. The same foot is advised by the manufacturers for an

80kg patient no matter if they are 5 feet or 7 feet tall, or if they intend to take part in competitive sprinting or leisurely family jogging.

Acknowledging the findings, conclusions and educated hypotheses of the authors in this review regarding synchronisation, the current prescription system appears to fall some way short of basic expectations and in many cases must be providing amputees with what can only be termed as the incorrect category of foot. It is in this area that the most important fundamental research must take place; putting science, logic and reasoning around how and why feet are prescribed. Hafner et al. write:

*'While the performance of the prosthesis will always be a vital component of prosthetic design, the ultimate goal will always be the optimum performance and health of the amputee.'* (Hafner et al. 2002, P6)

This means at the most fundamental level providing them with the correct prosthesis for their body and their desired activity.

Papers that discuss and investigate the dynamics of running feet during use are few. Evidently this is an area of limited research, but progress appears to be hampered by diverse approaches to understanding the problem. Results are varied with no definitive questions answered to aid the prosthetist. However, strong links between driving frequency and the resonant modes of the prosthetic system are suggested and investigated on a hypothetical basis by some authors (most notably Lehmann et al. 1993; Lechler et al. 2008; Noroozi et al. 2012a,b, 2014).

One particular area of foot dynamics that is briefly mentioned by only a single paper (Dyer et al., 2013) is that of the changing boundary conditions; the shifting of the ground contact point along the distal portion of the foot. If a single stride is examined, following foot strike, the tibia (in the case of an intact limb) progresses over the foot (tibial progression). This motion naturally transfers the weight of the runner from the extremity of the heel forward to the toe, until the foot leaves the ground (toe-off). This is demonstrated in figure 1.5.

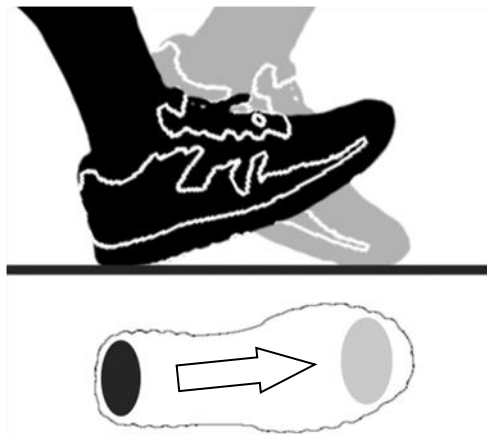


**Figure 1.5:** Projected ground contact point progression throughout a single stride on an unaffected leg.

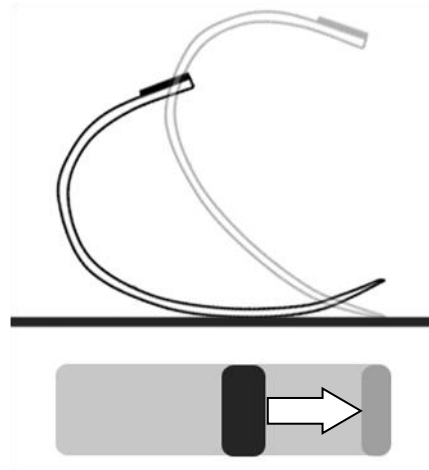


**Figure 1.6:** Projected ground contact point progression throughout a single running stride on an ESR running foot.

The same principle can be observed in an ESR running foot (for example with an Ossur Flex Foot). In this instance the lack of a heel means the initial ground contact point is with a posterior portion of the foot. As tibial progression occurs it is reasonable to suggest (and observable) that the ground contact point alters through to toe-off. This is demonstrated in figure 1.6. Given that the shank of the foot remains attached to the prosthetic socket at all times but the distal contact point changes, the spring rate of the foot must change as the length of the effective lever arm increases. The further rearwards (posterior) the contact point with the ground, the higher the spring rate must be. Conversely the effective stiffness decreases as the ground contact point progresses forward onto the toe.

This suggests that the spring rate of a foot is dependent on the running style of an individual. Even assuming straight level running, if the runner takes shorter strides or has a more digitgrade ('on the toes') characteristic set by the prosthetist, the ground contact will be different to that of a more relaxed user and thus a different spring rate variation will result.

Therefore this research sets out to investigate and add new knowledge on the dynamic characteristics of ESR prosthetic feet. What factors are important when prescribing a foot, and how do these factors interact with each other and the amputee? The

phenomenon of system resonance and the matching of driving oscillatory frequency is mentioned by a number of authors and this will be investigated in detail. Fundamentally, can the dynamic function of such a prosthetic device be understood, characterised and used to advise prosthetists when ascribing a category of foot to an amputee?

## CHAPTER 2: RESEARCH METHODOLOGY & PLAN

### 2.1 Research Questions

The literature review has identified what research has been carried out to date and where the areas for further work exist. As a result of this a research question was defined with a series of following sub-questions to assist in defining the most appropriate research objectives. It is by asking these questions that this work aims to most significantly add to the available knowledge of prosthetic running feet. The primary research question is stated below with the sub-questions detailed in the following sections:

***‘Is the current method of prescribing prosthetic ESR running feet (based on mass alone) appropriate and are there additional factors that should be taken into consideration?’***

Feet are currently prescribed according to the mass of an amputee with little or no consideration for other factors such as height, stride length or the intended running velocity of the amputee. This research intends to understand if this is an appropriate approach or if there are additional factors that could be taken into account that would benefit the prescription of suitable prosthetic devices and therefore the user experience of amputee athletes.

#### 2.1.1 Sub-question 1: What are the mechanical characteristics of a prosthetic running foot?

There is a wide disparity in figures published to date surrounding the efficiency of energy return of prosthetic running feet. It is not understood why this disparity exists and which figures are to be considered accurate. This research should identify what has caused these discrepancies and what the most appropriate testing method should be for such devices. What foot characteristics are important in amputee running and how can these be measured/ tested such that the future design of prosthetic feet can be advised.

### 2.1.2 Sub-question 2: Is the claim that a foot mimics Simple Harmonic Motion legitimate?

Authors have previously suggested that the action of a prosthetic foot follows the laws of Simple Harmonic Motion but no work has been conducted to validate this claim to date. If this is a realistic concept, the response characteristics of a prosthetic foot could be ascertained theoretically thus potentially allowing a more specific prescription for an amputee.

### 2.1.3 Sub-question 3: Can the action of a prosthetic running foot be modelled mathematically?

If the action of a foot could be modelled across a range of speeds this could be used to advise the prosthetist what foot is most suitable for an amputee, or advise the amputee how best to use a specific category of foot. Perhaps the limitations of a specific foot can be highlighted at an early stage rather than the 'trial and error' process that has been suggested previously (Strike & Hillery 2000, P.606).

### 2.1.4 Sub-question 4: Can the prescription of feet be changed such that the user experience of active amputees is improved?

The ultimate goal of any research concerning prosthetic feet is to improve performance and therefore user experience. If the current prescription methods employed by prosthetists can be shown to be lacking in any particular aspect, how can this be improved and what future work should be conducted to ensure a more specific and suitable prosthesis for an amputee?

## 2.2 Research Methodology

### 2.2.1 Qualitative vs. Quantitative Research

The research described in the literature review was carried out almost solely in a quantitative manner. Some studies have commented on user feedback in terms of self-selected running speeds (Czerniecki 2005; Hansen et al. 2004; Lehmann et al. 1993a,b) and others use qualitative measures for judging the suitability of participants for testing, for instance evaluating levels of comfort (Biswas et al. 2010). However the overwhelming majority of research in the field of prosthetic characterisation and running dynamics is carried out through quantitative measurement of specific variables. This is often conducted using equipment such as force plates (Arampatzis et al. 1999; Bruggemann et al. 2008; Lehmann et al. 1993a,b; Torburn et al. 1990; Wilson et al. 2009), high speed video capture (Strike et al. 2000; Hunter et al. 2005, Bruggemann et al. 2008; Grabowski et al. 2010) and reflective marker technology (Bruggemann et al. 2008; Lechler 2005; Torburn et al. 1990; Wilson et al. 2009). This methodology is appropriate but is perhaps limited at times by the specific artificial environment demanded by the measurement techniques.

To re-iterate section 1.3 the research objectives of this work are:

- To define the mechanical characteristics of a specific prosthetic running foot including spring rate and energy return efficiency.
- To measure, understand and explain the action of a prosthetic running foot when in use across a range of running velocities.
- To replicate the action of an amputee runner in a laboratory environment and manipulate variables to demonstrate the application of Simple Harmonic Motion.
- To define what limitations a prosthetic foot imposes on running performance.
- To suggest an alternative and improved method of running foot prescription based on the work conducted.

Following on from the majority of literature studied throughout the course of this research, the requirements of defining and understanding mechanical characteristics and running action fundamentally drives a quantitative research method. The above objectives all involve scientific measurement of specific variables and subsequent evaluation/replication of these variables in a laboratory environment. It is intended that the laboratory work be carried out without a human participant (for instance using a dynamic hydraulic test machine to ascertain foot spring efficiency) and as such a quantitative measurement approach is valid.

When testing with human participants (as is the intention for a portion of this research project) there should always be a qualitative element. This ensures suitability, comfort and safety of the participants and to aid this (and in line with research best practice) ethical approval was sought prior to testing. The approved ethics forms can be found in the appendix (Chapter 11, section A5.2) and considers the age, disability level, privacy and wellbeing of the participant.

Hafner et al. (2005) conclude their studies of the clinical prescription methods by writing:

*'Researchers must consider revising the test environments under which these prosthetic components are evaluated' (Hafner et al. 2005, p.9)*

And further:

*'Propelling research to match real-world environments such as stairs, hills, and uneven terrain may serve to better drive clinical prescription of prosthetic feet.'*  
*(Hafner et al. 2005, p.9)*

As such, quantitative measurement techniques proposed for this research include those mentioned above (force plates, high speed camera apparatus) as well as additional fabricated measurement devices suitable for data capture of specific variables over uncontrolled terrain. The specific measurement devices and methods are detailed in the chapters that follow and focus on a purely quantitative approach.

To conclude, it is proposed that this research take on a purely quantitative research approach with the exception of that which involves the human element. It is imperative that the wishes, comfort and on-going wellbeing of the individual are taken into account before, during and after testing and qualitative appraisal must be conducted. However this appraisal is not anticipated to form the backbone of the research. Whilst subjective feedback and advice from participants will no doubt advise the direction of the test work (to some extent) it is the data gathered from these various tests that shall be used to achieve the objectives defined in section 1.3.

### 2.2.2 Design of Experiments Methodology:

It is intended that each of the experiments to be carried out throughout the course of this research project be done according to best practice and in line with the principles set out by Ronald Fisher (Fisher, 1935). As such, particular attention shall be paid to the following factors:

- What and how many variables are being recorded?
- What control measures should be included?
- What resolution is required of these variables?
- How can they be recorded or measured?
- What frequency should they be recorded at?
- Dependant or independent variables?
- What external factors might affect accuracy and repeatability of the results?
- Should the participant be blind to the variables being measured?
- What is the sample size and is this sufficient to be representative?

The literature review in Chapter 1 has highlighted the variation in both measurement techniques and results for comparable tests. The adoption and careful application of these principles as well as the control of boundary conditions during the design of the experiments should serve to both improve accuracy and repeatability of the various investigations.

## 2.3 Chapter Summary

This thesis is split into 10 chapters and it is the purpose of this section to give the reader an overview of the contents of each. The chapters have been written to each cover a single manifold area of the research, each with clearly defined research objectives and conclusions that lead onto the following chapter. They are arranged in a logical and largely chronological order such that the story can be followed from the initial research questions (section 2.1) through to the final conclusions, discussion and suggestions of further study (Chapter 10). Contained in this section are summaries of each chapter and the rationale for the research contained within.

### 2.3.1 (Chapter 3): Static Characterisation

The objective of this chapter is to replicate the work conducted by previous authors in the field of foot characterisation, explain the disparity in results and aid in further understanding key factors in prostheses characterisation. This is carried out by slow-deflection testing of an Ossur Flex Run (Cat.6Hi) (Ossur, Iceland) prosthetic device in an Instron hydraulic test machine with various foot contact conditions. The true efficiency of the foot is calculated and the spring rate & linearity is stated. A new method for testing feet is defined and this technique is utilised throughout the rest of the project.

### 2.3.2 (Chapter 4): Dynamic Characterisation

This chapter defines typical input conditions for foot testing at representative velocities by measuring the relevant variables during amputee running. A sensing system was developed that could be worn by an amputee and was capable of collecting typical running data for foot deflection (amplitude, timing, rate) and ground contact point (along the base of the foot). The data gathered is averaged to define a single, typical, stride and this information was used to replicate the characterisation tests undertaken in Chapter 3 but with representative input conditions (displacement velocity & ground contact points).

### 2.3.3 (Chapter 5): Bringing Running into the Laboratory

If foot testing can take place in a laboratory environment without the use of an amputee volunteer, multiple conditions can be investigated without introducing variables (and the variability) associated with human participants. Therefore the aim of this chapter is to define, design, fabricate and calibrate a test rig onto which a prosthetic running foot can be mounted. The resulting rig can then be validated against the recorded data obtained during amputee running in Chapter 4. Using this rig it is possible to investigate the effects of modifying input conditions on foot response.

### 2.3.4 (Chapter 6): Changing SHM Variables on the Rig

Previous research work has suggested that a prosthetic foot dynamically mimics the action of Simple Harmonic Motion. This chapter aims to understand if this is legitimate by using a rig to simulate the action of an amputee runner. Each of the variables occurring in the equation for SHM (mass & stiffness) is modified in turn across a broad spectrum and the foot response measured.

### 2.3.5 (Chapter 7): Amputee Testing & the Effect of Speed Variation

The aim of Chapter 7 is to understand what effect running velocity has on the dynamic response of a prosthetic foot. All previous amputee testing was conducted at a single running speed and data was recorded and replicated in a laboratory. The same variables are again recorded (foot displacement, stride timing, ground contact progression) but additional information is gathered at a variety of running velocities. This chapter demonstrates that the stiffness of the prosthetic leg has the ability to limit the running speed attainable by the amputee.

### 2.3.6 (Chapter 8): Characterisation of Foot Categories

If a useful mathematical model is to be developed that describes running for a range of amputees, the role of the available foot categories should be understood and therefore characterised. The aim of this chapter is to define the meaning of the foot categories available for the Ossur Flex Run in a tangible manner. The entire range of

these feet was tested in an identical manner to the device described in Chapter 3 thus characterising each of the categories in turn.

### 2.3.7 (Chapter 9): Can the Action of a Foot be Modelled Mathematically?

The ultimate goal of this research project was to understand if the current prescription process is adequate. If a mathematical model can be developed that describes amputee running (as defined in the previous chapters of this thesis) the output can be compared with the current prescription method and discussed. A flowchart is developed that assembles the new knowledge into a congruent concept with a tangible output that can be measured and understood by both the prosthetist and amputee; stance length. Each of the contributing elements are examined separately and discussed and it is shown that the response time of the foot during running should not be predicted using the theory of Simple Harmonic Motion alone.

## CHAPTER 3: STATIC CHARACTERISATION

### 3.1 Introduction & Chapter Objectives

As mentioned in the literature review (Chapter 1) the static rating of prosthetic running feet has previously been conducted by authors of existing academic papers. The most notable work into foot dynamics has been carried out or summarised by Bruggeman et al. (2008), Nolan (2008), Geil (2001), Noroozi et al. (2012a,b, 2014) and Lehmann (1993a,b). Throughout these works particular attention was paid to the efficiency of energy return for the prosthetic foot on test, but figures generated vary dramatically. For example energy return rates for a composite ESR running foot are quoted as being 100% by Buckley (2000) whilst Nolan (2008) presents data suggesting an energy return of 63% for the same model of foot (an Ossur Cheetah). The wide discrepancies in these results would suggest either some degree of measurement error or inconsistent measurement techniques.

If a reliable understanding of the dynamic action of a foot is to be understood, these static rating methods should first be interrogated and testing repeated in a reliable and robust manner. The principle of comparing amputee running with a spring – mass system is a recurring theme when the associated literature is reviewed. The stiffness of the spring (or in this instance the prosthetic device) is fundamental to the frequency response of the system. Establishing a reliable figure of energy input versus return will also advise future research intended to improve the efficiency of amputee running.

The purpose of this chapter is to evaluate the work conducted previously by other authors, understand the reasons for the apparent discrepancies in results and to define an effective manner of characterising a prosthetic running foot. This test method can then be carried through into the following research chapters to ensure accurate and repeatable results.

## 3.2 Mounting Methods for Static Testing

### 3.2.1 Mounting Methods Shown in Existing Published Papers

The approach taken throughout the majority of this previous work has been to mount the prosthetic foot under test rigidly in a dynamic hydraulic test machine or to a sliding mass and exercise it vertically. The proximal end (shank) of the foot is mounted rigidly to the actuator or mass with the distal end free to slide on the ground surface of the machine. Usually this interface is aided by incorporating a low-friction material to allow the toe to slide against the ground plane as dictated by the geometry of the foot.

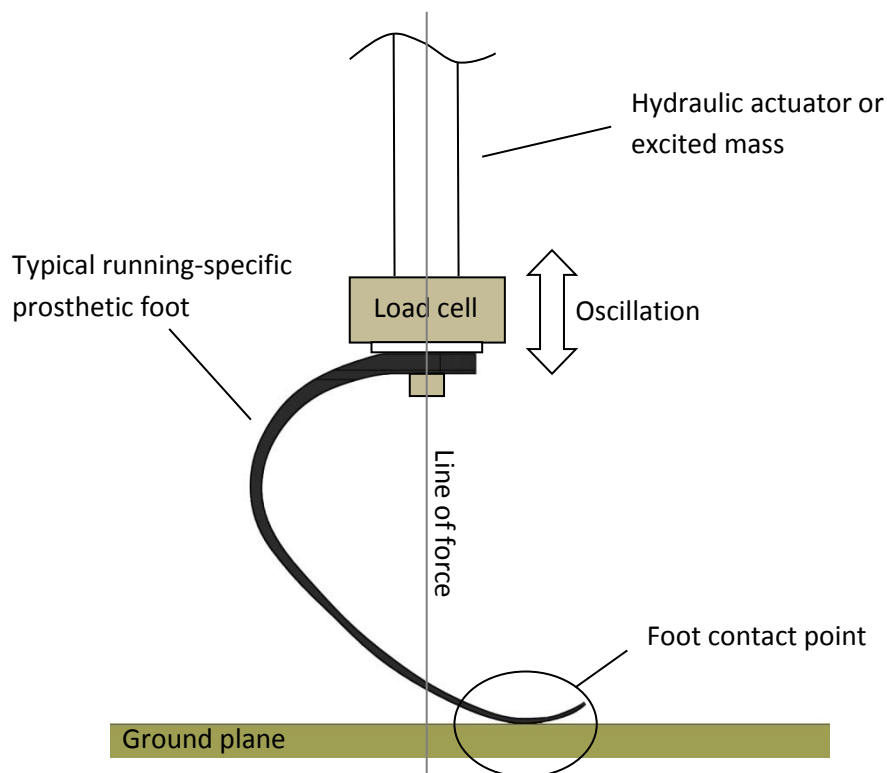


**Figure 3.1a:** Pictorial representation of ESR foot mounting strategy for previous investigations into static spring rate and efficiency of energy return.

Displacement data is collected from a linear transducer and ground force from a load cell located either between the proximal end of the foot and the actuator or under the toe of the foot. A pictorial representation of such a setup is shown in figure 3.1a and can be expressed as an illustration or free-body diagram (figure 3.1b).

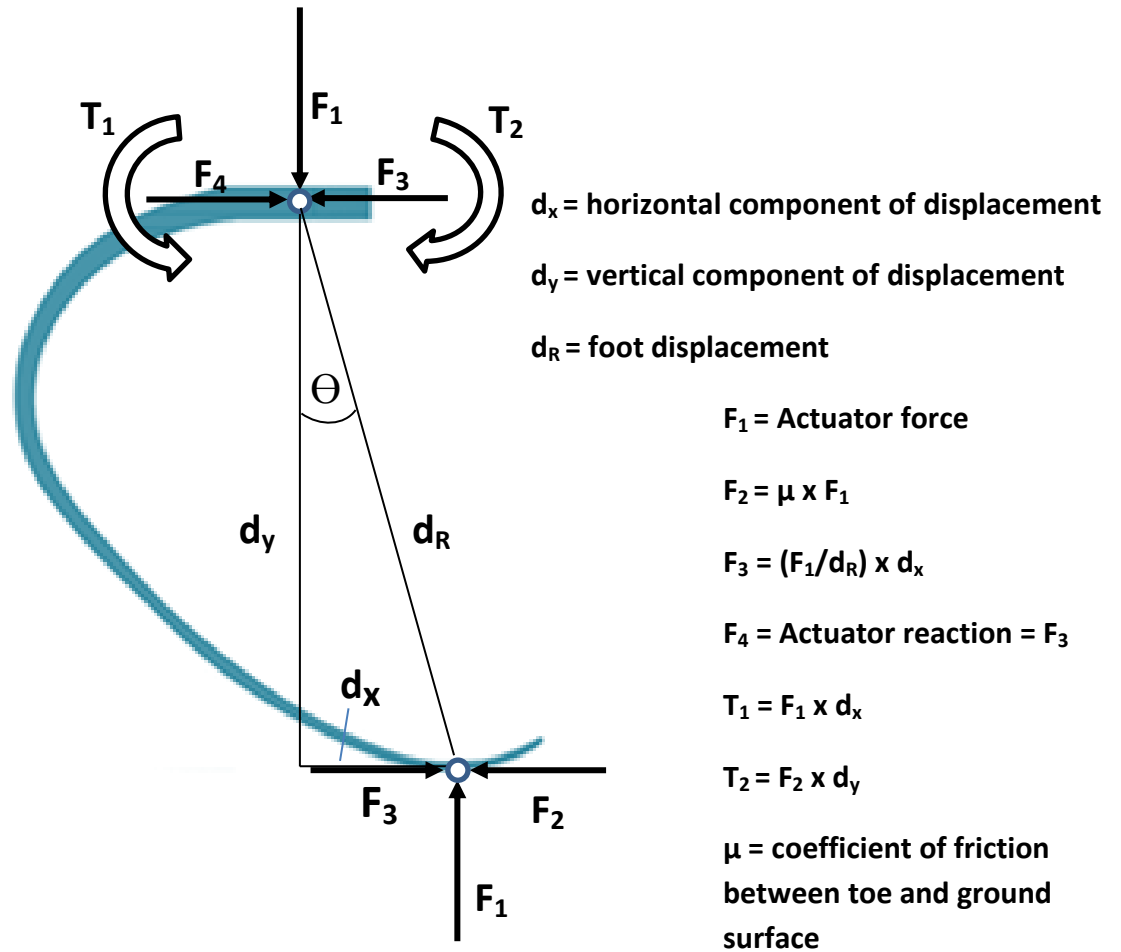


**Figure 3.1b:** Free body diagram of ESR foot mounting strategy for previous investigations into static spring rate and efficiency of energy return.

The test engineer then has to define the maximum amplitude of displacement and rate of deflection for the foot on test (particularly those testing using a programmable forced-displacement machine such as a hydraulic test rig where these parameters are required by the controller). From the data collected a force - displacement curve can be generated for both the compression and rebound phases resulting in a spring rate and hysteresis loop. Some papers (Geyer et al. 2004; McGowan et al. 2012) have suggested testing the foot 'dynamically' but it is not explained what dynamic motion means in this context.

### 3.2.2 Mounting Strategy Analysis

If the foot setup (as shown in figure 3.1a) is examined, it can be seen that the point of ground reaction is not in line with the input force from the actuator (or mass). This offset nature results in components of the force which can be defined as a function of foot geometry and is manifested as both a vertical and side load on the actuator.

These two components are reacted equally and opposite at the ground contact point (figure 3.2). Furthermore as the foot is deflected, the geometry naturally changes (as the foot is progressively loaded). This change in shape is illustrated by figure 3.3.

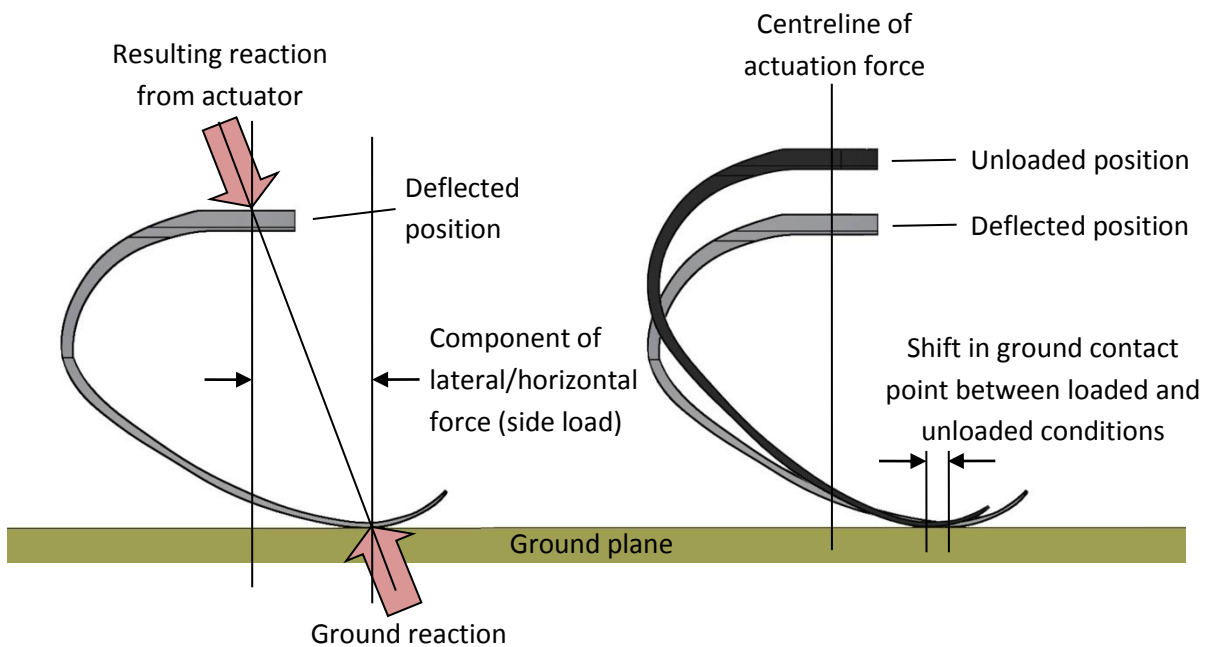


**Figure 3.2:** Illustration of the resulting reaction forces of the foot once a load is applied. The force can be divided into vertical and horizontal components as a function of geometry.

**Figure 3.3:** Illustration of the change in shape of a typical ESR prosthetic foot when load is applied and the foot is subjected to deflection.

As the shank of the foot is traditionally limited to purely vertical motion by the actuator and no rotation of mounting is permitted (the shank remains parallel to the ground plane at all times), the geometry of the foot exerts a lateral force at the toe. This lateral force is reacted by the friction between the toe and the ground plane meaning that longitudinal tension is built up in the foot. There are then two possible conditions:

1. The longitudinal forcing levels at the toe exceed the friction between the toe and the ground plane and the toe slides, thus shifting the ground contact point forwards. This is described in figure 3.4. The result of this is that the side load experienced by the actuator will momentarily diminish but the distance from the centre line of actuation force and the vertical line of ground reaction is increased.

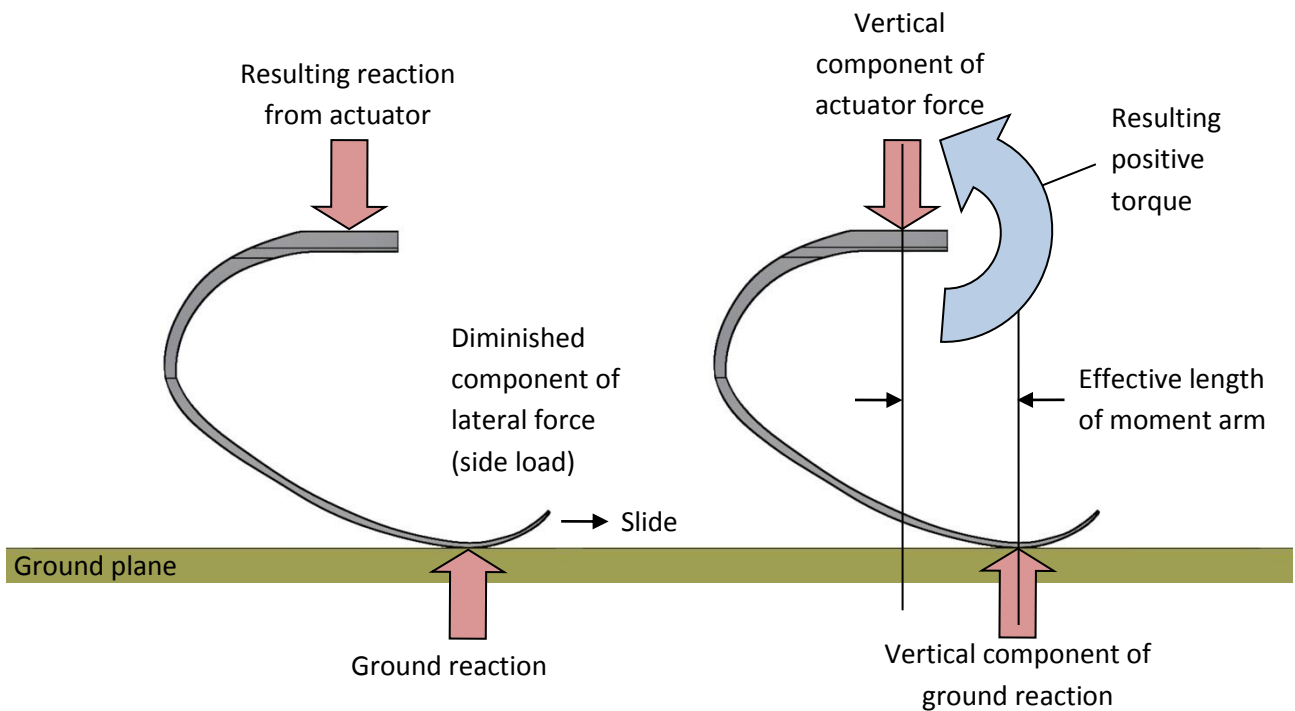


**Figure 3.4:** If the toe is allowed to slide the lateral component of the ground reaction force will be diminished according to the friction present between the toe and ground.

**Figure 3.5:** The resulting geometry and vertical component of ground reaction force will invoke a positive torque at the foot shank (viewed in the sagittal plane from the right).

This in turn will have two effects depending on the level of friction experienced at the toe.

- If friction is high, the increased distance between reaction lines will exaggerate the side load that exists at the actuator (by increasing the lateral component of the force shown in figure 3.2 and assuming an adequate reaction at the toe).
- If friction is low, the side load at the actuator will remain diminished. However for any given geometry and assuming the toe is moving freely against the ground plane, the foot becomes a lever arm with an effective length equal to the distance between

*reaction lines. This exerts a torque at the shank which translates into the actuator and can be seen in figure 3.5.*

Most likely a combination of these two effects will occur, exerting a lateral force and positive torque at the actuator (when viewed in the sagittal plane from the right hand side). Low-friction materials have been used in previous studies in an attempt to allow the toe to slide freely against the ground plane (Geil 2001).

---

2. The longitudinal forcing levels at the toe do not exceed the friction between the toe and the ground plane, preventing the toe from sliding. Once again the shank of the foot is rigidly fixed to the actuator and is only permitted a vertical motion but in this instance the toe is effectively fixed to its position on the ground plane. As described in figure 3.4 the geometry of the foot would ordinarily dictate that the toe position moves but in this instance the assembly is heavily constrained.

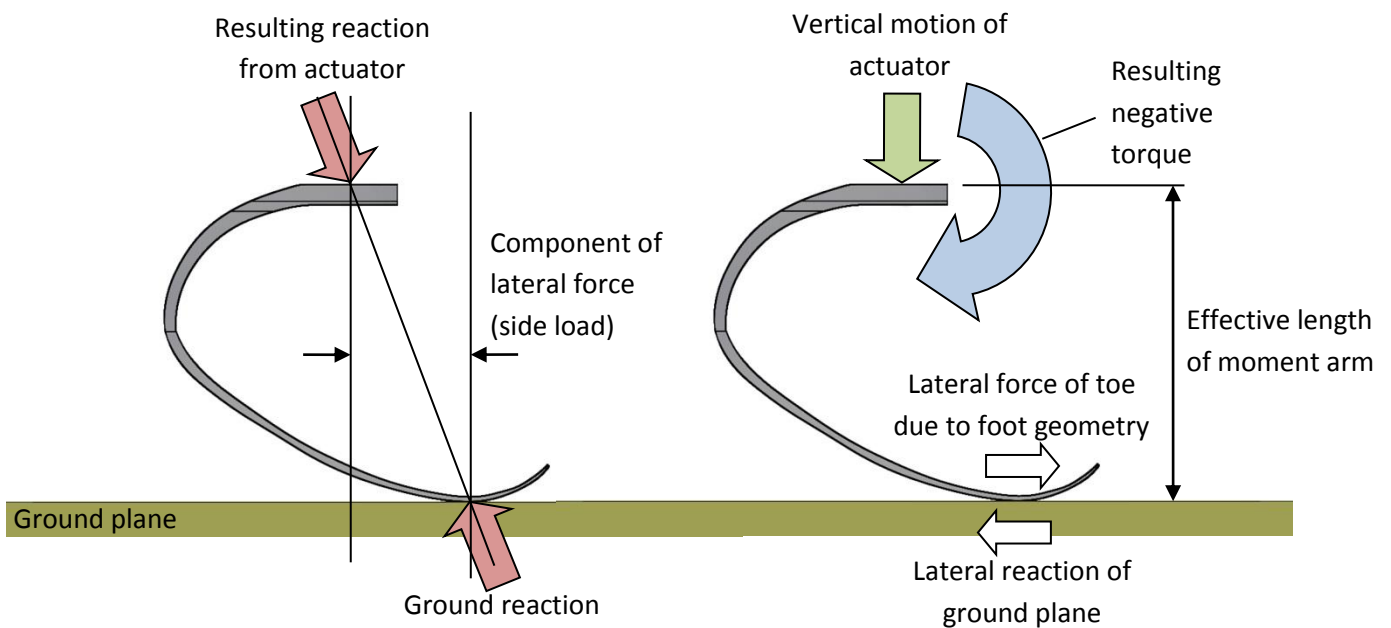


**Figure 3.6:** If sufficient friction exists between the foot and ground plane to prevent the toe from sliding the ground reaction components will remain, according to the foot geometry.

**Figure 3.7:** The friction that exists at the toe will provide a reaction force for the change in geometry of the foot (as displacement occurs) exerting a negative torque at the shank.

The actuator is again subjected to a side load proportional to the lateral component of the force (illustrated in figure 3.6), but in this instance the side load is not diminished as the toe cannot slide against the ground plane (as in figure 3.4).

In addition to this side load a negative torque (viewed in the sagittal plane from the right hand side) is exerted on the shank of the foot, again translated into the actuator that is rigidly attached. As previously mentioned and shown in figure 3.4, as the foot is loaded the geometry naturally exerts a force at the toe (due to the geometry of the foot). As this cannot occur due to friction, the ground plane reacts this force which is

manifested as a negative torque at the point where the foot attaches to the actuator. The moment arm for this torque is of a length equal to the distance of the shank above the ground plane (shown in figure 3.7) and is therefore inversely proportional to the deflection of the foot; as the foot is progressively displaced the lever arm reduces in length but the friction-derived lateral forcing level at the toe increases.

### 3.2.3 Conclusions of Foot Mounting Methods

It is clear from examining the mounting methods used previously that the actuator is subjected to significant side loads and torques as the foot is displaced. Depending on the nature of the foot interface with the ground plane the resulting friction could mean a positive or negative torque at the shank of the foot, or more likely a combination of the two at different amplitudes of deflection. The resulting forces and torques described in this section are not likely to be mutually exclusive and each of the factors described will occur with any such foot installation. For example, even if a low-friction substrate were located between the toe and the ground plane, a small amount of friction will inevitably occur. This will result in a negative torque as described in figure 3.7, but this will be added to a positive torque as described in figure 3.5.

Any restriction placed on the foot that reacts against the natural geometrical changes that occur due to displacement (for example friction at the toe) will result in an abnormal shape being forced on the foot. This is particularly apparent if the friction at the toe is greater than the lateral force, and it is a result of the shank being rigidly attached to the actuator. This abnormal strain being applied to the foot will theoretically, to an extent dependant on the level of friction at the toe, affect the spring rate of the foot. In addition the force required to overcome the friction (in the mounting instance described in figure 3.4) will affect the spring rate in a manner that will only be apparent on the compression phase of a full cycle. A different level of forcing will be apparent on the rebound phase and this disparity has the potential to significantly affect the recorded hysteresis values (and therefore measured efficiency) of a foot being tested.

Furthermore, despite the contact point between the toe and the ground plane moving forwards relative to the ground during progressive displacement of the actuator, if the end of the toe is used as the reference the point of contact actually moves rearwards. This directly contradicts what is observable during running and what is described in figure 1.6. The relevance of the ground contact point (relative to the end of the toe) is the topic of discussion later in this report and the consequence of this point moving rearwards during loading in a fixture shall be addressed.

Quantifying the discrepancies between these mounting methods is the subject of the following investigation. Using what is learned from these results, a practical and repeatable mounting method is specified for the purpose of defining the characteristics of prosthetic running feet.

## 3.2.4 Reproducing Previous Static Rating Test Methods

### 3.2.4.1 Theory

If a prosthetic ESR running foot were mounted in the manner described above and as in previous journal papers (Bruggeman et al. (2008), Nolan (2008), Geil (2001), Noroozi (2012a,b, 2014) and Lehmann (1993a,b)) in a dynamic hydraulic test machine (with the shank rigidly attached to the actuator), values for foot efficiency and hysteresis can be defined through collecting force - displacement data.

However in order to understand the relevance of the ground contact condition the level of friction between the toe and ground plate should be modified as a variable. Previous studies have reported foot efficiency values of between 63% and 100%. If a different level of friction existed between the toe and ground plane for these various investigations then this could explain the disparity in reported efficiency values. It is not yet understood how varying the friction affects the magnitude of the efficiency results and if it can do so by such a large margin. This investigation serves to further our understanding of the effectiveness of a rigid shank-actuator mounting mechanism for foot testing and the possible pitfalls of such an approach.

### 3.2.4.2 Method

An unused Ossur 'Flex Run' Cat6Hi prosthetic running foot was mounted in an Instron 8872 hydraulic test machine. This was done by rigidly attaching the foot with an M12 fixing to the load cell of the machine (attached to the actuator) and allowing the metatarsal region of the foot to contact the ground plane. In order to define input conditions for the testing, an amputee athlete was observed (subject to the relevant ethical considerations and approval as discussed in Chapter 2 and available in the

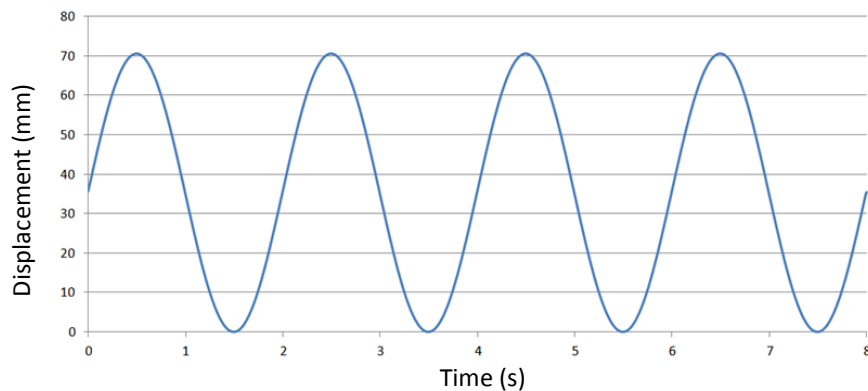


**Figure 3.8:** Typical displacement cycle of prosthetic foot under test displacing 70mm at a frequency of 0.5Hz.

Appendix) using an identical Ossur Flex Run foot to that on test. The manufacturer recommends that the amplitude of deflection should be between 1 and 2 inches on average. However when the amputee athlete was observed it was clear that the amplitude of deflection of his foot exceeded this maximum value, despite the foot having been prescribed by a qualified prosthetist in accordance with the manufacturer's instructions. In order to account for this overshoot of deflection and in the absence of more accurate data a maximum deflection of 70mm was chosen. At this stage of the investigation (and given the inevitable variation in foot deflection that will occur for different athletes) this value was judged sufficient to establish baseline characterisation information. Therefore the foot was displaced 70mm in a series of sine-wave oscillations. An oscillation frequency of 0.5Hz was chosen to simulate a static loading condition and force-displacement data was collected.

The driving oscillation wave is shown in figure 3.8 and a typical foot set up is shown in figure 3.9 in unloaded and at maximum deflection conditions.

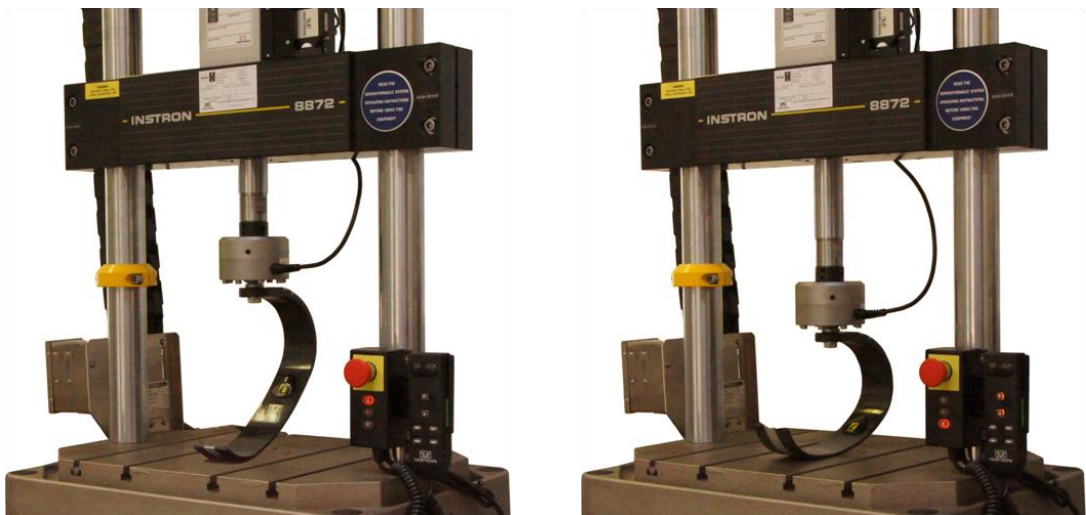


**Figure 3.9:** Typical foot setup in the Instron 8872 hydraulic test machine, shown at zero and maximum deflection (70mm). The ESR foot is rigidly mounted to the load cell attached to the actuator and the metatarsal region of the foot is directly in contact with the ground plane.

In order to further understanding of the role of ground friction, the interface of the foot with the ground plane of the machine was modified with solutions that varied the friction between the two surfaces. Each of these conditions is described in figure 3.10. These friction conditions are undefined in terms of their coefficient but for the purpose of this investigation they serve to demonstrate the trend of variability of the deflection results for different boundary conditions.

Force, displacement and time data for each of these conditions was captured using Instron DAX software. The data was then averaged using Microsoft Excel for the centre three oscillation cycles of each displacement phase (as shown in figure 3.8) to create a single representative displacement cycle.



**Condition 1: Low friction**

Bearing rollers were attached to the metatarsal region of the foot to simulate a virtually friction-free condition.

**Condition 2: Medium friction**

The carbon fibre surface of the foot was allowed to contact the cast iron bed of the test machine directly. No lubrication was added and the bed was clean and dry.

**Condition 3: High friction**

A proprietary running sole from Nike (Nike Inc.) designed for the foot on test was fitted as per the manufacturer's instructions to provide a high-friction condition.

**Condition 4: Ultra-High friction**

A sheet of ultra-high friction polymer material was placed between the foot and the bed of the machine. This material made slippage of the toe almost impossible when deflected.

**Figure 3.10:** Description of the various foot contact conditions that were used to alter the level of friction between the metatarsal region of the ESR prosthetic foot and the bed plate of the Instron test machine.

### 3.2.4.3 Results

The force - displacement data was averaged for each test condition and a hysteresis curve was generated for each. Condition 3 (using the Nike proprietary running sole) proved problematic as the lateral force exerted through the toe threatened to destroy the clipping system used to attach the sole to the metatarsal region of the foot. This is demonstrated in figure 3.11. Given that this foot sole designed to be used with the specific foot on test, this serves as a demonstration of how unrepresentative these test conditions are of amputee running. This test was aborted and results only generated for test conditions 1, 2 & 4.



**Figure 3.11:** Lateral force exerted through the foot threatened to destroy the fastening cleats of the proprietary running sole.

The efficiency of each test condition was determined by calculating the areas under the respective curve of the hysteresis graphs. This was done for both the compression and rebound phases of the displacement cycle. The value of hysteresis is defined as:

$$\text{EFFICIENCY \%} = \frac{\text{COMPRESSION PHASE ENERGY}}{\text{REBOUND PHASE ENERGY}} \times 100$$

Force – displacement graphs for each test condition can be seen in figures 3.12, 3.13 & 3.14 and table 3.1 gives an overview of the performance of each.

**Condition 1:** Low friction: 97% efficiency

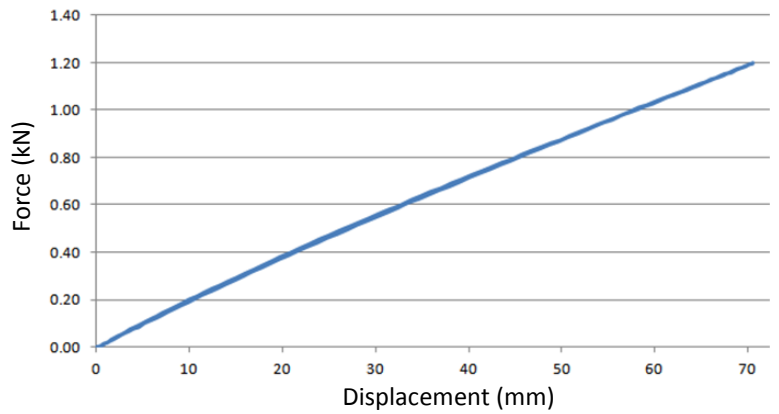
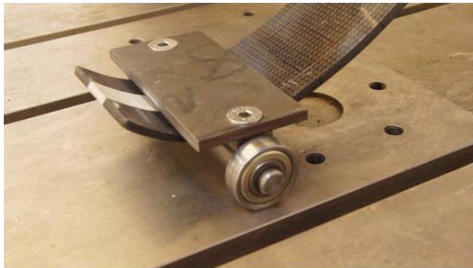


**Figure 3.12:** Hysteresis curve of the low friction condition. The efficiency can be seen as close to 100%.

**Condition 2:** Medium friction: 86% efficiency

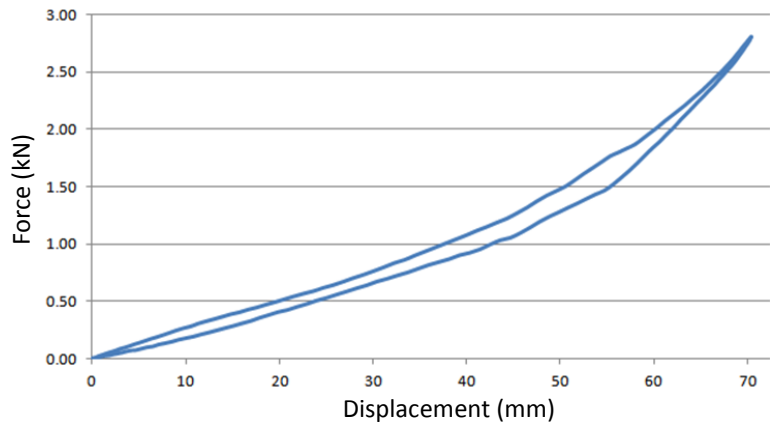


**Figure 3.13:** Hysteresis curve of the medium friction condition. Efficiency is reduced with an exponential spring rate trend.

**Condition 4:** Ultra-high friction: 71% efficiency

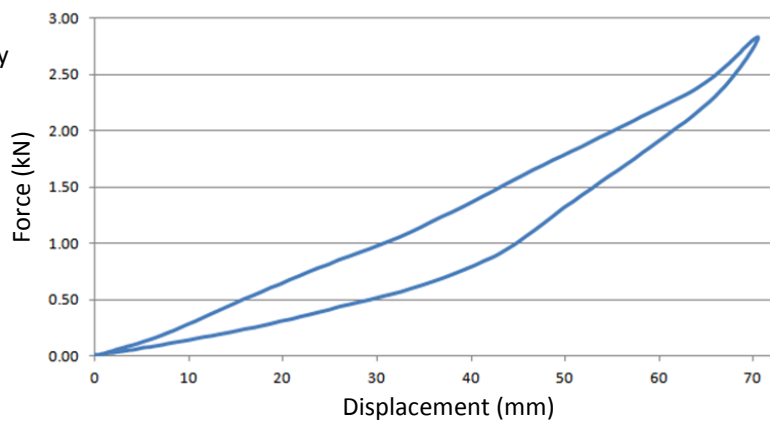


**Figure 3.14:** Hysteresis curve of the ultra-high friction condition. Efficiency is dramatically reduced over conditions 1 and 2.

	Peak displacement	Driving frequency	Peak force	Efficiency
Condition 1	70mm	0.5Hz	1.20kN	97%
Condition 2	70mm	0.5Hz	2.81kN	86%
Condition 3	<b>Aborted</b>			
Condition 4	70mm	0.5Hz	2.83kN	71%

*Table 3.1: Performance overview of each condition*

As can be seen in table 3.1 the efficiency values vary considerably across the test conditions. An interesting additional observation is the reaction force exerted by the foot at maximum deflection. For both of the conditions that involved restriction of the toe (with a friction element included in the setup) the peak force is similar at 2.8kN. However condition 1 was unrestricted and demonstrates a peak force of less than half that of conditions 2 and 4 at 1.2kN.

The reason for this disparity in peak force is the geometry of the test setup. As the foot deflects, the toe region exerts a force in the anterior direction (this is described in figure 3.3). Condition 1 features rollers to allow the free sliding of the toe region of the foot against the ground plane therefore not allowing any reaction force to act against this anterior force. To compound this effect the geometry of the foot is such that as the foot deflects the rollers move away from the centreline of the actuator. This results in lower amplitude of deflection of the foot for any given amplitude of the actuator.

A further observation is that test conditions 2 and 4 encouraged an exponential spring rate whereas test condition 1 demonstrated a near-linear rate. This is a result of the changing ground contact point of the foot relative to the toe (described in section 3.2.3). As can be seen in figure 3.9 the contact point shifts significantly rearwards (away from the toe) as deflection increases therefore shortening the effective lever arm of the foot and progressively increasing the rate. Condition 1 features a controlled ground contact point in that the rollers are in a fixed position on the foot. The effective lever arm of the foot therefore remains static and results in a near-linear spring rate.

### 3.2.4.5 Conclusions

This investigation has shown that mounting the foot in a variety of ways can change the apparent efficiency of the device. Despite identical input conditions the disparity in results is significant. There is a variation in efficiency of 26% and in reaction force of over 1.6kN by purely changing the interface condition of the toe with the ground plane of the test machine.

It is clear that if the ground contact condition is not controlled, the accuracy of data obtained from the foot when undergoing tests of this nature can be brought into question. If the toe is required to slide against the ground plane, any element of friction will introduce a value of hysteresis. It is important to note that the inefficiency measured throughout this investigation is as a result of energy dissipated at the toe interface. Not as a result of the characteristics of the foot itself. When rollers were introduced (therefore effectively eliminating friction at the toe in condition 1) the efficiency of the foot was measured at over 97%.

A further observation is that of the change in ground reaction force. Due to the geometry of the foot the toe exerts a lateral (when viewed in the sagittal plane) force (see figure 3.3). When a high-friction material was placed between the toe and the machine bed the foot was able to react against this and exert a higher load into the actuator (and therefore load cell). In the instance of the rollers no such reaction force was possible and the measured load was significantly reduced. Furthermore as displacement was increased this condition was exaggerated due to the geometry change of the foot.

Fundamentally this effect is driven by the offset from the centreline of the actuator and that of the ground contact point. The greater the value of the offset that exists, the greater the component of lateral force meaning a smaller vertical component (if the toe is mounted on rollers and therefore unable to react this lateral force). In order to control this variable and remove any lateral component for future testing the centreline of the actuator and the ground contact point should be aligned, regardless of foot deflection. This would also eliminate any torque acting on the load cell.

This testing has shown that the mounting of the foot, even for a simple displacement test, is fundamental to achieving repeatable and reliable results. If a foot were mounted in such a manner as described above on two consecutive days, it is possible that the level of friction will be different (due to contamination, humidity in the air or ambient temperature) and results will not be comparable. Also the ground contact point is undefined and unrealistic when compared with an amputee using the foot for running. This investigation suggests that if further testing is to be conducted using a rig-mounted foot the following mounting conditions must be satisfied:

- There must be effectively no friction at the mounting interfaces to dissipate energy
- The centreline of the actuator must always align with the ground contact point

The work carried out in this section is not intended to replicate running or to allow comparison with the action of a foot when used by an amputee athlete. It was designed instead to characterise the static deflection properties of a prosthetic device and to understand why authors conducting similar work previously came to such varied figures of foot efficiency.

### 3.3 Development of Mounting Fixtures

In order to avoid the complications of the changing boundary conditions as discussed in section 3.2.3 a mounting strategy was devised that allowed a single rotational degree of freedom at each end of the prosthetic foot (figure 3.15). Instead of the foot being rigidly mounted to the load cell the shank was allowed to rotate about its axis (when viewed in the sagittal plane) on a pair of fulcrums (figure 3.16) and the same was permitted of the toe interface (figure 3.17).



**Figure 3.15:** Testing fixture CAD design (left) and fabrication (right)

A steel cradle was designed and fabricated with a clamping bracket that could be attached at any point of the metatarsal region of the foot that not only allowed the same single degree of freedom as the shank on a pair of fulcrums, but also allowed precise definition of the ground contact point (Figure 3.17).

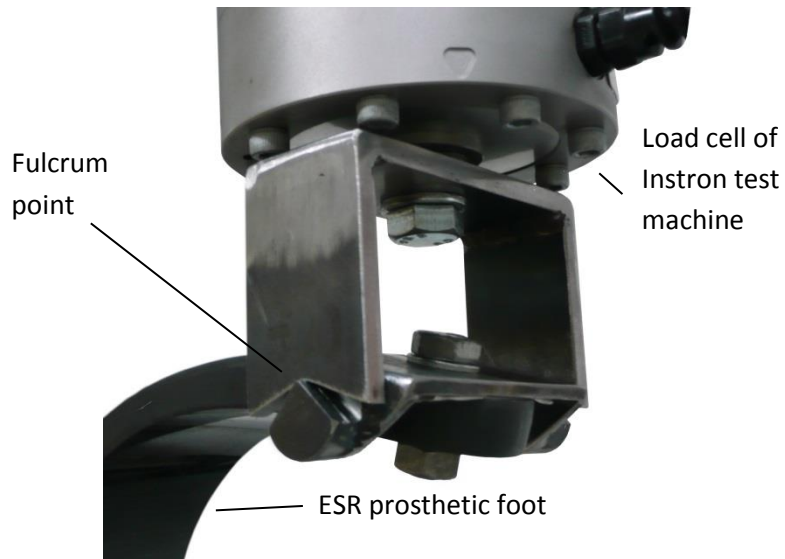


**Figure 3.16:** Detail of the fabricated bracket that clamps to the shank of the foot and provides the upper fulcrum points for attachment to the load cell of the Instron test machine.

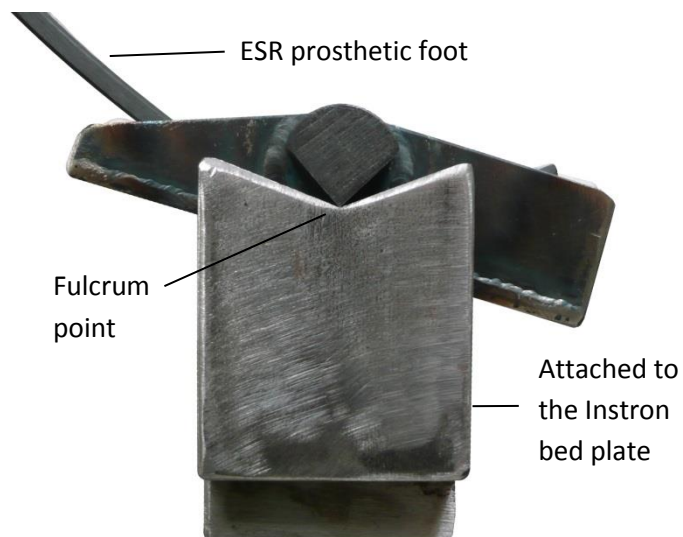


**Figure 3.17:** Detail of the fabricated bracket that clamps to the metatarsal region of the foot and defines the ground contact position with a pair of fulcrums.

This arrangement only allows flexibility in the sagittal plane and means that any prosthetic ESR foot of a similar style can be attached or removed without damaging or affecting the structure. To further protect the composite layup and improve safety, the distal end of the foot was cradled in a rapid prototyped (FDM) block that located inside the mild steel framework of the fixture and matched the curved profile of the toe region (figure 3.18). Between the upper and lower surfaces of the foot and the fixture was also inserted a thin ultra-high friction membrane to prevent slipping. A visualisation of the rig installed in the hydraulic test machine can be seen in figure 3.19.

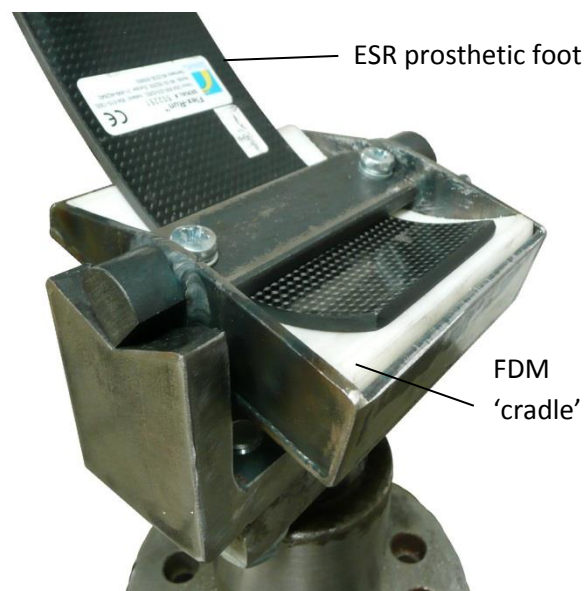


**Figure 3.18:** Detail of the fabricated bracket that clamps to the metatarsal region of the foot showing the FDM polymer cradle that supports the geometry of the foot. The ultra-high friction membrane is omitted for clarity.

As can be seen in figure 3.19, regardless of the amplitude of deflection of the foot the upper and lower interface points are always aligned. No lateral components of the force can exist and the actuator is only subjected to pure vertical loading conditions.

Furthermore because of the rotational degrees of freedom at each end of the foot it is not possible to establish a torque at either of the mounting interfaces.



**Figure 3.19:** Pictorial representation of foot displacement during testing, demonstrating the deflected position of the foot and the line of force superimposed through the fulcrum points.

## **3.4 STATIC CHARACTERISATION OF A SINGLE FOOT**

### **3.4.1 Theory**

Following the fabrication of a fixture that allows the effective mounting of an Ossur Flex Run foot, the Instron 8872 hydraulic test machine could be used to generate a hysteresis curve. By this means an accurate figure for energy return could be derived. This also allowed for a static spring rate to be defined for the foot.

### **3.4.2 Method**

The foot was subjected to an identical displacement cycle as the characterisation work conducted in section 3.2.4.2, driven with a sine wave of peak-to-peak amplitude 70mm and oscillation frequency of 0.5Hz. As before, the foot was subjected to a regime of four full waves and data from the centre three full cycles was averaged to generate a single representative displacement dataset. Data was once again collected from the load cell attached to the Instron test machine and the linear transducer of the actuator. Data was logged using the Instron DAX software (Instron) with a sampling rate of 100Hz.

### 3.4.3 Results

Figure 3.20 shows the resulting hysteresis loop from the foot on test. The compression phase is coloured blue and the rebound phase red, but despite this the two curves are almost indistinguishable with an energy return efficiency of 99.4%.

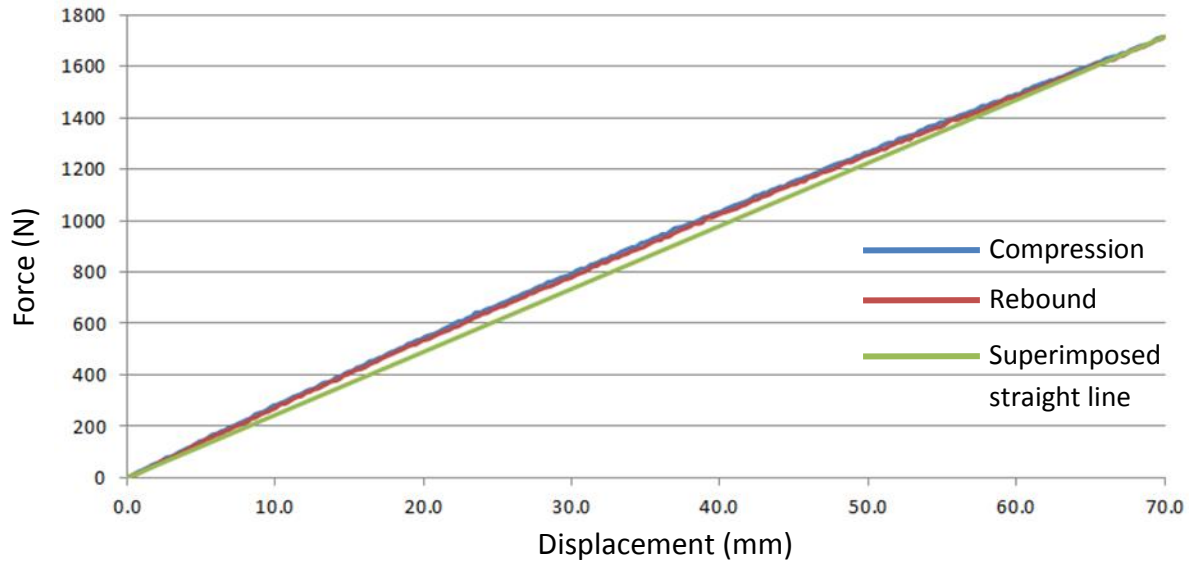


**Figure 3.20:** Hysteresis loop of Ossur Flex Run Cat.6Hi tested @0.5Hz, 70mm displacement and mounted with rotational degrees of freedom at shank and toe regions.

Further to this it should also be noted that the foot returned an almost entirely linear spring rate across the entire displacement. Figure 3.20 has a straight line superimposed over the compression and rebound curves and at its maximum point the deviation is 5.8% (800N of straight line vs. 851N of compression phase).

It can also be observed that the force reacted by the foot at maximum displacement is 1714N. If this figure is compared with the data collected in section 3.2.4.3 it can be seen that it does not align with that of any of the previous test methods (table 3.2). Condition 1 used rollers to virtually eliminate friction with the ground plane and offers figures closest to this new test regime in terms of efficiency but the peak force exhibited is over 500N adrift. This can be accounted for if the geometry of the test is examined. As discussed in section 3.2.4.5 as deflection increases in mounting condition 1, the lateral component of the force increases and the vertical component in turn will

decrease. Mounting condition 5 (figure 3.19) avoids this by ensuring the interfacing points (at the shank and at the toe) always remain aligned with the force. Therefore the geometry of the force cannot change.

	Peak displacement	Driving frequency	Peak force	Efficiency
Condition 1	70mm	0.5Hz	1.20kN	97%
Condition 2	70mm	0.5Hz	2.81kN	86%
Condition 3	<b>Aborted</b>			
Condition 4	70mm	0.5Hz	2.83kN	71%
Condition 5	70mm	0.5Hz	1.71kN	99%

**Table 3.2:** Hysteresis data for all foot mounting conditions demonstrating the change in both peak force and efficiency (energy return) despite identical input conditions.

#### 3.4.4 Conclusion

The results in table 3.2 demonstrate the importance of controlling the boundary conditions during testing of prosthetic feet. All of the mounting conditions tested used identical inputs but both the peak forces and values of foot efficiency measured varied significantly.

Mounting the foot on fulcrum points at both the medial and distal ends (at the shank and at the toe) means that the geometry of testing remains unchanged throughout the displacement cycle. The effective ground contact point remains the same both relative to the toe of the foot and also to the ground plane and results in an almost entirely linear spring rate. This is contrary to previous work conducted by other authors, most notably Dyer et al. (2013) (although this work was conducted with a different model of foot) and Geil (2001) who both present non-linear static deflection curves. Interestingly both of these authors conduct a similar test with the distal end of the foot sliding against a low-friction medium.

### 3.5 Chapter Conclusions

This chapter has demonstrated the importance of the mounting condition if an ESR prosthetic foot is being tested. The peak force, spring rate and efficiency of energy return are all affected by modifying the ground contact condition. The revised mounting method for the device on test (as described in section 3.3) has confirmed, statically at least, that the Ossur Flex Run foot has an energy return efficiency of >99% with a linear spring rate. Assuming that a single ground contact point can be defined, a linear spring rate for the foot can be established using this method to support the hypothesis of a spring – mass system.

Existing journal papers that address the efficiency of energy return from ESR prosthetic feet conduct their investigation with the shank of the foot rigidly attached to either the actuator of a test machine or to a mass that is restricted in the vertical plane. In doing this, as the amplitude of displacement increases and the foot is progressively deflected, the test geometry changes. The shape of the foot is influenced and according to the toe interface with the ground plate of the test machine a lateral force and torque is exerted on the actuator or mass. The discrepancies of historical test results from authors can therefore be explained and a new and novel mounting method is defined with which to continue the research.

It is important to note that this testing was not intended to replicate the action of a runner but instead to characterise the prosthetic device as a standalone component. If the individual elements can be understood, the prosthetic system can start to be built up such that modelling can occur.

All of the test work in this chapter has been carried out in what is referred to as a ‘static’ condition. That is the rate of deflection was sufficiently low to represent the foot in a static state. A natural progression for the research is to now characterise the same Ossur foot at higher, more representative rates of deflection. This would provide an understanding of the properties of the foot when being used by an amputee athlete and how, if at all, this differs from the characteristics established in this chapter.

# CHAPTER 4: DYNAMIC CHARACTERISATION

## 4.1 Introduction & Chapter Objectives

The term 'dynamic' is often misinterpreted, used as a subjective measure and as a loose undefined marketing term. However for the purpose of this report (and indeed in the case of vibration engineering) 'dynamic' refers to a system that is working in its intended manner, at the designed speed and frequency. Therefore in this instance it infers that the testing is being carried out at a realistic speed or, more tangibly, in a manner that replicates an amputee running. The previous work (chapter 3) was termed 'static' and although the actuator of the test machine was not at any time genuinely static, the head velocity was significantly lower than would be considered representative usage (previous tests were driven with a sine wave of 0.5Hz).

The purpose of this chapter is to improve understanding of the way an amputee runs, measure running variables and apply this knowledge to the way feet are testing in a laboratory. It is intended that the characterisation tests carried out in the previous chapter be repeated but at an actuator velocity that could be considered 'dynamic'. The values for the two test conditions (static and dynamic) can be compared which further characterises the prosthetic device as a component but also aids our understanding of the action of a runner. It assists in building a complete picture of how an amputee runs and therefore how this can be modelled.

In order for this to occur, firstly amputee running has to be understood with the relevant parameters recorded so that they can be replicated. These include typical values for foot deflection, stance phase timing and ground contact point change. Therefore a measurement technique needs to be developed that can record these key variables.

As mentioned in the literature review, dynamic analysis of gait and deflection models is typically performed using reflective markers and two- or three-dimensional motion capture systems with multiple high-speed cameras. Force plates can also be used to collect data of a small number of strides. Such an approach requires highly specialised

and expensive equipment in a controlled and unrepresentative environment within a large area for the setup of the apparatus. Additionally whilst such systems offer a high resolution this does not account for noise or the markers shifting on the subject during active use.

As such, the use of reflective markers was dismissed because of the limited field of view of a camera and the technical challenges of observing their relative changing positions over anything other than smooth level ground. Data collection should be taken outside of the gait laboratory and the measurement system must reflect this. Therefore the decision was made to develop a sensing system that could be worn by the amputee allowing the freedom to undertake their regular exercise regime.

## 4.2 Development of a Wearable Sensing System

### 4.2.1 Scope & Objective

The objective of this study is to obtain representative running data from an amputee athlete which can subsequently be used to advise further laboratory testing. Data shall be acquired from a single individual amputee volunteer and used to form laboratory input conditions (ground contact positions & deflection rates). The individual shall be chosen to be representative (be the user of a foot from within the interquartile range of feet available from the manufacturer), be a long-term and regular user of an ESR prosthetic foot and not suffer from extreme or influential pathologies such as restricted movement or chronic pain that might adversely affect running style or repeatability. Given that a single amputee is being used for data collection, every precaution should be made to ensure that the action of their running is not adversely affected by factors that could be mitigated such as excessive pain or discomfort. This process will be conducted following the Bournemouth University ethical approval process as set out in the Research Ethics Code of Practice, defined by the University Research Ethics Committee (UREC). Copies of the approved ethics forms can be found in the Appendix of this document.

A list of variables to measure is included in table 4.1. These were chosen for their role in describing the dynamic nature of what is anticipated as being a spring – mass system; the fundamental characteristics of the system.

Variable
Stride cadence
Ground contact time
Swing phase time
Timing of maximum displacement
Amplitude of maximum displacement
Rate of energy storage
Rate of energy return
Ground contact force
Ground contact point on foot

**Table 4.1:** List of possible variables to measure during amputee testing

Along with basic deflection and timing data it is viewed that the changing boundary conditions of the foot with the ground (progression of contact point) is of significant importance and is something that has not been found to be fully explored in the literature (see section 1.6).

#### 4.2.2 Design

ESR prosthetic running devices are regarded as functioning primarily in the sagittal plane meaning that the measurement of in-plane bending is adequate for understanding their dynamics. If this primary mode of operation can be observed accurately then many other factors can be recorded such as stride cadence, swing timing and rate of energy absorption/return (a complete list of measureables is shown in table 4.1).

Firstly, and fundamentally, an amputee had to be found who was willing to partake in these studies on a voluntary basis. As mentioned in section 4.2.1 he or she should be an active and long-term user of prosthetic ESR running feet. They should be representative of the age of competitive runners (circa 20 - 40 years of age), be unencumbered by limiting factors such as restriction of movement or chronic pain and have a foot prescribed to them that exists in the interquartile range of the available stiffness values from the respective manufacturer. Following some local searching, a male uni-lateral amputee was found that matched the description and ethical approval was obtained in October 2012 for the research to continue. He is 30-35 years of age and has a left-side trans-tibial amputation following trauma more than ten years ago. He has been the user of a category 6Hi Ossur Flex Run foot for over ten years and runs for leisure and fitness every day, has retained full joint articulation and suffers from no long-term pain or discomfort. He has a mass of 83kg and as such uses the correct stiffness category of foot according to the manufacturer's literature (table 1.2)

Five major pieces of apparatus were used for this investigation. They are summarised in table 4.2 and a table detailing what piece of equipment is associated with each specific variable is shown in table 4.3. Descriptions of each of the pieces of apparatus follow with an illustration of the complete instrumented foot shown in figures 4.1a & 4.1b.

Description	Manufacturer	Details
<b>1 Displacement Sensor</b>	Hartmann Automotive GmbH	Hall-effect rotary sensor
<b>2 Ground-Force Sensors</b>	Tekscan, Inc	Piezo-resistive sensor (0-100lb) (Flexiforce)
<b>3 Resistive Force Signal Conditioner</b>	Bournemouth University	4 channel conditioner/amplifier (0-5v output)
<b>4 Analogue Datalogger</b>	MSR Electronics GmbH	4 channel 1kHz 0-5v logger
<b>5 Battery Pack</b>	Generic	3 x AA alkaline cells (4.5v)

*Table 4.2: Summary of equipment used, manufacturer and details of the device.*

Variable	Units	Chosen measurement device
<b>Stride cadence</b>	Hz	Displacement sensor
<b>Ground contact time</b>	seconds	Displacement sensor
<b>Swing phase time</b>	seconds	Displacement sensor
<b>Timing of maximum displacement</b>	seconds after heelstrike	Displacement sensor
<b>Amplitude of maximum displacement</b>	mm	Displacement sensor
<b>Rate of compression</b>	mm/s	Displacement sensor
<b>Rate of rebound</b>	mm/s	Displacement sensor
<b>Ground contact force</b>	N	Displacement sensor
<b>Ground contact point</b>	mm posterior of toe edge	Piezo-resistive force sensors array

*Table 4.3: Summary of measurables and the specific measurement device proposed.*

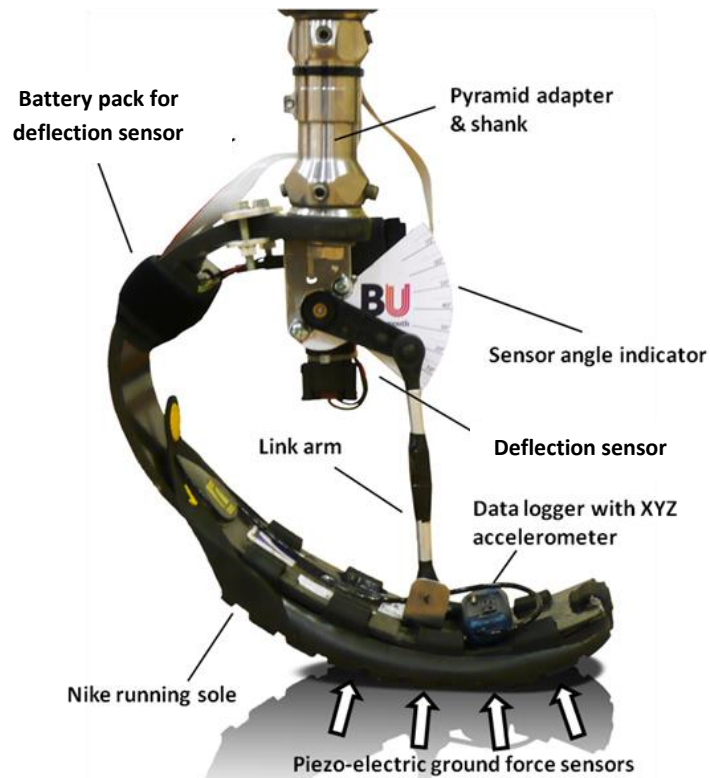


**Figure 4.1a:** Prosthetic running foot with instrumentation attached. An angle indicated was included as a visual check of deflection data acquired.

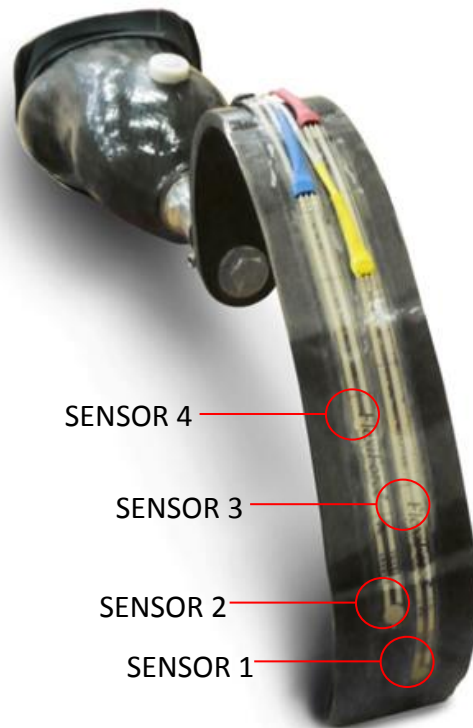


**Figure 4.1b:** Prosthetic running foot with instrumentation attached. Sole and angle/deflection sensor removed to clearly show piezo-electric sensor array.

A full and detailed description of the instrumentation can be found in Appendix 1 including design and set-up criteria.

### 4.3 Overview of Methodology

The foot used for the testing was a replica (identical model and stiffness category) of the foot already used by the amputee for over ten years. Therefore he was familiar with the device and his running on the foot was comfortable.

It should be noted that in order to ensure parity between the new model as tested and the aged historic foot as used by the runner for the previous ten years, a static deflection test was conducted with both feet prior to the test taking place. The methodology mirrored that of the static spring rate testing as detailed in Chapter 3 of this thesis although this specific investigation is not documented any further. The two feet were shown to have a static spring rate of within 1% of each other up to maximum displacement, therefore adding validity to the substituted foot and also credibility to the repeatability of the foot categories from the manufacturer.

Despite the near-identical nature of the substituted foot the amputee was allowed 30 minutes to warm up with the foot in the test environment (a 25 metre sports hall with wooden floor) to ensure the additional mass of the instrumentation (148 grams) would not cause any notable issues.

The testing routine consisted of the sustained running of ten lengths of the hall (250m with nine turns) with the entire sequence logged at a frequency of 128Hz. The runner was allowed to choose his own pace and cadence with which he felt most comfortable and familiar. Because the data logger was limited to four input channels, the deflection testing was conducted first followed by the ground-contact force testing. Identical runs were conducted and again logged.

## 4.4 Results

### 4.4.1 Foot deflection

The data acquired was filtered to avoid the portions of acceleration, deceleration and turning. A three-step portion at the centre of each run was isolated and the mean values calculated resulting in data for three averaged strides.

This filtered data is shown in figure 4.2. Displayed is the output voltage from the deflection sensor versus a time trace in minutes:seconds. This value of foot deflection was not calibrated into millimetres because doing so would falsely simplify the action of the foot. The value of deflection as a function of voltage reflects the position of the lever arm of the deflection transducer (figure 4.1) and as such a trend of foot deflection as measured at the point where the link arm meets the foot keel. However the keel deflection at any other point is different to this attachment point; the value of foot deflection as a function of millimetres depends on what point along the keel is being tested. Retaining the deflection as a function of voltage at this stage avoids misinterpretation of the results.

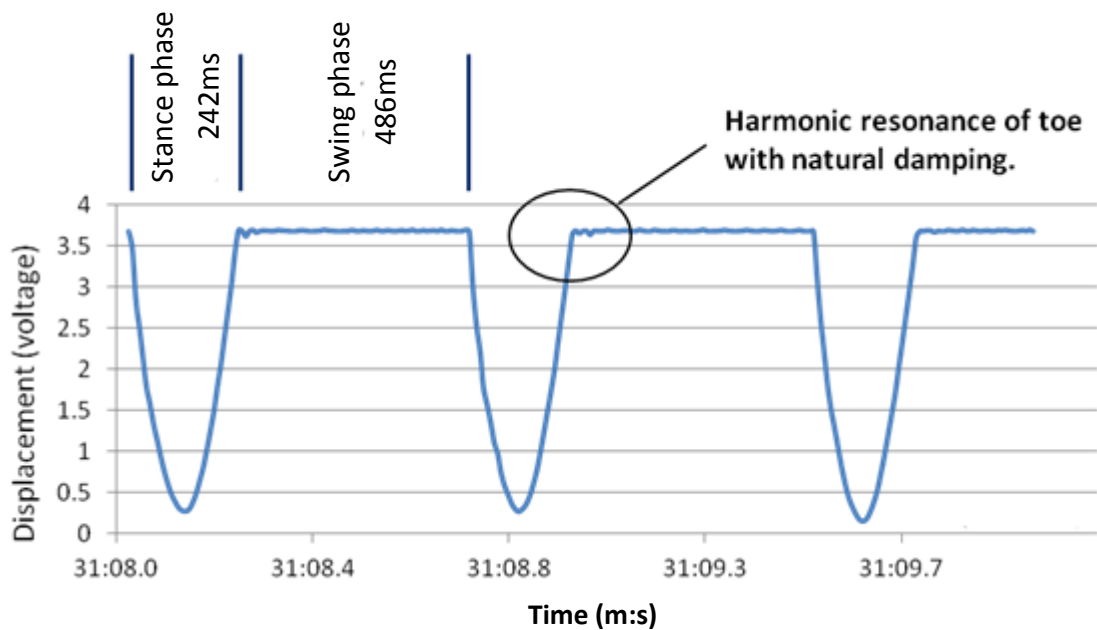


**Figure 4.2:** Trace showing the deflection characteristics of the foot tested (averaged raw data from rotary transducer with output in volts.  $SD = 0.021$ ).

Clearly visible is the timing sequence of the runner with well-defined stance and swing phases as well as the rate of deflection and energy return. The stance phase (occurring from heelstrike to toe-off (see figure 1.1 for definition)) occurs over a period of 242ms with the swing phase lasting 486ms until heelstrike for the next stride takes place.

Worthy of note is the clear demonstration of the natural harmonic frequency of the unloaded foot when toe-off occurs. The trace can be seen to resonate, diminishing with the natural damping of the device (provided by losses in the system such as air resistance and friction within the foot keel).

#### 4.4.2 Ground Contact Position

The data was once again filtered and averaged across all of the ten runs of the hall resulting in a single, typical, ground contact profile. Traces for each of the ground contact sensors can be seen in figure 4.3 with a measure of foot deflection overlaid to help visualise the heel strike and toe-off phases.

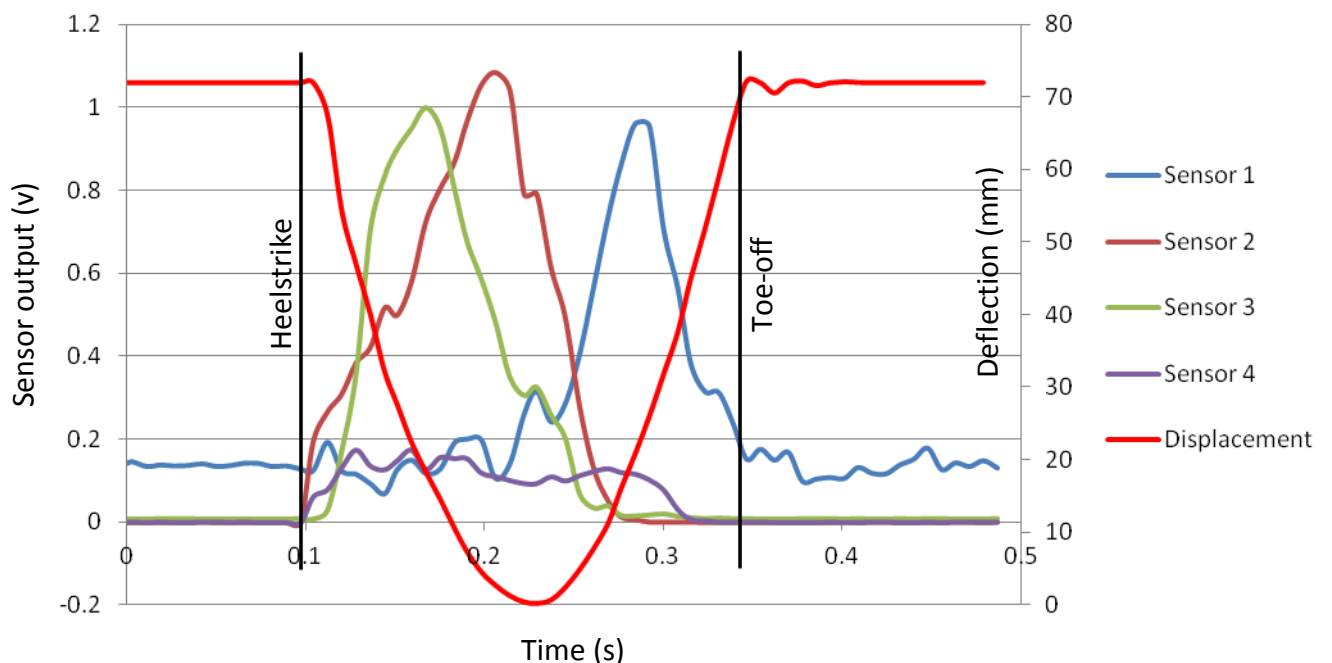


**Figure 4.3:** Force sensor outputs for a single stride with foot deflection overlaid

It is clear from this plot that only three of the sensors were useful (sensor 4 appears to represent only a baseline of contact). This is the posterior-most sensor and suggests that it is inheriting an input from the shoe sole attached to the foot but does not come into contact with the ground at any time. However the remaining sensors show a clear progression of the peak force with distinct and ordered outputs.

Sensor 1 suggests an error as it has a baseline output even through the swing phase of the stride. However this was investigated and is a result of its position on the toe. At this point of the foot, the profile forces the trainer sole into a curve which inherently exerts a force onto the position of the foot where the sensor is attached. Following testing the sole was removed and the sensor output returned to zero.

Time after heelstrike (s)	Distance of contact-point from distal end of foot (mm)
0.067	100
0.106	60
0.184	20
0.242	0

**Table 4.4:** Timing of the ground force peaks measured by piezo-resistive sensors

Now that timings of the peak forces at the various positions have been defined it is possible to record them in a table (table 4.4) and plot them in a graph against the time at which these peak forces occur (relative to heelstrike, figure 4.4) to visualise the progression of the ground contact point. From figure 4.3 it is clear that the foot first contacts the ground in a position somewhere between sensors 3 and 4 (between 110 and 130mm from the distal end of the foot) and toe-off occurs at a point forward of sensor 1 (within the end 20mm of the distal end of the foot). With this knowledge it is possible to begin to build up a more complete picture of the ground contact point progression and these extreme points (at the time of heelstrike and toe-off) can be extrapolated using the graph line and continuing the trend at either end.

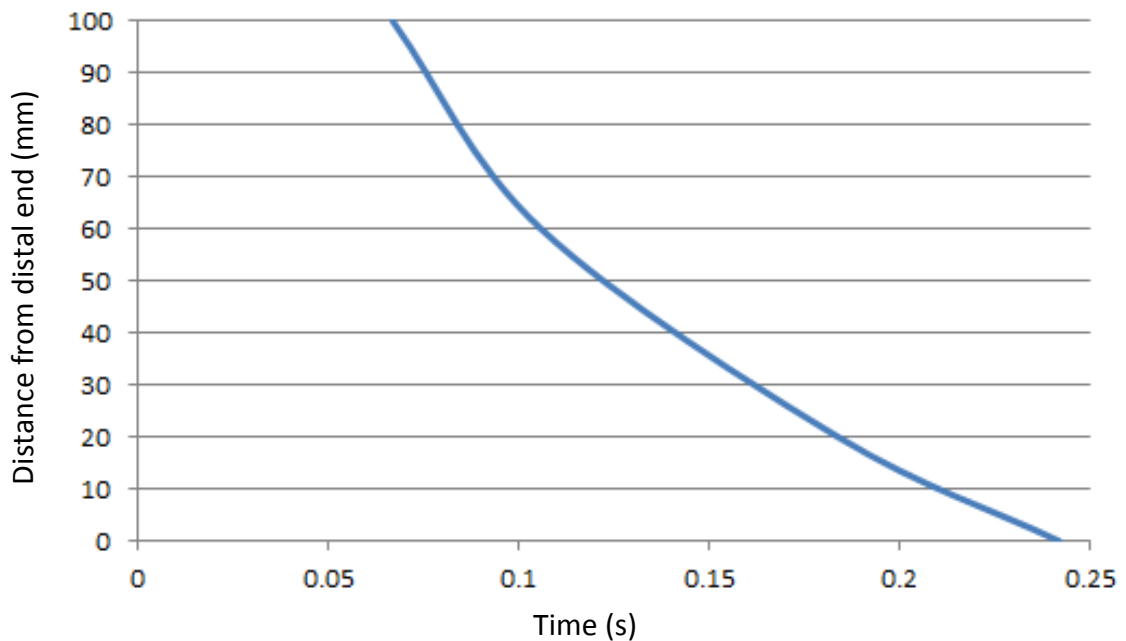


**Figure 4.4:** Curve demonstrating the shift in ground contact position relative to the distal end of the foot (toe region)



**Figure 4.5:** Force sensor locations demonstrating the line of progression of ground contact point.

Figure 4.5 shows a visualisation of the locations of the four sensors used and how the ground contact point progresses. As a validity check for the data gathered in this section a high-speed video was captured on the day of testing of the stance phase of a single stride from heel strike to toe-off. This video was captured using a Nikon Coolpix camera at 240 frames per second (10 times faster than standard broadcast video) at a resolution of 640 x 480 pixels. This was the maximum resolution that could be achieved by the camera without introducing significant motion blurring of the image.



**Figure 4.6:** Still frames extracted from high-speed video (240fps) taken of a single stance phase during data acquisition showing heel strike, mid stance and toe-off.

This sequence is shown in figure 4.6 and shows the foot first contacting the ground in the region between sensors 3 and 4 (as expected) and toe-off occurs at the very distal end of the foot, forward of sensor 1. Whilst this video was adequate for confirming the trend of ground contact progression from the rear of the foot to the toe, if further work is done involving high-speed video capture it should be done so at a significantly higher resolution and frame rate to allow the detail of the foot to be more visible (for instance the deflection guide added to the sensor).

## 4.5 Amputee Testing Conclusions

### 4.5.1 Summary

The objective of this chapter is to define representative test conditions for further laboratory testing. Whilst the work completed has improved our understanding of the dynamic function of a prosthetic foot, more work is required to translate this data into useful figures that can be applied to laboratory testing.

This investigation demonstrated profiles for both foot deflection and ground contact point over the duration of the stride. For the amputee on test with the specific foot used (an Ossur Flex Run Cat6.Hi) the foot response time (ground contact time) was 242ms with a symmetrical deflection profile. Mid-stance (maximum deflection) was achieved at 141ms. However the deflection is a value of voltage which would need to be calibrated to millimetres to enable programming of the Instron test machine controller.

The ground contact point can be seen to progress along the effective metatarsal portion of the prosthetic foot towards the distal end. However to translate this new information to a laboratory test procedure the Instron test machine (and fixture as described in section 3.3) requires a single ground contact point to be defined.

It should be noted that this method was not designed to capture the ground reaction force but instead provide a trend of how the contact point moves. Indeed a more accurate picture would be difficult to achieve with this method given that the foam running sole that was attached the foot offered a significant degree of load spreading onto the carbon section. This is shown by the overlapping of traces in figure 4.3.

There are a number of extensions to this work using the same ground force sensing devices and changing their locations on the base of the foot. For example if the sensors were placed at the extreme edges of the foot section (at the same distance from the distal end) some valuable gait data might emerge that could aid prosthetists with the lateral set-up of prosthetic devices, however it is considered that such work is outside of the remit of this project.

## 4.5.2 Further Work

Further work that should be conducted to benefit the dynamic understanding of such a prosthetic device is to repeat a static spring rate test (as in Chapter 3) with the effective ground contact point (the fulcrums of the fixture) positioned at each of these sensor positions. This would then provide an understanding of how the static spring rate changes throughout the course of a single stride. This is knowledge that is not published to date and is not considered by prosthetists during the prescription of a foot, but may prove fundamental to the style of running of an amputee.

In order to add tangible understanding to the action of the foot it would also be useful to calibrate the foot for a single point of ground contact. This means translate the voltage output of the rotary sensor to a measure of foot deflection in mm. As the foot effectively forms a lever, the further towards the toe the effective ground contact point is positioned the larger the deflection value will be for a given voltage logged at the sensor. For this reason it is not possible to define an absolute value of foot deflection because it depends on what portion of the foot is in contact with the ground at any given time. However if a ground contact point is defined, the deflection at this point can be ascertained.

These two further exercises are described in the following sections.

## 4.6 Spring Rate Calibration

### 4.6.1 Method

In order to define the spring rate of each of the ground contact positions the test method described in section 3.4 was repeated. However in this instance the lower fulcrum component of the fixture was attached such that the line of force acted through each of the locations of the three useful sensors from the ground contact testing in three successive tests. These were located at 20mm, 60mm and 100mm posterior of the edge of the toe of the prosthetic foot.

To run the test the programmable controller of the Instron 8872 test machine demanded figures of maximum and minimum deflection through which to exercise the foot. Due to the fact that the amount of deflection of the foot changes depending on the location along the metatarsal section of the foot that is under test, and to avoid over-strain of the foot (unrepresentatively high levels of deflection that might damage the foot) the rotary sensor was used to define the maximum level of deflection achieved. Regardless of what ground contact point was being tested, the foot was deflected until the rotary sensor gave an output of 0.5v – a level seen during amputee testing and safely within the working range of the foot. The data was once again logged using the Instron DAX software at 100Hz.

## 4.6.2 Results

The three ground contact points were tested and the data averaged into a single hysteresis loop as before (section 3.4). This was then displayed on a graph (figure 4.7) and, assuming a straight line approximation of each resulting curve, a spring rate was defined.

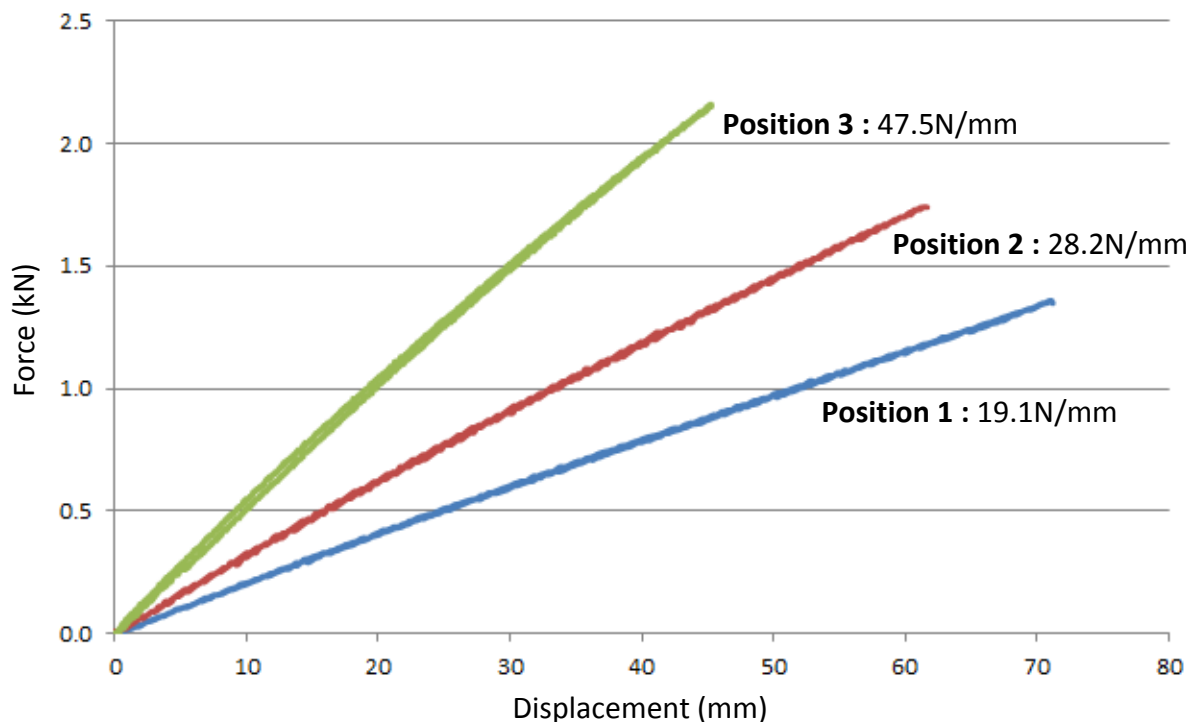


**Figure 4.7:** Graph demonstrating the difference in foot stiffness when altering the ground contact point along the metatarsal region of the foot. See table 4.4 for definitions of ground contact positions.

As with the previous static rate testing that was conducted the foot returned an almost completely linear spring rate regardless of what ground contact position was being characterised. Furthermore at each test position the hysteresis curves show an energy return of nearly 100%. However the spring rate varied from 19.1N/mm at position 1 (20mm from the toe) to 47.5N/mm at position 3 (100mm from the toe).

With this information, the measured stiffness of the foot can be plotted against the distance from the toe, theoretically allowing the stiffness of any point along this metatarsal region to be defined.

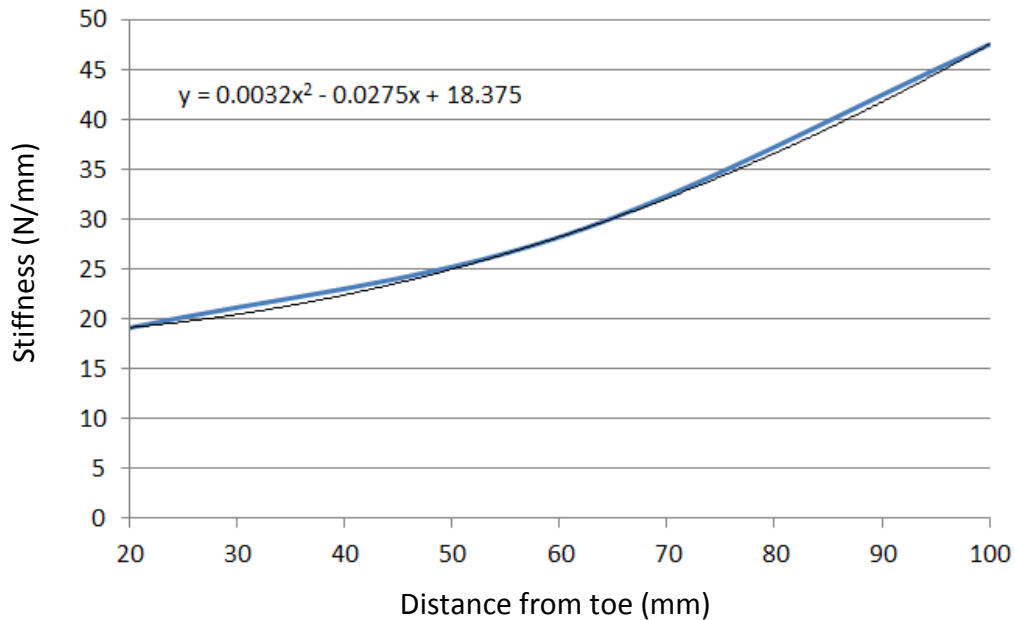


**Figure 4.8:** Graph demonstrating the difference in foot stiffness when altering the ground contact point along the metatarsal region of the foot. A line of best fit is added and equation derived to describe the relationship.

From this data it is very clear that the spring rate of the foot is dependent on the ground contact point and, as such, as the amputee progresses through the stance phase of the running stride, the foot dramatically softens. This change is purely a function of prosthesis geometry and the angle of attack of the foot during the stance phase of running. The variation in foot stiffness could be increased or decreased if the geometry of the metatarsal region of the foot were modified, but it cannot yet be suggested if this would be a positive or negative modification for the amputee.

The relevance of this phenomenon will become apparent when the action of the foot is being modelled mathematically. Immediately it is clear that a foot cannot behave in a manner that can be described using Simple Harmonic Motion (as suggested in previous studies and detailed in the literature review (Chapter 1)) as this equation assumes a single value of stiffness to establish the frequency of oscillation of the system.

## 4.7 Single Condition Calibration

### 4.7.1 Method

If the static and dynamic data is to be comparable it is fundamental that the toe clamp component of the testing fixture is attached at an identical position for each test. Therefore to remove any potential error the static testing was replicated (as conducted in section 3.4) with a newly-defined ground contact position (the position at which the toe-clamp should be affixed). This not only serves to provide a revised spring rate of the foot (at the new ground contact position) but also to generate a calibration curve for foot deflection in mm as a function of rotary deflection sensor voltage.

The actual ground contact position selected was 40mm from the toe which is the median value between sensors 1 and 2. However it is important to understand that because of the transient nature of the ground contact point and subsequently the variation in actual foot deflection (at that specific ground contact point) the actual chosen position is arbitrary. As long as the same position is used for both static and dynamic characterisation, the exact position is unimportant at this stage of the investigation.

Deflection data was gathered by logging the linear displacement of the Instron actuator and voltage data from the output of the rotary transducer simultaneously. The voltage was logged using the miniature foot-mounted MSR data logger (MSR electronics GmbH) at 128Hz and the linear displacement logged using the Instron DAX software (Instron) at 100Hz. They were then normalised to give a data rate of 100Hz. The setup of the foot mounted in the Instron test machine with instrumentation attached can be seen in figure 4.9. Also logged was a value of ground reaction force from the load cell of the Instron test machine.



**Figure 4.9:** Test set up of the Ossur Cat.6Hi foot installed in the Instron test machine with the displacement instrumentation attached prior to calibration.

At first the crosshead of the test machine was lowered, deflecting the foot, until the voltage output from the rotary transducer matched that of the maximum deflection of the foot during amputee testing (figure 4.2). This was then used as the limit for the machine (to avoid over-travel of the foot) and a low frequency (0.5Hz) sine-wave profile was run (as conducted in section 3.4) displacing the crosshead between 0mm (an unloaded foot) and the maximum deflection (maximum load) as just defined.

## 4.7.2 Results

Once the data rate was normalised the resulting voltage and deflection figures could then be plotted together to form a calibration curve for the rotary transducer with voltage plotted against deflection in millimetres (see figure 4.10).

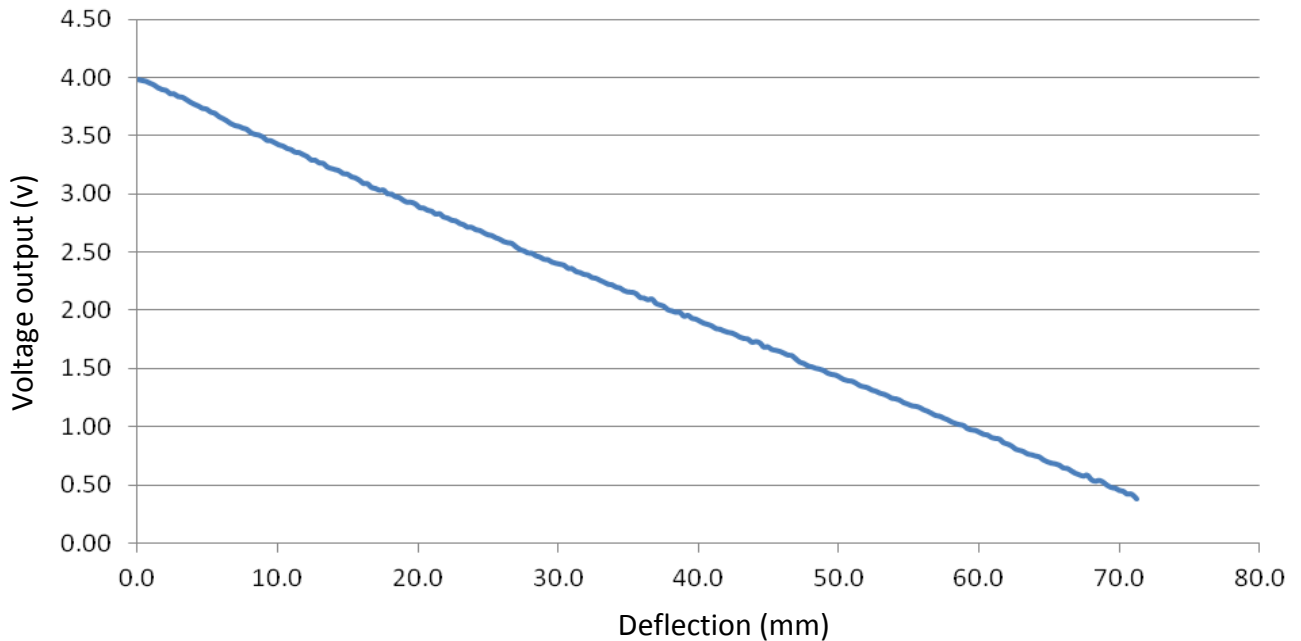


**Figure 4.10:** Calibration curve for rotary transducer

From the calibration curve generated, it can be seen that the foot deflects from an unloaded 0mm (at 3.95v) to a fully loaded condition at 72mm (0.35v) in a linear manner. Having these figures defined, an equation for this curve can be generated and therefore the output of the rotary sensor can be calibrated. Any subsequent test work in the laboratory can be done with real-world input conditions (as a function of deflection in mm) assuming this same ground contact position is used.

If the recorded trace of ground force is plotted against foot deflection a force-deflection curve is generated. This static deflection curve (figure 4.11) demonstrates once again the efficiency of the energy return from the foot at a slow crosshead speed and the linearity of the spring rate. A straight line is superimposed over the hysteresis curves and at maximum deflection (72mm) the resulting ground reaction force was recorded as 1648N. Therefore the resulting spring rate of this foot using a ground contact point 40mm from the toe of the foot is 22.9N/mm.

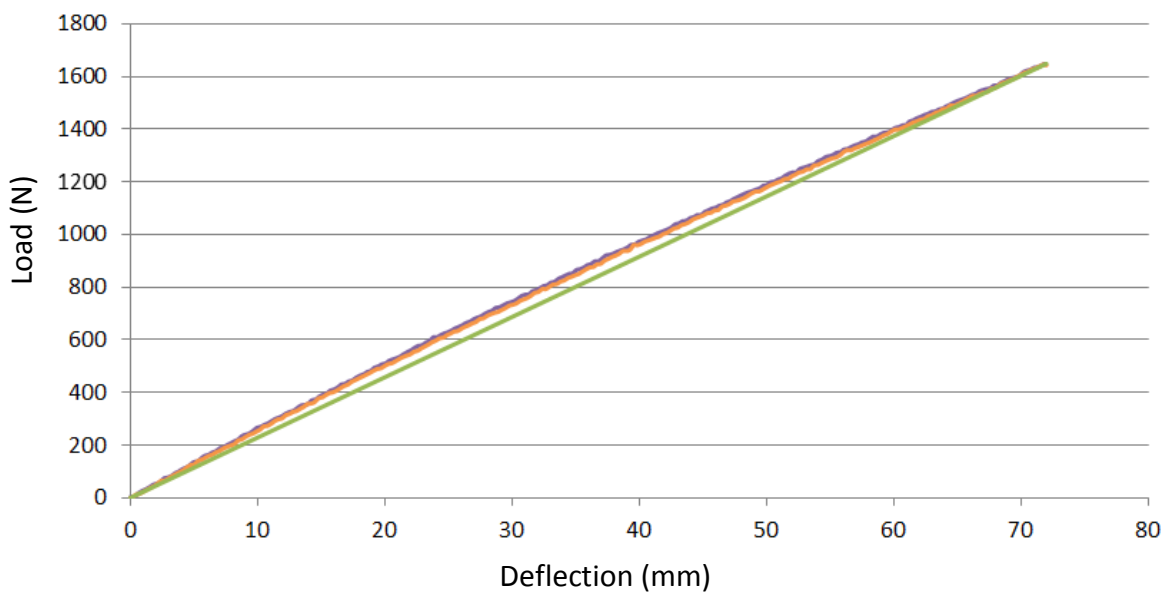


**Figure 4.11:** Calibration curve for static spring rate of foot (hysteresis loop) with a ground contact point 40mm posterior of the edge of the toe.

Figure 4.8 describes the relationship between ground contact point and foot stiffness and includes an equation describing this relationship. If the ground contact position used for this calibration (40mm) is substituted into this equation it can be used for data verification. Using this equation the theoretical foot stiffness is 22.4N/mm at 40mm rear of the toe; a variation of 2%.

## 4.8 Dynamic Spring Rate Testing

### 4.8.1 Method

In order to further characterise the foot dynamically the spring rate was measured in a similar manner to section 3.4 but with a higher crosshead speed. It is known that during initial data acquisition (section 4.3) the foot reached maximum deflection of 72mm in a time of 121ms (assuming the ground contact point defined in section 4.7). Examining the trace of foot deflection plotted against time in figure 4.2 it can be seen that the deflection of a foot can be considered symmetrical. If the data is interrogated it is made clear that the time from heelstrike to maximum foot deflection presents as identical to that from maximum deflection to toe-off (at a logging frequency of 128Hz). During laboratory testing this equates to an average crosshead speed of 0.60m/s. Alternatively it is known that the entire stance phase (consisting of a single compression and rebound of the foot) lasts for a duration of 242ms. To replicate this on the hydraulic test machine a frequency of  $1/0.242 = 4.1\text{Hz}$  is required (whilst matching the total deflection). To assume this is not quite correct and contains one large source of inaccuracy; the deflection trace generated by the rotary transducer during data acquisition is not a standard wave pattern. This precise shape cannot be programmed into the controller as it exists on the Instron 8872 machine available. Therefore the closest available standard wave shape was used (a triangle wave).

A further problem was encountered when attempting to match the crosshead speed to the deflection speed of the prosthetic foot during running. Once the foot was mounted into the hydraulic test machine and a waveform programmed into the controller it was found that the machine capacity was insufficient to deflect the foot 72mm at a velocity of 0.6m/s. The desired test frequency for a triangle waveform was 4.1Hz but if 3.0Hz was exceeded the calibration of the waveform became impossible and the crosshead failed to reach the required position in time, therefore shutting down the actuator. As such the maximum possible testing frequency with this machine was 3.0Hz.

A comparison of the two waveforms (as measured on the foot during data acquisition using a runner and the best-case generated by the hydraulic test machine) can be seen in figure 4.12. As such the testing that ensued was not truly dynamic as set out at the beginning of this section (4.1). However it is no doubt sufficient to boost the understanding of the nature of the foot during use.

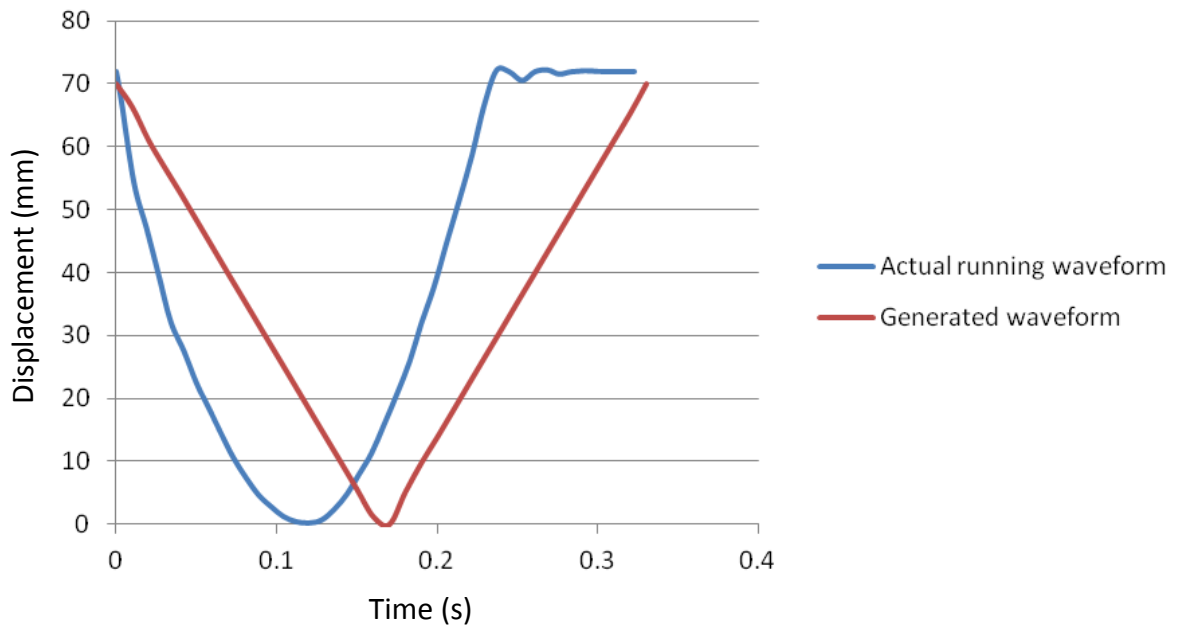


**Figure 4.12:** Recorded displacement waveform vs. best-case generated waveform

The foot on test (an Ossur Flex Foot Cat.6Hi) was mounted in the hydraulic test machine in an identical manner to that described in section 4.7.1 and subjected to a triangle wave of amplitude 72mm at a frequency of 3.0Hz. A total of six full phases of the waveform were completed following ramp-up and before ramp-down and can be seen in figure 4.13.

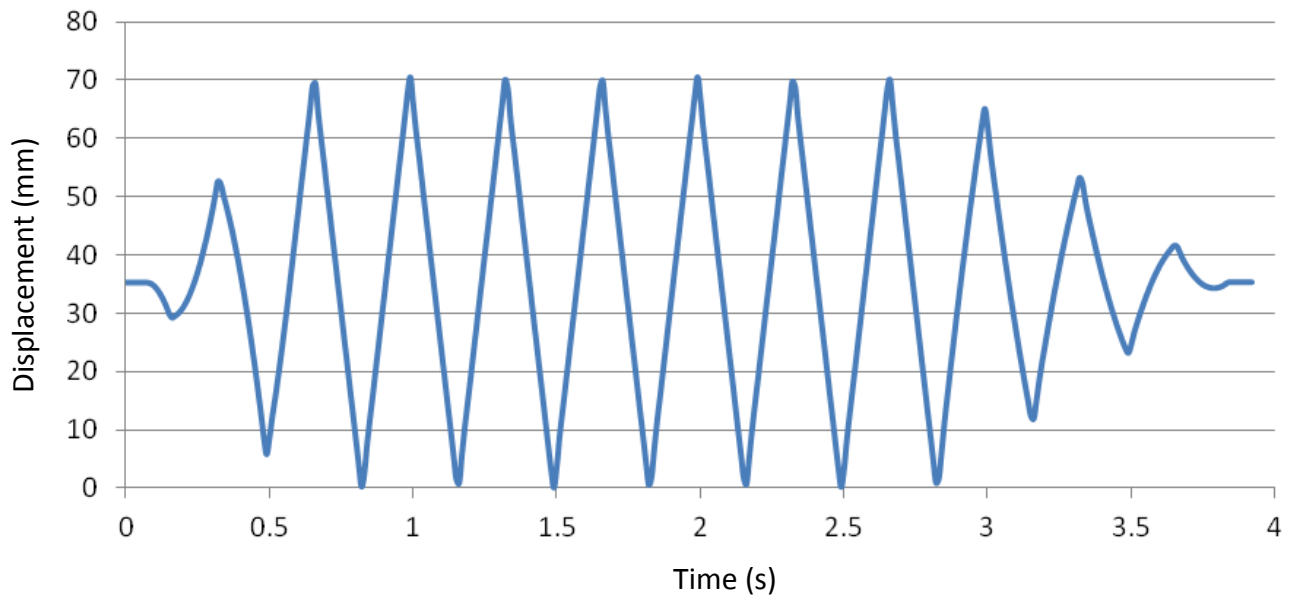


**Figure 4.13:** 'Dynamic' test procedure waveform (72mm amplitude @ 3.0Hz)

The data was recorded using the Instron DAX software at a sample rate of 100Hz. Data was collected for the entire sequence and the six full-wave phases were isolated and averaged to create results for a single wave. Data for both force and displacement were collected meaning that a hysteresis loop could be plotted.

During the generation of the hysteresis loop, at a frequency of 3.0Hz and amplitude of 72mm the crosshead velocity was 0.432m/s; somewhat lower than the 0.6m/s originally specified (for a frequency of 4.1Hz). This is however markedly different to that used for the static spring rate testing (Chapter 3 & section 4.7) where a crosshead velocity of 0.0288m/s was used. Operating the machine so close to its working limits introduced a further error. That is the calibration of the waveform proved very difficult meaning that the amplitude of displacement was smaller than requested. A maximum amplitude of 70mm was achieved whilst maintaining an accurate waveform (see figure 4.13).

## 4.8.2 Results

Because of the slower crosshead velocity the static testing (section 4.7) was able to achieve the full 72mm amplitude required from the controller and as such the maximum load recorded was larger (1.60kN dynamic vs. 1.65kN static) but assuming a straight line for each testing procedure, the spring rates are identical at this resolution (22.9N/mm for both static and dynamic tests). Figure 4.14 shows the resulting hysteresis loop for the dynamic testing.

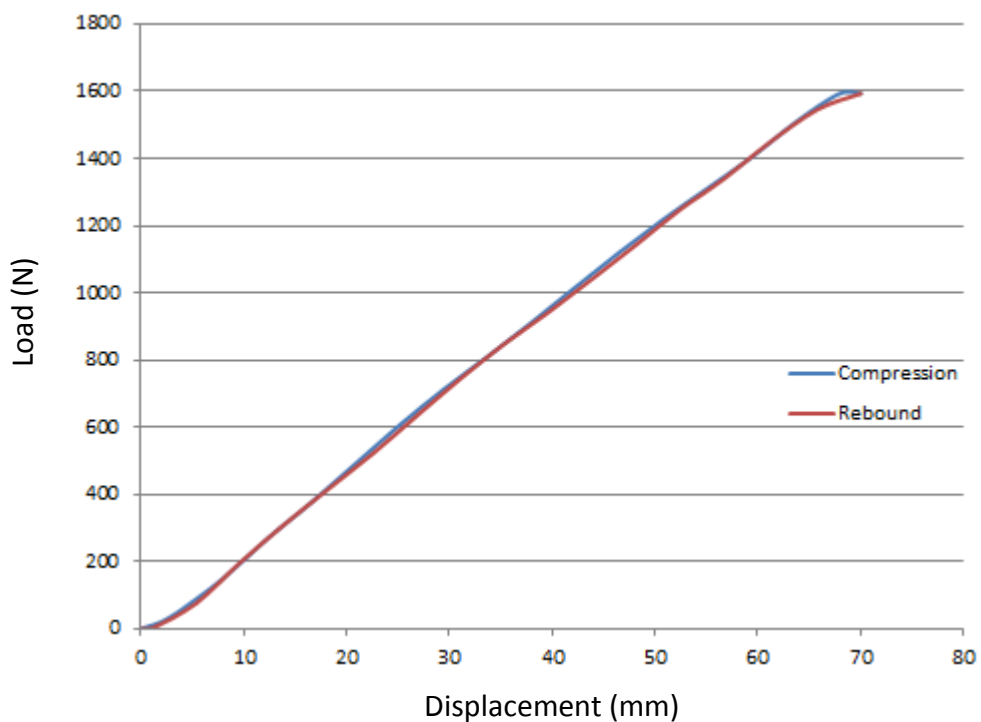


**Figure 4.14:** Hysteresis curve for Ossur Flex Run Cat.6Hi at crosshead speed of 0.432m/s

### 4.8.3 Conclusion

Whilst taking these sources of error into account, it can be seen from the hysteresis loop generated (figure 4.14) that the foot once again exhibits a very efficient energy return. The compression and rebound phases of the cycle are isolated and displayed in different colours and even so they are almost indistinguishable for the majority of the working phase. The largest discrepancy can be seen at the point of maximum displacement where the crosshead has to come to rest and accelerate in the opposite direction almost instantaneously. This area can be disregarded however. It is expected that this discrepancy is at least in part caused by the inertial properties of the fixture (a mild steel construction) acting on the load cell during this brief moment of extreme acceleration of the crosshead. But more importantly this period of change of direction is grossly exaggerated in the data collected during running from the rotary deflection sensor. This highlights the key difference between this semi-dynamic test and the foot being used in genuine running. When the foot reaches maximum deflection (and is attached to an amputee), it acts against the mass of the runner gradually changing the direction of the entire system. Conversely when the foot is being tested in the hydraulic testing machine the proximal end of the foot is attached directly to the actuator and is therefore driven to a definite position.

As such, and when observing the hysteresis loop in figure 4.14 it is apparent that the energy return from this specific Ossur Flex Run Cat.6Hi (being worked to a maximum deflection of 70mm at a shank velocity of 0.432m/s) is >99%.

## 4.9 Power Calculations

The reaction force of the foot during testing is known from logging the output of the load cell of the Instron test machine. The displacement is also known and therefore the energy stored in the foot can be calculated.

$$\text{Energy (J)} = \text{Force (N)} \times \text{Distance (m)}$$

Therefore:

$$\text{Energy stored in the foot} = 1601\text{N} \times 0.070\text{m} = \mathbf{112 \text{ Joules}}$$

This figure of 112 Joules should be halved however. This is because the maximum force of 1601N is not applied over the entire distance. Instead it can be considered that an average force of half the maximum (800.5N) is applied over the full distance of 70mm (0.07m). Therefore during the dynamic testing phase, the foot stores a theoretical 56 Joules of energy.

The time taken to deflect the foot the full 70mm is also known (167ms) meaning that the power used can also be calculated, given that:

$$\text{Power (W)} = \text{Energy (J)} / \text{Time (s)}$$

Therefore:

$$\text{Power to deflect foot} = 56\text{J} / 0.167\text{s} = \mathbf{335 \text{ Watts}}$$

The recorded level of energy efficiency makes sense if the power calculations are taken into account. Given that 335 Watts are used to deflect the foot at these speeds and amplitudes, any energy losses should quickly present themselves. However no audible emission was encountered from the foot and the surface temperature of the foot itself following the testing regime was not noticeably changed. Therefore the energy stored

in the foot must be returned into the load cell and actuator of the test machine rather than being dissipated as noise or heat.

These results contradict the work conducted by Geil (2001) whose study suggests a hysteresis level of nearly 25% for an Ossur Flex Foot. However as mentioned previously in this report, this work was conducted with little regard for the changing boundary conditions of the foot, in particular the ground contact point. The foot was mounted on slipping plates that could introduce errors into the data.

The results of this section suggest that there is little difference between the static and dynamic rating of an Ossur prosthetic ESR foot. Both the tests returned an almost perfect energy return efficiency and identical spring rates of 22.9N/mm.

It is clear that what can be termed 'dynamic' use for a prosthetic foot does not excite the foot at frequencies sufficient to cause a dynamic stiffening of the spring rate. Given the efficient nature of the foot in terms of energy return, it is also unlikely that any amputee is capable of driving the foot at a frequency that would cause dynamic stiffening and as such for the purpose of this project the stiffness of the foot shall be considered identical, regardless of static or dynamic use.

## 4.10 Chapter Conclusions

In order to quantify what could be considered 'dynamic' use of a prosthetic foot a wearable sensing system was developed, fabricated and tested, and through this means, true usage data was collected. This information defined the stance and swing phase timing of a specific amputee at a specific speed with one single style and model of foot. Additional information such as ground contact position of the metatarsal region of the foot was collected and this drove a series of laboratory tests designed to understand the dynamic nature of the prosthetic device.

This chapter has helped answer the research sub-question in section 2.1.1: **What are the mechanical characteristics of a prosthetic running foot?** Chapter 3 was able to describe how the spring rate of a prosthetic running foot is linear, but it is now known that the foot exhibits this same linear spring rate and energy return efficiency regardless of deflection speed (within reasonable limits as could be expected during amputee use). Further to this the ground contact point was shown to vary by over 100mm throughout the stance phase of the stride, equating to a change in spring rate of the foot of 249% (from 19.1N/mm at position 1 (20mm from the toe) to 47.5N/mm at position 3 (100mm from the toe)). This dramatic variation in spring rate would suggest that the action of an ESR prosthetic running foot is not so simple to be described adequately by Simple Harmonic Motion, given that this equation requires a single spring stiffness to be defined. This starts to address the research sub-question in section 2.1.2: **Is the claim that a foot mimics Simple Harmonic Motion legitimate?** However more work should be conducted before any conclusions are drawn in this respect.

Furthermore it is not yet known if the ground contact positions recorded in this investigation so far are typical of any amputee or usage profile, or if other factors will affect this value (for example mass of athlete, leg length, stride length, stiffness of foot, speed of running, etc).

This chapter has gone some way to improve understanding of the dynamic nature of prosthetic feet, but more work should be done to further this. The big challenge facing this investigation is that of the amputee athlete. If any parameters are to be changed (for example amplitude of oscillation or athlete mass) different amputee volunteers need to be found. However this introduces an infinite number of uncontrollable variables which is an area where previous research projects have struggled (see Chapter 1). Levels of amputation, limitations of individuals or even the availability of amputees who match the testing criteria all introduce uncertainty into the data produced.

Therefore the objective of the next chapter is to remove the amputee athlete from the equation and replicate an effective running action in a laboratory environment. A rig is designed and fabricated that can be used to test the changing of one variable at a time in a reliable and repeatable manner to define the characteristics of an ESR prosthetic running foot. By this means, the important factors that contribute to amputee running can be found and effective modelling of the running process should be made possible.

# CHAPTER 5: BRINGING RUNNING INTO THE LABORATORY

## 5.1 Introduction & Chapter Objectives

It was stated in the introductory chapters of this report that using amputee participants for the testing and analysis of prosthetic feet could be problematic, and it is clear that this approach has caused issues for other researchers (as discussed in the literature review, Chapter 1). An infinite number of uncontrollable variables are inevitably introduced that relate to subjectivity, repeatability, running style and the limitations of individuals. It was therefore deemed necessary to perform test work in a controlled laboratory environment at the earliest possible juncture in the project.

The objective of this chapter is to specify, design & validate a rig capable of replicating the dynamic response of a prosthetic foot during amputee running. This allows the variables that contribute to the response of a prosthetic foot to be manipulated and their effect understood. The research sub-question in section 2.1.2: **'Is the claim that a foot mimics Simple Harmonic Motion legitimate?'** can be investigated by the modification of those variables occurring in the equation for SHM (foot stiffness and mass) and the results compared with those anticipated and demanded by the equation.

Previously authors (Lehmann et al. 1993a,b; Noroozi et al. 2012a,b, 2014) have suggested the design of a dynamic response test fixture that aligns with the assumption of a spring-mass system. This means that for the purpose of analysis, the runner and foot makes up a simple spring-mass system with the intention of establishing a mathematical model for predicting foot response.

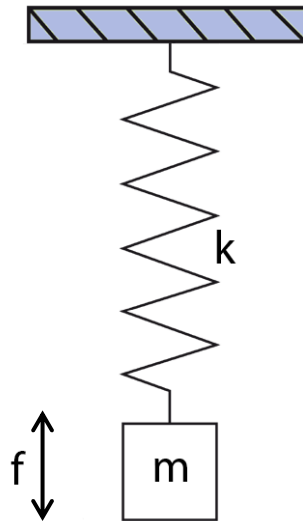


**Figure 5.1:** Basic ideal spring-mass system where  $f$ = frequency of oscillation,  $k$ = spring stiffness and  $m$ = mass

A representation of a basic spring-mass system is shown in figure 5.1. Assuming no losses the action of such a system is known to act according to Hooke's Law and thus the equation of Simple Harmonic Motion (SHM) as defined in figure 5.2.

$$\omega = \sqrt{\frac{k}{m}}$$

Which can be expanded for a function of oscillation frequency:

$$f = \frac{1}{2\pi} \sqrt{\frac{k}{m}}$$

**Where:**

$\omega$  = angular frequency (rads/s)

$f$  = frequency of oscillation (hz)

$k$  = spring stiffness (N/m)

$m$  = mass (kg)

**Figure 5.2:** Equation for Simple Harmonic Motion in ideal (zero losses) conditions  
(John R Taylor 2005, *Classical Mechanics*, P.163)

This equation can be rearranged to define the frequency ( $f$ ), mass ( $m$ ) or stiffness of the spring ( $k$ ). Assuming validity to this approach, a rig was designed that replicated this theoretical spring-mass system capable of 'Frequency Response Testing'. This is by contrast to the previous regime of test work that involved an Instron dynamic hydraulic test machine ('Driven Oscillation Testing'). During that series of test work the position of the foot was forced by a hydraulic actuator to understand the static and dynamic properties of the foot. A static spring rate, dynamic spring rate and hysteresis

loops were defined for the single category of Ossur Flex Run foot, but this did nothing to understand the 'response' of the foot. That is the characteristics of the unforced response of the foot to known inputs. Ideally a rig would be fabricated that would allow the reproduction of inputs (mass, deflection amplitude, foot stiffness) as defined by the amputee participant and the output (frequency response) could be compared to that measured during the testing of the participant. Once a correlation between the two systems (amputee and test rig) is established the true dynamic nature of the foot and the legitimacy of the suggestion of Simple Harmonic Motion can be understood.

The theoretical spring-mass system shown in figure 5.1 exhibits no losses and therefore purely requires an initial excitation in order to oscillate indefinitely. A rig would exhibit losses (by means of friction) and as such would require not only an initial excitation but also a source of input energy in order to maintain oscillation of the mass. As detailed in Chapter 1, Lechler et al. suggest:

*'The appropriate stiffness selection can reduce the metabolic cost when the driving frequency matches the resonance frequency of ambulation' (Lechler et al. 2008, P231)*

This view is shared by Lehmann et al. (1993a,b) and Noroozi et al. (2012a,b, 2014) but it has not been demonstrated conclusively. If the rig being designed and fabricated possessed the ability to record the timing and magnitude of input energy, this hypothesis could be proven. This could be as simple as a human interaction with the mass, applying a force in a timely manner to match the natural frequency of the system and allow the build-up of an oscillating displacement.

In order to define the dynamic nature of this system in a laboratory an exhaustive list of variables was compiled and captured, as detailed below:

- |  |   |
|--|---|
| <b>Mass applied to the system (kg)</b> | <b>Mass Displacement (distance moved) (m)</b> |
| <b>Stiffness of the spring (N/mm)</b>  | <b>Deflection of spring (m)</b>               |
| <b>Ground Reaction Force (N)</b>       | <b>Excitation force (N)</b>                   |

## 5.2 Rig Specification

It should be noted at this stage that to avoid confusing terms, 'deflection' refers to the change in distance between the shank and distal portion of the foot, whereas 'displacement' refers to the distance travelled by the mass of either the amputee or test rig.

The remit of this piece of work is to replicate the running action of the amputee participant, specifically the action of the prosthetic foot during the course of a single stride. The rig must be defined in a robust manner in keeping with engineering best practice. In summary, the design of the rig must allow for:

**- Up to 100kg mass to be applied safely.**

The runner used in the previous investigation at the time of testing had a mass of 83.0kg. Therefore to replicate his running action the rig should be able to withstand at least this mass to be applied. However in the interest of future testing and examining trends above and beyond the mass of this single amputee, a maximum capacity of 100kg was defined. The mass must be held in a stable manner to ensure that the operation of the device is safe for the user.

**- Effective boundary conditions to be maintained.**

In order to ensure parity with the previous test work and avoid unrepresentative tension build-up in the system the boundary conditions of the foot (specifically at the points where the foot interacts with the rig) must be controlled. This approach was taken for the Driven Oscillation Testing and can be found in Chapter 3.

- **A minimum of 200mm vertical displacement above the resting position of the foot.**

The vertical height achieved by the mass during testing represents the height gained by the centre of mass of the amputee during running. It is important to separate this from the height achieved by the prosthetic foot above the ground as this is influenced by flexion of the knee. Following video examination of amputee running it was deemed sufficient to allow for 200mm of vertical travel of the foot (ignoring deflection of the foot).

- **A variety of feet to be attached.**

Whilst the objective of this initial investigation is to reproduce the action of the amputee runner as defined previously, the rig should allow for future testing of other feet from the same and alternative manufacturers. Fortunately there appear to be only two mainstream foot attachment methods for prosthetic ESR running feet (pyramid mount & posterior mount). Examples of these are shown in figure 5.3.



**Figure 5.3:** Examples of posterior and pyramid-mounted feet (images source: Ossur.com)

The rig should possess the flexibility to adapt to these different mounting styles but not adversely affect the feet on test. They should be able to be mounted in an un-intrusive manner that does not require marking or damaging the foot.

**- A minimum calibrated resolution of +/-1mm for displacement/deflection instrumentation, +/-0.1N for load instrumentation and a minimum logging frequency of 100Hz.**

Any measurements taken from the system must be accurate to allow effective analysis following testing. All instrumentation must be calibrated before testing commences and a minimum logging frequency of 100Hz should be used in order to provide at least the same resolution as previous test work that was conducted. (Previously this figure of 100Hz was defined by the limitations of the data acquisition software of the Instron Hydraulic Testing Machine software). As previously stated (section 4.2.2) the action of a prosthetic running foot is understood to take place primarily in the sagittal plane. In addition, in order to simplify the system to be represented by a basic spring-mass system it was only necessary to allow the mass a single degree of freedom and travel in a purely vertical manner. However it must do so in a free and unrestricted manner in order to minimise any inefficiencies that might influence the results. Theoretically any inefficiency in the rig itself should be identifiable through the analysis of the data collected (by way of hysteresis curves from the force/displacement data).

## 5.3 Rig Design

### 5.3.1 Basic Design

A rig was designed, modelled and fabricated as shown in figure 5.4.

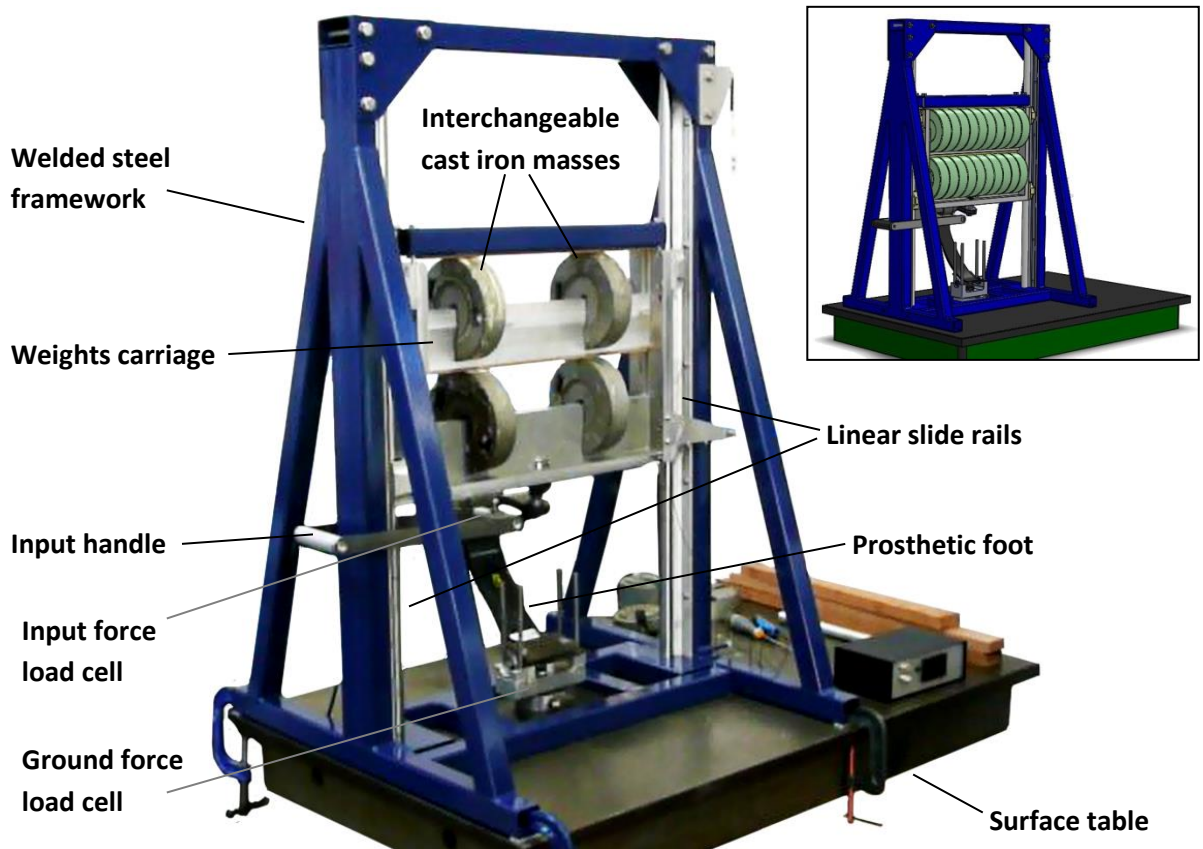


*Figure 5.4: CAD render and photograph of the frequency response rig with key components labelled.*

Figure 5.5 is a front view of the assembled rig and demonstrates the mode of action. Fundamentally this is a vertical sliding motion of a fabricated carriage that is able to securely retain various known cast iron masses that are commonly used in gym equipment, and on the lower edge a prosthetic foot can be mounted. Smooth action of the carriage is ensured with the use of ground linear slide rails with re-circulating ball bearings on each side.

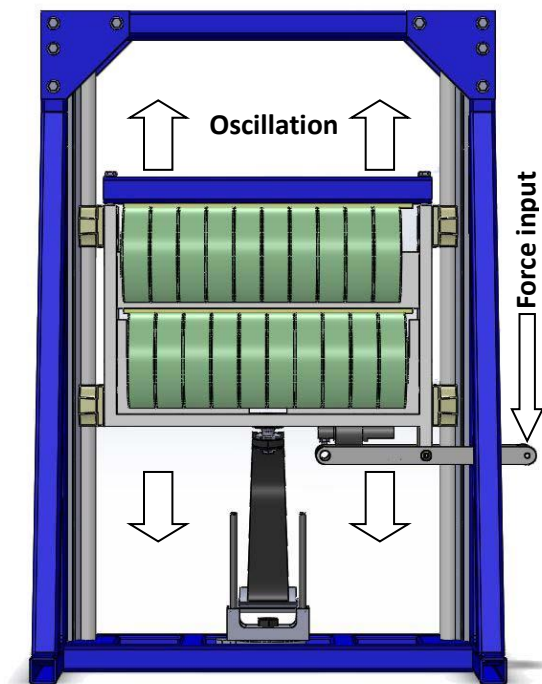


*Figure 5.5: Illustration of the designed mode of action of the frequency response rig design.*

Oscillation occurs when an input force is momentarily applied to the input handle. Energy is stored in the prosthetic foot and in accordance with the natural harmonic timing of the system is returned as gravitational potential energy. If a significant enough input force is again applied in a timely manner the resulting oscillation of the carriage will increase in amplitude. If the input force is not re-applied the amplitude of oscillation will inevitably decay until movement stops.

Although the principle of the rig is very simple there are a number of important details that ensure its function. Appendix 2 discusses the most important design aspects with information on fabrication and assembly.

### 5.3.2 Mounting of the Foot

As described in Chapter 3, when undergoing the forced oscillation testing the method of mounting the prosthetic foot on test is critical to ensure meaningful data. Most important is to allow the foot the required degrees of freedom at either end where it interfaces with the rig. Over constraint of the foot would result in tension build-up in the rig and this has the potential of adversely affecting the data gathered.

The correct mounting of the foot would result in purely vertical forces being applied to the rig in the -Y direction; this means all forces must be compressing the foot into the ground plane. At no point should the rig be subjected to lateral or torsional modes. In order to ensure this, three things must be provided:

- 1. All mounting points must be aligned with the vertical centreline of the rig**
- 2. The interface between the rig and foot at both medial and distal ends of the foot must be allowed to rotate in the sagittal plane.**
- 3. The distal (toe region) mounting point of the foot must be allowed to leave the ground plane if the energy stored in the system should be sufficient. This is to replicate the foot leaving the ground during amputee running.**

In order to accommodate for these requirements the foot was mounted using an automotive suspension ball joint at the medial end (at the shank) and between a pair of ball bearing races at the distal end. Importantly the saddle that cradled the ball bearing races at the distal end of the foot was located rigidly on the centreline of the rig and directly below the centre of the ball joint that attached the medial end of the foot to the chassis of the carriage. The ball joint in turn was mounted directly in the centre (in both X and Y directions) of the base plate of the carriage. This ensured that no lateral or torsional forces could be exerted on the carriage. This arrangement can be seen in the CAD model shown in figure 5.6. The view is sectioned for clarity with an Ossur Flex Run (category 6Hi) prosthetic foot installed.

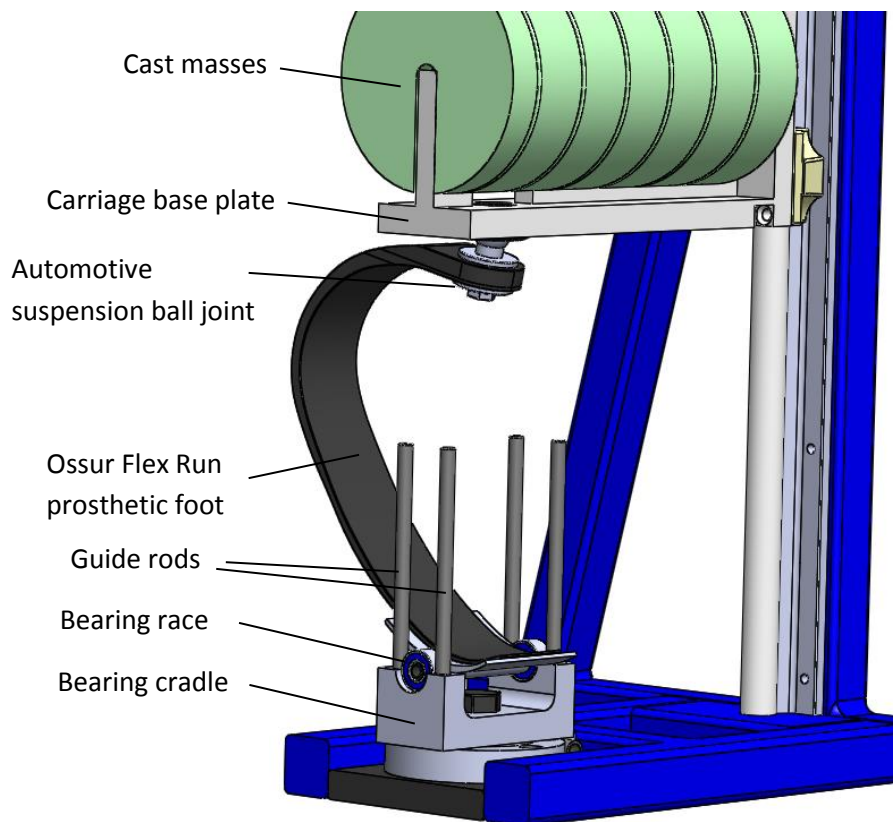


**Figure 5.6:** Cutaway CAD sectional view of the foot mounting arrangement. This setup ensures that the foot is allowed the relevant freedom of motion and the centreline of force is always aligned with the centreline of the rig.

To permit the free movement up away from the ground plane and allow the simulated effect of the runner's foot leaving the ground the bearing races were not captive but instead were cradled in machined cups. If the system possessed enough energy for the foot to leave the ground it was free to do so. However the distal end of the foot (and

bearing races) could not deviate from the centreline of the rig because of four guide rods inserted into the bearing cradle, one on each side of each bearing. This arrangement meant that if the bearings left their respective cradles, when the foot dropped again the bearings would return and relocate in their original positions. This action is demonstrated in figure 5.7.

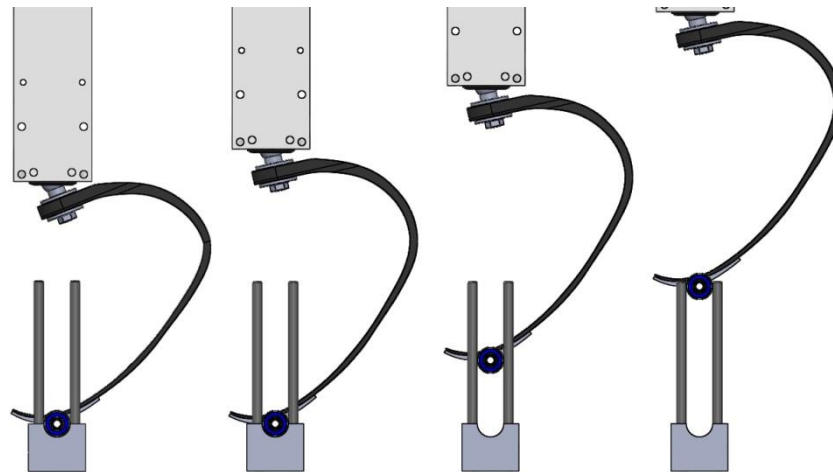


**Figure 5.7:** Diagram demonstrating the action of the foot during testing, and how the toe is free to leave the ground plane but can never deviate from the centreline

The medial end of the foot could be mounted to the ball joint by simply using the 12mm hole provided by the manufacturer for attaching the shank adapter. However the distal end of the foot has no features suitable for attaching any test hardware.

As such, a similar approach to mounting the foot was taken as used in the previous forced oscillation testing (Chapter 3) with the toe of the foot securely held in a purpose-built clamp. The clamp was fabricated from steel and machined such that the bearings were held in place using circlips. It was profiled so not to mark the finish of the foot on test. The clamp with bearings and bearing cradle can be seen in figure 5.8. This setup also means that throughout testing the effective ground contact point of the foot remains unchanged. This is important because, as defined in Chapter 4, as the ground contact point of the foot changes so too does the spring rate of the foot.

This approach relies on the bearing races (and associated brackets to clamp the foot) to be attached at the toe, adding an unrepresentative mass. During amputee running it is imperative that this portion of the foot is as lightweight as possible. This is because

throughout the course of a single stride the toe of the foot is subject to acceleration from toe-off through the swing phase to foot strike. Additional mass at this location would result in additional (perhaps unnecessary) energy expenditure by the amputee. However adding mass at this location on the rig is theoretically irrelevant for the purpose of recording the response time of the foot. Firstly this is because the swing phase does not exist (with the foot acting in a purely guided vertical plane). The second reason is that the response timing of the foot is defined by the ground contact time. During this period of ground contact the toe (and associated hardware) is effectively massless, being in contact with the ground plane. The response of the foot is dependent on the mass attached to the shank of the foot instead. It is anticipated that the natural oscillation of the unloaded foot be different to that witnessed during amputee running (as demonstrated in figure 4.2 & 4.3 when the foot is not in contact with the ground plane) but this can have no effect on the response time of the foot.

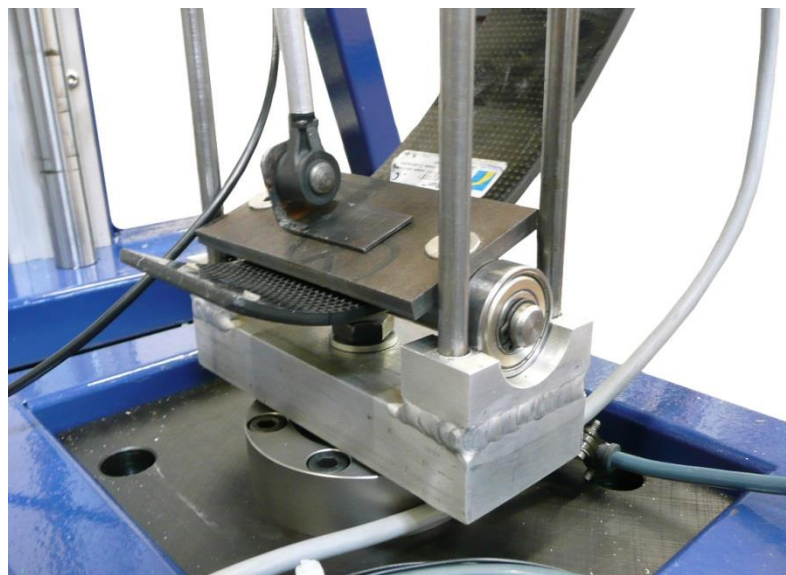


**Figure 5.8:** Photograph of the toe clamp that un-intrusively fixes to the distal portion of the foot and defines the ground contact point. Also visible is the load cell that measures the ground reaction force.

The practical result of this arrangement is that the ground contact point has to be defined prior to any test work being carried out. This is the topic of section 4.6 and is of great importance to the success of this investigation.

Below the bearing cradle as can be seen in figure 5.8 is the ground force load cell. This load cell is responsible for providing a reading of load going through the foot and is rigidly attached to the bearing cradle using a single screw. More information on this load cell and the other measurement devices used on the rig can be found in the following section and in Appendix 3.

### 5.3.3 Instrumentation

In order for the dynamic response of the foot to be understood a number of variables should be observed. As set out in section 5.1 these are shown again in table 5.1 along with details of the respective piece of instrumentation. Details of each are then given in Appendix 3 including information on calibration and set-up.

Variable Name	Units	Instrumentation	Manufacturer	Model	Working Range	Processing Hardware	Logging hardware
Mass applied to the system	kg	Ground force load cell & visual check	Applied Measurements Ltd	DSCR	10kN	In-house amplifier	MSR-165 datalogger
Ground Reaction Force	N	Ground force load cell					
Excitement force	N	Input force load cell	Thames Side	T66	100kg		
Distance travelled by mass	m	Linear resistive transducer	In-house design & fabrication	N/A	0 - 300mm		
Displacement of foot	m	Vario-resistive foot mounted sensor	Hartmann Automotive GmbH	8W83-3C279-BC	-45°/+45°	N/A	

**Table 5.1:** List of variables to be measured and the associated piece of instrumentation apparatus

## **5.4 Rig Validation: Can this rig be used as a valid comparison to amputee running?**

### **5.4.1 Introduction**

Before more investigative work can be conducted the validity of the rig as an alternative to amputee running should be evaluated. The reason for fabricating the rig is to allow the controlled testing of feet without the need for using an amputee. Variables (such as the mass applied, deflection amplitude and ground contact points) can be modified in a repeatable and iterative manner and the response of the foot can be examined. As mentioned in section 5.1 using amputees for comparative analysis has caused problems for researchers in the past and it is the intention of this investigation to avoid a repeat of such issues. However the rig makes some assumptions and the precise action is clearly different from a real-world environment in which no two steps are the same. For example the rig as described in section 5.3 can only allow a single ground contact point of the foot whereas it was proven in Chapter 4 that this is not the case in amputee running.

The most effective and robust manner of validating the rig is to attempt to replicate the action of the amputee runner as observed in section 4.4. This will give a direct comparison between the runner and the rig and allow conclusions to be drawn as to the effectiveness and suitability of further study using the rig.

As described in Chapter 4, during testing on flat level ground in a controlled environment the amputee runner exhibited the running characteristics (averaged values over 8 strides) as shown in table 5.2. This table indicates the key parameters that describe the running. It is these six parameters (highlighted in red) that should be replicated if the rig is to effectively match the amputee. Of these six parameters, three of them are purely a matter of using the same foot and adding mass to the carriage as to replicate the mass of the amputee.

<b>Height of runner</b>	180cm
<b>Weight of runner</b>	83kg
<b>Cadence of runner</b>	1.08 Hz
<b>Time for a single stride</b>	728ms
<b>Time for stance phase</b>	242ms
<b>Time for swing phase</b>	486ms
<b>Model of foot</b>	Ossur Flex Run
<b>Category of foot</b>	6 Hi
<b>Maximum displacement</b>	69.7mm
<b>Ground reaction force</b>	1.70kN

**Table 5.2:** Running characteristics of the amputee athlete during testing in Chapter 4

The remaining three are *stance phase timing* (or more appropriately in this instance 'ground contact time' as there is no stance phase of which to speak in the absence of a runner), *maximum foot deflection* and *ground reaction force*.

It is unrealistic to enter into this investigation assuming that all three of these variables can be matched. In reality only one can be purposefully replicated to that measured during amputee running. The remaining two variables will present themselves as a result of this first variable and the conditions of the foot and rig. For example if the rig were exercised with a progressively larger amplitude of the carriage until a ground reaction force of 'x' were achieved, the resulting ground contact time and maximum foot deflection could only be measured as a result of this ground reaction force. And the same is true if one of the other two variables were chosen as the driver.

Of these three variables, the most practical to choose as the driver is *maximum foot deflection*. This can be easily viewed by the operator during testing without the need for additional instrumentation by simply marking one of the stanchions of the test rig. The input handle runs very close to the framework and forms an excellent visual point of reference for amplitude achieved.

## 5.4.2 Ground Contact Point

One additional variable to take into account before testing can commence is that of the ground contact point. As demonstrated in section 4.4.2 the contact point that the foot holds with the ground varies throughout the stance phase of a single stride. While testing with the Ossur Category 6Hi foot and a single amputee athlete the contact point was shown to travel from over 100mm posterior of the front tip of metatarsal region of the foot (toe region) to the tip. However the rig is not capable of dynamically altering the contact point of the foot with the ground during the period of a single oscillation. Therefore as mentioned in section 5.3.2 a single ground contact point should be defined at which all testing must take place. Previously for the purpose of comparing static and dynamic characterisation (using the Instron test machine as part of the forced oscillation testing) this point was chosen to be 40mm from the distal end of the toe (section 4.7). However this figure should be revisited now that direct comparison with the amputee is being undertaken.

The main purpose of this specific investigation is to establish if the amputee and the rig can be effectively compared for the basis of future work. This requires the maximum values to align; the maximum foot deflection amplitude, maximum ground reaction force, maximum deflection timing, etc. Logically therefore the ground contact point chosen should be that which results at this same point of maximum foot deflection (& displacement)/ ground force during normal running use.

As mentioned in section 4.8 it was found that the timing of maximum deflection of the prosthetic foot during amputee running occurred (within measurable limits) exactly at the midpoint between heelstrike and toe-off. As shown in table 5.2 the total stance-phase time was 242ms meaning that maximum deflection must occur at  $242 / 2 = 121\text{ms}$ .

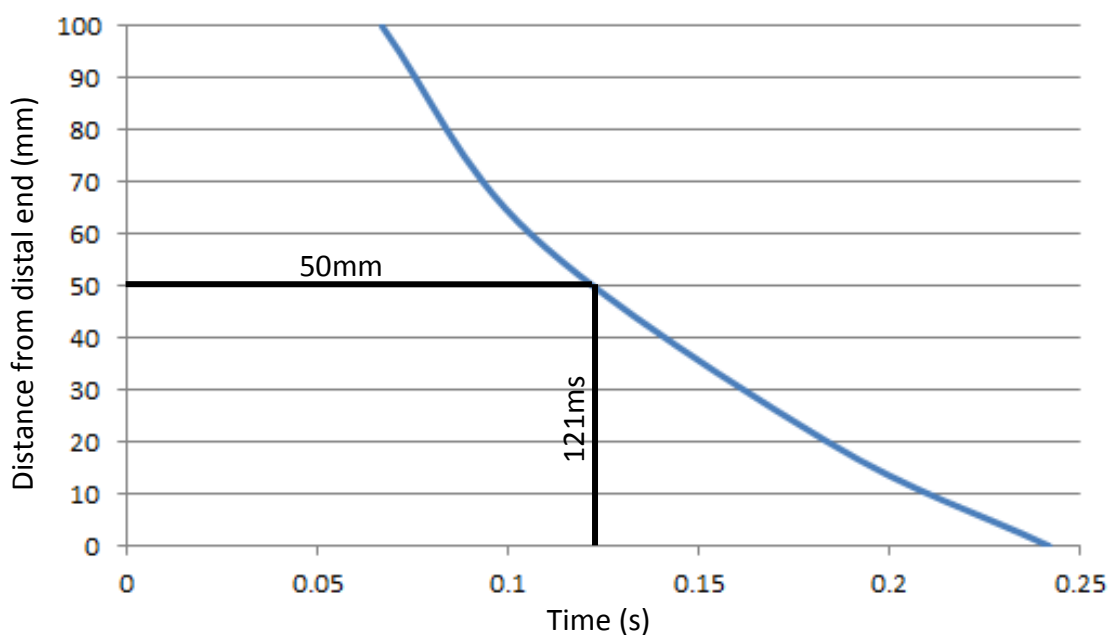


**Figure 5.9:** Curve demonstrating the shift in ground contact position relative to the distal end of the foot (toe region) with mid-stance position indicated

Using the graph defined in section 4.4.2 and shown in figure 4.4 (also figure 5.9) it can be seen that at 121ms after heelstrike the ground contact point of the foot is 50mm posterior of the tip of the foot. Therefore it was at this point that the toe-clamp portion of the rig was attached.

This modification in ground contact point is also the reason for the change in maximum deflection. The amputee testing conducted in Chapter 4 (and subsequent single point foot characterisation (section 4.7)) defined the maximum deflection of the foot as 72mm at a ground contact point of 40mm from the toe. The ground contact point for the purpose of this test work is being changed to 50mm from the toe meaning that this overall deflection value of the foot is invalid. The single point characterisation testing (as conducted in section 4.7) was repeated but with a ground contact point of 50mm rear of the toe. The resulting maximum deflection value was 69.7mm and it is this value that is to be replicated by the rig.

### 5.4.3 Method

Figure 5.10 shows the test setup with the masses added to the carriage of the rig. The carriage has a mass of 16.0kg before any additional weights are added. Therefore to achieve a total mass of 83kg a further 67kg are required. A summary of the test conditions is shown in table 5.3.



*Figure 5.10: Apparatus set-up to replicate the mass of the amputee athlete.*

The logger was started and the carriage exercised up and down using the input handle. Force was applied downwards on the input handle and it quickly became apparent at what moment in the oscillation cycle the force should be applied to ensure the most efficient build-up of energy in the prosthetic system. This coincided with the natural harmonic resonance of the system and is the subject of further discussion in this chapter. Energy was applied in this timely manner until the target maximum foot deflection was achieved. As discussed previously a mark was added to the right-hand

stanchion where the edge of the handle passes at 69.7mm below the unloaded condition of the foot to act as a visual reference to the user.

Test Conditions	
Test Name	Running Replication
Foot on Test	Ossur Flex-Run Cat6Hi
Carriage Mass	16kg
Added Mass	67kg
Total Mass	83kg
Driving Variable	Foot displacement
Variable Value	69.7mm

**Table 5.3:** Test conditions for replicating amputee running

When the edge of the handle coincided with this mark the maximum deflection value had been reached. Having the required deflection been achieved it was found that the input force could be reduced in order to maintain the desired amplitude. This is demonstrated in figure 5.11 which is a trace of handle input force and foot deflection against time.

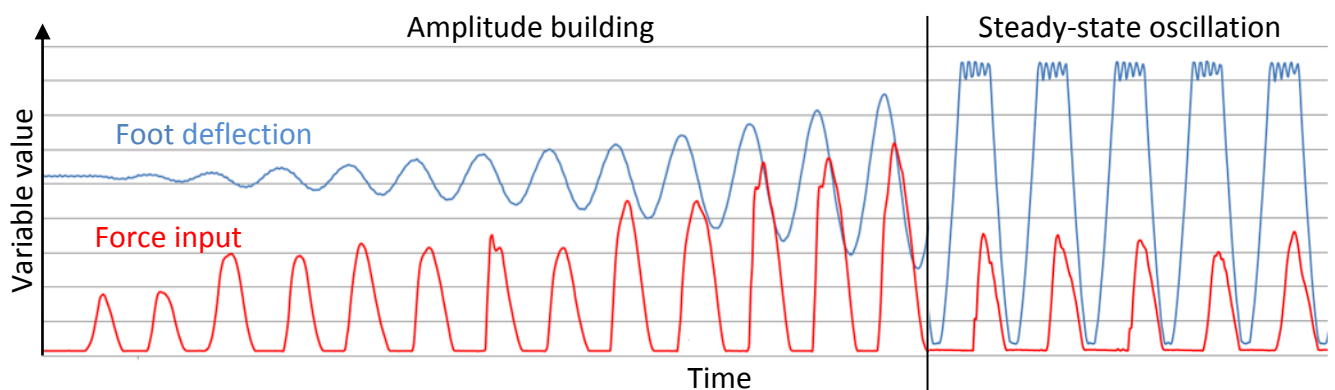
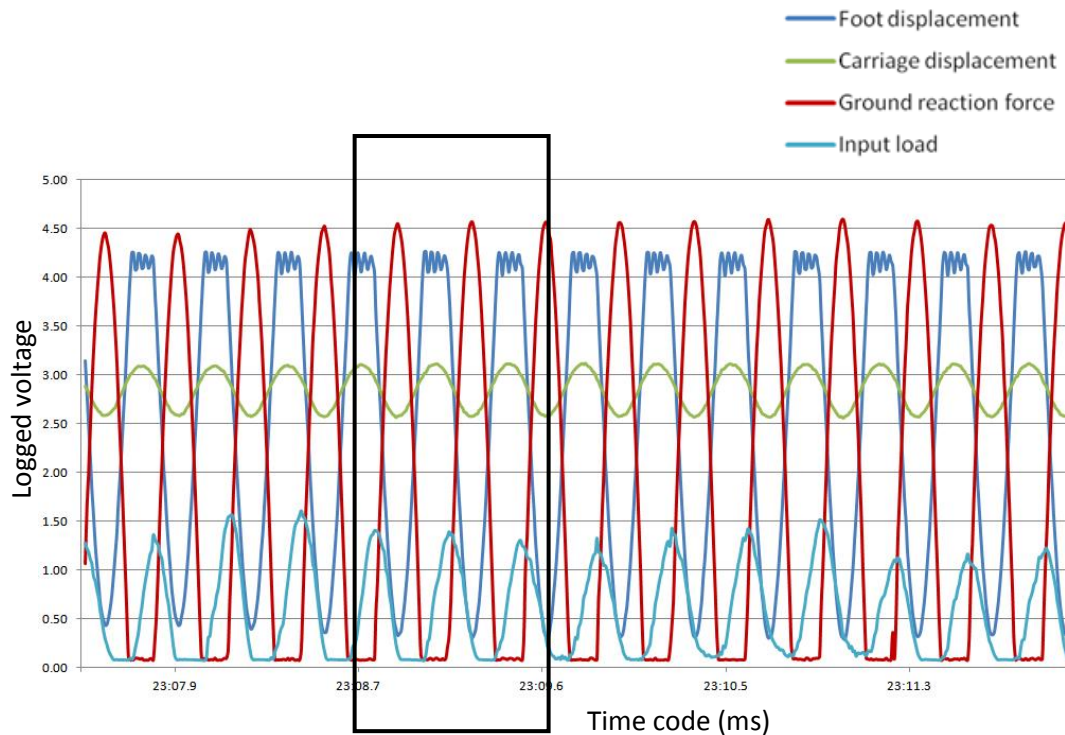


**Figure 5.11:** Graph demonstrating the input force required to build-up the amplitude of oscillation of a prosthetic foot mounted on the test rig, compared with that required to maintain steady-state amplitude

After approximately 15 full-displacement oscillations of the carriage the input force to the handle was removed and the carriage was allowed to settle, the amplitude of oscillation decaying naturally. Once the carriage was stationary the logger was stopped and the data could be collected.

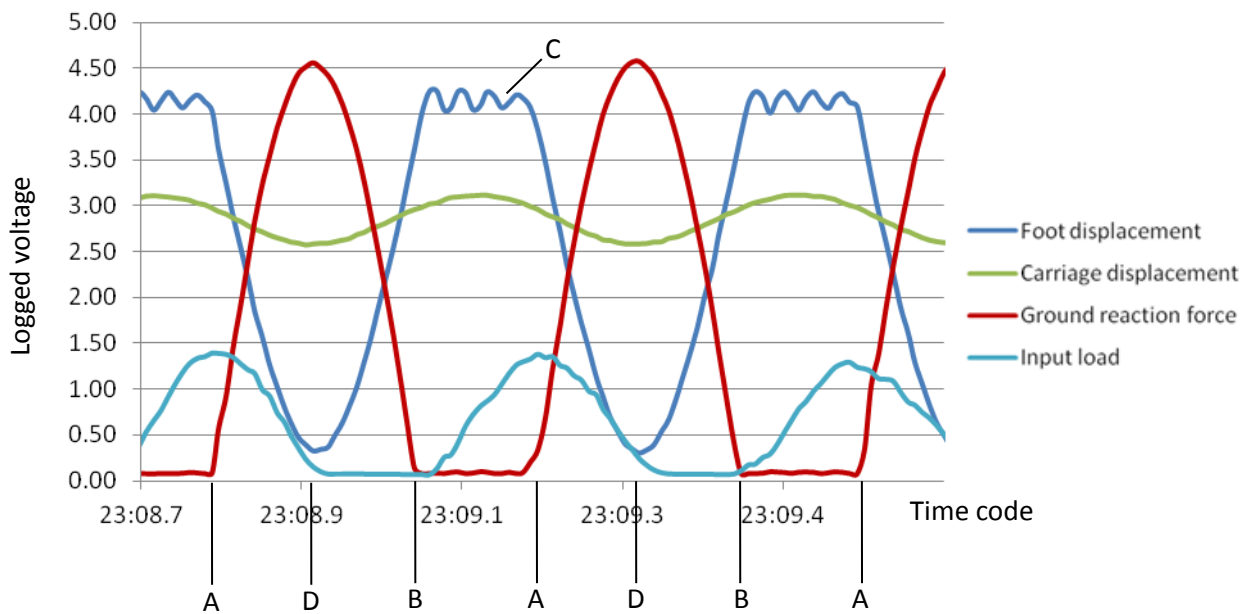
#### 5.4.4 Results

Figure 5.12 shows the raw data that was collected for the 15 full-displacement oscillations. The X-axis is the time code as generated by the data logger and the Y-axis is displayed in volts as collected by the data logger.



**Figure 5.12:** Raw data captured from all four logged channels with isolated oscillations (figure 5.13) shown

The data displays well on the graph with few or no apparent anomalies. However it is difficult to interrogate when shown in this manner. In order to understand the dynamic action of each of the variables a smaller sample of this trace is shown in figure 5.13 with some of the key points labelled. Shown are two full 'strides' (or complete oscillations) of the rig with all four channels overlaid. The X-axis is still expressed as the time code generated by the data logger and the Y-axis expressed in voltage as logged, and the important events of the stride are labelled.



**Figure 5.13:** Isolated oscillation cycles from figure 5.12 with key stride events labelled A, B, C, D.

Point A is the equivalent of heelstrike in amputee running (for comparison an equivalent trace for amputee running with labels can be seen in figure 4.2). This is the moment the foot first touches the ground plane and deflection begins. At this point the mass is moving in the -Y direction at its maximum velocity. At point A it can be seen that the foot deflection and ground reaction force react simultaneously and mirror each other in an opposing apex.

The moment of maximum foot deflection (and maximum ground reaction force) is labelled as D at which point the velocity of the carriage is zero and the kinetic energy of point A has been converted into potential energy stored in the foot. The carriage changes direction and accelerates towards point B; the equivalent of toe-off in amputee running.

The foot leaves the ground plane and as it does so the toe of the foot, now unsupported by the rig, enters its own resonance. This harmonic is visible on the trace of foot deflection as measured by the vario-resistive sensor mounted to the foot and is labelled as point C. Before the resonance has time to decay to zero the carriage returns towards the ground plane and once again the toe of the foot comes into contact with the ground reaction force load cell and is shown again as point A.

Throughout this single oscillation the carriage displacement can be seen as a smooth sine wave and the trace of force input from the handle can also be seen. As described in section 5.4.3 the timing of the input force was entirely dictated by the operator.

In order to generate more meaningful data from this information the time code was converted into milliseconds and each channel converted into a value of its native unit by using the specific calibration equation as generated in Appendix 3. Additionally the X and Y values of each of the measured variables was split and displayed on a separate graph. Only the centre ten oscillation cycles were used for data analysis to ensure the 'warm-up' (amplitude build-up) and 'warm-down' (amplitude decay) phases did not influence the data. The maximum value achieved by each variable for each oscillation during test was recorded and the mean calculated, as shown in figures 5.14 to 5.17.

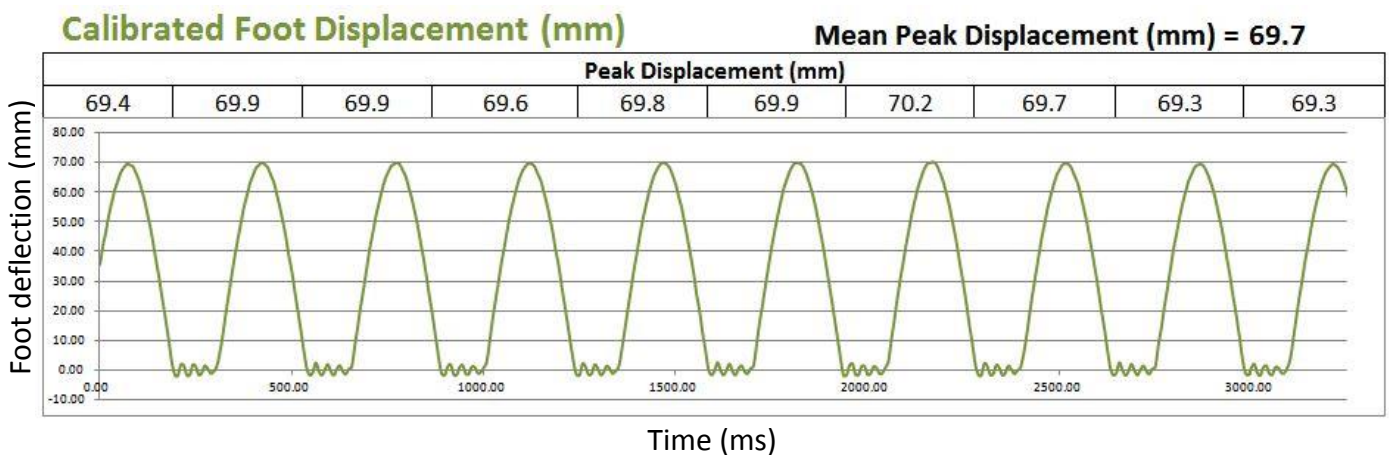


**Figure 5.14:** Trace of foot deflection (83kg)

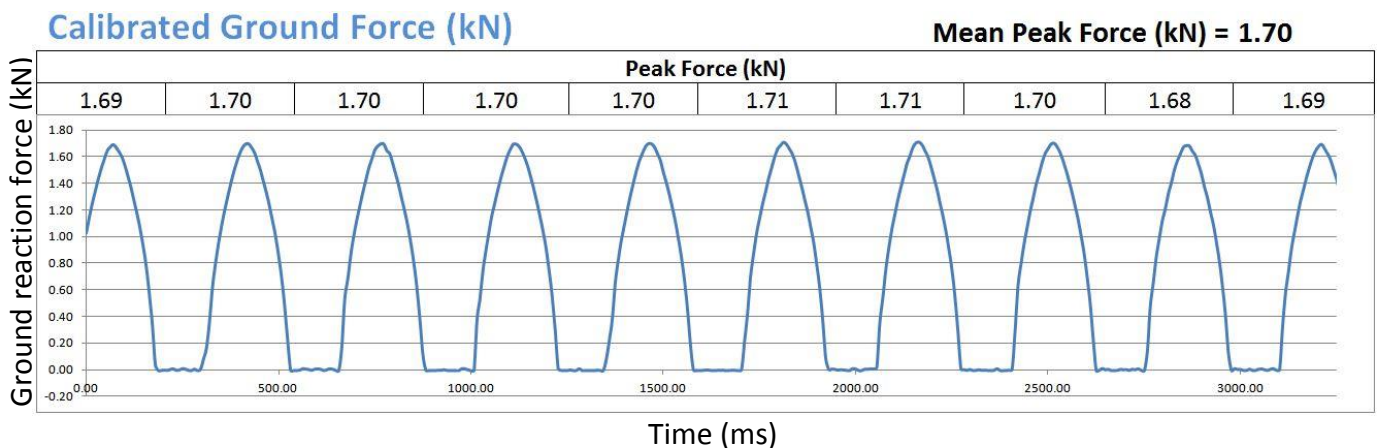


**Figure 5.15:** Trace of ground reaction force (83kg @ 69.7mm)

### Calibrated Input Force (N)

Mean Peak Force = 43.5

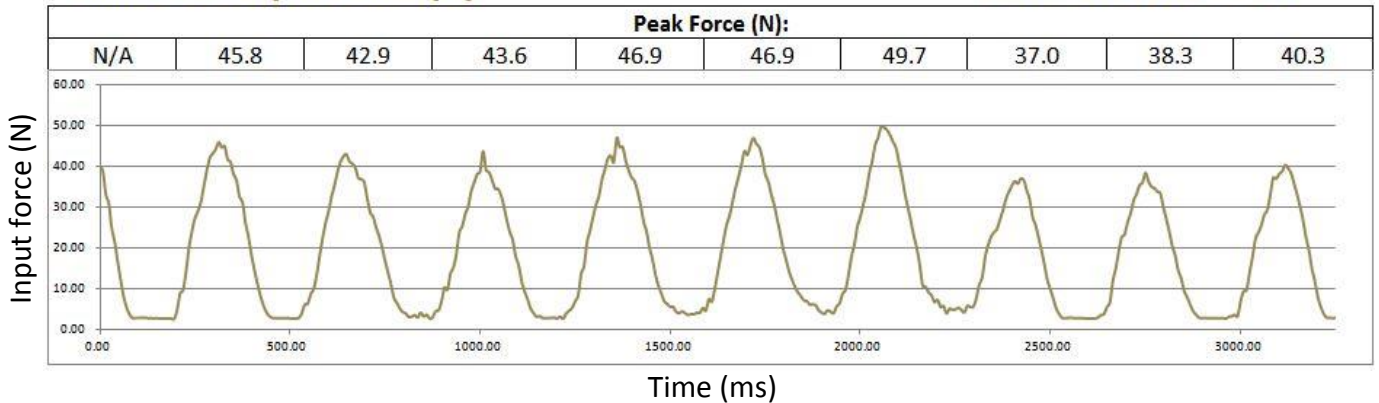


**Figure 5.16:** Trace of input force (83kg @ 69.7mm)

### Calibrated Carriage Displacement (mm)

Mean Peak Displacement = 9.5  
Mean Trough Displacement = 70.1

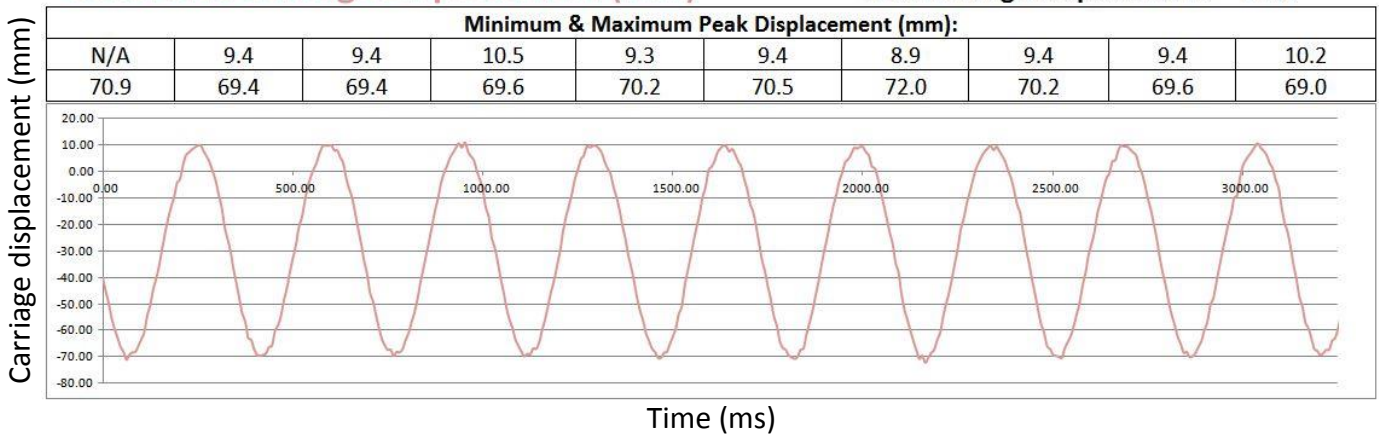


**Figure 5.17:** Trace of carriage displacement (83kg)

Important to note is that due to the offset of the peaks of the various traces, the input force (figure 5.16) and the carriage displacement (figure 5.17) only feature 9 peaks instead of 10. The mean peak of each of these traces was calculated and is tabulated in table 5.4 where it is compared with the values obtained from the amputee athlete who was being mimicked.

As shown in table 5.4, if the maximum mean values are examined, within measureable limits the running action of the amputee subject is identical to the oscillation of the rig. For the purpose of this investigation the driving variable was foot deflection; this is the variable that was set out to be replicated from the recorded amputee running of

section 4.3. As can be seen in figure 5.14 the intended value of 69.7mm was not always perfectly achieved (as is inevitable with a human-operated system) but over the ten measured oscillations the mean value is ideal. The ground force is also identical which stands to reason. If the foot deflection is the same, then for this given deflection the force exerted must also be the same as previously measured. Above all, this result serves to confirm the repeatable setup of the foot deflection instrumentation and the accurate calibration of the ground force load cell.

Variable name	Averaged Peak Value		
	Rig Measurements	SD	Amputee Measurements
Ground Force (kN)	1.70	0.01	1.70
Foot Displacement (mm)	69.7	0.28	69.7
Minimum Carriage Displacement (mm)	9.5	0.49	N/A
Maximum Carriage Displacement (mm)	70.1	0.89	N/A
Input Force (N)	43.5	4.28	Unknown
Stance Phase Timing/Ground Contact Time (ms)	235 - 245	0	235 - 245

**Table 5.4:** Averaged data over 10 strides for rig vs. amputee running with identical input conditions (values of Standard Deviation listed).

It is logical to expect the recorded values of foot deflection and carriage displacement to align as it is the displacement of the carriage that is driving the deflection of the foot, but there is a discrepancy of 0.4mm. This could be a measurement or calibration error, but more likely it is a result of the misalignment between the medial mounting point of the foot to the base of the carriage and the centreline of the deflection transducer attached to the foot. As shown in figure 4.1 the setup of the deflection transducer requires the pivot of the rotary transducer to be directly below the centreline of the shank adapter used for attaching the foot to an amputee, but this is when the shank is perfectly vertical. When installed in the rig the shank is not vertical and indeed when the foot goes through deflection the shank portion of the foot rotates in the sagittal plane. The result of this is that the pivot of the rotary deflection transducer can never perfectly align with the centreline of the rig and as such will inevitably measure a small error when compared with the true vertical motion of the carriage. However it should be noted that for the purpose of this investigation it is the deflection of the foot that is more important as it is this variable that is being directly compared with what was measured during amputee testing.

Equally important is the apparent ability of the rig to replicate the timing of the amputee. The ground contact time between the amputee and the rig is identical (to the nearest 10ms). At a logging frequency of 128Hz it is impossible to differentiate between the two. This apparent replication of running style can be examined further by comparing the foot deflection data for the entire stance-phase and is shown in figure 5.18. Data from ten strides (in the case of the amputee)/oscillations (in the case of the rig) is averaged in to a single set and the two resulting curves are overlaid.

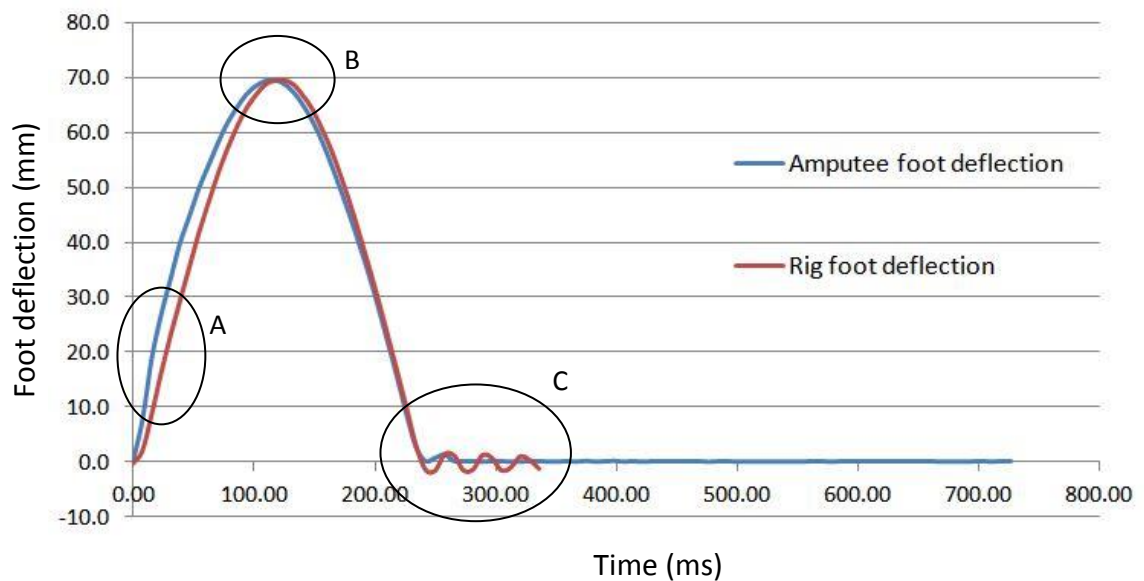


**Figure 5.18:** Traces of foot deflection (83kg) for both the rig and amputee testing phases

Figure 5.18 illustrates that whilst the overall ground contact time of the foot is identical between the rig and the amputee there are some notable differences in how the deflection of the foot progresses over the period of a single stride.

Firstly when the foot first comes into contact with the ground the rate of deflection is greater during amputee running than it is on the rig (labelled A in figure 5.18). This is particularly apparent at the very early stages after heelstrike. However at approximately 30mm deflection this situation changes and it appears that the gradients of both traces become aligned. The data shows that the foot measured during amputee running reaches its point of maximum deflection fractionally before that from the rig (labelled B), but after the apex it can be seen that the opposite is

true. The steeper gradient belongs to the data from the rig and as a result the two traces tend towards each other until they reach 0mm deflection at the same time.

This phenomenon is a result of the ground contact point changing along the metatarsal region of the foot. Discussed in section 4.4.2 as the stance phase of a single stride progresses during amputee running the point at which the foot contacts the ground changes, tending towards the distal end of the foot until toe-off occurs. However the rig set-up uses a single effective assumed ground contact point. As such, when the amputee first lands (heelstrike) the portion of the foot that touches the ground first is posterior to that point used on the rig. This results in a decreased lever-arm ratio of the foot which equates to a higher relative stiffness and as such an increased rate of deflection. As the ground contact point progresses forward towards the anterior edge of the foot the reverse is true. The effective stiffness of the foot becomes progressively less and the subsequent rate of deflection lower. The moving ground contact point exhibiting itself in this way and the fact that both feet exhibit the same ground contact time adds validity to the assumed ground contact point used on the rig (discussed in section 5.4.2).

The second notable difference is the resonance that occurs after toe-off (when the foot leaves the ground, labelled C in figure 5.18). Both methods of testing exhibit resonance at this stage of the stride but the nature of this oscillation is different. During amputee testing it was apparent that the toe underwent one or two progressively decaying oscillations. During rig testing however this changed to four distinct and marginally decaying oscillations at significantly greater amplitude. The oscillations are always arrested by the foot coming into contact with the ground plane once more.

This harmonic disparity is a result of the different setup of the two investigations. During amputee testing every effort was made not to add mass to the distal end of the foot so not to influence the running action of the individual. Added mass at the distal end of the foot might have affected the swing phase of the stride as the amputee works to reposition his foot. However during rig testing the mounting of the foot was a critical concern and (as discussed in section 5.3.2) hardware was added to the

metatarsal region in order to clamp the foot. This hardware included the two bearings that allowed the rotational degree of freedom in the sagittal plane as required by the mounting strategy that was used. The addition of the extra mass at the distal end of the foot serves to slow the resonant frequency of the toe in accordance with the equation for simple harmonic motion (figure 5.2). Furthermore this additional mass stores more energy than the smaller mass of the toe alone and therefore forces a larger deflection following toe-off.

The third difference is that of the duration of 'zero deflection' following toe-off. This is represented by the length of each of the traces. However this is easily explained as what is probably the greatest difference between testing using an amputee and on the rig. The traces shown in figure 5.18 illustrate the duration of a single stride or oscillation. On the rig the foot returns to the ground plane after approximately 330ms to begin another cycle. However the foot of the amputee does not come into contact with the ground until approximately 720ms because the process is interrupted by the action of the contralateral leg. The foot of the amputee is in the air for a significantly longer time whilst the other leg is undergoing the stance phase of the stride.

## 5.5 Characterisation of Rig Efficiency

It has been suggested that the rig operates in accordance with the equation for Simple Harmonic Motion (section 5.1) but this equation does not account for any losses. It has been established in Chapter 4 that the foot itself is >99% efficient in terms of its energy return, but when considering the measured response of a more complex system (such as the foot mounted to the rig) the entire system should be taken into account. Rig components are restrained with various devices (for example linear slide rails with recirculating ball bearings), all of which inevitably subtract from the overall efficiency by means of friction.

The efficiency of the rig was ascertained using three separate methods:

**Method 1: Hysteresis curves**

**Method 2: Input energy vs. stored energy**

**Method 3: Carriage amplitude decay**

Detail of the methods used for evaluating the efficiency of the rig can be found in Appendix 4 with an overview provided in table 5.5.

Method 1: 88.9%	}	<b>Mean value = 89.4%</b>
Method 2: 90.3%		
Method 3: 88.9%		

**Table 5.5:** Results of the three separate methods for determining rig efficiency

## 5.6 Chapter conclusions

It has been demonstrated that the rig is capable of closely mimicking the action of an amputee runner during steady-state running, assuming that the following are true:

- *The mass of the runner is equivalent to that of the carriage (with masses attached)*
- *The same (or an identical) foot is used*
- *The ground reaction force OR foot deflection is copied*
- *The ground contact point selected to represent the running action is equivalent to that achieved at the point of maximum foot deflection during amputee running (in this case 50mm rear of the toe tip)*

If these four conditions are satisfied this rig can effectively replicate the running action of an amputee runner and return the same ground contact time. This establishes a known and understood link between the rig and amputee, but at this stage it is not useful for working backwards; this means using the rig to predict how an amputee will run. The main reason for this is that the amplitude of deflection of the foot will vary depending on how much energy the amputee is exerting. For instance it has been shown that the ground force maintained by a runner increases at higher velocities (Munro et al. 1987; Keller et al. 1996). This change in load will inevitably result in a change in amplitude of deflection of the foot, but it is not yet understood if this change will result in a modified ground contact time. In other words, if the ground contact time changes for different values of foot deflection, the rig can only be used to predict one if the other is known. The ground contact time can be demonstrated if the foot deflection is known and vice versa.

It has also been shown that if a small input force is applied in a timed and sympathetic manner to the prosthetic spring-mass system the amplitude of oscillation (and therefore energy stored in the system) increases. This agrees with the hypothesis stated in section 5.1 and the views of Lechler et al. (2008), Lehmann et al. (1993a,b) and Noroozi et al. (2012a,b, 2014). This baseline of energy input is required to maintain the amplitude of oscillation and overcome the frictional inefficiency of the rig (defined in section 5.5 as 10.6%). If greater amplitude is to be achieved, a greater force

input is required (in the same timely manner) as can be seen in figure 5.11. If the input force is removed the amplitude of oscillation will decay to zero according to the frictional losses in the system. The system can be seen as being grossly under-damped (more information on the efficiency of the system can be found in Appendix 4) and as such the frequency response contribution from the effective damping of the system is considered negligible and has been ignored.

The objective of this chapter was to design and fabricate a rig that was able to mimic amputee running and would allow individual variables to be modified. This objective has been satisfied and the rig can now be used to not only improve our understanding of amputee running but more specifically help answer the research sub-question set out in section 2.1.2: **'Is the claim that a foot mimics Simple Harmonic Motion legitimate?'**

If an amputee can be compared to a spring-mass system as authors have previously suggested then the ground contact time will be predictable in accordance with the equation for simple harmonic motion (section 5.1). This states that for a given mass and spring rate the frequency of the system (and therefore ground contact time) will remain constant regardless of fluctuations in amplitude (ignoring any losses). It is therefore critical to the progress of this thesis that further investigations are conducted to understand if the equation for SHM can be applied to amputee running. Individual variables can be manipulated and the response time observed to establish if SHM is a valid trend.

Furthermore the ground contact point assumed for this amputee athlete (50mm rear of the tip of the toe) could change depending on running velocity, foot deflection, stride length, stride frequency or even the individual set up of the prosthetic foot. Previously it was shown that the change in ground contact point (and therefore the boundary conditions) has a dramatic effect on the effective stiffness of the foot. Additional investigations should address this in order to understand both the magnitude of change of the ground contact area for different styles of running (across a range of speeds, stride lengths, etc) and how relevant this change would be to the measured frequency of oscillation.

# CHAPTER 6: INVESTIGATING SHM VARIABLES

## 6.1 Introduction & Chapter Objectives

Previous studies (Lehmann et al. 1993a,b, Noroozi et al. 2012a,b, 2014) have suggested that the action of an ESR prosthetic foot can be assumed to act according to the equation for Simple Harmonic Motion. This equation can be seen in figure 5.2 and relies on the values of two variables to provide a value of frequency of oscillation of a spring-mass system, namely Mass ( $m$ ) and Spring Stiffness ( $k$ ).

Having established a connection between amputee running and the frequency response rig (section 5.4.4), the rig can be used to explore how applied mass and spring stiffness affect the frequency response of the prosthetic foot. Investigations can be conducted to test the response of the foot across a range of applied masses or foot stiffness values to understand if the observed trends coincide with those expected and required by the equation for SHM.

The objective of this chapter is to explore the relevance of Simple Harmonic Motion to amputee running and answer the research sub-question set out in section 2.1.2: **'Is the claim that a foot mimics Simple Harmonic Motion legitimate?'**

## **6.2 Exploring the Principles of SHM**

### **6.2.1 The Effect of Mass Variation**

The first SHM variable explored was that of varying the mass. According to the equation of SHM (figure 5.2) if the mass of a spring-mass system is increased the frequency of oscillation will be reduced. This phenomenon is easily investigated by exercising the rig through a certain displacement (as conducted in previous tests, for example section 5.4.3) but modifying the mass of the carriage of the rig. The effective ground contact point (clamp position) must remain constant and the same foot must be used for all tests (therefore maintaining identical spring stiffness for all tests. The equation of SHM makes no reference to the amplitude of displacement and as such for the purpose of this investigation the amplitude is ignored.

#### **6.2.1.1 Method**

The rig was assembled as shown in figure 5.10 with an Ossur Category 6Hi ESR prosthetic foot attached to the carriage. The toe clamp was located in an identical position to the testing in section 5.4.2 at 50mm from the toe meaning that the data gathered in Chapter 5 is comparable.

Masses were added to the rails of the carriage according to table 6.1, secured using the clamping beam (see Appendix 2) and the data logger initiated. The masses chosen for this investigation were selected as the median value of those recommended by the manufacturer (Ossur) for each category of their feet (table 6.2) up to the maximum design load of the rig (100kg).

The rig was exercised using the input handle (see figure 5.4) at a frequency that subjectively matched the resonant frequency of the system until the amplitude of oscillation was such that the toe comfortably left the ground plane. This amplitude was maintained for a series of at least ten oscillations at which point the input force was removed and the amplitude of the carriage allowed to naturally decay. Of the data recorded, a series of 8 oscillation cycles were isolated and averaged to provide a single

typical 'stride'. This method was then repeated for the next successive applied mass until all seven loading conditions had been satisfied.

Test condition:	1	2	3	4	5	6	7
Mass (kg):	40.5	48.5	56	64	73	83	94.5

**Table 6.1:** Test conditions with associated masses to be fitted to the carriage. Masses were chosen as the median values of those published by the foot manufacturer up to a limit of 100kg.

WEIGHT KG	37-44	45-52	53-59	60-68	69-77	78-88	89-100	101-116	117-130
WEIGHT LBS	81-96	97-115	116-130	131-150	151-170	171-194	195-220	221-256	257-287
High to Extreme Impact Level	1	2	3	4	5	6	7	8	9

**Table 6.2:** Flex Run stiffness prescription guide (Source: Ossur.com)

### 6.2.1.2 Results

Figure 6.1 shows the traces of deflection plotted against time for each of the seven mass conditions.

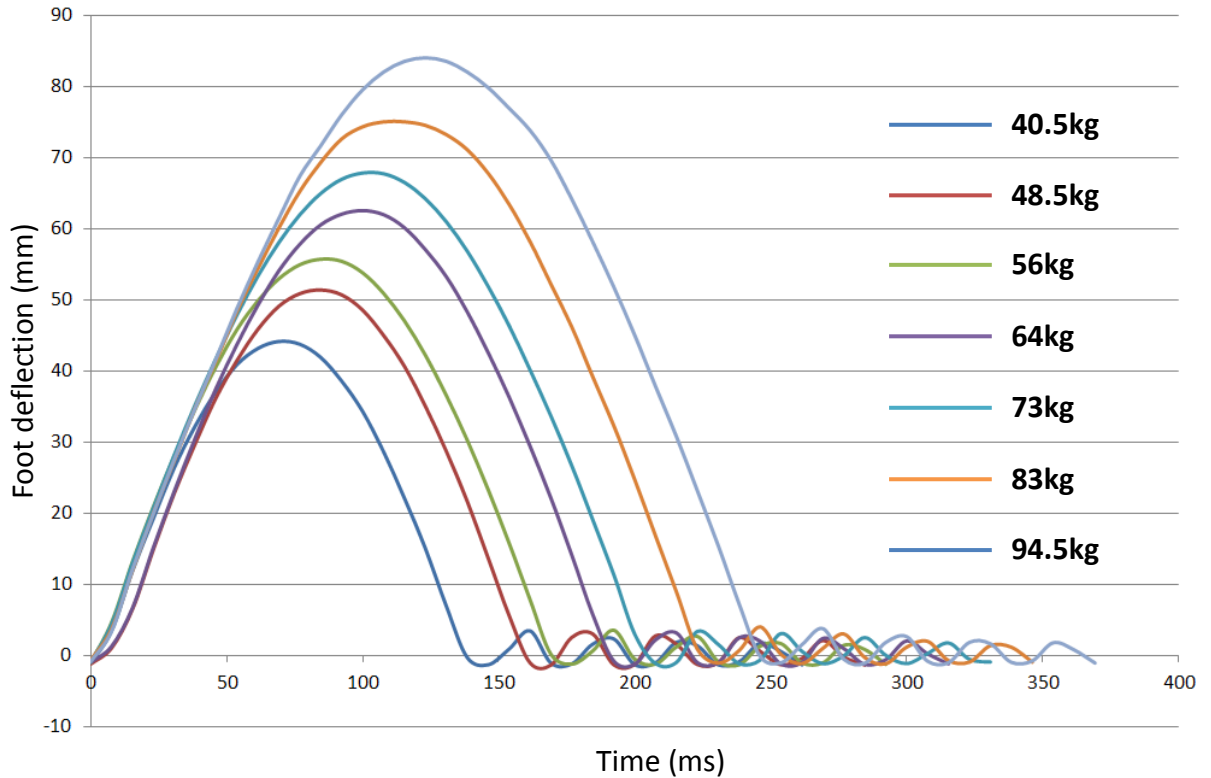


**Figure 6.1:** Traces of foot deflection for each successive mass applied to the carriage plotted against time. The foot response slows proportionally as mass increases.

As the mass of the carriage increases there are two significant effects:

1. The amplitude of displacement increases. The amplitude was controlled by the amount of energy applied through the input handle of the rig and as such was variable, but in order to establish comparability of the data, displacement (& deflection of the foot) was defined in each case by the toe leaving the ground plane. However with the increase in mass, more stored energy in the foot is required to enable this. Therefore a greater deflection is required. It should also be noted that the nominal value of foot deflection (that which occurs in a static loading condition) is also naturally greater with the increased load on the foot.

- The frequency response of the foot is slower, proportionally to the increase in mass. This trend is expected according to the equation for SHM, but it is not yet known if the size of the change is congruent with the equation.

The same trend can be seen if the same investigation is expressed in terms of the ground reaction force measured in kN, shown in figure 6.2.

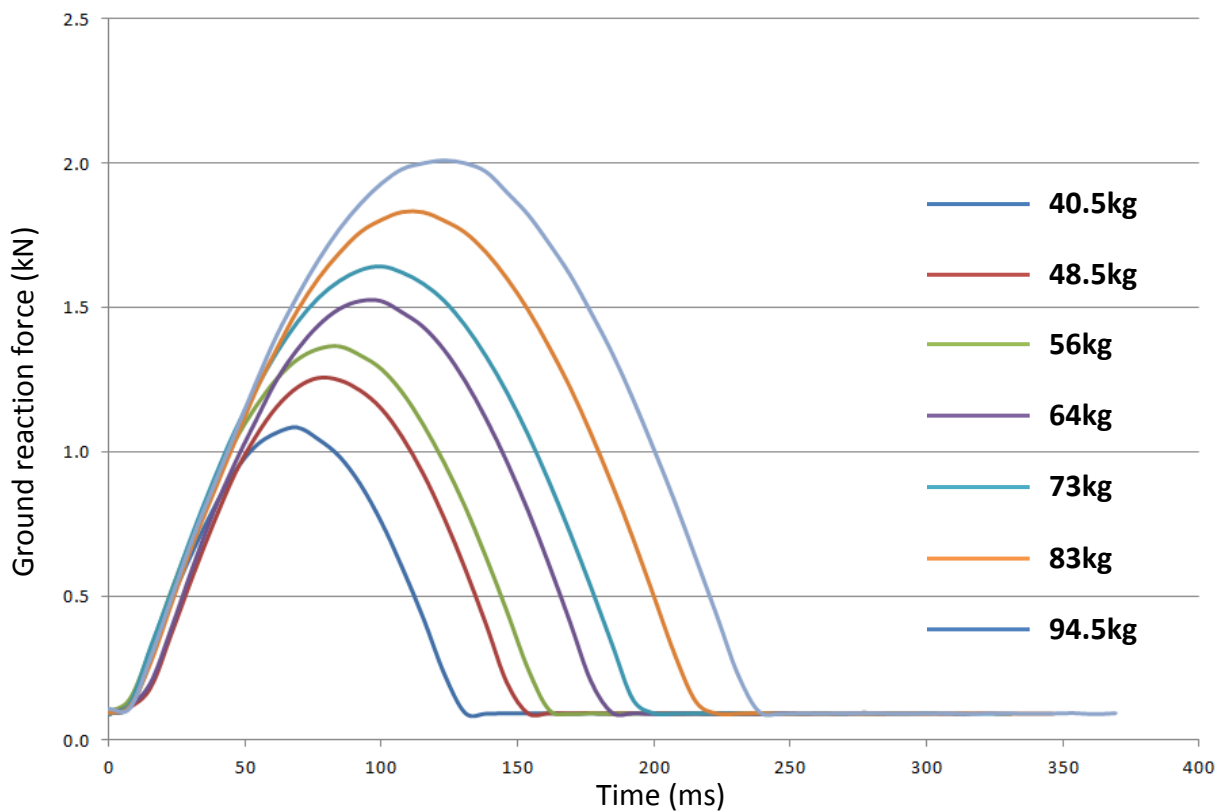


**Figure 6.2:** Traces of ground reaction force for each successive mass applied to the carriage plotted against time. The foot response slows proportionally as mass increases.

For each successive loading condition it can be seen that the ground reaction force increases according to the deflection of the foot (shown in figure 6.2). Given that each loading condition takes place with the same foot and ground contact position, this is exactly the trend that would be expected and suggests that the deflection data captured is valid. A further validity check that can be conducted is to plot values of force and deflection for each of the loading conditions on the same graph, therefore creating a force- deflection curve and a series of hysteresis loops (figure 6.3).

It can be seen that each of the loading conditions exhibit the same linear spring rate for the loading phase (see section 3.2.4.3 for an explanation of hysteresis curves and energy efficiency) and when plotted together as in figure 6.3 it is impossible to differentiate the individual conditions from one another.

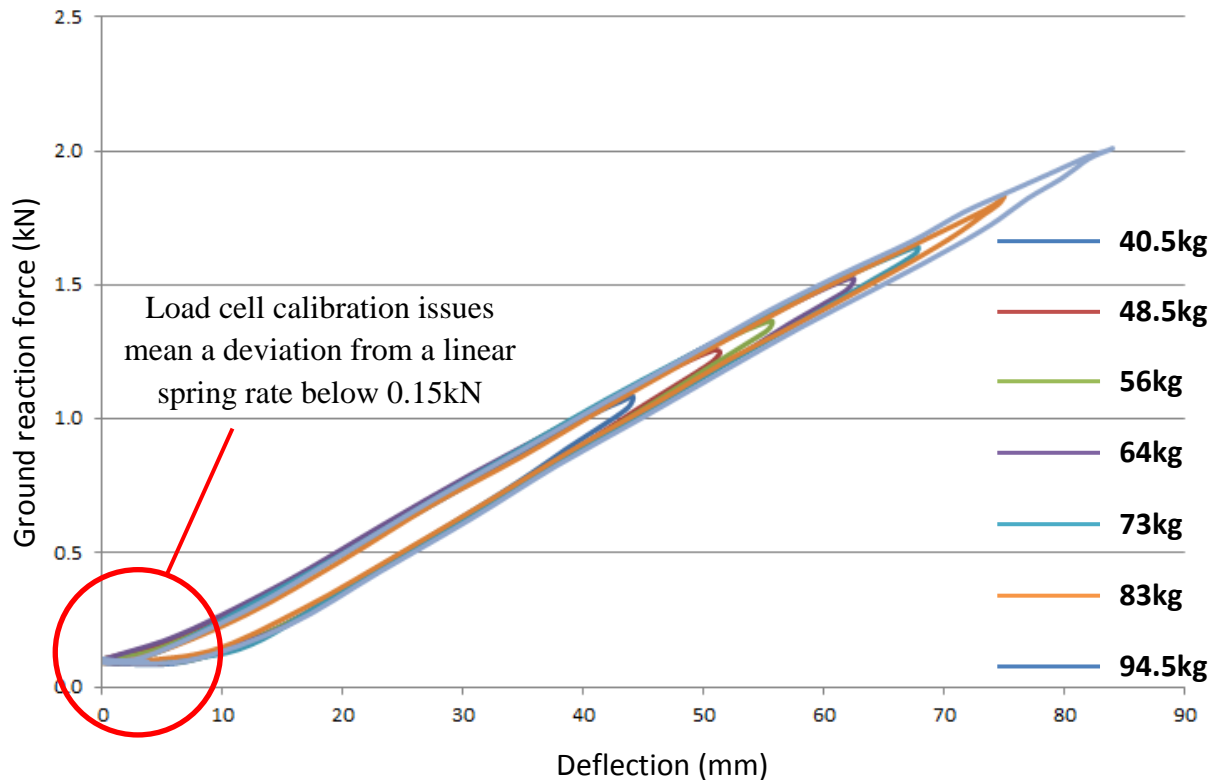


**Figure 6.3:** Hysteresis loops for each successive loading condition of the foot demonstrating the uniform linear spring rate of the foot on test, regardless of how much load is applied.

As discussed in Appendix 3 the load cell accuracy diminishes significantly below 0.2kN and this is evident in figure 6.3 where the load apparently never reaches a value of zero, despite the foot being airborne. The spring rates plotted in figure 6.3 show a margin of hysteresis (and therefore inefficiency). This is an effect of the frictional losses of the rig and is covered in detail in Appendix 4.

To further add validity to this data figure 6.4 shows the same data but with the original spring rate data from section 5.4.2 overlaid that was measured on the Instron test machine for an identical ground contact position. As can be seen the spring rates are nearly identical.

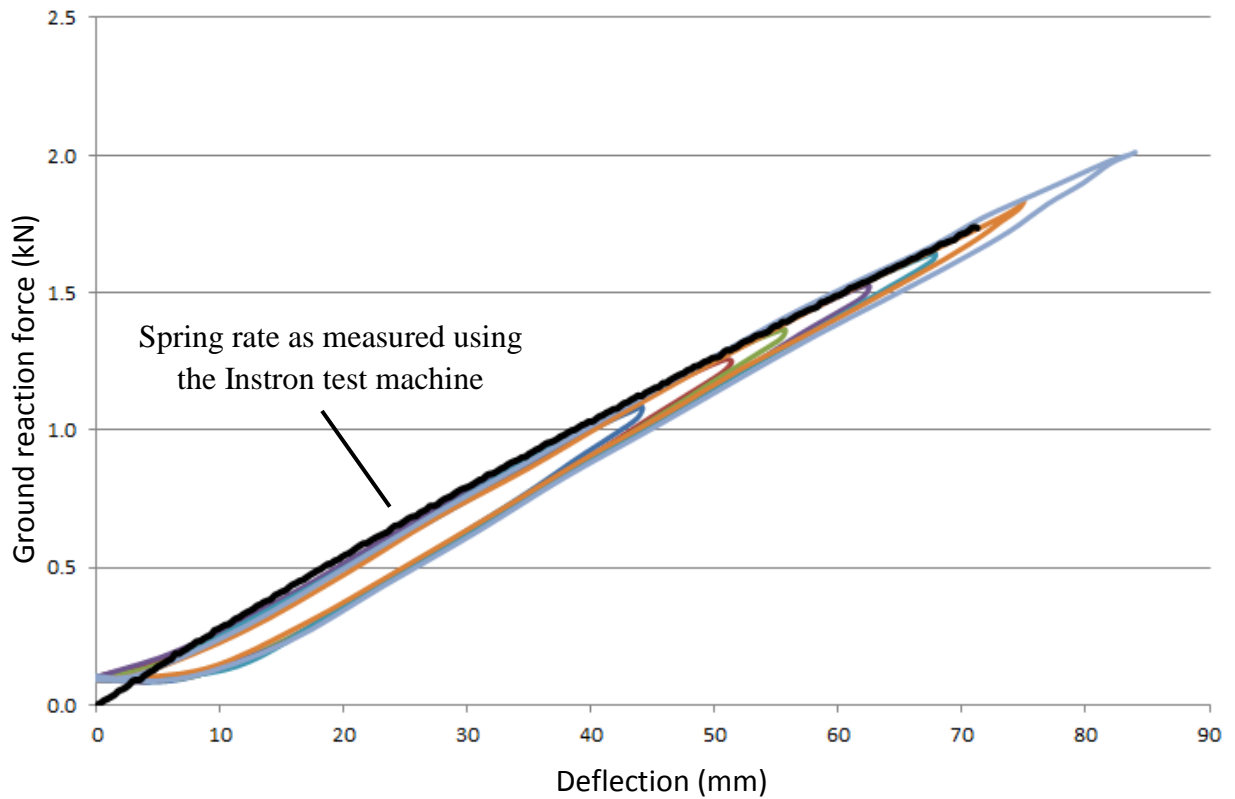


**Figure 6.4:** Hysteresis loops for each successive loading condition of the foot with the originally recorded spring rate of the same foot from the Instron testing phase (section 5.4.2).

This correlation in spring rate data serves to confirm the calibration of the load cell of the rig versus that of the Instron test machine.

## 6.2.2 The Effect of Stiffness Variation

The second SHM variable to explore was that of varying the stiffness of the foot. The equation for SHM dictates that as the stiffness of the spring rate increases, the frequency response time will decrease meaning that the mass will respond faster, resulting in a higher frequency of oscillation.

In a similar manner to the previous investigation, this can be explored using the rig and prosthetic ESR foot. As discussed in section 4.6 the stiffness of the foot changes depending on the effective ground contact position. This is the point at which the toe is clamped into the rig fixture prior to testing, and figure 4.8 demonstrates how the stiffness alters along the length of the metatarsal region of the foot on test.

### 6.2.2.1 Method

In order to affect a stiffness variation for the purpose of this test the same approach was used, modifying the position of the toe clamp to provide three different foot stiffness values whilst maintaining the mass as a constant. The three positions chosen were identical to those used to generate the data in figure 4.7 and mirror the ground force sensor positions from the amputee testing phase of this report (section 4.4.2).

A mass of 83kg was mounted to the rig and for each of the ground contact positions the carriage was exercised by the operator in a resonant manner using the input handle. Maximum amplitude of oscillation was achieved and defined as the toe comfortably leaving the ground. This was maintained for a minimum of ten cycles. Data from 8 of these cycles was then isolated and averaged to demonstrate a typical stride for each of the ground contact positions (effective values of foot stiffness).

### 6.2.2.2 Results

The resulting average strides can be seen in figure 6.5 with deflection plotted against time in milliseconds.

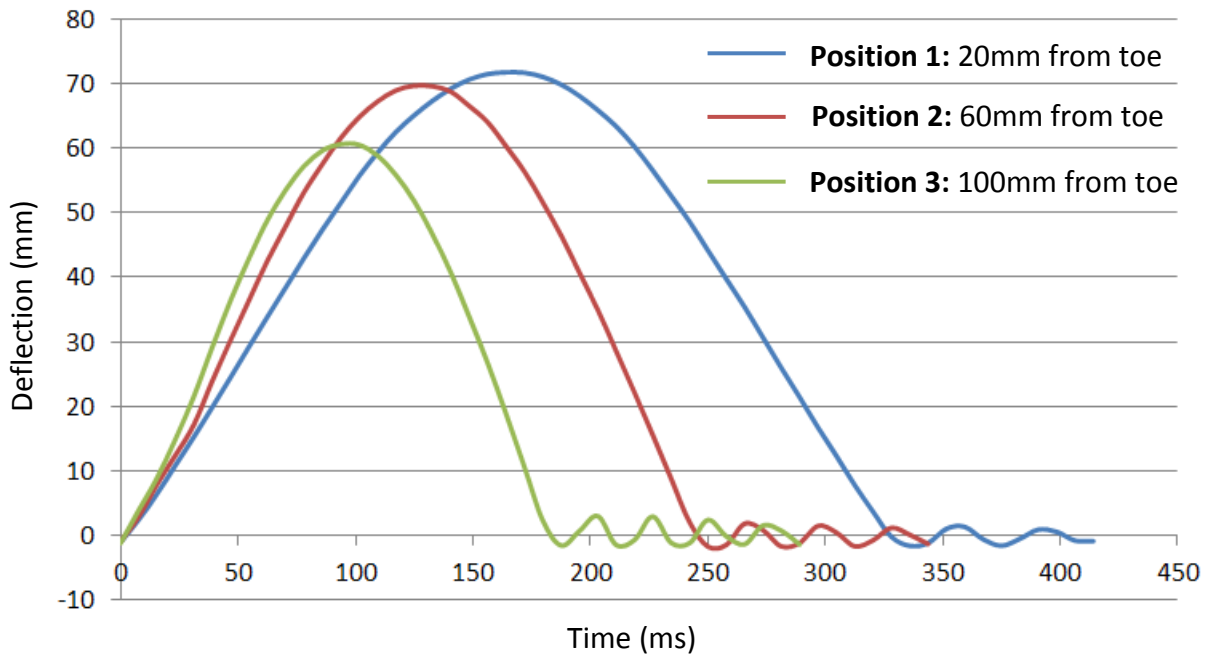


**Figure 6.5:** Traces demonstrating the response time in terms of foot deflection of the Ossur Cat.6Hi foot with varying ground contact points. As the stiffness increases, the contact time decreases.

In accordance with the expected trend for Simple Harmonic Motion, as the effective stiffness of the foot increases (as the ground contact point moves further rearward on the foot) the frequency response of the foot becomes faster.

What can also be observed is that as the foot spring rate is diminished, the amplitude of oscillation increases. Given that the mass remains unchanged throughout the testing this is to be expected as a lower spring rate will permit a larger deflection for the same given loading condition. It should also be noted that the nominal deflection of the foot (that deflection achieved when the system is at rest and at equilibrium) was larger for the softer foot condition.

An identical trend can be seen if the ground reaction force for this testing is examined (figure 6.6).

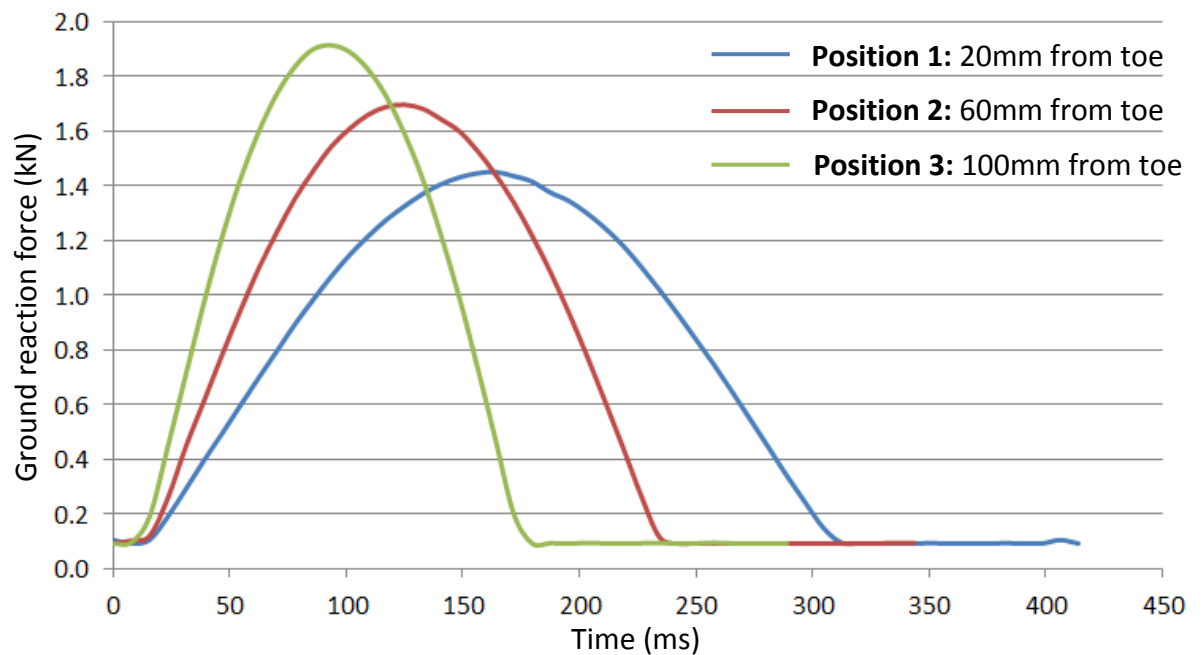


**Figure 6.6:** Traces demonstrating the response time in terms of ground force of the Ossur Cat.6Hi foot with varying ground contact points.

The timing is identical (as it is the same dataset that is being examined) but in this instance the ground reaction force for the stiffer foot condition (position 3) is greater (1.91kN versus 1.70kN and 1.45kN for the softer conditions).

As the amplitude was not accurately controlled in this investigation (the purpose being to understand the trend of foot stiffness versus response timing) it is difficult to comment on the relevance of this increased ground reaction force. However when the deflection of the foot and the ground reaction force are compared with one another it is reassuring to observe that the stiffness of the foot is increased as the contact position moves rearwards. This trend aligns with the work carried out in Chapters 4 & 5.

### 6.2.3 Variation Conclusions

If the link between the action of a prosthetic running foot and the equation for Simple Harmonic Motion is valid it should be observable that:

1. If the mass of the amputee is increased, the response time of the foot is increased (the foot responds slower) assuming the stiffness of the foot is constant.
2. If the stiffness of the foot is increased, the response time of the foot is decreased (the foot response faster) assuming the mass of the amputee is constant.

The previous two investigations have demonstrated that these proportionate trends exist when testing using the frequency response rig as detailed in sections 6.2.1 & 6.2.2. However it cannot yet be concluded that amputee running is purely a function of Simple Harmonic Motion. The data gathered does not quantitatively conclude that the frequency of oscillation is congruent with the equation for SHM; only that the qualitative trends exist.

As such, very little reference has been made to the importance and relevance of deflection amplitude. The equation for Simple Harmonic Motion (figure 5.2) does not require a value of displacement to define a value of response timing for a simple spring – mass system meaning that assuming no losses exist, the timing for such a system will be the same regardless of oscillation amplitude.

From a dynamic response point of view, a prosthetic foot can only have three true independent variables:

- **Mass applied** (that which it has to act against during the response phase)
- **Spring stiffness**
- **Deflection amplitude** (representing the energy stored in the system as a function of spring stiffness).

In order to define the response time using the equation for Simple Harmonic Motion only the first two of these variables are required as the displacement value does not

affect system timing. Therefore the final test that can be conducted to confirm the trend for Simple Harmonic Motion is to investigate the effect of changing the amplitude of oscillation of the system whilst maintaining the system mass and spring stiffness as constant.

If the foot returns identical values of timing (foot response) across a broad range of values of foot deflection, the system can truly be considered to act in accordance with the equation for Simple Harmonic Motion. If however the response time varies across a range of deflection values it can be deduced that such a link is more complex than academic papers have previously suggested.

## 6.2.4 The Effect of Deflection Amplitude Variation

Assuming validity to the concept of comparing amputee running to Simple Harmonic Motion, regardless of the amplitude of oscillation the response timing of the foot will always be identical. Using the fabricated response rig (figure 5.4) this can be investigated by maintaining as constant the foot stiffness and mass applied to the carriage and observing the timing of the foot across a range of deflection amplitudes.

### 6.2.4.1 Method

Because of the qualitative nature of this specific investigation the value of mass or foot stiffness is irrelevant providing they are kept constant throughout the process. However to aid comparability and continuity an Ossur Cat.6Hi prosthetic running foot was mounted in the rig (in an identical manner to sections 6.2.1 & 6.2.2) with a mass of 83kg applied as in previous tests. The toe clamp (that defines the effective ground contact point and therefore ultimately the stiffness of the foot) was attached at an identical position (50mm from the toe).

To provide a range of deflection values the carriage was exercised using the input handle in a harmonic manner until a maximum value of 70mm was achieved. Because of the large amount of energy required to deflect the foot 70mm (and the limited amount of power able to be applied by hand to the input handle in a single moment) the overall level of deflection builds up over a number of oscillation cycles. With each successive cycle, the energy applied to the input handle is added to the kinetic energy of the mass travelling under gravity. As a result the foot achieves a progressively larger deflection with each successive oscillation of the mass (less the losses inherent in the rig, discussed and quantified in section 5.5 and Appendix 4).

This gradual build-up of amplitude provides a broad range of values of foot deflection and their corresponding response timing that can be interrogated and displayed. Foot deflection data was again collected at a frequency of 128Hz using the MSR data logger.

### 6.2.4.2 Results

Building up the amplitude of oscillation in the manner just described to a value of 70mm required a series of 28 oscillation cycles of the spring–mass system. A trace of foot deflection plotted against time is displayed in figure 6.7. deflection can be seen tending from a value of 28mm which is the nominal deflection value when the foot is at rest (and the system is in equilibrium). This is the point at which the reaction force of the foot (a function of spring rate multiplied by deflection) equals the force exerted by gravity on the mass of the system.

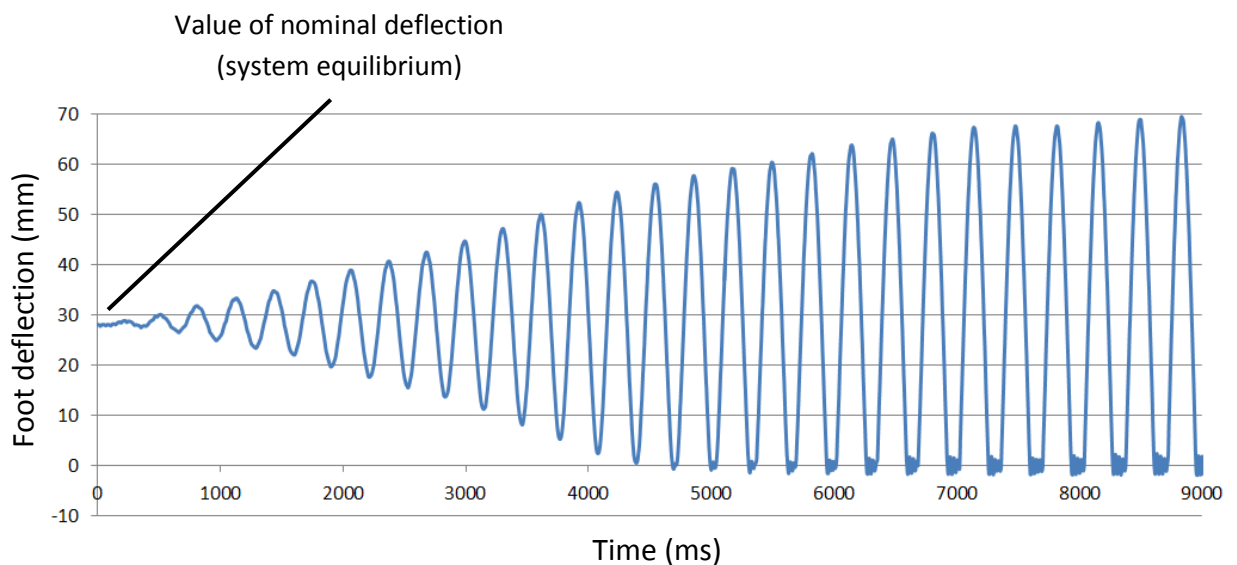


**Figure 6.7:** Trace of oscillation build-up, the values of which were used to demonstrate the frequency response of the foot at different values of deflection.

Interesting to note is the point at which the foot begins to leave the ground at the upper-apex of mass travel (occurring at around 4700ms in figure 6.7). With each progressively larger deflection of the foot, the amount of stored energy (as gravitational potential, kinetic or spring potential energy) in the system increases and propels the foot further from the ground plate.

Each of the foot deflection cycles was isolated and plotted over one another in figure 6.8. This is to demonstrate the frequency response of the foot across the range of deflections such that they can be compared with one another. In order to make the plotting of data more practical, every other oscillation cycle was plotted (resulting in  $28/2 = 14$  individual deflection curves).

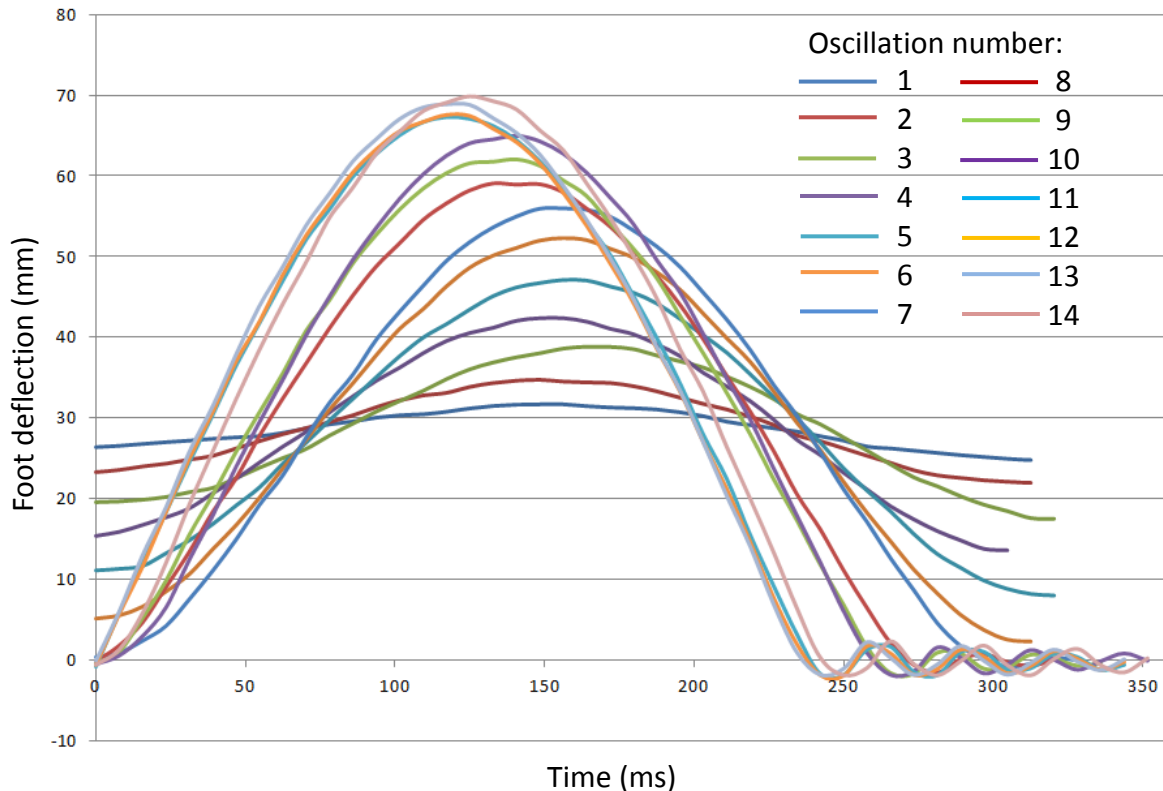


**Figure 6.8:** Graph displaying oscillation cycles of the rig with progressively increasing values of foot deflection. Foot on test was Ossur Flex Run Cat6.HI with 83kg mass applied.

If Simple Harmonic Motion is relevant to amputee running it is expected that the response timing of each of these deflection cycles should be identical. However figure 6.8 shows that the response timing changes significantly across the range of amplitude. The graph shows the response timing expressed as the time between points of minimum deflection for each deflection cycle. Values for each of the oscillation cycles were defined and are displayed in table 6.3.

Oscillation number	1	2	3	4	5	6	7	8	9	10	11	12	13	14
Max. Displacement (mm)	32	35	39	42	47	52	56	59	62	65	68	68	69	70
Start Displacement (mm)	26	23	20	15	11	5	1	0	0	0	0	0	0	0
$\Delta$ Displacement (mm)	5	11	19	27	36	47	55	59	62	65	68	68	69	70
Response time (ms)	313	311	309	305	303	297	289	273	258	258	242	234	233	233

**Table 6.3:** Summary of figures representing the progressively large values of deflection with details of response timing. Importantly, the response time changes depending on foot deflection amplitude.

The values of foot response time can be seen to vary from 233ms to 313ms. If these figures are accurate they directly contradict the suggestion that a prosthetic running foot acts in accordance with the equation for Simple Harmonic Motion which requires them to be identical.

As shown in figure 6.7 all foot deflection tends from the value of static deflection; that is the value of foot deflection at static equilibrium when the system is at rest. In this instance (for a mass value of 83kg, an Ossur Flex Run Cat.6Hi foot and an effective ground contact position of 50mm posterior of the edge of the toe) this static or 'nominal' deflection figure is 28mm. Before the foot begins to leave the ground (at the greater amplitudes of oscillation) it can be seen in figure 6.7 that a sine wave of foot deflection is established with progressively expanding amplitude. In recognition of this the data displayed in figure 6.8 was rearranged such that  $t=0$  for each trace was at this nominal value of 28mm deflection. Once again the resulting traces were plotted over one another and are shown in figure 6.9.

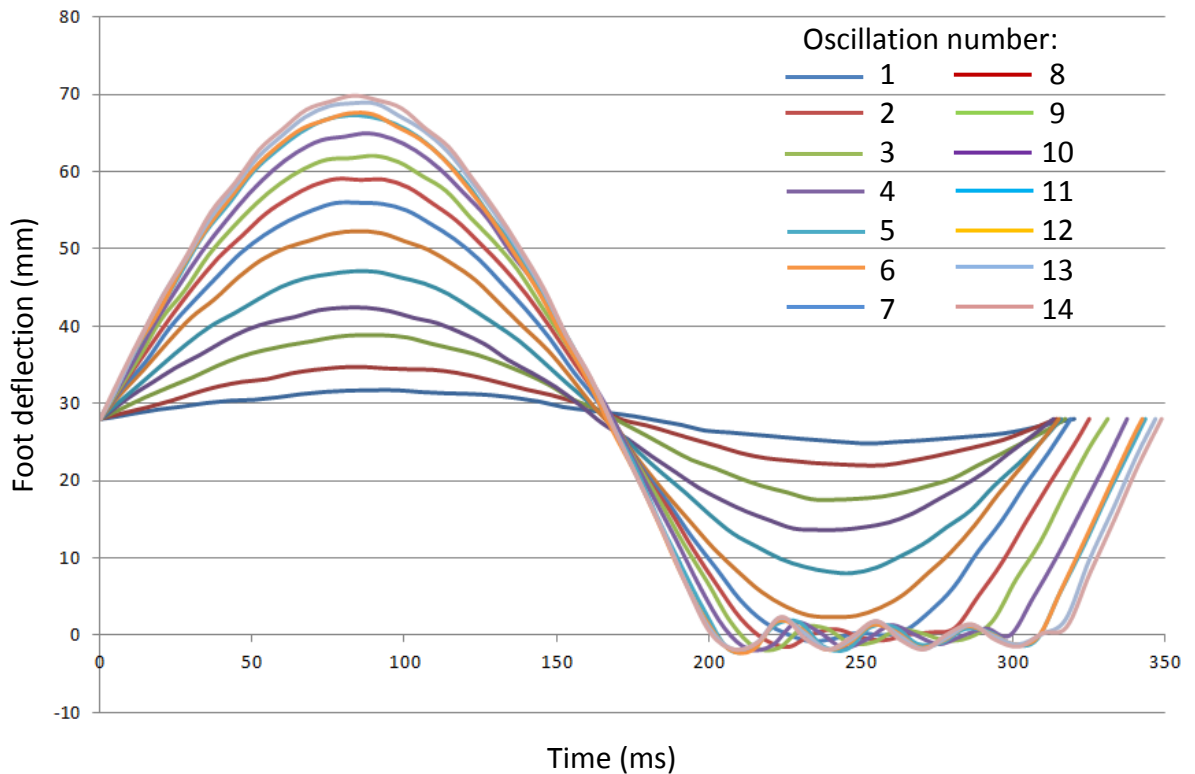


**Figure 6.9:** Graph displaying oscillation cycles of the rig with progressively increasing values of foot deflection, rearranged such that 28mm deflection occurs at  $t=0$ .

When the data is rearranged such that the nominal deflection value for each curve occurs at  $t=0$  it can be seen that regardless of amplitude the response time of the foot to return to this same nominal value is virtually identical. At a logging frequency of 128Hz the response time presents as 160ms for all but one deflection series. Further to this, the second half of the period reflects the first; that is the time from  $t=0$  to the point the deflection returns to the nominal value (28mm @  $t=160$ ms) is also the time taken to complete the second half of the deflection cycle thus confirming the sine wave nature. This is true up until the moment the foot leaves the ground plane and becomes airborne (from the 7<sup>th</sup> cycle onwards). From this moment onwards (as the deflection progressively increases further) the foot spends a greater period of time in the air and as such extends the second half of the deflection cycle before returning to the nominal deflection value.

### 6.3 Chapter Conclusions

Although initially appearing not to follow the trend described by Simple Harmonic Motion, if the data is displayed in the correct manner (with deflection occurring either side of the nominal value of the loaded foot at rest) it can be suggested that the reverse is true.

It was shown in sections 6.2.1 and 6.2.2 that if the mass or the stiffness of the system is modified (whilst maintaining all other variables as constant), the resulting response timing follows the trend expected of Simple Harmonic Motion. Figure 6.9 demonstrates that the amplitude of oscillation (or foot deflection) is irrelevant to the frequency response of the system assuming two things:

1. The data is viewed as beginning at the nominal value of deflection.
2. The foot does not leave the ground.

At the point where the foot leaves the ground the mass is no longer attached to the spring that was reacting against it and as such cannot be assumed to function as a spring–mass system.

This is the first time in this or any published investigation that the overall ground contact time has not been considered as the response timing of a foot. It is clear that if the action of a runner is to be modelled, the ground reaction time is secondary to the time taken for the foot to reach maximum deflection and return to this same value of nominal deflection. For the purpose of this investigation this is to be known as the ‘Half-Wave Timing’ or HWT.

What is also clear from examining figure 6.7 is that a sine wave could be used to model the action of a foot up until the point where the toe leaves the ground (which of course it always must do during running). At this moment the action of the foot no longer ascribes to Simple Harmonic Motion.

It is known from table 6.3 that the ground contact time (GCT) of the foot under test varies considerably with foot deflection. Given that the HWT is always the same regardless of deflection (assuming a constant mass and foot stiffness) this means the

time from nominal deflection (following maximum deflection) until the foot leaves the ground must vary depending on foot deflection. This can be observed in figure 6.10 and more easily in Figure 6.11 which is a detail view of the points of the foot leaving the ground for the various traces of foot deflection.

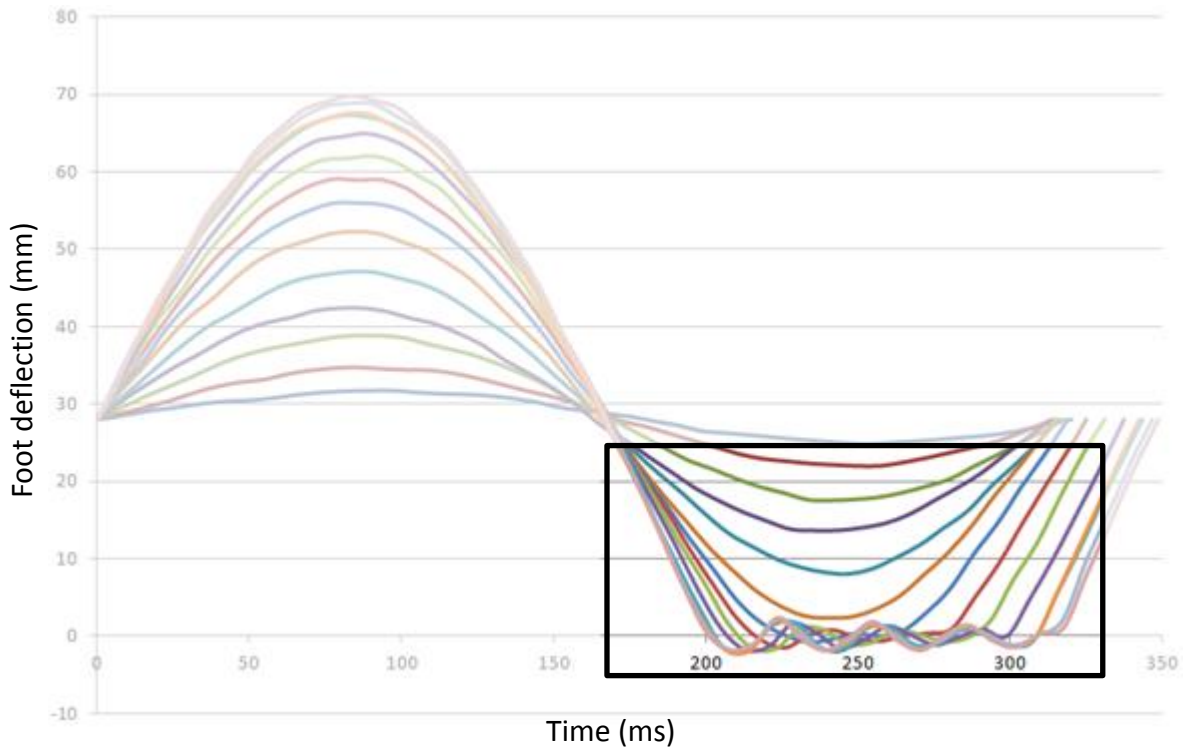


**Figure 6.10:** Graph displaying oscillation cycles of the rig with progressively increasing values of foot deflection, rearranged such that 28mm deflection occurs at  $t=0$ . A detailed view of the isolated section can be seen in figure 6.11.

The various points at which the foot leaves the ground plane during testing are displayed in figure 6.11 for the different traces of deflection. It can be seen that the gradient of the curve at the time it hits the nominal deflection value defines the ground contact time. The greater the value of foot deflection, the steeper the gradient of the deflection curve at the end of the HWT (at nominal deflection) and the shorter the period of time until the foot leaves the ground (toe-off).

Therefore it can be concluded that the GCT of an amputee runner is directly related to the amplitude of deflection achieved. The greater the deflection that is achieved, the shorter the GCT is for that specific stride.

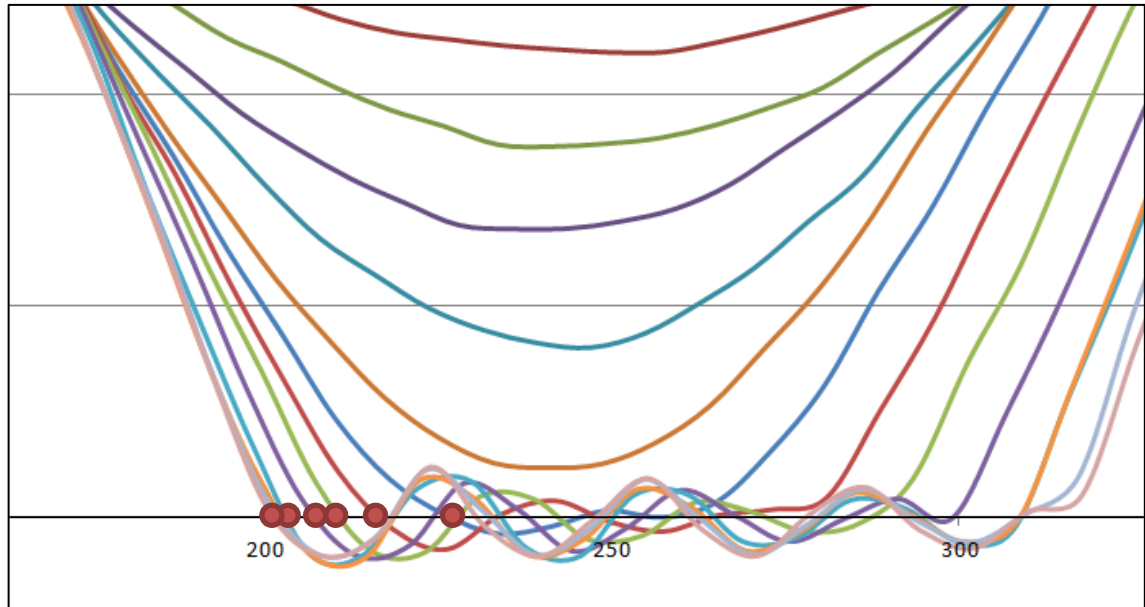


**Figure 6.11:** Detail of figure 6.10 showing the change in timing of when the foot leaves the ground plane across a range of values of foot deflection.

If this is the case it should be understood what foot deflection occurs during a variety of running activities. The information gathered to date (during the amputee running phase of this investigation in Chapter 4) only provides data captured for a single running velocity with a single category of foot.

The research sub-question set out in section 2.1.2: **‘Is the claim that a foot mimics Simple Harmonic Motion legitimate?’** has been answered by this new information. It can be concluded that a prosthetic running foot can be described by the equation for simple harmonic motion but providing two conditions are met:

1. The nominal position is used as a reference for the start of the response phase
2. A single ground contact point is defined and this does not change for the duration of the stride.

Clearly these two conditions are not useful for describing amputee running. The nominal position is arbitrary for a prosthetist and cannot be observed during running, and as shown in Chapter 4 the ground contact position changes throughout the stance phase of the stride. However the rig was able to replicate the ground contact time of the runner by assuming a single median ground contact position.

It appears that the dynamic response of a prosthetic foot cannot be actively altered by the amputee and the response timing (HWT) depends on the mass of the amputee and the stiffness of the foot alone. Therefore it could be suggested that the amputee can only affect a larger ground reaction force in order to change their velocity. It stands to reason that this larger ground reaction force will invoke larger deflection amplitude and therefore a shorter ground reaction time.

It is therefore proposed that in order to continue this investigation more should be learned about the effect of different running velocities on the prosthetic foot. Does a higher velocity mean a shorter GCT and are there any other effects that might influence the dynamic response of the foot? It should also be understood how an amputee affects a greater running velocity if the response of the foot is fixed.

# CHAPTER 7: THE EFFECT OF SPEED VARIATION

## 7.1 Introduction & Chapter Objectives

The previous chapter has demonstrated that the action of a prosthetic running foot can be effectively described by the equation for Simple Harmonic Motion providing a single stiffness is defined. This stiffness would inevitably be an assumption of foot characteristics and in section 5.4 was used effectively to replicate the ground contact time of an amputee on the dynamic response rig (figure 5.4). The ground contact point of the foot (and therefore effective stiffness of the device) has been shown in Chapter 4 to vary across the metatarsal region of the foot as the stance phase of a single stride progresses. What is not yet known is how this ground contact progression changes when a different running speed is required. This is essential knowledge if the research question stated in section 2.1.3: **'Can the action of a prosthetic running foot be modelled mathematically?'** is to be answered.

This chapter serves to improve understanding of the effect of running velocity on the dynamic response of a prosthetic foot. It is known that an amputee can alter his or her velocity during running but no literature has been found to describe what mechanism is used to affect this. This investigation has so far determined that the dynamic response of a prosthetic foot is fixed and governed by its properties (stiffness, mass applied, amplitude of deflection) but if this is the case, which of the mechanisms for increasing running velocity can the amputee employ?

A series of tests were proposed that require a unilateral trans-tibial amputee to run at a variety of speeds. Stance length, foot deflection and ground contact data was collected to understand the mechanism of speed variation in amputee running and how this can be modelled mathematically.

## 7.2 Velocity Testing (Part 1)

### 7.2.1 Method

Following the relevant ethics considerations and approval (as can be seen in the Appendix) an investigation was carried out at a running track to determine the ground contact time (overall foot response time) and ground contact point progression of the foot across a range of running speeds. These are the same variables that were measured during amputee testing in Chapter 4 and an identical apparatus was used as described in section 4.2. The aim was to understand if the boundary conditions of the foot (ground contact point progression and therefore foot stiffness) change at different running speeds.



*Figure 7.1: Image of the amputee running during one of the 400m test runs. A total of six runs were completed.*

During the previous amputee testing (Chapter 4) the individual was asked to run at a single self-selected running velocity and stride data was gathered. On this occasion the runner was asked to carry out a series of 400 metre runs of an established athletics track (figure 7.1) at subjective self-selected 'slow', 'comfortable' and 'fast' speeds. The times for these runs were recorded and an average velocity defined for each. In order to improve the data resolution from previous tests the ground contact data was

recorded at a frequency of 512Hz as a function of voltage (previous tests were conducted at a logging frequency of 128Hz).

It should be noted that this testing was conducted using a different amputee athlete to the individual involved in the previous test work. Further to this, during the course of this research the manufacturer of the Flex Run model of foot (Ossur) released an updated design of foot, changing the detailed geometry of the toe region. More information on this change can be found in section 8.1. From this point onwards all testing conducted was done so with the newer style of Ossur Flex Run foot.

## 7.2.2 Results

The amputee completed the three 400m runs according to the times and speeds in figure 7.2. Also displayed is a graphical illustration of the ground contact profile at each speed. Ten strides were isolated from the steady-state portion of each of the 400m runs and averaged into a single dataset as displayed. For information on sensor position see section 4.2.2.

Figure 7.2 demonstrates the change in stride characteristics at the three different velocities ( $11.8\text{kmh}^{-1}$ ,  $15.8\text{kmh}^{-1}$  &  $18.2\text{kmh}^{-1}$ ). The progression of ground contact point is similar to that measured in the previous amputee testing (figure 4.3, although this is with the previous geometry of Ossur Flex Run and these results should not be directly compared) for sensors 1, 2 and 3 and is consistent across the three running speeds. However a progressively large reading from sensor 4 can be observed as velocity increases. This sensor is the most posterior-mounted and these results suggest that the initial ground contact point moves rearward as speed increases.

Another trend that changes as the speed increases is that of the overall stride duration (stance and swing phase combined). It is assumed that foot strike occurs at the moment of initial reading from the rear-most mounted sensors (sensors 3 and 4) and as such the overall stride time decreases from 692ms at  $11.8\text{kmh}^{-1}$  to 576ms at  $18.2\text{kmh}^{-1}$ .

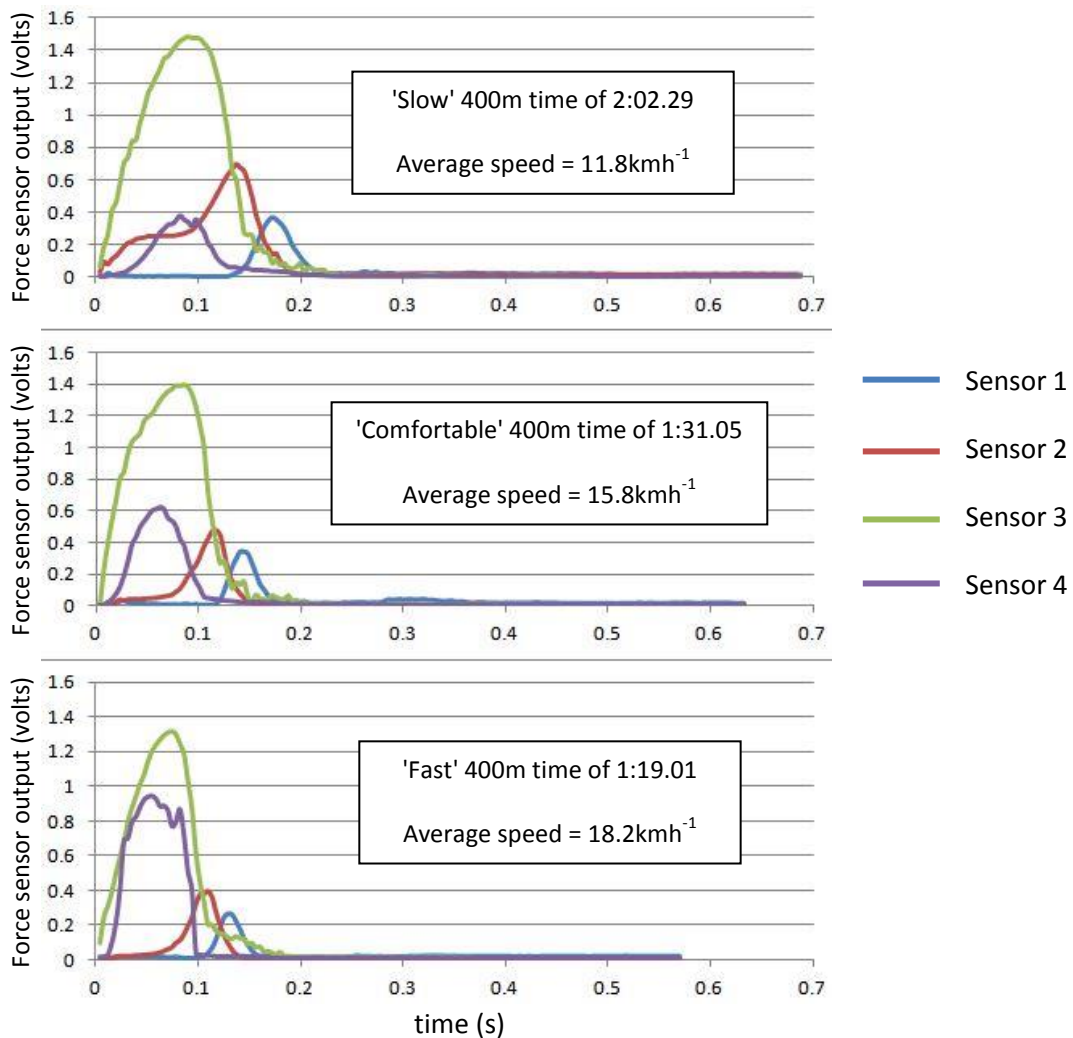


**Figure 7.2:** Times and speeds for the three 400m runs completed by the amputee athlete along with ground contact profile curves for an entire stride (averaged data for ten individual strides).

### 7.2.3 Conclusions

Whilst there is a suggestion of ground contact point change, it cannot be concluded that a higher running velocity means a further-rearward heelstrike position. If the profiles shown in figure 7.2 were equivalent and showed little or no variation in pressure progression it could be suggested that speed does not have a considerable impact on the boundary conditions of the foot, but these results serve only to justify more work in this area. The concept of using ground force sensors for determining the

ground contact position is valid, but the limitations of the data logger available (with four channels) means that only four sensors can be used.

In section 4.6.2 it is demonstrated that the magnitude of stiffness change of the foot with a small change of ground contact point is significant. If an accurate understanding of foot stiffness is to be gained, the ground contact progression should be demonstrated in a less ambiguous manner.

Furthermore due to the limitations of the data logger used, only the ground contact progression was measured for the entirety of this investigation (only four channels are available on the data logger used). A more comprehensive understanding of the effect of running velocity on stride characteristics would be obtained if the foot deflection were also measured (as in section 4.4.1). The nature of testing on a running track means that at any given point the running velocity is unknown (with the speed shown in figure 7.2 derived as the average speed for the entire run). Another drawback of testing on the track is that the runs are not repeatable. If any one of the tests was to be repeated the speeds obtained would inevitably be different. This work should be repeated in a more controlled environment and using more accurate data capture techniques.

## 7.3 Velocity Testing (Part 2)

Following the suggestion that increased running speed shifts the heelstrike position rearward (in relation to the toe of the foot) further testing was conducted to understand the effects of velocity on stride characteristics.

The fundamental principles of the test remain unchanged from that carried out in section 7.2. However more attention was paid to two things:

- Accurate definition of running speed
- Accurate measurement of foot characteristics (ground contact progression as well as foot deflection)

### 7.3.1 Method

In order to make the testing more repeatable and to address the points above, following ethical approval (as shown in the Appendix) test work was conducted using a treadmill. In this way the speed could be defined and assured. The use of a treadmill also allowed video to be captured of the event in the sagittal plane and used to understand the action of running, specifically the ground contact progression at the various test speeds instead of using the ground force sensors as previously (sections 4.2 and 7.2).

The foot was marked with highly visible plastic pins inserted into the Nike running sole at known locations (every 20mm from the toe up to a value of 180mm) such that when viewed on the video, the pin located nearest to the ground contact point could be identified. In order to determine the ground contact point the pins could therefore be counted from the toe. This set up is shown in figure 7.3.



**Figure 7.3:** Image showing the pins that were inserted into the foam of the Nike running sole to demonstrate the ground contact position when filmed in HD super-high frame rate video.

The minimum logging frequency found effective in previous test work for all data collected was 100Hz (as defined by the Instron hydraulic test machine controller). Therefore the video footage should also demonstrate a minimum resolution of 100Hz, or in the case of video 100 frames per second (fps). The standard frame rate for video cameras used in broadcast television (and therefore the vast majority of available video cameras) is 24fps. Should a higher frame rate be required, the camera used becomes a specialist piece of equipment.

However it is not enough to simply specify a frame rate of 100fps. Because of the speed of movement of the foot during running (particularly at higher speeds) blurring can occur when the video is paused (necessary to understand the ground contact points and effectively identify the pin locations relative to the ground plane). For this reason it could be necessary to record the action of the foot at a significantly higher frame rate than 100fps. The precise frame rate required cannot be accurately defined unless the velocity of the subject in the image is known (in this case the velocity of the toe of the foot, which is not known) or unless tested and calibrated on the day of testing. Therefore for the purpose of this test a camera was sourced that permitted a

significantly faster frame rate than could be considered practical for this manner of investigation whilst maintaining 1080P resolution (1080 x 720 progressive scan, more commonly known as High Definition).

The camera used was a Phantom Flex model from Vision Research Inc. capable of up to 2570fps in HD resolution. This was coupled with two 500W halogen lights to provide sufficient light required for the high frame rate recording. This set up can be seen in figure 7.4.



**Figure 7.4:** Image showing set up of the Phantom camera used for recording the action of the running foot on test with the two 500W halogen lights attached with a tripod.

The camera and lights were set up on a tripod on the left hand side of a treadmill such that the running was viewed directly in the sagittal plane on the side of the affected leg of the amputee. The camera was calibrated to use the lowest frame rate that still resulted in no visible motion blur when paused at the highest running speed (the treadmill had a maximum speed setting of  $18\text{kmh}^{-1}$ ).

Measuring rules were also added on the near and far edges of the treadmill meaning that a virtual line could be drawn through the equivalent measurements on each side

and the stance length determined. This can be seen in figure 7.5. In this instance the term 'stance length' refers to the distance travelled by the foot when in contact with the belt of the treadmill. In normal running, away from a treadmill, it is very difficult to observe this attribute and represents the distance the centre of mass of the amputee travels during the stance phase of the stride. Traditionally the term 'stride length' also accounts for the distance travelled by the athlete during the swing phase as well as the stance phase and is therefore not appropriate.

Because the ground force sensors were not being used for ascertaining ground contact

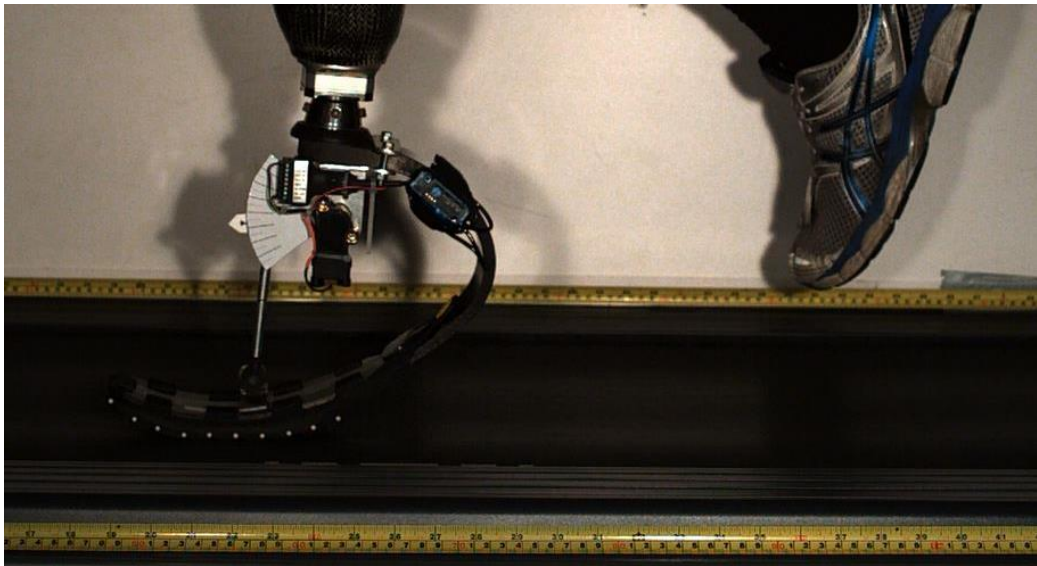


**Figure 7.5:** Image showing the treadmill used during testing with measuring rules set up at the front and rear edges (as viewed by the camera) used for establishing stance length.

progression they were removed and the deflection sensor (figure 4.1) was reinstated. This allowed for both the ground contact progression (via video) and foot deflection to be recorded simultaneously. Once again the data from the deflection transducer was recorded using the MSR data logger at a frequency of 512Hz.

In order to gain a complete understanding of the effect of running speed on the action of the prosthetic foot the amputee athlete was asked to run at a range of speeds from  $8\text{kmh}^{-1}$  to  $18\text{kmh}^{-1}$  at  $1\text{kmh}^{-1}$  intervals.  $8\text{kmh}^{-1}$  is the speed at which walking becomes running for this particular amputee athlete (and as such this was the slowest possible speed at which running occurs) and the treadmill maximum velocity was  $18\text{kmh}^{-1}$ . Coincidentally the maximum speed the amputee could comfortably run in the previous

test work (section 7.2) was  $18.2\text{kmh}^{-1}$  and as such this was judged sufficiently representative of the amputee's range of running speed.

Data was captured using the Phantom camera and deflection sensor simultaneously for each speed and a summary can be seen in the following sections. Appendix 5 details the statistical analysis that was conducted to understand the legitimacy and accuracy of this measurement technique. This includes:

- An intra-rater reliability analysis for a single running velocity. This analysis demonstrates a Standard Deviation of 2.0 with a mean of 669.7 across the ten measurements showing a statistically insignificant variation in the data.
- A t-test analysis across the entire velocity range comparing the visually observed camera data and the logged deflection sensor data. A P-value of 0.9173 is generated which is regarded as statistically insignificant.

## 7.3.2 Foot Deflection

### 7.3.2.1 Results

The data gathered was expressed in terms of output voltage from the deflection transducer as calibration was not required; a single point of ground contact was not yet being interrogated as was previously the case in section 6.2.1.1. The data gathered at this stage serves to provide a trend of deflection when understanding the timing of the foot (for example the stance phase timing) and when comparing one trace of deflection with another.

From the recorded data, ten steady state steps were isolated (for example in figure 7.6 showing the data for the steps at  $18\text{kmh}^{-1}$ ) and averaged into a single 'typical' stride.

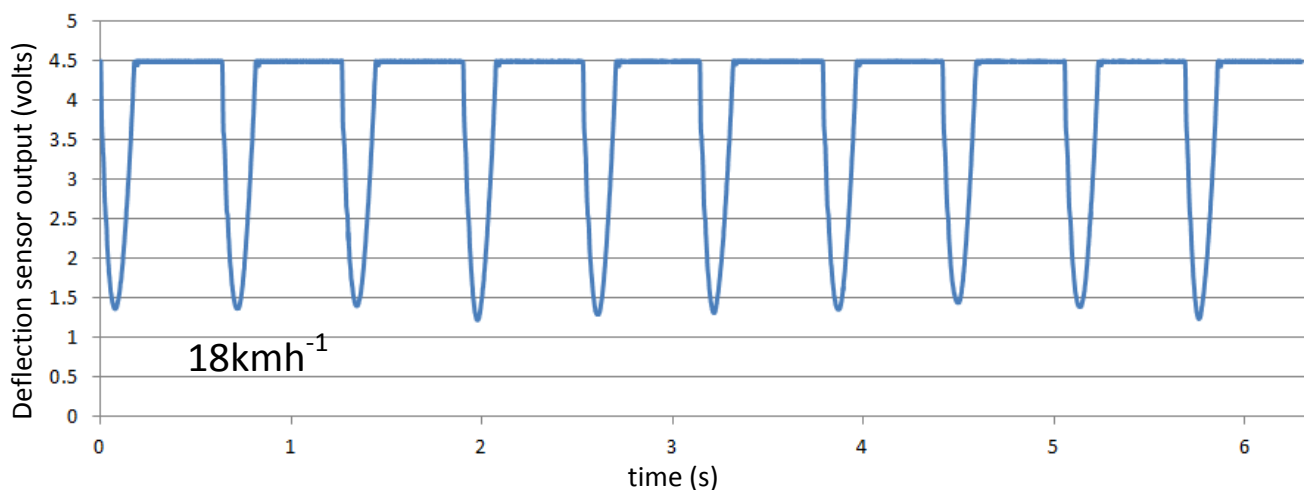


**Figure 7.6:** Trace of the deflection values recorded for the ten individual strides at  $18\text{kmh}^{-1}$  that were then averaged into a single 'typical' stride as shown in figure 7.7.

From each of these sets of averaged data (for each running speed from 8 – 18kmh<sup>-1</sup>) the following information could be derived:

- Stance phase timing (ground contact time)
- Swing phase timing
- Rate of energy absorption vs. return
- Amplitude of deflection (when compared with similarly generated traces)

When all of the traces for the individual running speeds are collated on a single graph the effect of speed on the dynamic response of the foot can be seen (figure 7.7)

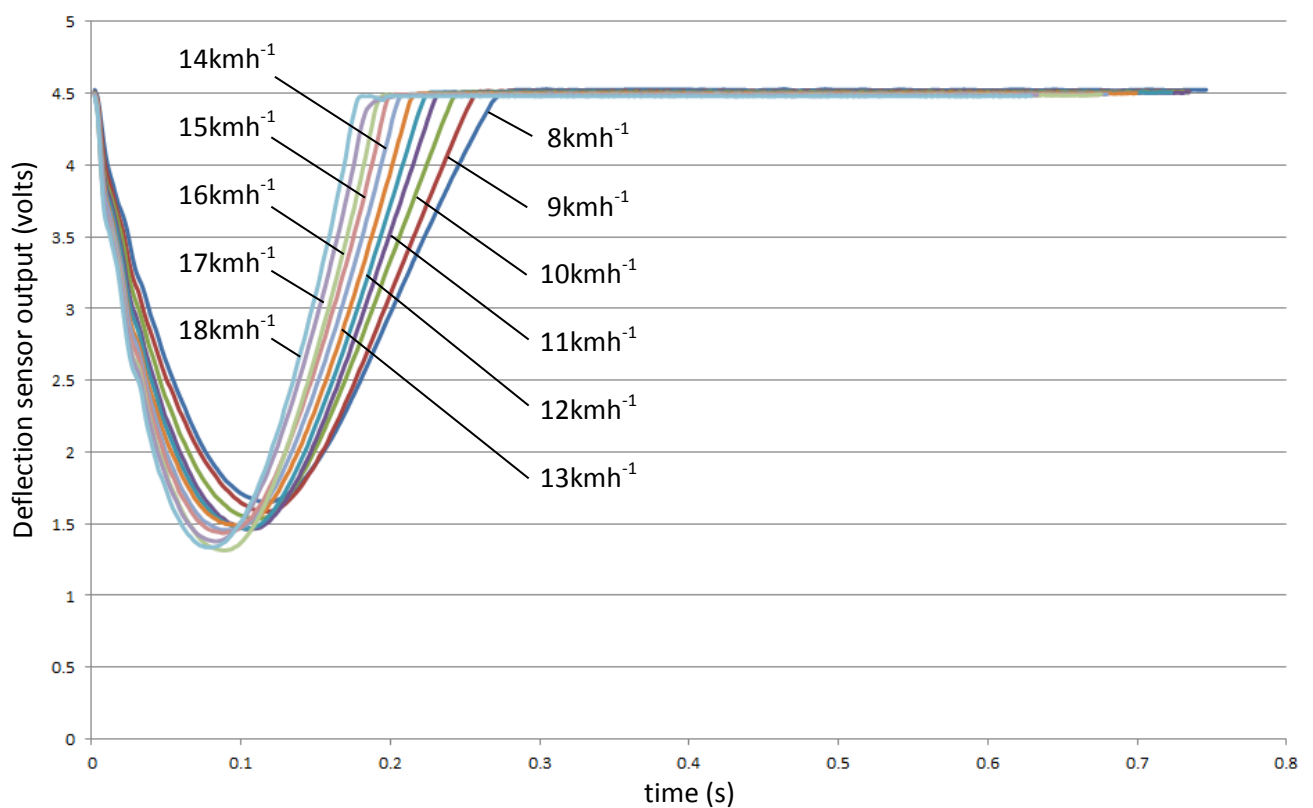


**Figure 7.7:** Graph showing traces of the averaged strides for each of the speeds tested from 8kmh<sup>-1</sup> – 18kmh<sup>-1</sup>.

It can be seen that as running speed increases there are two notable effects:

1. The response timing (ground contact time or stance phase timing) decreases. Despite the stiffness of the foot remaining unchanged and the mass of amputee constant throughout the testing, the dynamic response timing changed from 275ms at 8kmh<sup>-1</sup> to 182s at 18kmh<sup>-1</sup>.
2. The amplitude of deflection increases. Although the value of deflection is not calibrated into a tangible measure (it instead is displayed as a function of voltage output) the amplitude of deflection can be seen increasing by 12% across the range of running speeds tested.

The timing data for all of the strides was collected and can be seen in table 7.1. Mid-stance is defined as the time of maximum deflection of the foot.

Velocity kmh	Velocity m/s	Ground contact time ms	Mid-stance time ms	Stride time ms
8	2.2	275	119	746
9	2.5	260	117	734
10	2.8	246	111	734
11	3.1	232	104	730
12	3.3	227	102	723
13	3.6	217	100	699
14	3.9	209	90	680
15	4.2	203	88	676
16	4.4	197	86	668
17	4.7	193	84	633
18	5.0	182	80	629

**Table 7.1:** Summary of the response timing data of the prosthetic foot on test across the range of running speeds.

### 7.3.2.2 Deflection Conclusions

Given that the amplitude increases it is not a surprise to see that the response timing has decreased. During the test work conducted using the rig (section 6.2.4) it was shown that the foot responds about the true half-wave timing (HWT) represented by the amplitude of deflection in a statically loaded condition of equilibrium. As such, as the amplitude of deflection increases, the overall ground contact time decreases whilst the HWT remains identical. However the order of change is much larger than could be expected if this were the only factor affecting the timing.

The increase in amplitude would suggest that as running speed increases, the ground reaction force also progressively increases. This would support the conclusions of Weyand et al. (2000) who state:

*'We conclude that human runners reach faster top speeds not by repositioning their limbs more rapidly in the air but by applying greater support forces to the ground.'*

In this instance it also suggests that more energy is being stored in the foot throughout the stance phase which is progressively released towards toe-off and stored through the swing phase in the body mass in the form of gravitational potential energy.

### 7.3.3 Ground Contact Progression

The captured video was analysed using the specialist software supplied with the camera (Phantom Camera Control – PCC) and each recording was trimmed to show a single stance and swing phase of the affected leg. Before testing began the camera was calibrated to film at a suitable frame rate that eliminated visible motion blur when paused, achieved at 1500fps. Selecting a higher frame rate than this was unnecessary and served only to increase the file size of the data capture.

#### 7.3.3.1 Stance Length Results

For each running speed a virtual line was superimposed onto the video at the point of heelstrike (aligning with the two measuring rules attached at the near and far sides of the treadmill) and a second line superimposed at the point of toe-off. These measuring rules and the superimposed lines can be seen in figure 7.8 which shows the important segments of the stance phase along with a measure of stance length for that particular speed (in this instance  $18\text{kmh}^{-1}$ ). The values for stance length at each running speed were observed to the nearest whole cm (therefore  $\pm 5\text{mm}$ ) and can be seen in table 7.2.

Velocity		Stance length (prosthetic)
kmh	m/s	mm
8	2.2	500
9	2.5	530
10	2.8	580
11	3.1	610
12	3.3	640
13	3.6	670
14	3.9	700
15	4.2	710
16	4.4	730
17	4.7	740
18	5.0	740

**Table 7.2:** Summary of stance length of the prosthetic foot on test across the range of running speeds ( $8 - 18\text{kmh}^{-1}$ ).

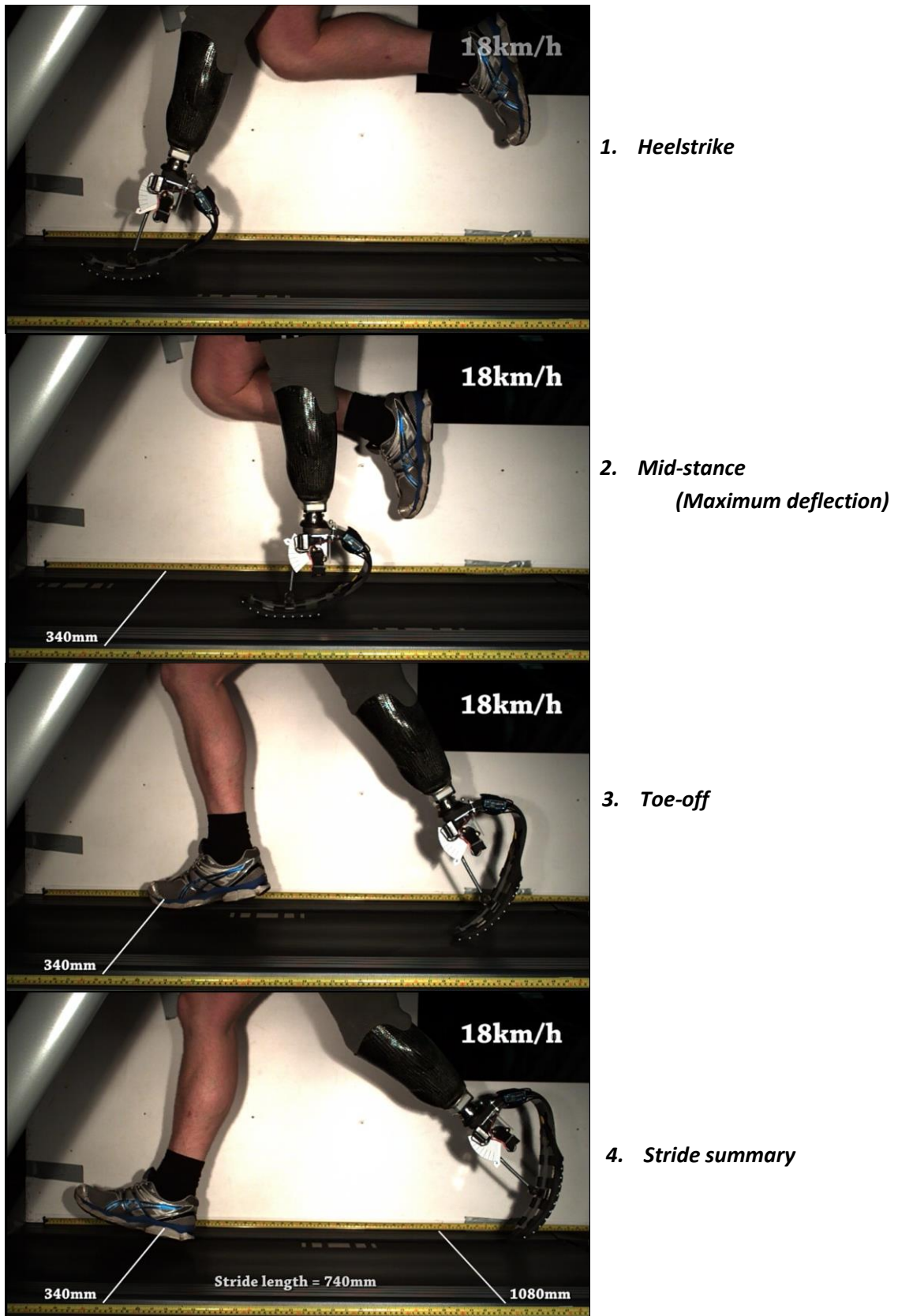


**Figure 7.8:** Series of images (still frames) capturing the progression of a single stride at  $18\text{kmh}^{-1}$ . The measuring rules used to determine the stance length can be seen on the near and far edges of the treadmill with lines superimposed to show the points of heelstrike and toe-off.

When this data is plotted on a graph (figure 7.9) it can be seen that a linear trend is established from  $8\text{kmh}^{-1}$  until  $16\text{kmh}^{-1}$ . However above this speed the gradient becomes shallower, levelling off at  $17\text{kmh}^{-1}$  and  $18\text{kmh}^{-1}$  both with a stance length value of  $740\text{mm}$ .

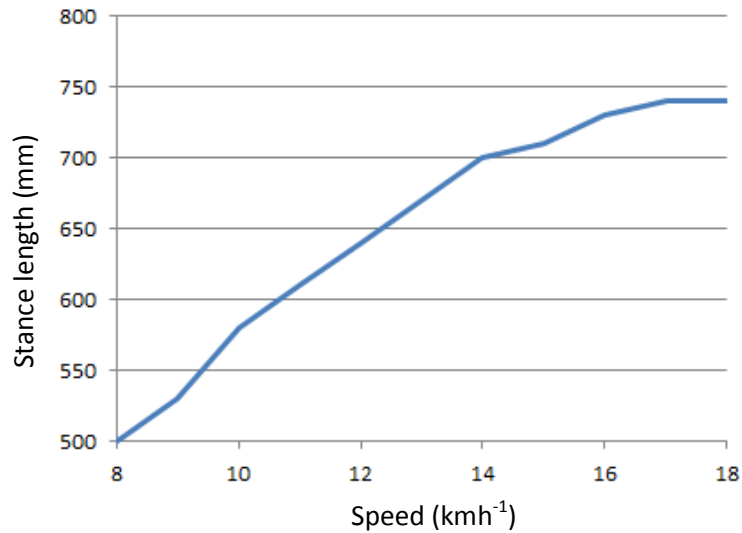


**Figure 7.9:** Trace showing how the stance length of the affected leg changes at different running speeds

It appears that above  $16\text{kmh}^{-1}$  with the specific foot that was fitted (an Ossur Flex Run Cat.7Lo) the amputee under test reaches his maximum stance length ( $740\text{mm}$ ).

### 7.3.3.2 Ground Contact Progression Results

In addition to measuring stance length the video could be paused at the moment heelstrike occurs and shifted (jogged) forward or backward frame by frame to understand the ground contact point at any moment.

By this means (and according to figure 7.10) the ground contact point of the foot at the moment of foot strike could be defined.

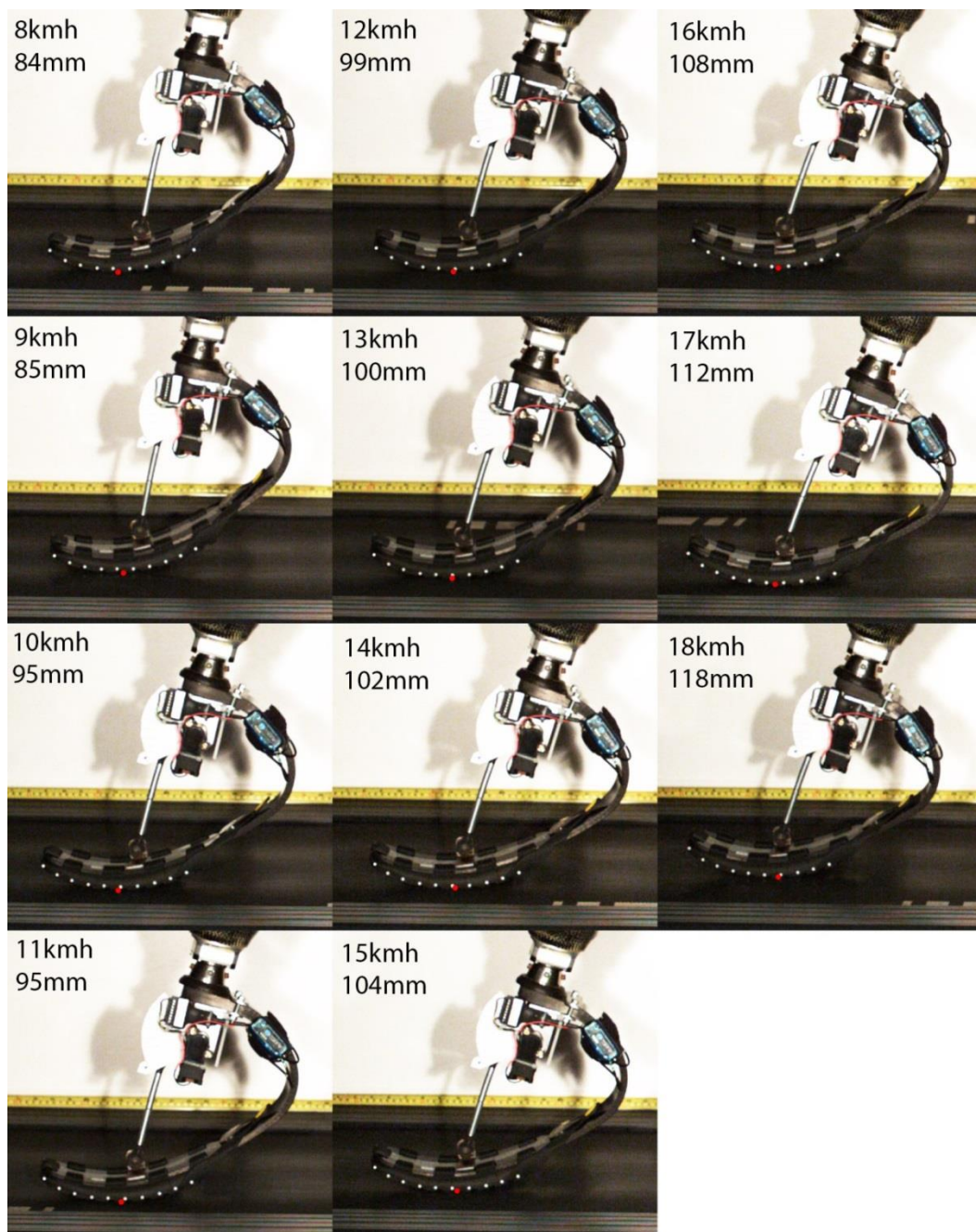


**Figure 7.10:** Collection of images of the prosthetic foot at the moment of foot strike at each of the test speeds demonstrating the change in ground contact point (defined as mm rear of the toe).

Figure 7.10 shows a collection of images (still frames) from the video, captured at the moment of heelstrike for the range of tested running speeds. The figures located in each of the frames demonstrate the running speed as well as the ground contact point as a function of distance rear of the edge of the toe. There is a superimposed red dot indicating the ground contact point in each condition. As each white pin was located 20mm apart, the ground contact position can be defined by counting the pins from the toe. As such the data gathered was deemed accurate to +/-1mm.

It can be seen that as speed increases, the ground contact point at heelstrike moves progressively rearwards. This information was plotted and can be seen in table 7.3 and figure 7.11.

Velocity kmh	Velocity m/s	Heelstrike position (relative to toe) mm
<b>8</b>	2.2	83
<b>9</b>	2.5	86
<b>10</b>	2.8	92
<b>11</b>	3.1	95
<b>12</b>	3.3	98
<b>13</b>	3.6	100
<b>14</b>	3.9	103
<b>15</b>	4.2	104
<b>16</b>	4.4	108
<b>17</b>	4.7	112
<b>18</b>	5.0	118

**Table 7.3:** Summary of stance length of the prosthetic foot on test across the range of running

Figure 7.11 suggests a linear relationship between the ground contact point of the foot at heelstrike and running speed. As the velocity increases, the ground contact point moves further rearward on the foot up to a value of 118mm rear of the toe at 18kmh<sup>-1</sup>; a change of 35mm posterior across the range of speed. It was found in section 4.6.2 that the stiffness of the foot decreases towards the tip of the toe, meaning that as the running speed is increased the effective stiffness of the foot is also increased.

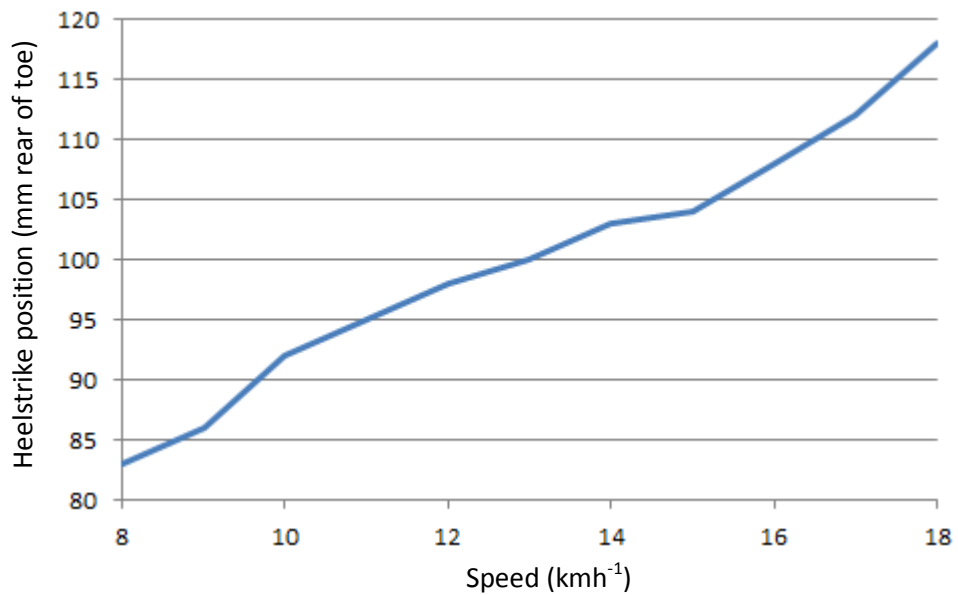


**Figure 7.11:** Trace showing how the heelstrike ground contact point of the affected leg changes at different running speeds

It should be noted that toe-off occurred at the same location for all test speeds at the tip of the toe; effectively at 0mm. Therefore the range of ground contact point for each speed can be considered as being from the posterior-most figure listed in table 7.3 and 0mm.

Using the same method of video interrogation the progression of ground contact point can be observed throughout the course of the stride. This will help furnish an understanding of how the effective foot stiffness changes throughout the stride and at different running velocities.

As mentioned previously the video was filmed at 1500fps meaning that 15 frames = 10ms. This ratio was used to generate the ground contact point data for each running speed. The video footage was paused at the moment of foot strike and the contact point read from the screen (by counting along the white markers pinned to the sole of the foot). The video could then be advanced 15 frames and the second ground contact position read before advancing the video another 15 frames. This process was repeated until toe-off occurred. By this method the ground contact point of the foot

could be ascertained for every 10ms throughout the course of the stride. It was repeated using video capture for each of the test speeds (8 – 18kmh<sup>-1</sup>).

It was anticipated that the point of ground contact would progress smoothly from the posterior to anterior portions of the foot throughout the duration of the stride (as tibial progression occurs – see figures 1.5 & 1.6). However the video demonstrated how the geometry of the foot and most notably the *deflection* of this geometry meant that this is not the case.

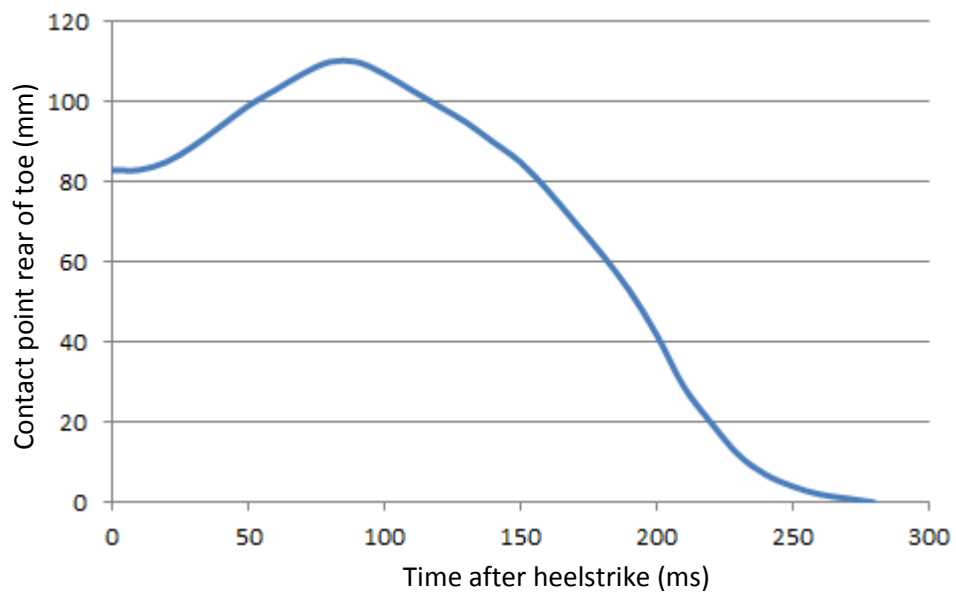


**Figure 7.12:** Trace demonstrating the progression of ground contact point at 8kmh<sup>-1</sup>

Figure 7.12 shows a trace of ground contact point (expressed as a distance in mm rear of the tip of the toe) plotted against time after heelstrike in milliseconds for a running speed of 8kmh<sup>-1</sup>. It can be seen that immediately following heelstrike up to a value of 90ms the ground contact point actually moves posterior despite the knee of the amputee progressing over the top of the foot. It can be observed from the video capture that this phenomenon is caused by the bending of the foot and how its geometry interacts with the ground.

Figure 7.13 shows two screenshots (freeze frames) selected from the video of 8kmh<sup>-1</sup> running (corresponding to the trace in figure 7.12 above) at heelstrike and 90ms after heelstrike. The position of ground contact is indicated by a red marker and it can be

seen that it moves rearwards along the base of the foot. The bending action of the foot as deflection occurs changes the geometry of the toe and forces the ground contact point rearwards.

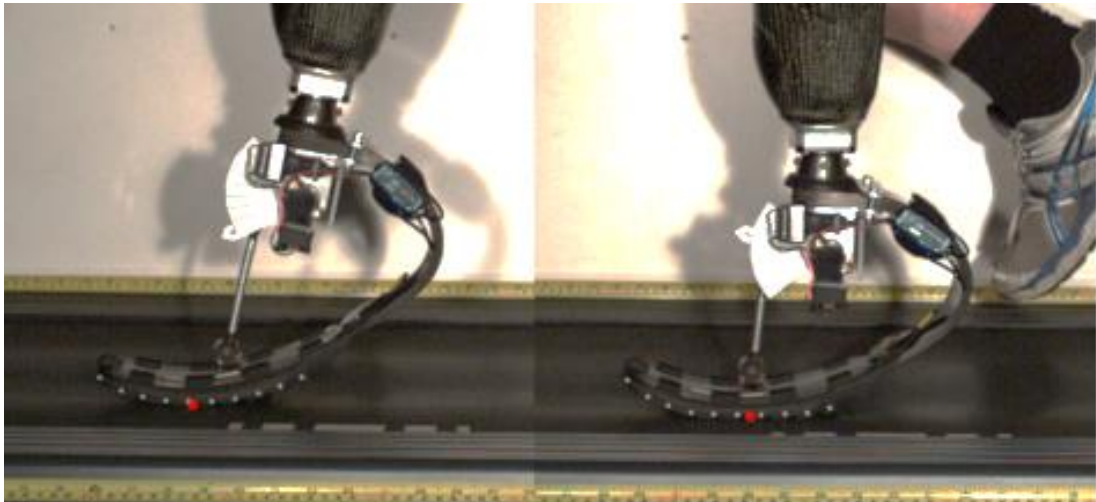


**Figure 7.13:** Screenshots of the prosthetic foot during running at 8kmh at heelstrike and 90ms after heelstrike demonstrating the contact point moving posterior (82mm – 110mm).

This change in geometry would appear to conflict with the progression of the knee over the foot in its effect of changing the ground contact point (the knee moving over the top of the foot would encourage a naturally anterior-moving ground contact point). It suggests that the speed at which each occurs defines the resulting moving of ground contact point.

In order to demonstrate this, figure 7.14 shows the curves for both the 13kmh<sup>-1</sup> and 18kmh<sup>-1</sup> tests added to the graph of 8kmh<sup>-1</sup> displayed in figure 7.12. It can be seen that as running speed increases the posterior movement of the ground contact point reduces until, at 18kmh<sup>-1</sup>, there is no longer any posterior movement at the start of the stance phase. This suggests that the speed of progression of the knee over the foot is sufficient to counteract the effect of the foot bending and results in the contact point remaining static for the first 60ms of the stance phase of the stride.

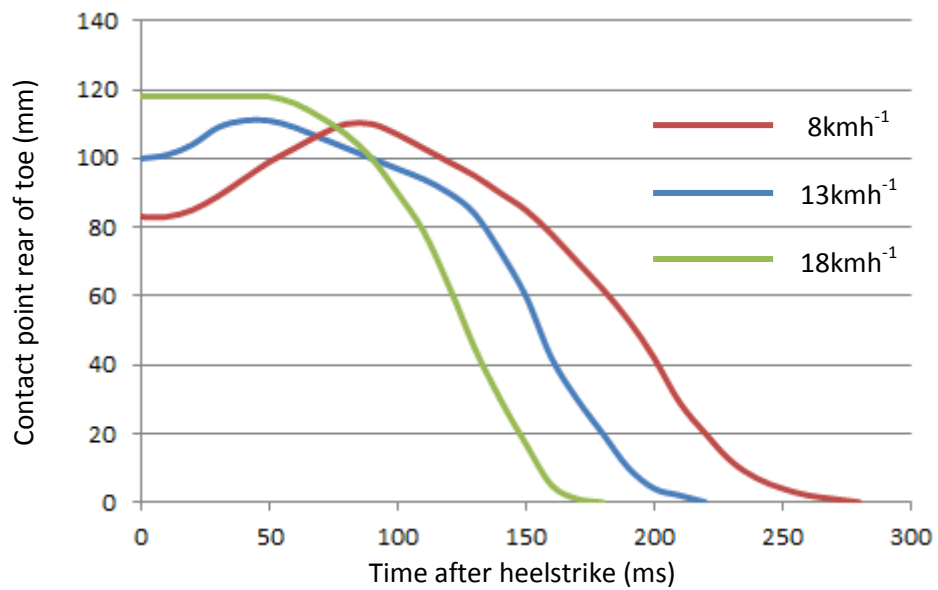


**Figure 7.14:** Trace demonstrating the progression of ground contact point at 8, 13 & 18kmh<sup>-1</sup>

### 7.3.4 Foot Stiffness Progression

It has been shown in section 7.3.3.2 that the ground contact point of the foot changes throughout the course of the stride and figure 7.14 defines a profile of this progression for three running speeds. Fundamentally this change in ground contact point means a change in foot stiffness, and it is this stiffness that interacts with the system as a tangible measure. If the dynamic nature of the foot is to be understood, the change in foot stiffness should be defined.

If a value of stiffness could be defined for various positions along the metatarsal region of the foot, these could be plotted and a profile of foot stiffness vs. ground contact point could be generated. Using the equation generated from this curve, the stiffness of any specific point along the foot could be defined mathematically without the need for further stiffness testing. This is an identical approach as taken in section 4.6.2.

### 7.3.4.1 Method

An investigation identical in nature to that carried out in section 4.6 was conducted but using the newer geometry of Flex Run foot (Cat7.Lo as used for amputee testing in section 7.2 & 7.3). Also different were the effective positions of ground contact point chosen (toe clamp positions – see table 7.4).

The foot was installed in the Instron hydraulic test machine as shown in figure 4.9 with the deflection transducer attached. This was used for defining the maximum deflection at each effective ground contact point.

Three ground contact points were chosen for testing (defined as 15mm, 75mm and 135mm rear of the toe). Providing that these chosen points represent a broad variation in ground contact point and that they were well defined and repeatable, the actual location of these chosen points was unimportant. This is because they would be used to define a curve to characterise the stiffness of the foot at any given position.

For each clamp point the foot was deflected to the maximum value observed in amputee running (section 7.3) as defined by the deflection transducer (1.35 volts at mid-stance at  $18\text{kmh}^{-1}$ ). Because of the change in the effective lever arm of the foot, the further anterior the toe clamp was attached, the higher the amplitude of

Toe clamp position (description)	Toe clamp position (mm from toe)	Required actuator displacement (mm)
rear	135	45
mid	75	58.1
front	15	88

**Table 7.4:** Summary of toe clamp positions chosen to demonstrate the change of foot stiffness along the metatarsal region with the actuator displacement required to mimic maximum foot deflection at each point.

displacement requirement of the Instron actuator to achieve the deflection transducer target voltage. Table 7.4 summarises the required displacement at the different ground contact points to achieve 1.35 volts at the transducer.

As in previous test work of this nature (section 4.6) the foot was deflected in a sine wave at a frequency of 0.5Hz up to the maximum deflection summarised in table 7.4. Data was recorded from the linear transducer and the load cell of the Instron at a frequency of 100Hz therefore providing the necessary data to generate a force – displacement curve for each ground contact point.

### 7.3.4.2 Results

Figure 7.15 plots the force–displacement data that was recorded for the Ossur Flex Run Cat.7Lo foot on test for each of the simulated ground contact positions. These are described as ‘rear’, ‘mid’ and ‘front’ positions but are defined in table 7.4.

As can be seen in figure 7.15 (and as previously demonstrated with the older model of Flex Run in section 4.6) the foot exhibits an almost entirely linear spring rate for each of the ground contact conditions with an energy return efficiency of >99%. The data shown forms a hysteresis loop with traces for both compression and rebound phases. However the efficiency of the foot is such that the two phases are indistinguishable.

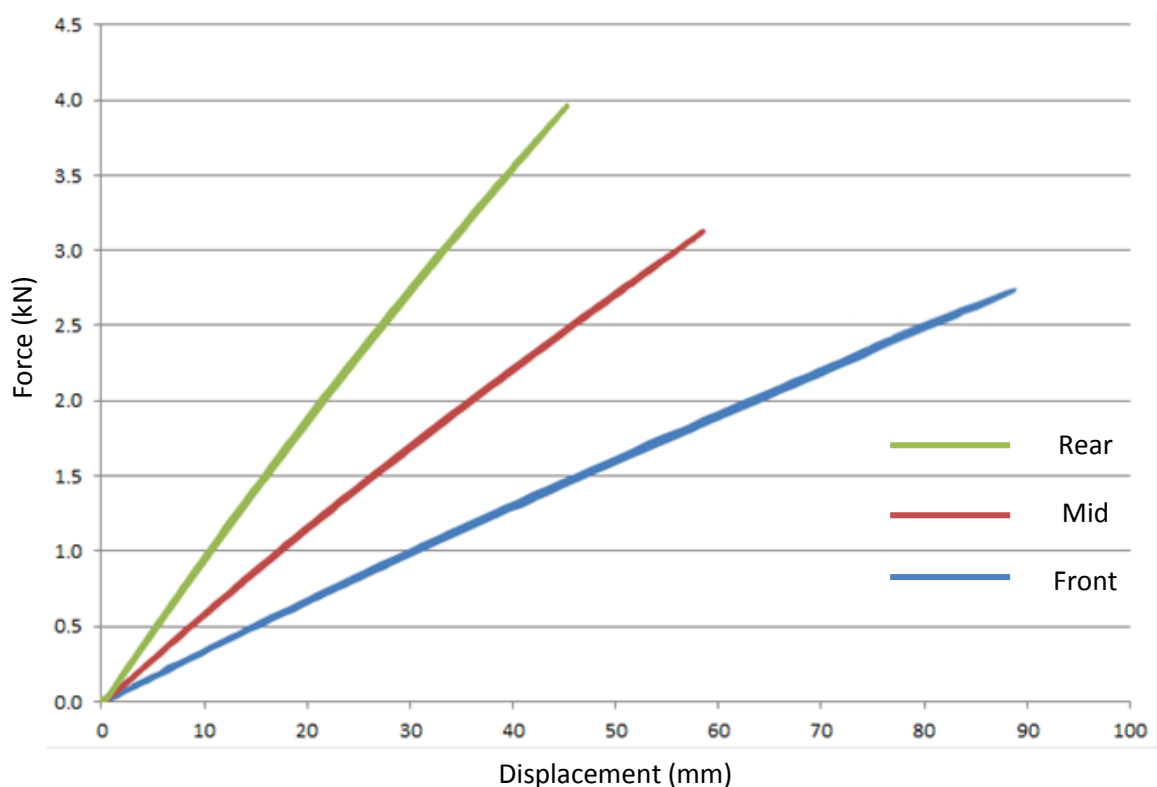


**Figure 7.15:** Graph comparing the force – displacement data for the Ossur Flex Run Cat.7Lo foot with three different simulated ground contact positions (defined in table 7.4).

The spring rate of each of these simulated ground contact conditions was calculated by dividing the maximum force by the maximum achieved displacement, therefore providing a value for stiffness in N/m. This method of defining spring rate assumes a completely linear force – displacement relationship and this is the topic of discussion in section 3.4.3. The resulting spring stiffness is summarised in table 7.5.

Position		Stiffness
Description	mm rear of toe	N/m
<b>Front</b>	15	31482
<b>Mid</b>	75	53599
<b>Rear</b>	135	87622

**Table 7.5:** Summary of foot stiffness values for the three simulated ground contact positions.

These values of stiffness were plotted on a graph against their position on the foot (mm rear of the toe). The resulting curve is shown in figure 7.16.

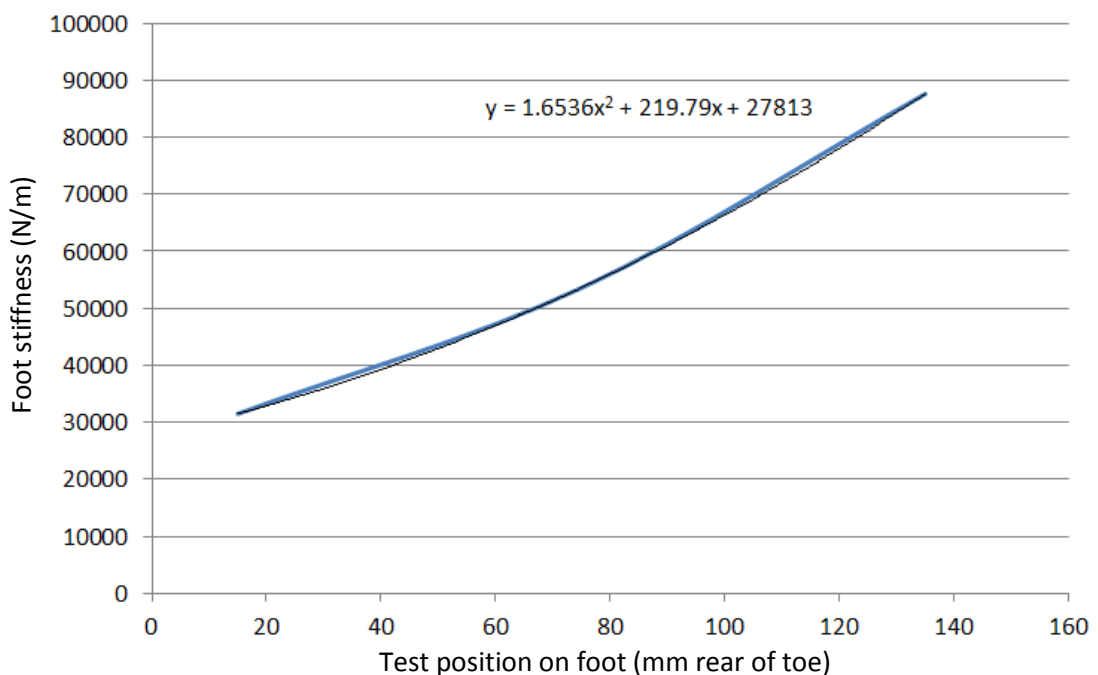


**Figure 7.16:** Curve of foot stiffness plotted against the effective ground contact point along the metatarsal region of the foot. A 2<sup>nd</sup> order Polynomial equation was derived from the curve and is displayed.

A 2<sup>nd</sup> order Polynomial equation was derived from the curve and is displayed in figure 7.16. Using this equation the stiffness of the foot can be defined for any specific ground contact point and as such the change in stiffness throughout the progression of the stance phase of the stride can be calculated.

Figure 7.12 shows the ground contact progression over the base of the foot during a single stride for the amputee running at  $8\text{kmh}^{-1}$  with an Ossur Flex Rub Cat.7Lo foot. It is now possible to express this data in terms of stiffness instead of as a function of contact point from the toe (in mm). This is done by substituting each value of ground contact point used to generate figure 7.12 into the equation displayed in figure 7.16. The resulting graph is shown in figure 7.17.

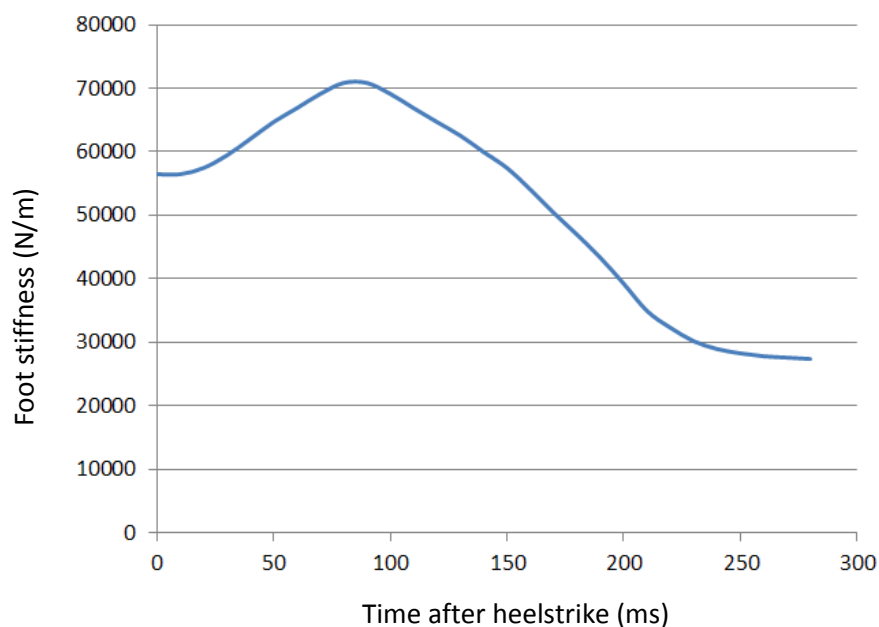


**Figure 7.17:** Trace displaying the changing effective stiffness of the prosthetic foot throughout the course of a single stance phase. This curve mirrors that shown in figure 7.12 and is based on the same data.

This new stiffness profile highlights the amplitude of change of the foot stiffness throughout a single stride. At its maximum value the foot stiffness reaches  $70839\text{N/m}$ , contrasting with the stiffness of  $27380\text{N/m}$  at the toe; alternatively expressed, the stiffness of the foot alters by a factor of 2.6 times throughout the course of a single step.

This highlights the importance of understanding the ground contact conditions of the foot during running if its response is to be understood and modelled.

### 7.3.5 Data Validity Check

In order to establish a validity check for the data gathered in this section a relationship between stance length, running speed and ground contact progression can be established.

By definition, the stance length is the distance travelled by the ground contact point of the foot in the time defined by the dynamic response of the system (ground contact time). This ground contact time is known (table 7.1), the stance length has been defined through interrogation of the video (table 7.2, figure 7.8) and the change in the Ground Contact Point is detailed for each running speed in table 7.3. The belt speed was defined for each test and as such these factors can be correlated as follows:

$$\text{Stride length (m)} = \text{velocity (m/s)} \times \text{GCT (s)} - \text{GCP change (m)}$$

Working through the example for 18kmh (shown in figure 7.8):

$$\text{Velocity} = 18 \text{ km/h} = 5.0 \text{ m/s}$$

$$\text{Ground Contact Time (GCT)} = 0.182 \text{ s}$$

$$\text{GCP change} = 0.118 \text{ m}$$

$$\text{Stride length (m)} = 5.0 \text{ m/s} \times 0.182 \text{ s} - 0.118 \text{ m} = 0.792 \text{ m}$$

Velocity kmh	Velocity m/s	Stride length (actual) mm	Ground contact time ms	GCP shift mm	Stride length (calculated) mm	Variation %
8	2.2	500	275	83	528	5.6
9	2.5	530	260	86	564	6.4
10	2.8	580	246	92	591	2.0
11	3.1	610	232	95	614	0.6
12	3.3	640	227	98	659	2.9
13	3.6	670	217	100	684	2.0
14	3.9	700	209	103	710	1.4
15	4.2	710	203	104	742	4.5
16	4.4	730	197	108	768	5.1
17	4.7	740	193	112	799	8.0
18	5.0	740	182	118	792	7.0

**Table 7.6:** Summary of stance length, ground contact conditions and the correlation accuracy (% variation) of these factors for each running speed tested.

Table 7.6 summarises the values of stance length and the ground contact conditions that exist for each running speed from 8 – 18kmh<sup>-1</sup> along with values for the theoretical calculated stance length that should occur if all of the numbers are completely accurate.

As can be seen the calculated and actual figures of stance length exhibit a maximum deviation of 8% from one another with an average variation of 4.2%. However it should be noted that the largest variations occur at the extremities of speed tested. The data assumes accurate measurement of the actual stance length, ground contact time (defined by the deflection transducer) and the shift in ground contact position along the metatarsal region of the foot, all of which have been measured and recorded throughout the course of this research. Additionally, and fundamentally, the data assumes the belt speed of the treadmill to be accurate. The fact that the largest discrepancies appear at the extremities of test speed (18kmh<sup>-1</sup> was the highest achievable belt speed of the machine) suggest that this could be a factor in the value of % variation.

## **7.4 Chapter Conclusions**

From the data presented it is clear that in order to run faster, an amputee will increase their stance length therefore covering more ground with each stride. This is information that has not been found in any of the literature studied to date. As defined in Chapter 6 the response time of the foot is fixed and governed by foot stiffness, amplitude of deflection and the mass acting on the foot. Therefore the amputee cannot demand a change in response timing and will instead alter his or her stance length according to the speed desired.

The subjective feedback from the amputee at the time of testing was that he was not comfortable running faster than 18kmh<sup>-1</sup>, likening the feeling to trying to ride a bicycle in a gear that was too low. It is possible to ride the bicycle faster by spinning the pedals more rapidly (increasing cadence) until the point where the pedals cannot be turned any faster. At this time it would necessary to change gear to go faster.

As such there must be a maximum speed that can be achieved by an amputee with a specific prosthetic foot, defined by the response time and the stance length that amputee is capable of achieving. If a higher running speed is required, either the stance length must be increased further or the response time must be decreased. This means that for a given running speed, the foot will respond faster and thus shorten the stance length at that speed. The amputee regains the ability to increase his or her stance length and achieve a higher velocity. In the instance of the amputee athlete tested it appears that his maximum velocity was achieved on the treadmill at  $18\text{kmh}^{-1}$  as a function of the limitations of the foot. However simply assigning a stiffer foot category does not immediately mean a faster running speed can be achieved. It would purely mean that the response time of the foot is no longer the limiting factor and some other constraint is placed on the runner (leg power, ability to reposition limbs fast enough, fitness, etc).

As the speed of running increased it can be seen that the initial point of ground contact moves posterior along the metatarsal region of the foot. In section 7.3.4.2 it was once again shown that the stiffness of the foot decreases towards the toe, meaning that as running speed increases the effective stiffness of the foot is also increased. It could therefore be suggested that the foot is to a certain extent self-adjusting to the demands of a higher running speed. As mentioned previously the limiting factor in amputee running can be the stiffness of the foot (or lack thereof) and the resulting response time being slow. As the speed increases it can be observed that the foot effectively becomes stiffer due to its geometry and therefore the response time will be shorter. It could also be suggested that if the initial point of ground contact were not to move in a posterior direction as speed increases, the maximum speed able to be achieved on that specific prosthetic foot would be lower and more limiting to the amputee.

Throughout testing across the entire range of running speeds the (unilateral) amputee was able to maintain symmetry (measured subjectively by feedback from the amputee and by examining video of the runs with a qualified and experienced prosthetist). This suggests that the unaffected leg is matching the action (timing, stance length) of the prosthetic leg in order to preserve symmetry.

This chapter has demonstrated that if the action of a prosthetic foot were to be modelled (in response to the research sub-question put forward in section 2.1.3: **Can the action of a prosthetic running foot be modelled mathematically?**) it is not sufficient to purely take into account the stiffness of the foot and mass of the amputee. It has been shown in this chapter that the effective stiffness of the prosthetic running foot varies depending on running velocity. Further to this and in response to the primary research question in section 2.1: **Is the current method of prescribing prosthetic ESR running feet correct?**, it can also be suggested that the desired running speed of the amputee should be taken into account when prescribing a running foot. Currently the manufacturer advises prescribing a running foot based on the mass of the amputee alone. However this chapter has demonstrated that without understanding the dynamic response of that foot, this prescription method has the potential to limit the maximum running speed of the amputee. It therefore can be concluded that whilst undoubtedly assigning a competent category of foot to many amputees, the current prescription has the potential of limiting the activities of amputee athletes.

All of the work carried out to date (in Chapters 3, 4 & 6) has involved the characterisation of a single category of foot. Chapters 3 & 4 were conducted using an older model of Flex Run foot. If the research question in section 2.1.3: **Can the action of a prosthetic running foot be modelled mathematically?** is to be answered, a deeper understanding of the foot categories available should be gathered. Following a study of the categories, Wilson et al. (2009, P.221) comment '*The exact stiffness categorization was somewhat arbitrary*'. Ossur currently manufacture 9 different stiffness categories of Flex Run foot (each with a 'Hi' or 'Lo' variant) and currently there is no literature available that refers to their stiffness characteristics.

It is proposed that the following chapter be concerned with furthering our knowledge of the mechanical properties of these stiffness categories in anticipation of modelling their action mathematically.

# CHAPTER 8: CHARACTERISATION OF FOOT CATEGORIES

## 8.1 Introduction & Chapter Objectives

As discussed in Chapter 1, Ossur as a manufacturer offer a range of prosthetic running feet. The most popular is the Flex Run model which has been the subject of this research project, but within this individual model there are a broad range of stiffness classifications available.

Work to date has been concerned with amputee testing and subsequently the replication and investigation of this running in a laboratory environment. This has all been conducted with the style and category of foot that was already in use by the amputee athlete who was tested, therefore ignoring the majority of the available range of feet. The Flex Run is available in 9 stiffness categories (named Cat.1 through to Cat.9, the latter being the stiffest model). Within each of these categories there exists a 'Hi' and 'Lo' variant. Following feedback from the manufacturer, it has become known that this Hi and Lo denomination is a result of manufacturing tolerances. Each of the feet is individually rated for spring rate at the time of manufacture and if the foot stiffness sits within the upper half of that specific category stiffness tolerance band it is awarded 'Hi' status. The same is true for the Lo rating but for the lower end of the stiffness tolerance band.

The first 12 months of work in this research project was carried out using an Ossur Flex Foot Cat.6Hi dating from 2003. The knowledge gained from testing with this foot has set the tone for the entire project and established the trends upon which the theory is based. However in 2012 Ossur redesigned the Flex Run foot with a modified geometry rendering the specific nature of the work in this project irrelevant to any newly prescribed foot thereafter. The trends are useful to our understanding (for example when comparing the function of a foot with the equation for simple harmonic motion in Chapter 6) but any absolute data should be updated with information obtained from repeat testing with the newer geometry of Flex Run. A summary of the geometrical changes can be seen in figures 8.1 & 8.2.

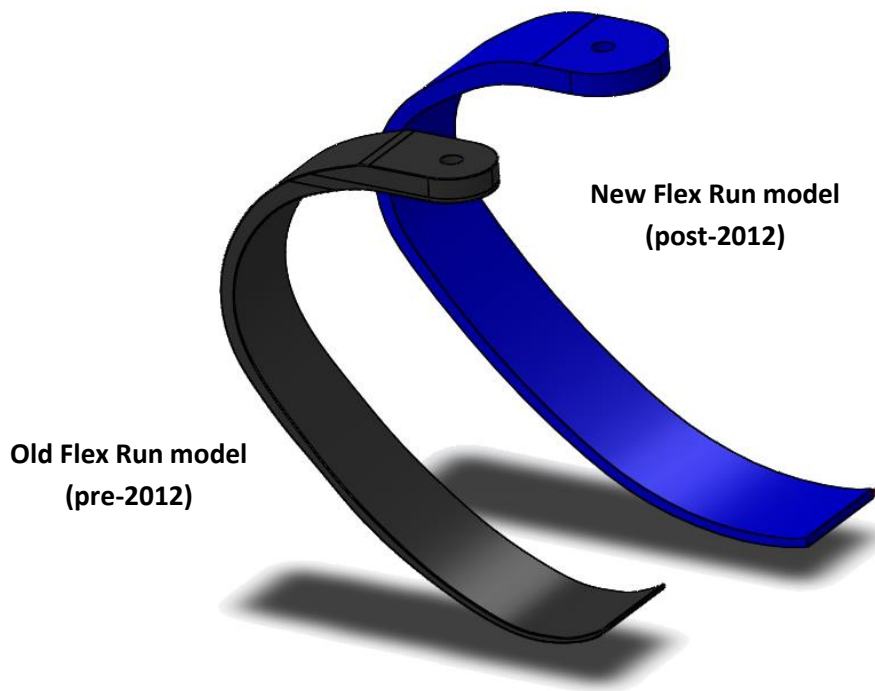


**Figure 8.1:** CAD image of the new and old style Ossur Flex Run. The geometry for every category is identical; the number of carbon fibre laminate layers defines the stiffness category.

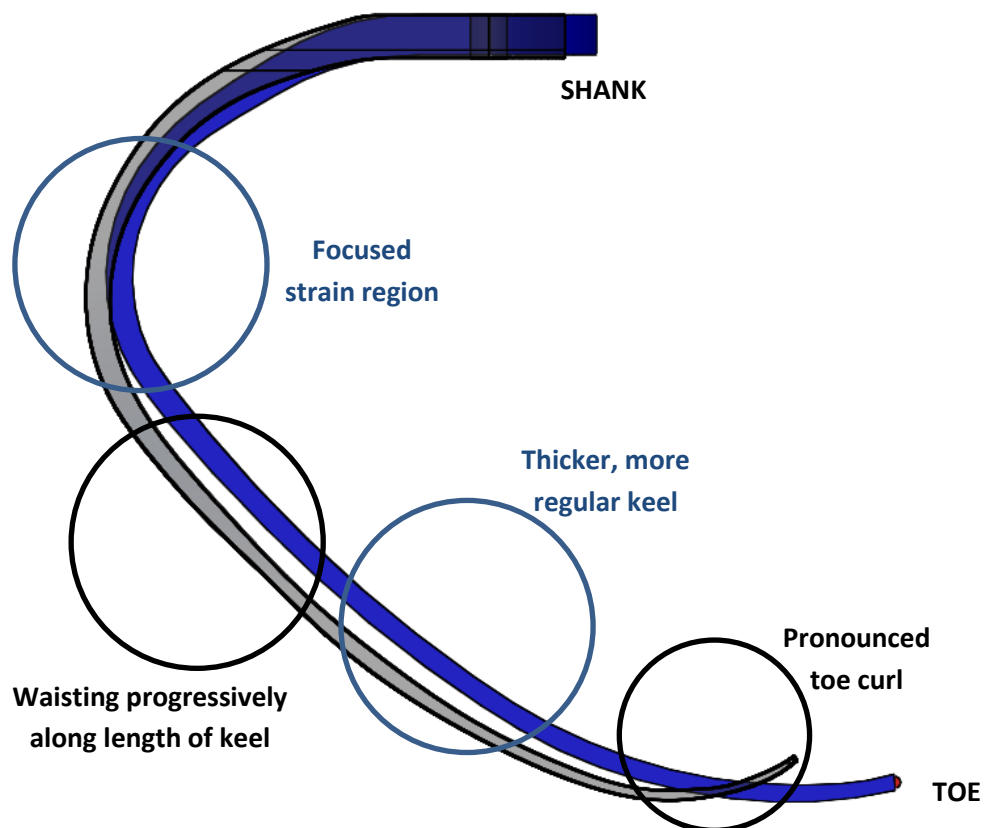


**Figure 8.2:** CAD image of the new and old style Ossur Flex Run overlaid with the key differences highlighted (viewed in the sagittal plane).

The feet are the same fundamental design but differ in their detail. The most prominent difference is that the older model (pre-2012) waists along its length from the toe to the shank meaning that the keel gets progressively thinner towards the toe. The result of this is that the strain of the foot bending is spread along the length of the foot. By contrast the new design appears to focus the strain on a particular region. This has been done by thickening the section of the keel without tapering towards the toe. Given that it is this area of strain that will predominantly provide the spring rate of the foot, it could be suggested that this has been done in order to better control the stiffness of the foot.

The second most obvious change is on the toe of the foot. The older model features a pronounced curl which has been eliminated on the newer model. There appears to be no clear advantage to this feature, but it could be suggested that it better controls the ground contact point at which toe-off occurs. With a curl in the toe the ground contact point at the moment of toe-off might change depending on the speed of running and length of the stride, whereas this cannot be the case with the newer model. Alternatively the explanation could be as simple as more easily allowing the fitment of the Nike running sole that was designed and released at the same time as the newer model of foot.

Fundamentally the designs are significantly different enough to warrant all future testing be conducted with the newer model. As such one foot from each of the 9 categories was sourced from the manufacturer and all subsequent work was conducted with the newer model of foot. The objective of this chapter is to further understanding of what the categorisation means (in terms of mechanical stiffness) such that the research question set out in section 2.1.3: **'Can the action of a prosthetic running foot be modelled mathematically?'** can be answered. If a value of stiffness for each of the available feet can be defined, this could be substituted into a model in order to understand the theoretical dynamic response characteristics.

## 8.2 Category Testing

Having access to the entire range of feet meant that an investigation could be carried out into what the category system means from a stiffness point of view. Do the feet ascribe to a regular array across the stiffness range or are their categories less controlled?

### 8.2.1 Defining a Datum

In order for the stiffness categories to be characterised, each of the feet needed to be installed in the Instron hydraulic test machine as conducted in section 3.4. The feet could then be deflected according to a pre-defined programme, therefore generating a force – displacement curve for each of them. As carried out in section 4.6 the toe clamp could be moved in order to simulate a change in ground contact point and generate a stiffness profile. The location of the toe clamp was previously defined as a distance from the toe of the foot, but upon inspection when the feet were compared with one another it quickly became clear that this was not possible.

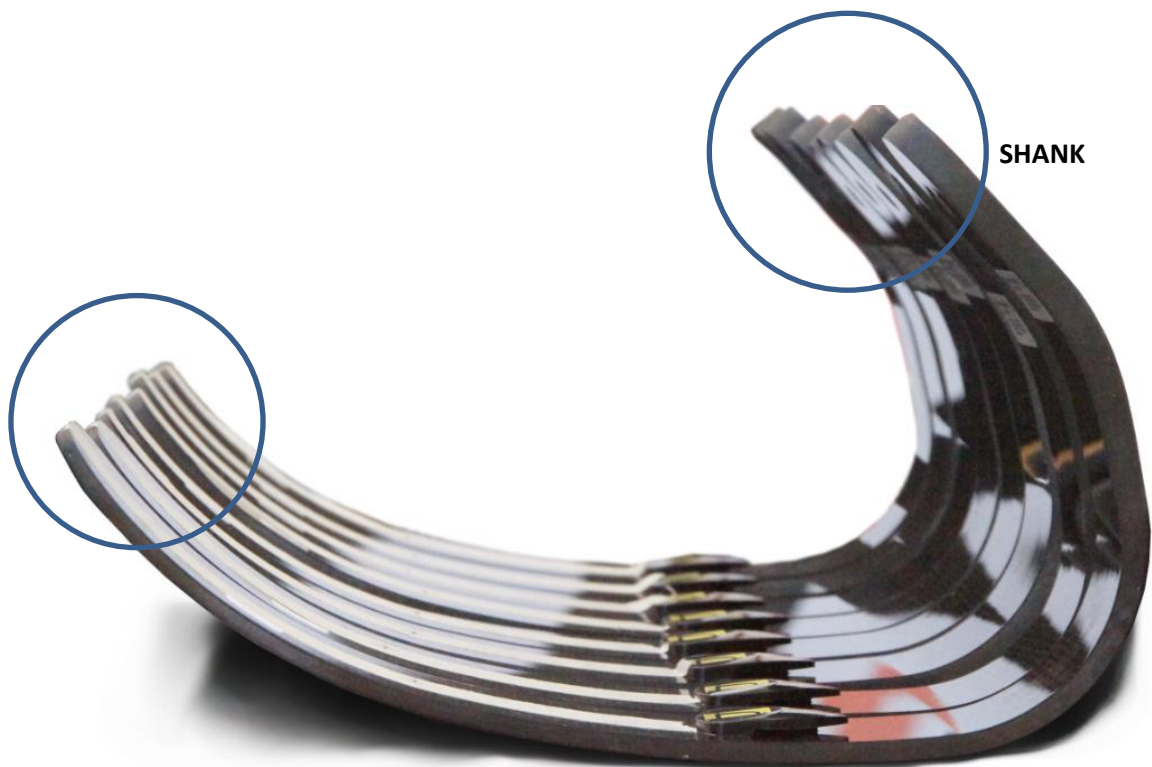


**Figure 8.3:** Image demonstrating the disparity in toe length and shank shape when a range of Flex Run feet are aligned. The upper shank surfaces for all feet are parallel.

Figure 8.3 is an image of the Flex Run feet obtained from the manufacturer aligned next to one another. The upper surface of each shank was arranged with a straight edge along the line of feet and each was laid on a flat surface. However despite best efforts to align the feet, the length of the toe differed on each device to the order of 6mm. In addition the shank edges did not align and upon inspection, the shape of this portion of the foot was irregular. It was confirmed by the manufacturer that this area was hand-finished during manufacturing (figure 8.4).

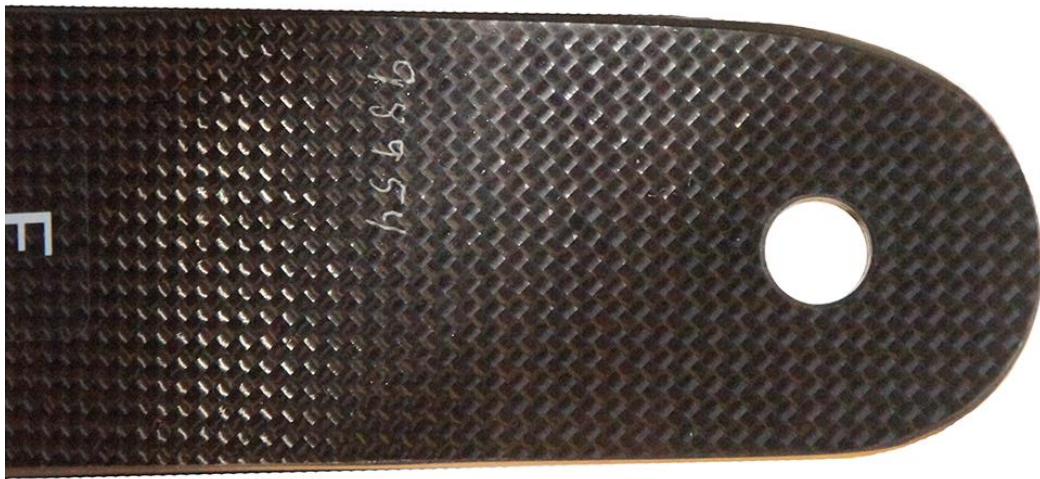


**Figure 8.4:** Image showing the detail of the shank with hand-finished edges. The irregularity of the curve makes the edge unsuitable as a datum point.

Before any characterisation work can occur with the feet, a reliable and repeatable datum point needs to be established across the entire range. It is about this point that measurements for the attachment of the toe clamp are to be taken, but it is clear that there are no surfaces of the foot that are comparable from one device to another. The datum point needed to be in relation to the foot geometry as the precise location of any of the edges of the feet is irrelevant.

The one remaining feature of the foot that could be used was the drilled hole for attachment of the pyramid adapter. The manufacturer confirmed that this position was drilled relative to the foot geometry (using a drilling jig that fastened to the foot

geometry, not relying on the position of any of the edges) and as such a method was devised of using this as the datum point for all testing.

Instead of physically measuring from the mounting hole around the curve of the foot geometry it was decided to use the mounting position to project a mark onto the keel of the foot. To do this a laser pointer was modified such that it attached through the mounting hole of each of the feet. This was complicated by the variation in drilling sizes of the mounting hole (categories 7,8 & 9 feature a 12mm hole whereas all of the lower categories feature a 10mm hole) but a small cylindrical aluminium component was fabricated that achieved the goals. The laser pointer device was pressed securely into one end and on the other were machined two threads; the first M12 and the second M10 with a corresponding shoulder to morph from one size to the other. This allowed the component to be attached to any of the feet regardless of hole size. Through the centre of the component was drilled a 0.5mm hole, 20mm long which aligned with the laser. This hole ensured that the light emitted by the laser was directionally accurate, aligning exactly with the cylindrical component. The device can be seen in figure 8.5 and the entire assembly mounted to a foot in figure 8.6.



**Figure 8.5:** Image showing the fabricated cylindrical component attached to a generic laser pointer. This could be mounted to the shank of any Flex Run foot for marking the datum.

This laser device could therefore project a point onto the upper face of the metatarsal region of the foot that was repeatable across all of the feet on test and irrespective of the hand-finished edges (but instead consistent with the foot geometry).



**Figure 8.5:** Image showing assembly of the laser device and foot prior to marking the position of the datum.

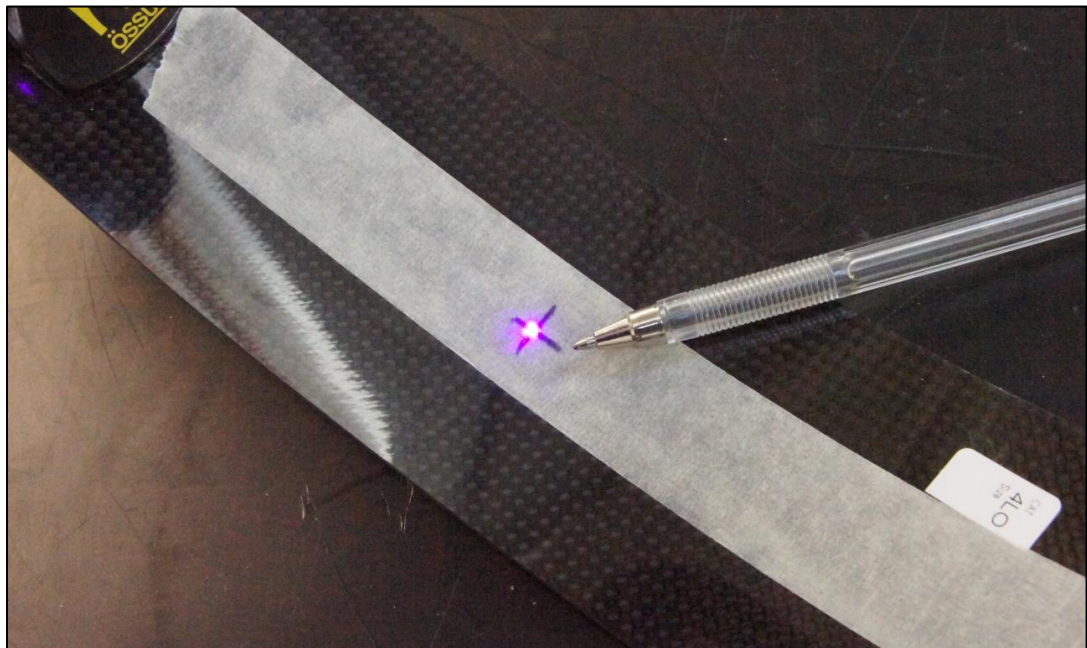


**Figure 8.6:** Image showing the projected laser datum and marking of this datum on the metatarsal region of the foot.

In order to avoid damaging the foot with a datum point, masking tape was added to the upper surface of the metatarsal region of the foot and using a pen the datum was marked (figure 8.6).

All of the feet (9 in total) were marked with a datum including the Cat.7Lo foot (that was used in Chapter 7). This foot had already undergone stiffness characterisation testing (section 7.3.4.1) and as such the positions of the toe clamp that were used in this previous work were repeated. The measurements used to define the position of the toe clamp (table 7.4, previously values in relation to the edge of the toe) were converted to locations in relation to the new laser-generated datum point.

## 8.2.2 Method

Once the toe clamp locations (used for defining the effective ground contact positions) were defined the stiffness characterisation for each foot could take place. The methodology for this is described in section 7.3.4.1. A summary of the new toe clamp locations can be seen in table 8.1.

Toe clamp position (description)	Toe clamp position (mm from toe)	Toe clamp position (mm from laser datum)
rear	135	-8
mid	75	52
front	15	112

**Table 8.1:** Detail of the toe clamp positions for the new laser-guided datum point as transposed from the previous datum of the front edge of the toe for the Cat.7Lo foot. A negative value means posterior of the datum point.

### 8.2.3 Results

Each foot in turn was characterised in terms of stiffness versus effective ground contact position. As conducted in section 7.3.4.1 each foot was subjected to a force – displacement measurement at three separate points along the metatarsal region, thus producing three individual force – displacement curves. An example is shown in figure 7.15 for the Cat7.Lo foot.

This means that as previously completed in section 7.3.4.2 an equation describing the stiffness of each of the foot categories could be derived as a function of ground contact position. The relevance of this equation becomes apparent when trying to model the action of all categories of foot mathematically, predicting the dynamic response and is the topic of the following chapter.

In addition the force – displacement data for each ground contact point can be plotted on a single graph in order to compare the distribution of foot stiffness across the range (for example for the mid contact point as illustrated in figure 8.7).

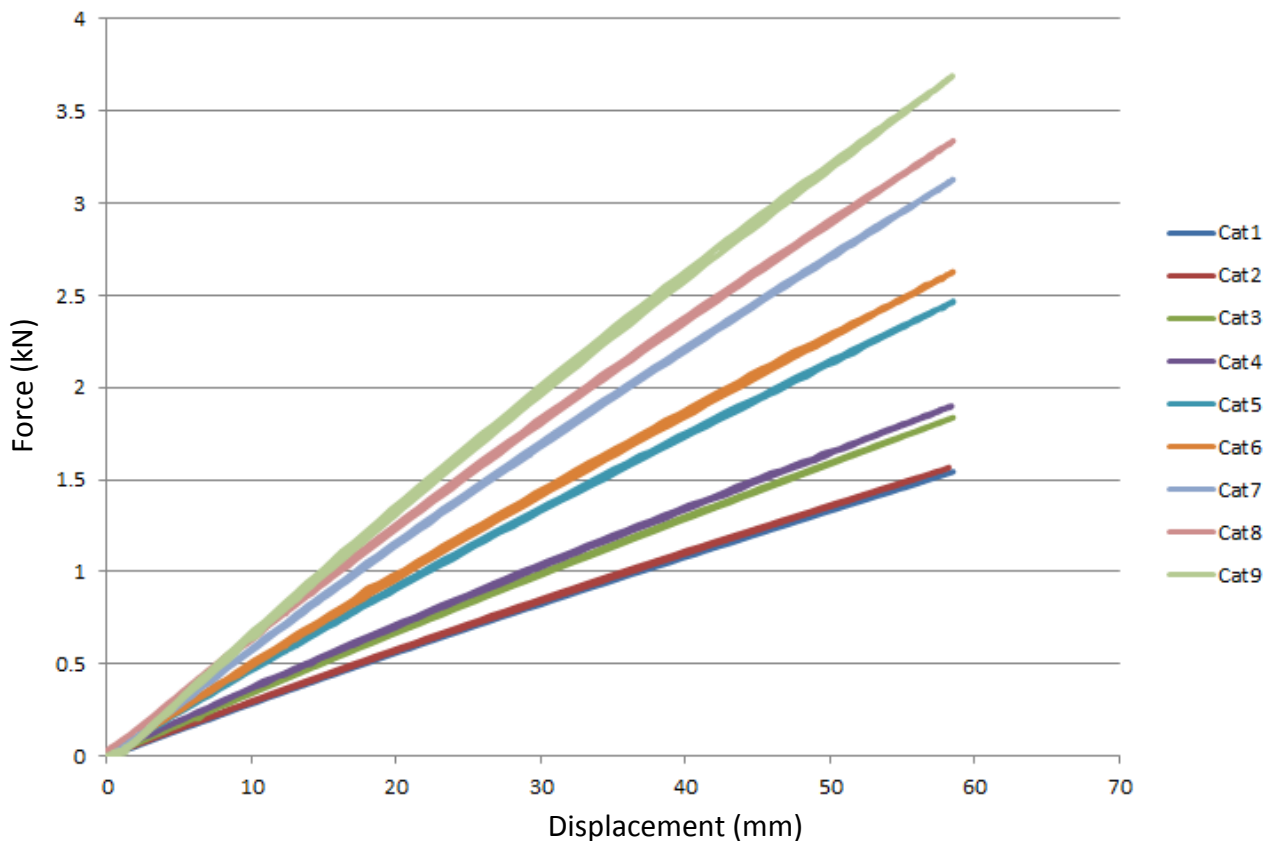


**Figure 8.7:** Graph comparing the force – displacement data for the entire range of Ossur Flex Run feet when tested at the ‘Mid’ position (see table 8.1).

It can be seen in figure 8.7 that the foot categories cover a range of stiffness and if the peak force is divided by the peak displacement a value of foot stiffness (at that specific 'mid' location) can be derived. The stiffness information for all feet at all contact positions is shown in table 8.2.

Category	Measured stiffness (N/m)		
	front	mid	rear
9	38451	63138	108705
8	34570	57287	97050
7	31482	53599	87622
6	27656	45098	76387
5	25862	42330	71460
4	22554	32548	53935
3	19406	31396	54024
2	16895	26919	44901
1	16569	26894	44307

**Table 8.2:** Overview of stiffness of all categories of Flex Run foot available from Ossur tested at three locations as described in table 8.1.

Interesting to note is that the feet do not appear to cover this range of stiffness in regular intervals. For example categories 1&2 are almost indistinguishable from one another, both returning nearly identical spring stiffness (a deviation of 0.1%). Likewise categories 3&4 share similar stiffness values (deviating 3.5% from one another). As demonstrated previously (in sections 3.4 & 4.7) the feet tested all exhibit an energy return efficiency >99% with a linear spring rate. However as described in Chapter 3 this efficiency and linear spring rate is as much to do with the mounting strategy of the foot as it is to do with the foot itself.

Using the data in Table 8.1 and Table 8.2 it was possible to generate a graph to describe the stiffness of each foot at any ground contact point. This is a similar process to that carried out in section 4.6.2 and as displayed in Figure 4.8, the main difference being that on this occasion the reference point was the laser datum instead of the edge of the toe of the foot. An example of this can be seen in Figure 8.8 as selected for the Cat.7 foot.

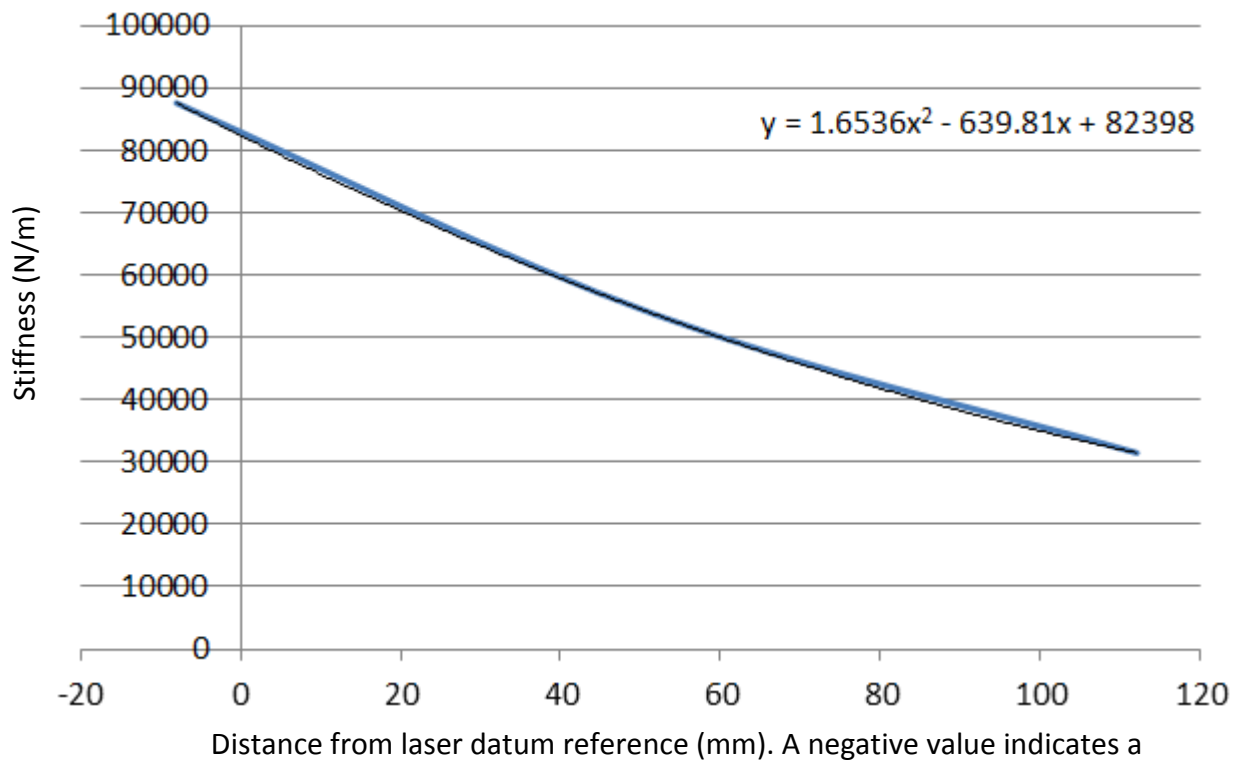


**Figure 8.8:** Graph demonstrating the difference in foot stiffness when altering the ground contact point along the metatarsal region of the foot. A line of best fit is added and equation derived to describe the relationship (Cat. 7 example).

As in section 4.6.2 a 2<sup>nd</sup> order Polynomial equation was sufficient to describe this curve and allow the definition of the foot stiffness for any ground contact point.

### 8.3 Chapter Conclusions

This chapter has demonstrated the variation of mechanical stiffness values across the range of Flex Run prosthetic foot categories, albeit for a sample size of one for each category. It can be seen that the categories do not sit at regular intervals through the stiffness spectrum, but it is likely that this occurs because of the variation in manufacturing tolerance.

It was acknowledged by the manufacturer that each category of foot can exhibit a range of stiffness, and in response to this a 'Hi' or 'Lo' classification is added. This also means that the foot could sit at any point within these classifications and as such the foot stiffness can only be defined within a working tolerance band. It is not possible to generate this tolerance band by testing one foot from within each stiffness category and instead this would be a useful extension of this research project.

Whilst every care was taken to ensure the accuracy of the toe clamp that was fitted for the testing (to define the effective ground contact point) it was assumed that the shank mounting hole was always perfectly aligned. However it was found that the mounting hole could also be in a variable position across the width of the foot and was not always drilled perfectly normal to the mounting face of the foot. The unrepeatable nature of this mounting hole could also be a source for error.

Having defined the stiffness of each foot at three points along the metatarsal region an equation was defined for each that described the stiffness of the foot as a function of ground contact position. These equations can now be used to specify foot stiffness (as a value of N/m) for any ground contact point. This information can now be used to advise the following chapter and takes the research one step closer to answering the research question set out in section 2.1.3: **Can the action of a prosthetic running foot be modelled mathematically?**

Now that the stiffness of the various feet is understood at any ground contact point, and Chapters 4, 6 & 7 have defined how this ground contact point changes with running velocity, the following chapter is aimed at understanding whether amputee running can be defined by a mathematical model.

# CHAPTER 9: MATHEMATICAL MODELLING OF A FOOT

## 9.1 Introduction & Chapter Objectives

This research has been able to characterise the action of a prosthetic running foot, defining mechanical properties and how these properties affect the action of an amputee athlete. If this learning can be applied to a mathematical model that is capable of describing amputee running, this can be used to judge not only the effectiveness of the current prescription technique but also to understand if and how the method of prescribing feet can be changed to improve the user experience for amputees, thus answering the primary research question stated in section 2.1: ***Is the current method of prescribing prosthetic ESR running feet correct and could it be more appropriately advised by taking into account any additional factors?***

If the action of a foot could be modelled mathematically, the understanding from the previous chapters could be generalised and used to benefit a wide range of amputee athletes. For instance it was shown in Chapter 7 that as speed changes there is a dramatic difference in foot response (resulting from a change in ground contact position and therefore foot stiffness). This change in ground contact position could be compounded depending on other factors such as amputee leg length or available stance length. Currently these factors are not taken into account when prescribing a prosthetic foot, the process relying solely on the mass of the amputee to assign a category of foot.

Furthermore it was shown in section 7.3.3 that the foot itself can provide a throttle on the maximum running speed available to an individual. Currently there is no method of understanding if a prescribed foot will allow the amputee to run in the manner that they desire.

This chapter is dedicated to the task of modelling the action of a foot mathematically such that the dynamic response of a foot can be ascertained for any amputee and the restrictions of that foot be understood.

## 9.2 Theory

Before undertaking any modelling it is important to establish what it is that is being defined. The ultimate goal is to assist the prosthetist in prescribing a foot, so what does the prosthetist need to know?

Throughout the course of this research project it is the dynamic response time that has taken precedent (otherwise referred to as Ground Contact Time). It is the natural output of the equation for Simple Harmonic Motion and has been shown in Chapter 6 to be a direct result of amputee mass, foot stiffness and the amplitude of deflection. If the response time of a foot could be defined for any amputee for any level of activity with any prosthetic running foot, would this help the prosthetist in making an accurate prescription?

The answer is probably not. Whilst the response time of the foot is an interesting variable to quantify, it is not a tangible measure for those who prescribe or use the prosthetic device. It means little to the prosthetist and amputee.

However it was shown in section 7.3.5 that if a running speed is specified, the ground contact time of the foot defines the stance length of the amputee. That is the distance travelled by the ground contact point of the foot in the given response time when using a treadmill. Stance length is a measurable that can be appreciated by the runner and observable by the prosthetist. It would therefore be logical if the output of any modelling was the resulting stance length that would need to be achieved by the amputee for any given running speed. This would require the amputee to specify their desired speed of running and providing that they or the prosthetist understands the limitations of the individual's stance length capabilities, the suitability of the foot being modelled can be judged.

Figure 9.1 shows a diagrammatic representation of this process, derived from the research carried out in the previous chapters and how each of the contributing factors interacts with the final output of defining stance length. Each of the criteria is addressed in the following sections of this chapter.

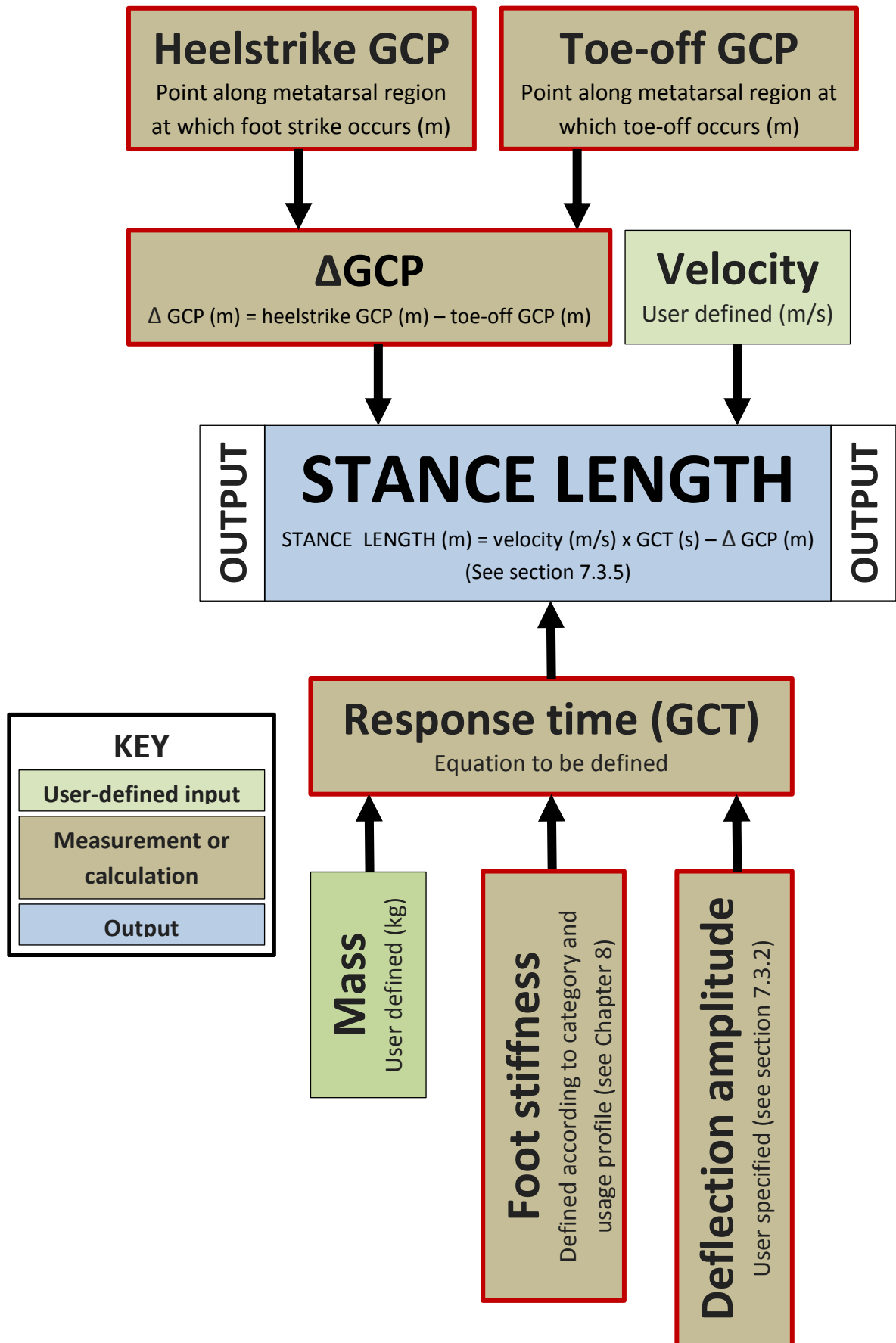


**Figure 9.1:** Flow diagram of the criteria that define the stride length of an amputee athlete using a Flex Run foot. Elements highlighted in red are knowledge gained during this research project.

## 9.3 Contributing Factors

### 9.3.1 $\Delta$ GCP

It was shown in section 7.3.3 that the ground contact point of the foot changes not only throughout the course of a single stride (progressing in an anterior direction towards toe-off) but also for different running speeds. As amputee running speed increases the position of foot strike moves rearwards (and on to an effectively stiffer portion of the foot).

In order for the equation that defines the stance length (section 7.3.5) to work effectively this change in ground contact position (from heelstrike to toe-off) has to be defined. This value represents the distance along the metatarsal region of the foot that the ground contact point progresses throughout the course of a single stance-phase of a stride.

It was demonstrated in section 7.3.3 when observing amputee running that at all speeds the toe-off position is identical, always occurring at the tip of the toe. The foot strike position was defined for the amputee being tested across a range of running speeds (table 7.3), but it is not known how this would change for athletes of differing proportions.

When observing the action of the amputee runner in section 7.3.3 it was observed that regardless of running speed his foot strike always occurs with a straight leading leg (little or no flexion of the knee is apparent). An example of this action can be seen in figure 7.1 which shows the amputee runner on a track, captured a fraction of a second prior to foot strike. The flexion in a knee when running (and particularly at the moment of foot strike) is a contentious issue ([www.scienceofrunning.com](http://www.scienceofrunning.com) 2014) in the running community but if it is assumed that the leg is straight (or has a small degree of flexion) at the moment of heelstrike then the ground contact point of the foot becomes a simple geometrical condition. The foot is still in an un-deflected state and the geometry of all categories of Ossur Flex Run feet is identical. This means that the ground contact point is a function of the angle of attack of the leading leg at the moment of heelstrike.

### 9.3.1.1 Foot Strike Position Simulation

A CAD simulation was constructed using a model of the Ossur Flex Run foot and a virtual representation of leg and hip joint. A screenshot of this model can be seen in figure 9.2. The foot was marked with pins in an identical manner to the testing in section 7.3 and the virtual hip was constrained in a way that allowed the position of the foot to be moved to rest on the ground plane. In addition the virtual leg length of the model could be changed. This way any stance length could be represented with any length of leg and the ground contact point be 'read' from the model.

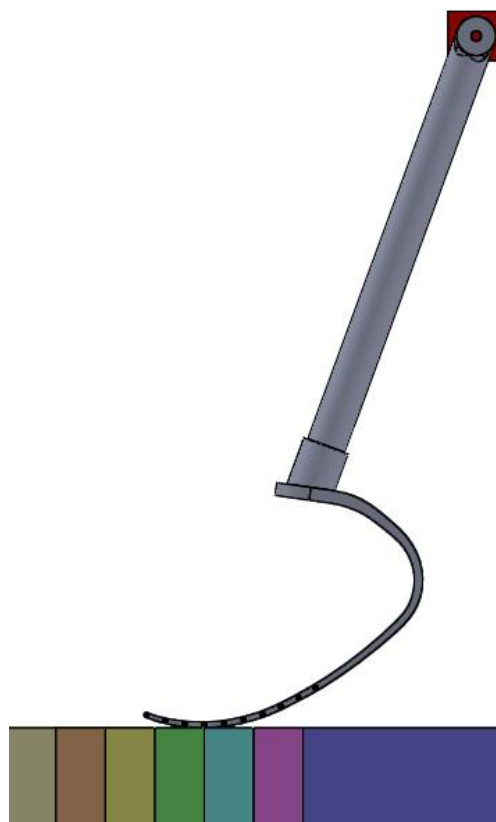


*Figure 9.2: Screenshot of CAD model developed to predict in part the ground contact point on the metatarsal region of the prosthetic foot for a variety of stride and leg lengths*

It should be noted that the foot model was mounted to the virtual leg as best it could be by following the manufacturer's instructions (Ossur Instructions for Use, 2012). However these instructions are vague and proved impractical to follow to the letter. They call for the ground contact point when standing to be 25 – 40mm anterior of the load line (figure 9.3). Even if the larger value of 40mm is affected the angle of the foot

(when viewed in the sagittal plane) is unrealistic. When the manufacturer was consulted their advice was to align the foot with the shank parallel to the ground plane and so this is the approach that was taken but this results in the ground contact position being 124mm forward of the load line. It can only be assumed that these instructions were not modified when the geometry of the foot was changed in 2012. This foot installation was an area of confusion and is not conducive to a repeatable set up. The suggestion of this research is that the guidelines to prosthetists be revisited and updated, although a prosthetist will no doubt use their experience and amputee feedback to generate a more effective foot alignment.

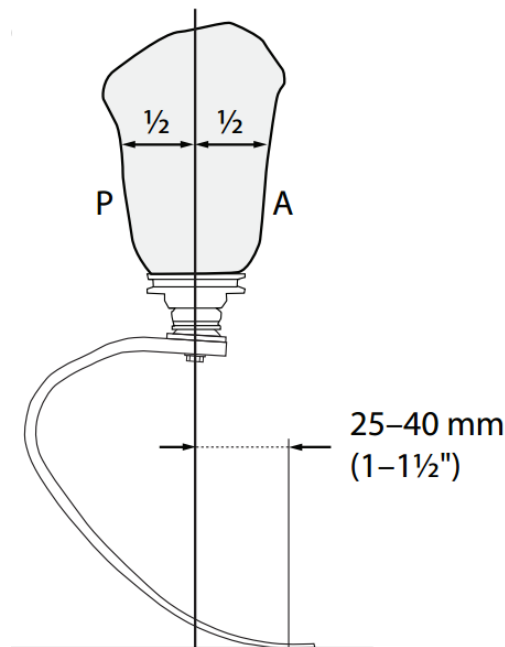


**Figure 9.3:** Extract from the Ossur installation guidelines (Ossur Instructions for Use 2012) calling for the initial ground contact position to be 25-40mm forward of the load line.

The model was used to define the ground contact position (GCP) for leg and stance lengths as detailed in table 9.1. This table was used to create a series of curves to represent each leg length and these can be seen in figure 9.4. The length of the stride was divided into two because it is only the distance forward of the static resting point that concerns this particular investigation. It was ascertained in section 4.4 that the

compression and rebound phases of the stance phase of the stride are symmetrical meaning that the same stance length will occur rear of the mid-stance position.

		Leg length						
leg		742	692	642	592	542	492	442
leg + foot		1000	950	900	850	800	750	700
Stride Length/2	124	34	34	34	34	34	34	34
	200	50	50	50	52	54	56	60
	250	60	61	63	67	71	76	80
	300	72	76	79	83	88	94	98
	350	84	89	92	97	102	108	117
	400	95	100	105	111	118	127	-
	450	106	112	119	129	138	-	-

**Table 9.1:** Summary of the foot strike positions (mm measured from the toe) along the metatarsal region of the virtual prosthetic foot for different leg and stride lengths. All dimensions are in mm.

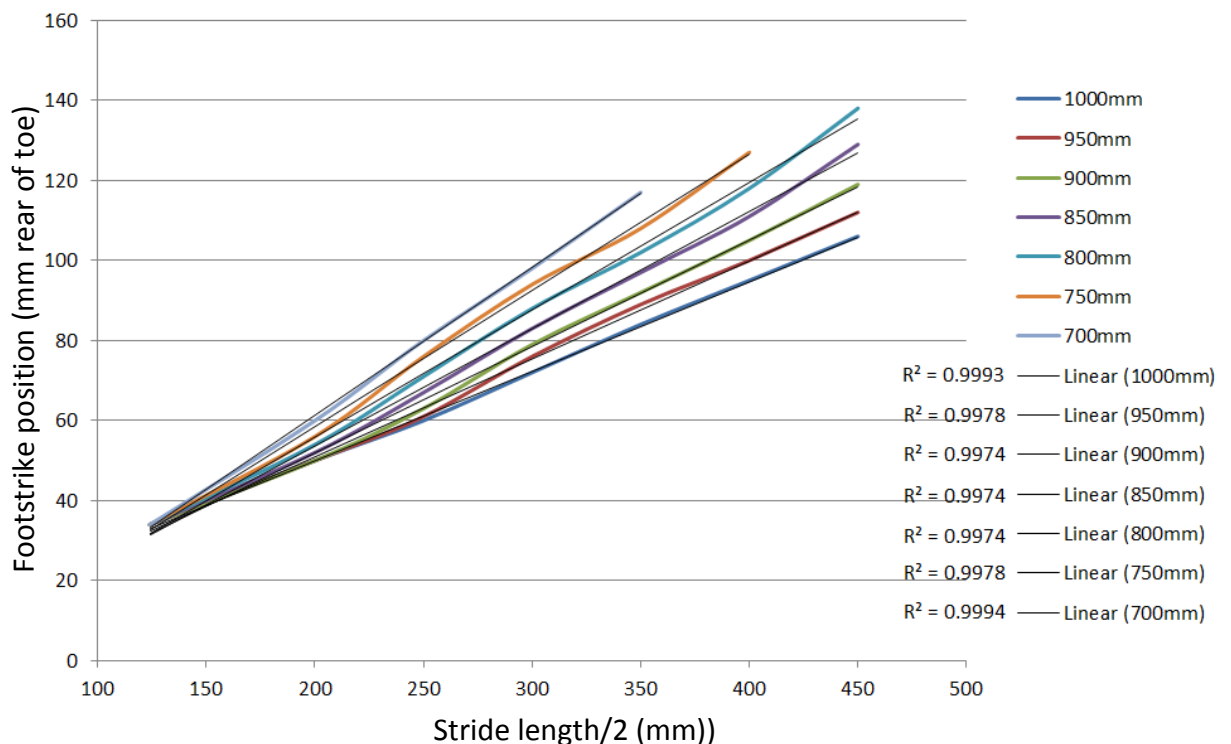


**Figure 9.4:** Traces of foot strike ground contact point against stride length for a variety of simulated leg lengths. Each curve has a linear trendline added with  $R^2$  values quoted.

A linear trendline was applied to each of the curves shown in figure 9.4 as a function of  $y=m(x)+c$ . The terms 'm' and 'c' were split apart and the extreme values of these (from the 1000mm leg length trace and the 700mm leg length trace) and were used as boundary figures to create a trace of 'm' terms and a trace of 'c' terms plotted against leg length. These traces can be seen in figure 9.5.

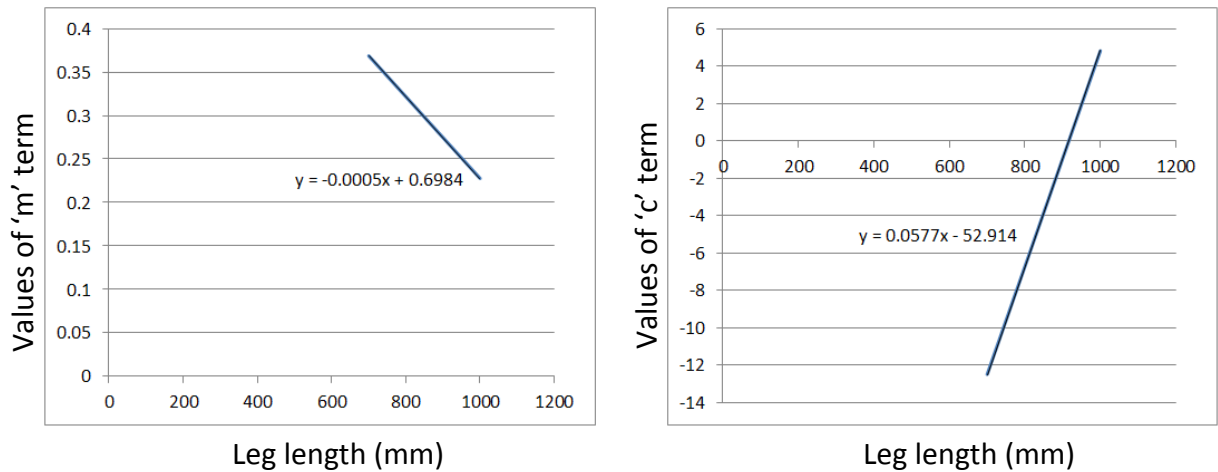


**Figure 9.5:** Traces of 'm' and 'c' terms extracted from the straight line equations  $y=m(x)+c$  for the trendlines shown in figure 9.4. Equations derived from these two graphs were used to develop a formula capable of describing heelstrike position for any stride and leg length.

An equation (in the form of  $y=m(x)+c$ ) was developed using the output of these two traces (as a function of leg length) to form the 'm' and 'c' terms with 'x' being a value of stance length. Using this equation it was possible to define the ground contact point of a foot at foot strike by defining values of leg length and stance length.

		Leg length						
Max variation	2.5	742	692	642	592	542	492	442
Min variation	-2.5	1000	950	900	850	800	750	700
Stride Length/2	124	31	31	31	31	31	32	32
	200	48	50	52	54	56	58	60
	250	59	62	65	69	72	75	78
	300	70	75	79	83	88	92	96
	350	82	87	93	98	104	109	115
	400	93	100	106	113	120	126	-
450	104	112	120	128	136	-	-	

**Table 9.2:** Summary of the foot strike positions (mm measured from the toe) along the metatarsal region of the virtual prosthetic foot for different leg and stride lengths. All dimensions are in mm. Cells in green indicate the number is within the defined tolerance.

As a verification exercise the data from the original measurements (shown in table 9.1) was cross-checked with an identical table with each cell filled with output data from this developed equation. This can be seen in table 9.2. The cells in green are those in which the measured data and calculated data correlate to an accuracy of +/-2.5mm.

It can be seen that all figures generated by the equation fall within this tolerance with the exception of the shortest stance length. This is the stance length generated from the leg at 0°, or vertical, and as such is not a realistic test condition.

Given that the original foot setup (with the shank parallel to the ground) is unlikely to be used in a real-life situation, the equation had added to it a bias factor that would be modified by the prosthetist according to the individual set up requirements of the amputee. This factor simply biases the ground contact point forward or rearwards (inevitably this would always be rearwards due to the extreme angle of the foot at initial setup). For the amputee tested in Chapter 7 this value was 24mm posterior (as defined by the prosthetist aligning the foot) meaning that his static ground contact point was 100mm forward of the load line (with the shank aligned parallel with the ground this value is 124mm as can be seen in table 9.1).

	Stride length (mm)	Measured GCP (mm)	Calculated GCP (mm)	Variation (mm)
Leg length = 1003mm	500	83	83	0
	530	86	86	0
	580	92	92	0
	610	95	95	0
	640	99	98	1
	670	102	100	2
	700	105	103	2
	710	106	104	2
	730	109	108	1
	740	110	112	-2

**Table 9.3:** Summary of the heelstrike GCP figures (in mm) for the amputee (as measured in Chapter 7) for both the measured and calculated methods with the variation defined. The stride length varies as running speed increases.

As a data verification exercise the data collected from the amputee in Chapter 7 (foot strike ground contact positions, stance lengths and the amputee leg length) was compared with that generated by the equation developed in this section. The results can be seen in table 9.3. It can be seen that the maximum variation is 2mm, at greatest a deviation of 2%. The mean deviation is 0.96%.

### 9.3.1.2 Conclusions

Using this method of simulation, a general equation has been developed in the form of  $y = mx+c$  (with the  $m$  &  $c$  terms derived from the CAD simulation exercise in section 9.3.1.1) that describes the ground contact point of the foot for any given stance or leg length. The data verification exercises suggest this can be completed to an accuracy of  $\pm 4.5\text{mm}$  ( $\pm 2.5\text{mm}$  originating from table 9.2,  $\pm 2\text{mm}$  from table 9.3) across the entire calculation range. This data was verified against that captured during the amputee testing phase in Chapter 7.

In order for the calculations to work the user must enter values for leg length and stance length. The leg length is a simple measurement from the centre of rotation of the hip (head of the femur) to the base of the unloaded prosthetic foot. The stance length however presents complications in some circumstances. If the prosthetist (or user of this equation) is experienced and competent in predicting a suitable stance length for the amputee then a value should be forthcoming. However if the stance length needs to be predicted by a further element of this modelling exercise (as suggested in figure 9.1) there will be a conflict of values. The stance length cannot be defined without knowing the change in ground contact point, and the ground contact point cannot be defined without a value of stance length.

It is possible that this creates a circular calculation that tends closer to an accurate product with a number of iterations. If this cannot be achieved an alternative method would be required, perhaps in the form of a look-up chart of typical values that can advise the prosthetist.

This method of calculating the ground contact point at foot strike relies on two assumptions that could be the subject of further study.

1. The affected (prosthetic) leg is straight at the moment of foot strike (i.e. there is little or no knee flexion). This is the style of running employed by the amputee athlete previously tested (Chapter 7) but is by no means the only style of running used by individuals able-bodied or otherwise. Further study should be conducted that establishes the variation in running styles with a view of defining the variation in knee angle at the moment of foot strike. A flexed knee will mean that the leg length is slightly (almost certainly insignificantly) reduced but also exhibit a rotation in the sagittal plane of the prosthetic device. This rotation will serve to bias the foot strike position forward towards the toe and could adversely affect the accuracy of the resulting data.
2. The stride is symmetrical about the point of mid-stance (in terms of stance length). It has been shown to be so during testing with the amputee in section 4.4 but further investigation should be undertaken to confirm this assumption if additional runners are to be considered.

### 9.3.2 Foot Stiffness

The stiffness of the prosthetic foot on test was investigated in section 7.3.4 where the stiffness variation along the length of the keel (metatarsal region) was defined, and in section 8.2 where the same exercise was conducted across the category range of available Flex Run feet. It was shown that the stiffness of the foot changes throughout the course of a single stride and the stiffness at each instance shown in table 8.2.

What is not known at this stage is how this stiffness or rather this change in stiffness affects any modelling of the response time that might occur.

Section 6.2 shows that when attached to the rig the foot and mass as a system acts according to the trends of Simple Harmonic Motion (if the nominal foot deflection is used as the reference for response timing). Crucially though, this testing was conducted with a single defined ground contact point and therefore foot stiffness. The purpose of this section is to identify the magnitude of stiffness change that occurs during running (as investigated in Chapter 7) and if this can be approximated to a single value. The mathematical modelling of the foot using the equation for Simple Harmonic Motion relies on a single value of foot stiffness and if this cannot be found, alternative modelling methods should be used.

### 9.3.2.1 Defining the True Spring Rate of the Foot

Traditionally the rating of a spring is conducted by generating a force – displacement curve. The linearity of the spring can be understood, as can the level of force required for any specific level of deflection. Whilst the testing did not directly produce the relevant data to generate a force – displacement curve for the foot, it can be calculated using what was captured.

At no stage in this research project has direct force data been captured from amputee testing. This is because of the specialised equipment that is usually required in a controlled test area. Instead the deflection of the foot at a known position was recorded (section 8.2) and the stiffness at all locations calibrated. Figure 7.14 displays the results describing how the ground contact point of the foot (as being used across a range of running speeds by an amputee athlete) progresses throughout the stance phase of the stride. It provides a value of contact point rear of the toe plotted against time in the stride (originating from foot strike at  $t=0$ ). Figure 7.16 is the resultant curve of a series of Instron-based testing that defines an equation describing the stiffness of the same foot for any given ground contact point along its length. As such, if these are combined the graph in figure 9.5 can be generated, defining foot stiffness against a value of time through the stride. For the purpose of simplifying the data, at this stage this exercise is only concerned with a single category of foot (Cat.7Lo) as used by an amputee (97.5kg) running at a single velocity (13kph). It can be seen that the effective foot stiffness changes from 65000N/m to 28000N/m throughout the course of the stride, having increased to 71500N/m at 45ms after foot strike.

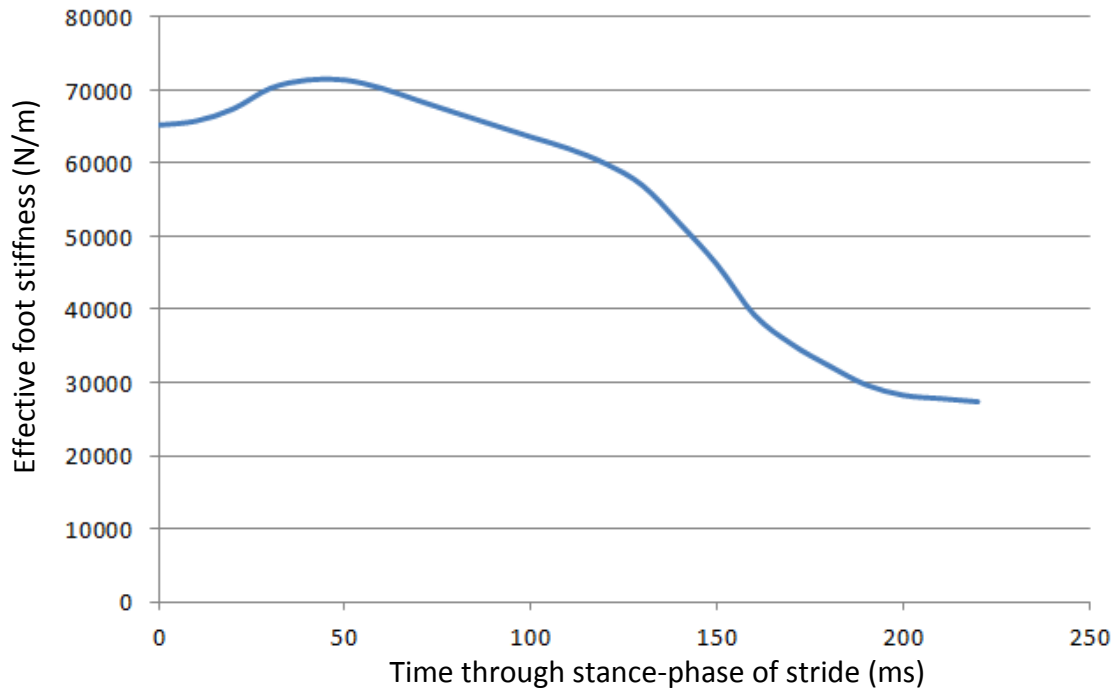


**Figure 9.5:** Trace demonstrating the variation in foot stiffness throughout the course of a single stance phase of the stride. The change in stiffness is caused by the shift in ground contact position.

The deflection work that was carried out (section 7.3.2) used the deflection transducer mounted to a single specified location on the keel of the foot. This location is irrelevant providing it is constant, however it can be used as a reference for all deflection testing at other foot locations.

Section 7.3.4.1 describes how three selected ground contact locations were chosen for calibration work and figure 7.15 displays force – displacement data for these positions. The middle of these three locations (defined as ‘mid’ and 75mm rear of the toe with a linear stiffness of 53599N/m) was used as a datum reference, it being a point with known characteristics. Using this ‘mid’ point as a position for the toe clamp (therefore defining the ground contact point) a calibration curve was generated for the foot using the Instron hydraulic test machine showing displacement (mm) against a value of volts as recorded by the MSR data logger during test. The static characterisation testing procedure is described in section 3.4. This curve is shown in figure 9.6.

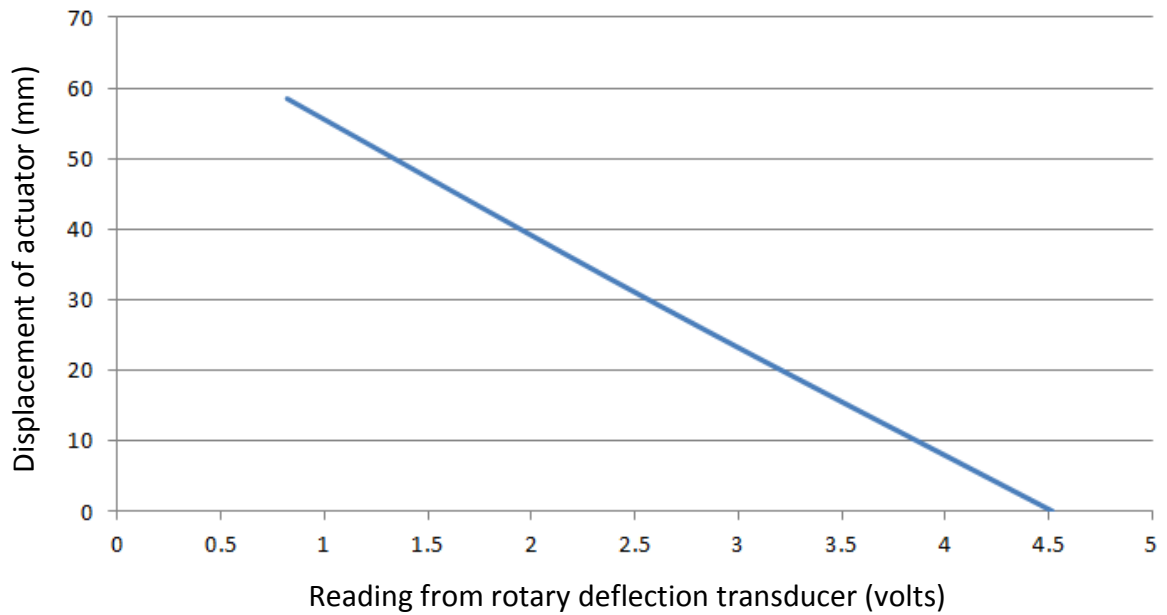


**Figure 9.6:** Calibration curve for the 'mid' ground contact position (75mm rear of the toe) using the rotary deflection transducer as a reference.

An equation for the resulting straight line was generated meaning that for any given value of voltage measured by the deflection transducer during amputee running, a value of deflection in mm can be defined. It should be noted that this value of deflection (in mm) is only valid at this exact point along the foot (75mm rear of the toe). However this information can be used to generate a value of deflection at any point along the toe.

The stiffness at this 'calibration point' is known to be 53599N/m. It is also known that  $f=kx$  (force = stiffness x extension) meaning that the extension at any given time throughout the duration of the stride can be defined by the ratio of foot stiffness (apparent at this specific time) and the calibrated point stiffness of 53599N/m.

Therefore at every given time throughout the stride (every 0.00159 seconds in this case as the calibration work was conducted at 512Hz) the ratio of foot stiffness for the respective time through the stance phase of the stride (as defined in figure 9.5) and known calibrated point stiffness (53599N/m) was calculated. This ratio, when multiplied by the deflection achieved at the known calibrated point, provides a value of foot deflection in mm for the specific point on the foot where ground contact occurs at that specific moment. This resulting value of foot deflection is the only true measure

of foot deflection and is something that has not previously been discussed or defined in any academic sources. It is defined by the blue line in figure 9.7.

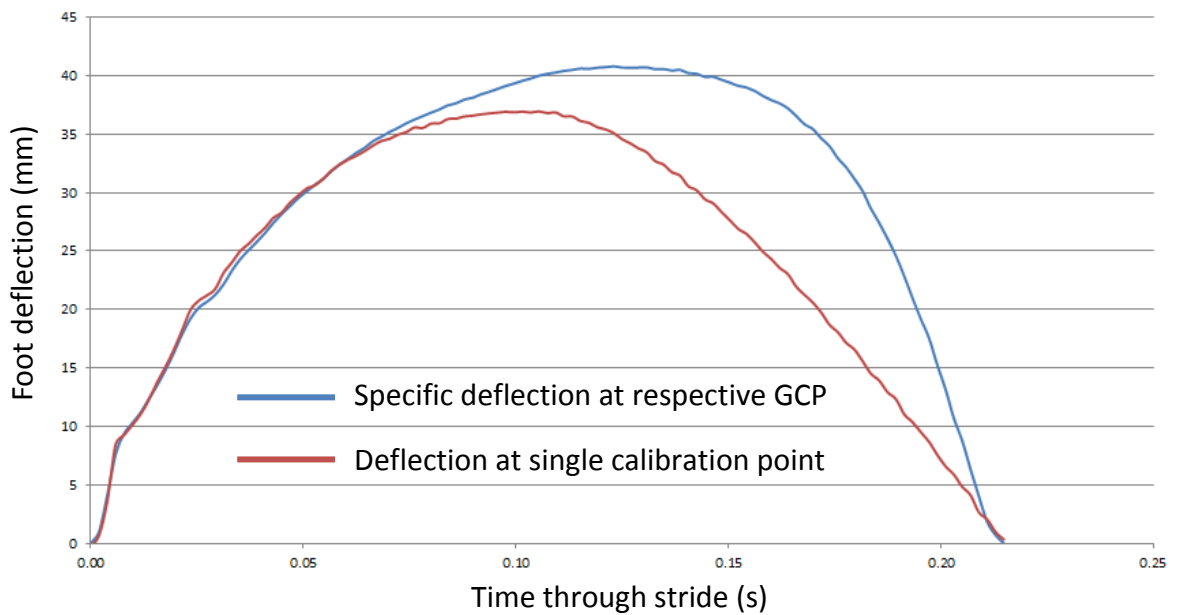


**Figure 9.7:** Curves demonstrating the disparity between foot deflections as measured at a single location and at the ground contact point as it progresses through the stride.

This information transforms the knowledge we hold about the deflection of the foot. Up until this point the stride characteristics have always been considered symmetrical about the position of mid-stance with maximum deflection occurring equidistant between foot strike and toe-off. This graph demonstrates that this is true if a single point of measurement is used, but not if that point of measurement is the ground contact point (which progresses throughout the stride). Instead the red line (representing displacement of the single point) should be considered a trend of **foot strain** but not **specific deflection**.

Further to this it can also be suggested that the form of the blue curve (representing specific deflection) will change depending on running velocity. Figure 7.14 demonstrates how the ground contact point progression changes based on running speed, and as such the stiffness progression will also change. The specific deflection is based on this progressive change in foot stiffness and as such the shape will inevitably be altered.

Further to this, because  $f = kx$  (force = stiffness  $\times$  extension) the force at the ground contact point can be calculated at any given moment throughout the stride by multiplying the stiffness of the foot at that point with the value of deflection shown in figure 9.7. With this new information a force – deflection curve can be generated for the foot using true values of force and deflection at the specific ground contact point employed by the foot on test. This can be seen in figure 9.8.

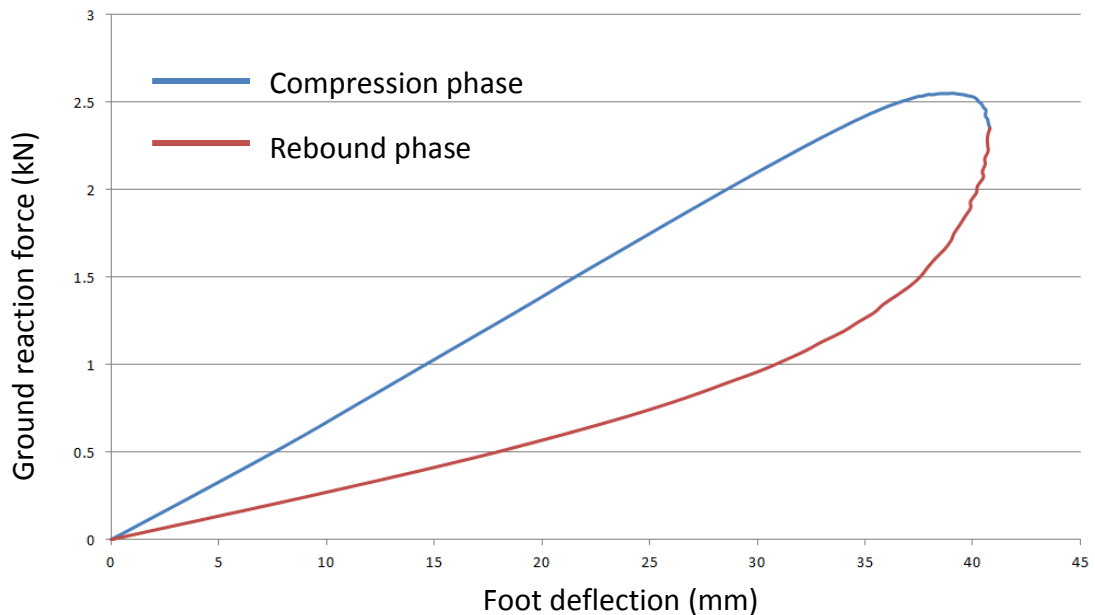


**Figure 9.8:** True force – deflection curve for the Cat.7Lo Flex Run foot on test when used by a 97.5kg amputee athlete to run at 13kph

The resulting force – deflection curve is unusual in that it demonstrates a high value of hysteresis if viewed in the traditional manner; that is the disparity between the compression and rebound phases of the cycle. This graph would normally suggest a poor level of energy return efficiency. However this is only relevant if the compression and rebound phases are symmetrical in their spring geometry; this is not the case. Furthermore the compression and rebound phases (as demonstrated in figure 9.8) are reversed to a traditional force – deflection curve. If a symmetrical spring (that which follows the same geometry in the compression and rebound phases) were to produce a curve of this nature it could be concluded that the spring has a high level of damping (and thus energy inefficiency) and the compression curve would be the lower of the two (indicated in red on this graph). The curve in figure 9.8 suggests, counter-intuitively, that the ‘spring’ requires less energy to be compressed than it returns in the rebound phase. The spring rate is significantly lower on the rebound phase, but

what is not clear from this figure is that this change in spring rate is a result of geometrical change. The spring rate of the foot softens towards the toe and as such this is demonstrated in the rebound phase of the force – deflection curve.

### 9.3.2.2 Conclusions

Following this investigation two things become clear:

1. The spring rate of the foot will vary depending on the running speed. It is shown in section 7.3.3.2 that as speed increases, the amputee uses a more posterior portion of the foot thus increasing stiffness. Further to this, and as shown in figure 7.14, the additional bending of the foot at higher running speeds means the ground contact progression forms a different profile. If a model were to be developed that predicts the foot stiffness it would need to take into account the ground contact position change at foot strike and throughout the stride. Both of these factors were discussed in section 9.3.1 and a model for the prediction of the initial ground contact point developed for any given leg and stance length. The ground contact progression has proven to be crucial for understanding the foot stiffness profile. Whilst a model of the information already recorded can be developed (in a manner similar to that in section 9.3.2.1), the effect of different users (amputees of different heights, weights, running styles, etc) is not understood and was considered outside the scope of this work.
2. Traditional response models (such as the equation for Simple Harmonic Motion) cannot solely be used for modelling the behaviour of an Ossur Flex Run prosthetic running foot. This approach requires a single, linear spring stiffness value to be defined and although figure 9.8 demonstrates a linear compression-phase stiffness value, the rebound phase is distinctly different. If the concept of Simple Harmonic Motion is to be pursued, some manner of assumption has to be made that takes into account the variation in foot stiffness and allows the definition of a single linear foot stiffness for the purpose of the model.

### 9.3.3 Calculating Response Time

Previously authors (Lehmann et al. 1993a,b; Noroozi et al. 2012a,b, 2014) have suggested that the action of a prosthetic foot could be considered to mimic the equation for simple harmonic motion with the deflection of the foot during running forming half of a sine wave.

This was discussed in Chapter 6 and was found to be incorrect. Instead the discovered trends suggest that the function of the foot can be compared with simple harmonic motion if done so about what was termed the Half Wave Timing (HWT) and if a single foot stiffness is assumed.

The equation for simple harmonic motion as expressed in figure 5.2 gives a value for oscillation frequency for the full phase of a sine wave (in Hz). The reciprocal of this value provides a value of time (in seconds) to complete this oscillation. As such, half of this value would give the time to complete one half of one oscillation, but it was shown in section 6.2.4 that this one half of one oscillation can only exist from the point of nominal deflection (the amount of deflection achieved when the amputee is standing on one leg in a static state of equilibrium).

Therefore when comparing the deflection of a prosthetic running foot as fitted to an amputee with simple harmonic motion, this value of static 'nominal' deflection should be defined. This task holds its own challenges:

1. The amount of deflection under static loading changes depending on what the ground contact point is at that moment. It has been shown in section 4.6.2 that the stiffness of the foot changes along the length of the metatarsal region. Therefore if a load is applied at a soft region (towards the toe), the deflection if measured at that same point would be larger than if the same load were applied to a more posterior section of the foot.
2. The amount of deflection changes depending on what position of the foot is measured. This is the reason that in section 4.4 and throughout this research project the traces of foot deflection were expressed as values of transducer output in volts and not calibrated into millimetres.

A further and perhaps much more significant challenge is that the equation for simple harmonic motion demands a value of 'k' or spring stiffness. This should therefore be completed with a value for foot stiffness (in N/m) but it was shown in section 7.3.4.2 that the ground contact point (and therefore the effective stiffness of the foot) can change by a factor of 2.6 times throughout the course of a single stride. Additionally the ground contact point is not repeatable and can also be seen changing depending on the velocity of the amputee athlete.

### 9.3.3.1 Method

#### Nominal Foot Deflection

In order to address the issue of defining a nominal foot deflection position, the same approach was taken as that in section 6.2.4.2. During amputee testing the foot deflection was measured using the rotary transducer, the output of which is voltage. This voltage if left uncalibrated demonstrates the trends of running (contact timing, swing phase timing, etc) but not defined figures for deflection in mm.

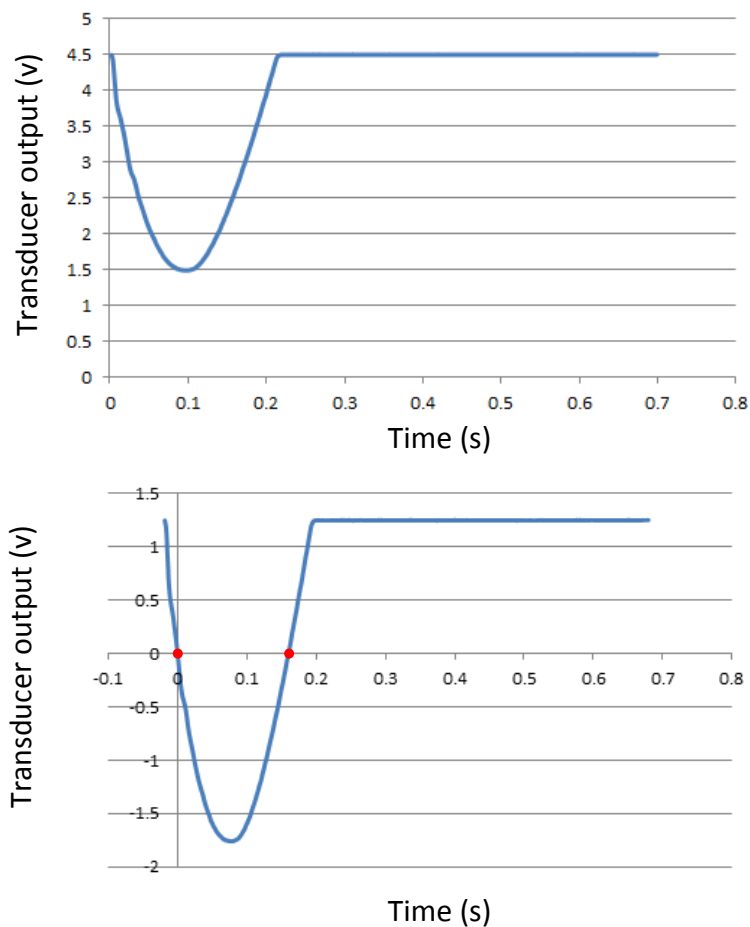


**Figure 9.9:** Foot deflection as a function of transducer output voltage as raw collected data (above) and corrected about the nominal voltage at  $t=0$  (below) for a 97.5kg amputee @13kph. The duration of half-wave timing is indicated by the red markers.

This section is primarily concerned with the timing of the stride, it being this that is being replicated by mathematics. Therefore the uncalibrated trace of foot deflection was used throughout this section. The nominal position was measured by requesting the amputee stand still on his affected leg for a period of a few seconds, and thus the

output of the rotary transducer could be recorded at nominal deflection for the prosthetic installation conditions specified by the prosthetist.

The raw trace of voltage from the deflection transducer as captured during amputee running at  $13\text{kmh}^{-1}$  is shown in figure 9.9 along with the same data corrected about the nominal voltage at  $t=0$ . As measured, the nominal voltage (representing nominal deflection of the foot) was 1.25v and this second trace shows the nominal timing (half-wave timing or HWT) as 160ms. The overall foot contact timing was 217ms.

This same exercise was conducted with data from all of the running velocities tested in Chapter 7 and tabulated as shown in table 9.3.

Velocity kmh	Velocity m/s	Ground contact time ms	True half-wave timing ms
8	2.2	275	181
9	2.5	260	179
10	2.8	246	172
11	3.1	232	168
12	3.3	227	165
13	3.6	217	160
14	3.9	209	153
15	4.2	203	150
16	4.4	197	147
17	4.7	193	141
18	5.0	182	135

**Table 9.4:** Tabulated figures of full stance phase (ground contact) and half-wave timing for a 97.5kg amputee running on an Ossur Cat.7Lo prosthetic foot across a range of speeds.

It is these figures of half-wave timing that should be replicated if an effective equation can be developed to model the response timing of the foot. The link between HWT and GCT can then be established but as discussed in section 6.3 it is anticipated this link will be a function of overall foot deflection.

### 9.3.3.2 Assumption of a Single Foot Stiffness

It was suggested (and tested) in section 5.4.2 that the stiffness of the prosthetic foot can be assumed to be the median-point stiffness. This means that if the foot strike position is 120mm rear of the toe and toe-off occurs at 0mm (i.e. at the toe), the stiffness that can be assumed to represent the range of variation is that which occurs at 60mm rear of the toe. This value can be defined from the information in section 7.3.3.2 and is displayed in table 9.5.

Velocity kmh	Velocity m/s	Heelstrike (ref. toe) mm	Heelstrike (ref. laser) mm	Median GCP (ref. toe) mm	Median GCP (ref. laser) mm	K at median point N/m
8	2.2	83	46	41.5	87.5	39075
9	2.5	86	43	43	86	39604
10	2.8	92	37	46	83	40685
11	3.1	95	34	47.5	81.5	41237
12	3.3	98	31	49	80	41796
13	3.6	100	29	50	79	42173
14	3.9	103	26	51.5	77.5	42745
15	4.2	104	25	52	77	42937
16	4.4	108	21	54	75	43714
17	4.7	112	17	56	73	44504
18	5.0	118	11	59	70	45714

**Table 9.5:** Tabulated heelstrike positions and the resulting figures for the median ground contact point (GCP) for a 97.5kg amputee running on an Ossur Cat.7Lo prosthetic foot for a range of speeds.

These values of median ground contact position were transposed into values of foot stiffness using the equation generated in figures 8.7 & 8.8 and these figures then substituted into the equation for Simple Harmonic Motion (as in figure 5.2). This is demonstrated in the following example for 13kmh<sup>-1</sup>:

#### 13km/h:

Equation derived in Figure 8.7:

$$y = 1.6536x - 639.81x + 82398$$

where:

$x$  = GCP from laser datum (mm)

$y$  = Foot stiffness (N/mm)

Substituting values for a median GCP of 59mm (Table 9.5):

$$\text{Foot stiffness} = (1.6536 \times 79) - (639.81 \times 79) + 82398 = 42173 \text{ N/m}$$

This stiffness value of 42173 N/m can then be transposed into the equation for Simple Harmonic Motion (shown in figure 5.2) along with the mass of the amputee (97.5kg) to provide the theoretical halfwave response time, as follows:

$$f = \frac{1}{2\pi} \sqrt{\frac{k}{m}}$$

where:

f = Frequency

k = Foot stiffness = 42173N/m

m = Mass = 97.5kg

Therefore:

$$f = \frac{1}{2\pi} \sqrt{\frac{42173}{97.5}} = 3.31 \text{ Hz}$$

The reciprocal of this represents the full wave frequency response time = 0.302 seconds

Therefore half of this value represents the halfwave response time = 0.151 seconds

This process was repeated for all running velocities for the same amputee athlete mass of 97.5kg and the same prosthetic foot. The resulting frequency response times are shown in figure 9.10, plotted as time against running speed and compared with the measured values from table 9.4.

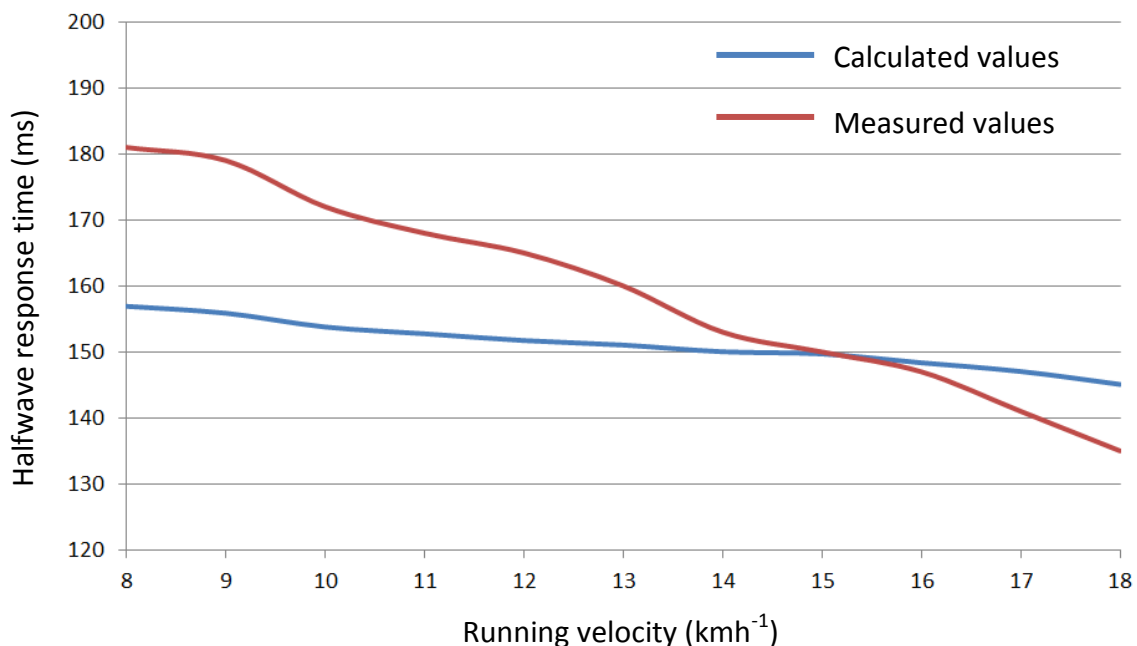


**Figure 9.10:** Traces of response time (median calculated and amputee measured) for the HWT for a 97.5kg amputee running on an Ossur Cat.7Lo prosthetic foot for a range of speeds. This uses median GCP data to generate a single value for foot stiffness.

The figures show a maximum disparity of 24ms (at 8kmh<sup>-1</sup>); a variation of 13%. This is a more significant variation than would be expected from the equation of Simple Harmonic Motion and suggests that this method of assuming foot stiffness is not addressing all of the issues. Indeed this is a simple mechanical principle that is being applied to a very complex (perhaps infinitely complex) system. Some level of error is to be expected but 24ms could be considered excessive.

Although this method of assuming the median foot stiffness is representative takes into account the shift rearward of the ground contact point, it does not take into account the profile of progression forward. No allowance is given for the amount of time the foot spends at the rear of the contact area (the stiffer area) versus the time spent at the softer areas.

As such the next logical step is to use the mean ground contact point of the data presented in figure 9.5. The average value will present a foot stiffness that takes into consideration both the magnitude of foot stiffness and the time spent at that stiffness value. Similar data to that displayed in figure 9.5 was gathered for all running speeds, the mean value of ground contact point was defined and an identical procedure to that conducted above was completed. The results are plotted in figure 9.11.

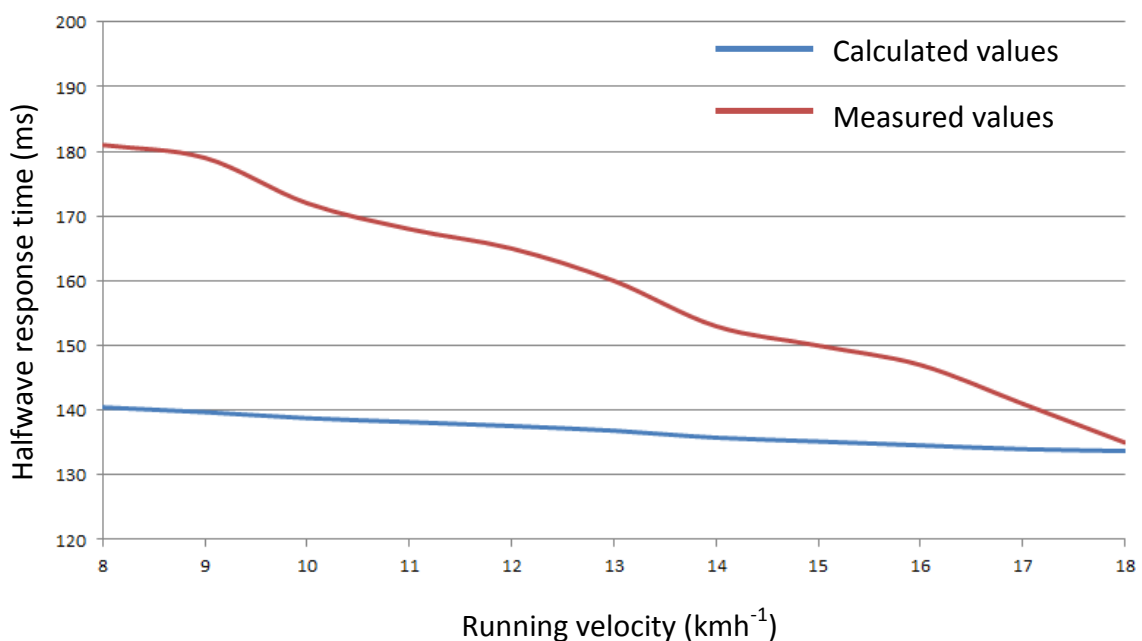


**Figure 9.11:** Traces of response time (average calculated and amputee measured) for the HWT for a 97.5kg amputee running on an Ossur Cat.7Lo prosthetic foot for a range of speeds. This uses mean GCP data to generate a single value for foot stiffness.

Using the mean values of foot stiffness across the range of running speed proved to be less accurate than the results using the median stiffness values. In this instance the variation was 41ms or 23%.

To better illustrate the values of stiffness used for this testing figure 9.12 shows identical data to figure 7.14 but with the assumed values of stiffness (for the median values and average values) superimposed on to each of the three curves.

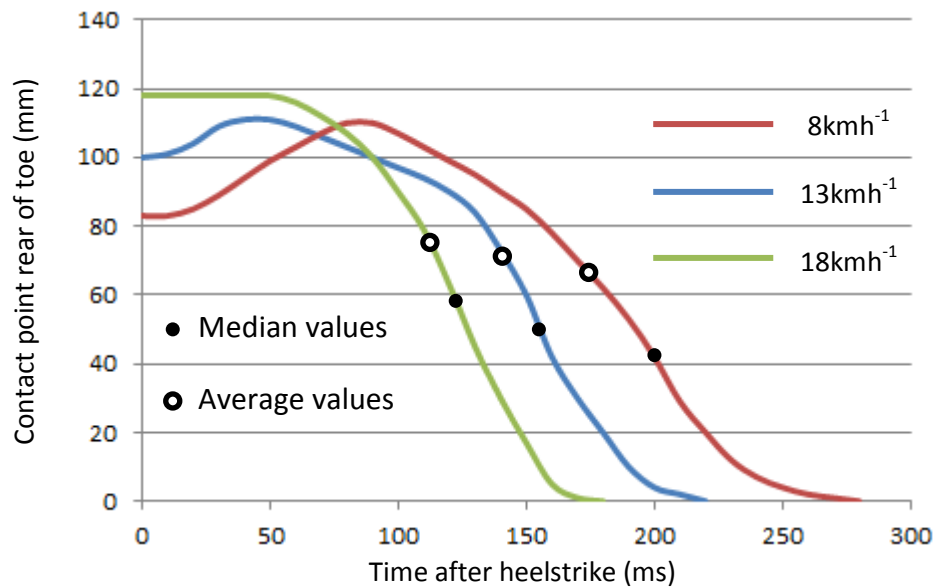


**Figure 9.12:** Trace demonstrating the progression of ground contact point at  $8\text{kmh}^{-1}$  with the assumed GCP locations marked.

These curves represent the progression of the ground contact point for 8, 13 and  $18\text{kmh}^{-1}$  running. To put the error into perspective figure 9.13 is identical with the exception of the superimposed contact points. On this occasion the equation was rearranged such that the output was the foot stiffness required in order to achieve exactly the foot response recorded during amputee running. This foot stiffness was converted back into a value for the ground contact point (rear of the toe) and marked on the traces.

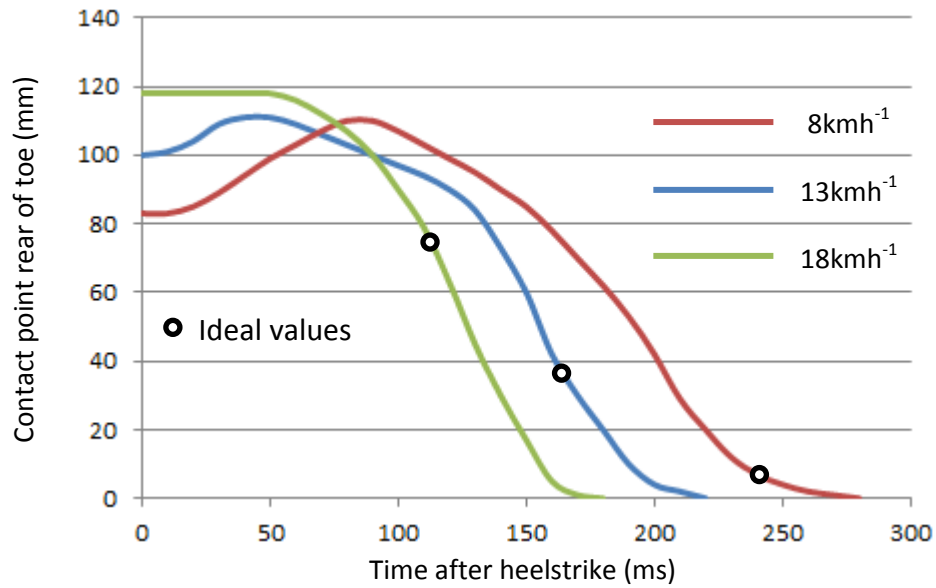


**Figure 9.13:** Trace demonstrating the progression of ground contact point at  $8\text{kmh}^{-1}$  with the ideal GCP locations marked.

It can be seen that the ideal locations of ground contact position are varied suggesting there are other factors that have yet to be appreciated. Whilst the average value for GCP at  $18\text{kmh}^{-1}$  is close to the ideal value ( $77.5\text{mm}$  versus  $73\text{mm}$ ), the values for  $13$  and  $8\text{kmh}^{-1}$  are progressively extreme. The GCP that provides the ideal value of foot stiffness required for Simple Harmonic Motion to mimic the action of a prosthetic foot at  $8\text{kmh}^{-1}$  appears to occur at  $7\text{mm}$  from the toe; a value at the extremity of the range of stiffness that the foot can provide. This appears to not take into account the portion of the stride that exists at the rear of the foot (the stiffer region).

## 9.4 Chapter Conclusions

This work could support one of two possible conclusions.

1. The foot and amputee as a system does not act in accordance with simple harmonic motion. Chapter 6 concluded that the foot could act in accordance with SHM if the nominal value of foot deflection is used to establish the timing. However despite this there appears to be no correlation between measured values and those recorded during amputee running. The trends are in the correct directions but when absolute figures are demanded, this approach falls some way short of providing useful data. To assume that SHM is capable of replicating the running action of an amputee is to ignore a large number of very significant factors and it could be these assumptions that are the root causes of the data disparity. For example it is assumed that:
  - the amputee and foot operate in a purely vertical motion both in terms of amputee motion and in-plane foot bending.
  - there is no influence from the speed of running with the exception of the shift in ground contact position (no braking forces on the foot, frictional losses, etc)
  - the body of the amputee is perfectly rigid.
  - the amputee is unable to generate power.
  - the ground contact points defined throughout the amputee testing are precise points. In reality the load of the ground is spread across an area of the foot by the soft running sole
  - the overall foot deflection is the same regardless of speed
2. Using the mean or median positions for assuming a single stiffness are not adequate for modelling the response of the foot and a third condition exists that is being overlooked. All of the assumptions mentioned above are still present but their effect is insignificant to the generation of a predicted foot response time.

As discussed by Geyer et al. (2004, p.315) ‘*The planar spring-mass model is frequently used to describe bouncing gaits.....in human locomotion*’ and Grabowski et al. (2009, p.201) suggest that ‘*Running-specific prostheses (RSP) emulate the spring-like behaviour of biological limbs during human running*’. Research has been carried out that defines leg stiffness, comparing it with a value of spring stiffness used in the equation for Simple Harmonic Motion. A simple explanation for the disparity in figures achieved in this investigation (in support of these suggestions) would be that the foot does act according to SHM, but it is not purely the spring rate of the foot that is in question; moreover the spring rate of the entire system.

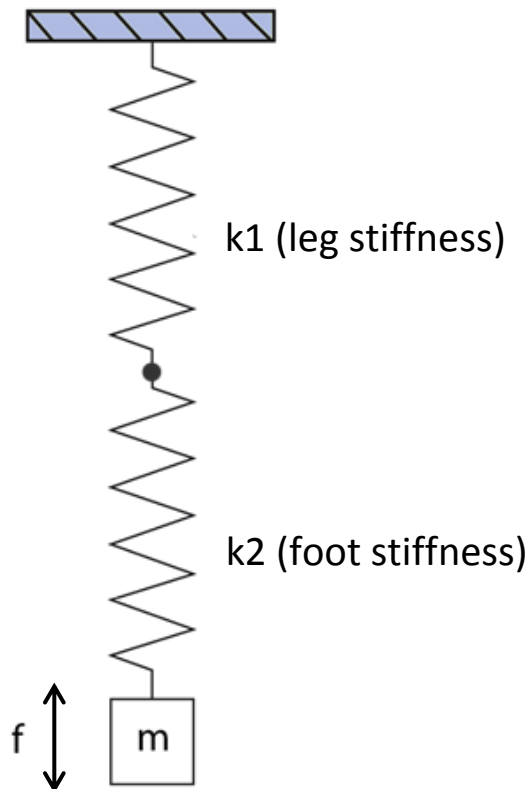


**Figure 9.14:** Suggested addition to the spring-mass system of an amputee using a running foot, where  $f$ = frequency of oscillation,  $k$ = spring stiffness and  $m$ = mass

This system includes the amputee’s affected residual leg providing an effective spring rate, and it could be this that is influencing the results. The excessively low value of foot stiffness shown in figure 9.13, to achieve a theoretical response time in line with  $8\text{kmh}^{-1}$  running, could be explained if a second spring were arranged in series with the prosthetic foot. An illustration of this concept is shown in figure 9.14.

If this is the case then any modelling that takes place should concern the entire amputee as a system. The results shown in this section suggest that if the foot is viewed in isolation, any simulated response times will be variable not only across a range of running speeds, but also the range of feet and the infinite range of running styles employed by amputee athletes.

Addressing the research question set out in section 2.1.3: **Can the action of a prosthetic running foot be modelled mathematically?** the results are inconclusive. Whilst the action of the prosthetic running foot alone can be modelled (assuming the ground contact points and representative values of stiffness are understood), when the amputee is introduced and the prosthetic system is examined the equation becomes more complex. By including the amputee, an infinite number of variables are introduced which will vary from one individual to another.

Suggested further work in this area would be to use the data shown in figure 9.11 to understand the stiffness of the affected limb of the amputee athlete when placed in series with the prosthetic. The relationship between the two curves appears to be linear and as such a progressive spring rate for the residual limb could be defined thus allowing mathematical modelling. However this work could not occur without significantly more amputee testing to validate the concept and define the relevant factors to allow the various datasets to align. Therefore this exercise was deemed outside of the remit of this research project.

## Chapter 10 Discussion & Conclusions

### 10.1 Discussion

In Chapter 2 (in response to the literature review) a single research question was defined with four sub-questions and it is around these questions that the research has been focused. This chapter addresses each of the research sub-questions in turn with reference to the chapters contained within this thesis and follows by examining the main research question.

#### 10.1.1 Sub-question 1: What are the mechanical characteristics of a prosthetic running foot?

In hindsight this research question can be split into two separate components. The majority of the work carried out in the field of dynamic characterisation to date has concerned the prosthetic foot as a standalone component, ignoring the ‘system’ (including the amputee during running).

Chapter 3 was concerned with the static characterisation of the Ossur Flex Run foot as a component and was initially aimed at understanding why previous work (as detailed in the literature review) had resulted in significantly different figures. (Bruggeman et al. (2008), Nolan (2008), Geil (2001), Noroozi et al. (2012a,b, 2014) and Lehmann et al. (1993a,b)) have conducted work into the efficiency of dynamic response of similar running feet and have published figures ranging from 63% to 100%. Through repetition of the work detailed in the literature but modifying the boundary conditions it was shown that grossly different figures of energy efficiency could be generated by manipulating the ground contact friction coefficient. Using this learning, a new concept of mounting fixture was designed such that the foot was not over-constrained. Using this fixture the foot demonstrated an energy efficiency >99%, a linear spring rate and in Chapter 4 the stiffness of the foot along the length of the keel was ascertained.

It was found that the stiffness of a prosthetic running foot is dependent on the location at which it touches the ground. Therefore in a laboratory environment the foot will

exhibit stiffness proportional to the rig fixture that is being used to test it. However the amputee test work carried out in Chapter 4 suggests that the ground contact point changes throughout the course of a single stride, meaning in turn that the stiffness of the foot varies correspondingly. Further to this it was demonstrated in Chapter 7 that the ground contact point for a single amputee is also dependent on running velocity. The contact point at the moment of foot strike moves posterior as speed increases (section 7.3.3.2). Chapter 9 goes further and models the ground contact point of the foot with the ground for a range of different leg length and stance length conditions, demonstrating that for a given stance length the initial ground contact point at the moment of foot strike moves rearwards as leg length is decreased. It was also shown that if the prosthetist biases the foot in a posterior or anterior direction this has the ability to modify the ground contact point and therefore effective stiffness of the foot.

Finally the stiffness characteristics of the foot depend on what manufactured category that foot belongs to. Chapter 8 demonstrates the variation in foot stiffness across the range of Flex Run feet available from Ossur. Each exhibits a linear spring rate with >99% energy return if tested in the manner described in sections 3.3 & 3.4, and each shares the characteristic of stiffness changing along the length of the keel.

This research has demonstrated that whilst a prosthetic running foot is a passive device with fixed properties, the exhibited mechanical characteristics are a function of:

**In a laboratory during rig testing:**

- Foot category
- Mounting condition
- Boundary conditions (frictional losses)

**When being used by an amputee:**

- Foot category
- Running speed
- Leg length
- Initial setup by the prosthetist

As long as these mechanical characteristics are appreciated and it is understood how they interact with the amputee during running, this knowledge can advise the design of future feet. The properties of the feet available are primarily a function of their geometry. The profile of stiffness progression throughout the stance phase of the stride is a result of the shape of the toe and how this interacts with tibial progression (the knee progressing over the foot).

### 10.1.2 Sub-question 2: Is the claim that a foot mimics Simple Harmonic Motion legitimate?

The theory of Simple Harmonic Motion replicating running (both able-bodied and amputee) is a recurring theme in the literature from the previous three decades, but no definitive answers are forthcoming when reviewing what has been published.

In Chapter 5 a rig was designed and manufactured with the aim of replicating the action of an amputee in the laboratory, replacing the amputee with a series of cast iron masses. This allowed individual variables (stiffness, mass, foot deflection) to be altered and the response of the prosthetic foot to be observed. It was shown that a prosthetic foot aligned with the expected trends of Simple Harmonic Motion assuming a single ground contact point was used (resulting in a single foot stiffness) and if the foot deflection was expressed about the nominal point. This means the value of deflection occurring in a static loading condition equivalent to the amputee resting all of their mass on the prosthetic device in static equilibrium. It is in this condition that the response time of the foot was not modified by the amplitude of deflection of the tests (as required by the equation for Simple Harmonic Motion).

However as discovered in Chapter 4 and compounded in Chapters 7 & 9 the stiffness of a prosthetic foot cannot be expected to be defined by a single figure. The stiffness of the foot has been shown to change throughout the course of a single stride and as such the equation for Simple Harmonic Motion can no longer apply. Despite the rig work aligning with the equation, when a prosthetic system is being considered it was shown in Chapter 9 that additional variables are introduced. It was concluded that even though the stiffness of the foot was understood at all points throughout the

stride, the total stiffness of the leg of the amputee was quite different and resulted in foot response times that did not correlate with the assumption of Simple Harmonic Motion.

### 10.1.3 Sub-question 3: Can the action of a prosthetic running foot be modelled mathematically?

The objective of Chapter 9 was to assemble the factors that were shown to affect the characteristics of the prosthetic foot, understand their relationship with each other and model each of them such that a useful output could be defined. It was suggested that the most productive output from a model of running is that of stance length. It is a tangible measure that an amputee or prosthetist can observe and as demonstrated in Chapter 7 has the ability to define the maximum speed the amputee can run assuming the dynamic response of the foot is known.

There were two issues identified in this section that prevented the action of a foot from being modelled. These were:

1. In the assembled flowchart shown in figure 9.1, stance length was a product of the response time of the foot. However it was shown in section 9.3 that an accurate response time of the foot cannot be generated without first defining the stance length (the ground contact point and therefore foot stiffness and response time depending on both the stance length and leg length of the amputee). It was suggested that some manner of circular calculation be set up such that each of the factors (stance length and response time) be defined in an iterative manner but this concept was not investigated further.
2. Understanding the stiffness of the foot and predicting the response time using the equation for Simple Harmonic Motion is not sufficient to predict the response time of the foot when attached to the amputee. It is suggested that the leg stiffness and positive work done throughout the duration of the stance phase of the stride affects the response time.

#### 10.1.4 Sub-question 4: Can the prescription of feet be changed such that the user experience of active amputees is improved?

The response time of the prosthetic foot has been shown (in Chapter 7) to limit the speed at which an amputee can run. It was shown in Chapter 9 that the response time of the foot is based on the stiffness category of the prosthesis as well as other factors such as stance length, amplitude of deflection and leg length all of which affect the ground contact position of the metatarsal region of the foot, and this in turn affects the stiffness of the device. As such it is proposed that the following factors be taken into account when prescribing a running foot:

- **Amputee mass**
- **Leg length**
- **Desired running speed**
- **Stance length**

Figure 9.1 describes the relationship these factors have on one another and ultimately on the response of the foot. Chapter 9 was able to provide mathematical models to describe the effects of leg length and stance length on foot response time, but fell some way short of predicting the ground contact time when used during running. It was suggested that a factor be included in the calculation to include the latent effect of the amputee on the overall spring rate and further work can be conducted in order to validate this concept (further testing with amputee athletes using alternative stiffness categories of feet). This tool should take into account the factors listed above and result in a value of stance length for that specific amputee at that specific running speed using the category of foot selected. A visualisation of the proposed tool is shown in figure 10.1.

Boxes shown in green are completed by the prosthetist and include a bias factor that describes the anterior or posterior movement away from the neutral alignment of the foot required by that amputee.

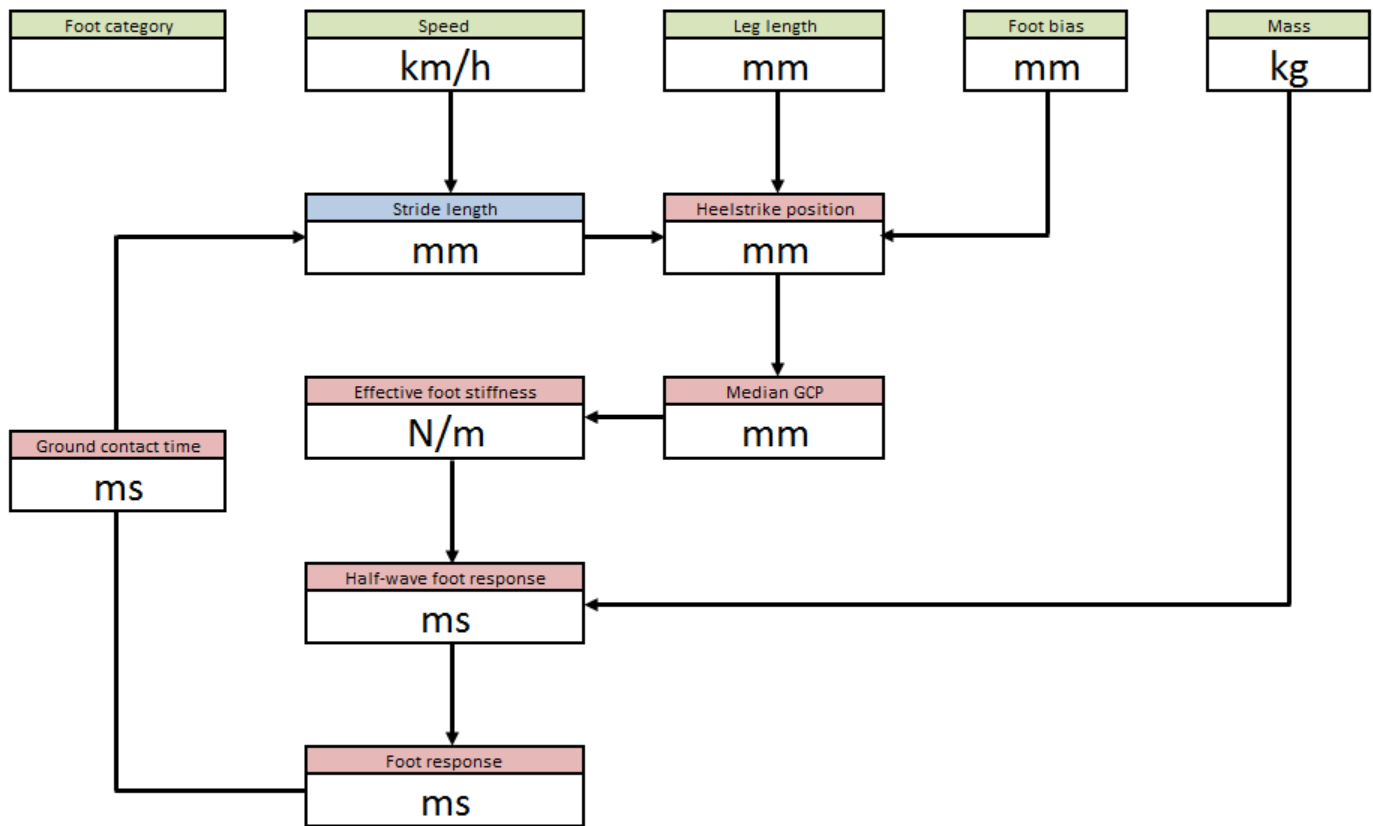


**Figure 10.1:** Suggested flowchart tool to aid the prescription of prosthetic running feet. The prosthetist would be responsible for completing the boxes shown in green. The output (stance length) is displayed in the blue box.

If this manner of tool were developed it would be capable of assigning the relevant foot category to an amputee based on their specific requirements and fitness regime.

10.1.5 **Primary Research Question:** *Is the current method of prescribing prosthetic ESR running feet (based on mass alone) correct and could it be more appropriately advised by taking into account any additional factors?*

During testing in Chapter 7 it was demonstrated that the maximum achievable running speed of the amputee was approximately  $18\text{kmh}^{-1}$ . As his running speed increased, so too did his stance length (given the fixed response characteristics of the foot being used) until his maximum available stance length was reached. At this point the only way to affect a faster running speed was to decrease the response time of the foot by replacing it with a stiffer category.

The amputee was using the correct foot as assigned by a qualified prosthetist in accordance with the manufacturer's literature and current prescription practice. If the intended exercise regime of the amputee had involved running at a velocity in excess of  $18\text{kmh}^{-1}$  this foot would have limited his abilities. Therefore undoubtedly there are instances whereby the incorrect foot stiffness is prescribed to an amputee. Currently the desired running speed of the amputee is not taken into account when prescribing a foot, the selection process instead being based solely on the mass of the amputee.

Section 10.1.4 details the additional factors that this research has highlighted should be taken into account when prescribing a prosthetic running foot (Leg length, desired running speed, stance length) and as such the primary research question (and thus objective of this piece of research) has been answered.

## 10.1.6 Contribution to Knowledge

This research has contributed to knowledge in a number of areas and this section is dedicated to stating this novel work.

### **Influence of mounting conditions on laboratory foot testing**

Chapter 3 details the static characterisation of ESR feet and highlights the effect of changing the boundary conditions as a result of different mounting configurations. This work explains the disparity in results observed in the published literature and details a novel mounting configuration that ensures accurate and repeatable test results.

### **Application of SHM to amputee running**

As described in the literature review authors have suggested a link between Simple Harmonic Motion and amputee running. Chapter 6 investigates this claim and demonstrates that SHM can only be used to describe the response of a prosthetic foot if the nominal deflection value is used and assuming a single ground contact point.

### **Factors describing the dynamic response of ESR feet**

It has been hypothesised that the stiffness and mass of an amputee affects the dynamic response of an ESR prosthetic device. This research has shown that further to these, additional factors that affect response include leg length (chapter 9), stance length (chapter 9), posterior/anterior setup bias (chapter 9), deflection magnitude (chapter 6) and running speed (chapter 7).

### **The ESR prosthetic limits running speed**

Chapter 7 details the effect of speed variation on foot response. It was found that as running velocity increases the fixed response characteristics of the ESR foot force a lengthened stance until the amputee loses the capability to extend further. Therefore the prosthetic device limits maximum running speed. As an extension to this it can be seen that the foot stiffness category serves to 'tune' the stance length of the amputee and this could be a method employed by prosthetists to improve the comfort of amputee athletes.

### **True foot stiffness profiling**

Reference to the stiffness categorisation of ESR feet can be found in the literature but a translation of the various categories into tangible stiffness measures does not appear to exist in the public domain. Further to this the characterisation of stiffness versus ground contact point of the foot during running was not found in the available literature and this is defined in chapter 3. In addition the progression of the ground contact point during amputee running is a novel measure that was defined in chapter 4 and this data can be converted into a true foot stiffness profile of the foot as defined in section 9.3.2.1.

### **True deflection & forcing data**

As an extension to the ground contact progression data captured in chapter 4, true values of foot deflection and ground force were defined in chapter 9. These figures are defined by the deflection and forcing level at the exact point of foot contact with the ground and can be seen in section 9.3.2.1. This information cannot be found in the available literature and describes the true spring co-efficient of the prosthetic foot when used by an amputee. This is a measure that to date has not been replicated in a laboratory.

## 10.2 Conclusion

The current design of Flex Run foot from Ossur means that as the stance phase of the stride progresses, the foot softens. Therefore during running the amputee lands on the stiffest portion of the foot at the moment of foot strike. It could be suggested that the opposite would be advantageous to the amputee; landing on the soft portion of the foot and allowing a smooth deceleration of their mass with the foot stiffening towards the moment of toe-off, providing a more firm platform against which to apply force.

Contrary to this previous statement however, the geometry of the foot means that as running velocity increases the amputee employs a stiffer portion of the foot. This has the effect of increasing the overall effective stiffness of the foot, inevitably resulting in a quicker response time. It was shown in Chapter 7 that a slow response time of the foot can limit the upper speed attainable by the amputee and this slight stiffening of the prosthetic naturally assists in obtaining a faster running speed.

It was also found in Chapter 7 that an amputee can run at any speed with a prosthetic leg up until either they reach their physiological limit (strength, fitness, etc), or their stance cannot extend any further at which point the foot response time can be considered too slow for any further acceleration. Therefore it is suggested that the stiffness of the prosthetic foot serves to tune the stance length of the amputee for their chosen running speed. If the amputee has reached their desired running speed but their stance length appears abnormally short, the stiffness category of the foot could be reduced thus increasing the ground contact time and lengthening the stance.

This research has highlighted that the prescription of a passive prosthetic running foot is a very specific task. The dynamic response of the foot will dictate the stance length of the amputee at any given running speed and ultimately limit the speed that runner can achieve. Another approach to improving the prescription process could lie in the fundamental design of the prosthetic device. McGowan et al. (2012) conclude their studies of prosthetic running feet by stating:

*'The inability to modulate RSP stiffness also likely impairs the ability to accelerate and reach maximum speed. Thus, an RSP that allows for stiffness adjustments within stance*

*or from step to step might allow users to attain even better sprinting performance.'*  
(McGowan et al. 2012, p.1982)

If a prosthetic device were designed that allowed the user to modify its stiffness based on the activity being undertaken, the specific nature of the prescription could be generalised allowing more freedom with a single foot than is currently possible.

It is the finding of this research that the current prescription method of ESR feet is inadequate and more factors should be taken into account if the user experience of an amputee athlete is to be improved. The available prosthetic devices that were tested proved to be highly efficient and very effective, but there are inevitably instances where the prosthetic foot prescribed is limiting the activity of the user, forcing a stance length or running speed that is undesirable. Factors such as desired activity, running speed and leg length should become an intrinsic part of the prescription process and further work should be conducted in this area.

It should also be noted that if the prescription method were to change and advise a softer foot than is currently the case (as a result of the existing prescription process) the structural integrity should be understood.

## 10.3 Further work

This research has highlighted a number of areas of further study that have the potential of improving our understanding of the dynamic action of prosthetic running feet. These are detailed in the following sections.

### 10.3.1 Improve Understanding of the Amputee 'System'

It was shown in Chapter 9 that the prosthetic foot cannot be considered solely responsible for the effective spring stiffness of the leg of the amputee. Further to this McGowan et al. (2012) comment:

*'It is likely that the fixed stiffness of the prosthesis coupled with differences in limb posture required to run with the prosthesis limits the ability to modulate whole leg stiffness.'* (McGowan et al. 2012, p.1982)

The effective stiffness of the affected leg appears to be variable from one individual to the next and depend on multiple factors including foot stiffness, running style, leg length and limb posture.

If the dynamic response of the amputee (not just the foot) is to be predicted more work should be conducted to understand the relationship between these factors. This could be done by isolating variables and controlling them in a known state. For instance it was shown in Chapter 7 that the effective stiffness of a foot not only changes throughout the course of the stride but also for different speeds of running. In order to control the stiffness of the foot at a single value a fixture could be fabricated that allows the amputee to land purely on a single ground contact point along the metatarsal region of the foot. The change in running response could then be examined and the effect of the ground contact point changing can be understood.

It is also suggested that this manner of investigation should also include modifying terrain (running up or down hill) and ground contact conditions (for instance cross-country running with a soft sole versus track running with spikes). This should also take into account the effect of biasing the foot in an anterior or posterior direction to include multi-directional loading and its influence on running dynamics.

### 10.3.2 Investigate the Suitability of Including a Modification Factor

In section 9.4 it is concluded that the predicted response of the prosthetic foot does not align with that measured during amputee running and it is suggested that a modification factor be employed to account for the disparity. This factor would be derived from the measured results (as opposed to being derived from first principles as the response model has been) and as such appears to be a reaction to the inaccuracy of the original concept. It represents the intrinsic stiffness of the residual limb of the amputee. However if further work could be conducted to confirm the principle of such a factor, the result would be an accurate mathematical model of the action of an amputee. This model could then be used as a tool to advise prescription (as discussed in section 10.1.5).

It is anticipated that this work would involve the replication of that carried out in Chapters 7 & 9 with a variety of amputee athletes. Their running response characteristics could be recorded and this data used to establish a correlation factor across a range of individuals using a range of stiffness categories of feet.

### 10.3.3 Increase Sample Sizes of Feet Tested for Category Characterisation

Chapter 8 is concerned with the characterisation of the mechanical properties (essentially stiffness variation) of the range of Flex Run feet available from the manufacturer, Ossur. It was shown in this chapter that the feet make up a spectrum of stiffness values, but do not occupy an equal distribution within the range. This suggests either a measurement error or deviation within a manufacturing tolerance within the categories.

If a mathematical model could be effectively implemented to improve the prescription of these prosthetic devices it would need to rely on accurate values of foot stiffness. Therefore it is suggested that further characterisation testing (in the manner described in Chapter 8) is conducted to increase the sample size of tested devices and better define the mechanical properties of the range of feet available.

#### 10.3.4 Designing the Next Generation of Prosthetic Running Foot

Information gathered during the course of this research project has shown that the feet currently available can limit the activities of the athletes using them despite a correct prescription (according to the manufacturer's guidelines). One approach to remedy this issue is to improve upon the prescription process and this has been a recurring theme throughout this thesis. This could mean that multiple running feet are prescribed, each to address a particular desired running speed and activity.

An alternative approach would be to modify the design of the running foot such that a specific prescription is not required. For example if a foot were designed that had the capacity to have its spring rate modified, this could then be adjusted by the amputee to suit the specific activity being undertaken. An extension to this would be to design a mechanism with the ability to dynamically adjust the foot stiffness such that the response of the foot could be tailored from one stride to the next, or even throughout a single stride. Such a development could mean activities with a range of running requirements (for example field sports like rugby or football) could be catered for in a more controlled and efficient manner.

Another issue facing amputee runners is that of dorsiflexion. The individual is not able to induce flexion in their ankle to raise the height of the toe during the swing phase of the stride and as such must raise their knee height to clear the ground with the toe of the foot. This is particularly evident during the acceleration phase of sprinting. In order to address this issue the concept of pre-loading the foot should be investigated. This means that the foot is held in a slight state of deflection by mechanical means thus allowing a greater ground clearance. At the moment of foot strike the spring rate of the foot will be identical to an unrestrained model but the preload will mean the deflection (as experienced by the amputee) will begin from a load greater than zero (as is currently the case). Theoretically the response time of the foot will be identical because the spring rate (and ground contact progression) will remain the same as the unrestrained version. However it is possible that this method will introduce additional loading into the physiology of the amputee via higher landing forces onto a preloaded foot.

## References

- Alexander, R. 1976. Mechanics of bipedal locomotion. Perspectives of Experimental Biology, Oxford, UK: Pergamon Press. PP.493-504.
- Alexander, R. 1992. A model of bipedal locomotion on compliant legs. Philosophical Transactions of the Royal Society of London. B 338, pp.189–198.
- Arampatzis, A., Bruggemann, G-P., Metzler, V. 1999. The effect on leg stiffness and joint kinematics in human running. Journal of Biomechanics. 32, pp.1349-1353.
- Au, S., Berniker, M., Herr, H. 2008. Powered ankle-foot prosthesis to assist level-ground and stair-descent gaits. Neural Networks. 21, pp.654-666.
- Biswas, D., Roy, S., PK, L., Kumar, R. 2010. Energy Cost and Gait Efficiency of Below-Knee Amputee and Normal Subject with Similar Physical Parameters and Quality of Life: A Comparative Case Study. Online Journal Of Health And Allied Sciences. 9(3), pp.1-4.
- Blickhan, R. 1989. The spring–mass model for running and hopping. Journal of Biomechanics. 22, pp.1217–1227.
- Blickhan, R. & Full, R. J. 1993. Similarity in multilegged locomotion: bouncing like a monopode. Journal of Comparative Physiology. A 173, pp.509–517.
- Bobbert, M.F., Yeadon, M.R., Nigg, B.M. 1992. Mechanical analysis of the landing phase in heel-toe running. Journal of Biomechanics. 25(3), pp.223-234.
- Borelli, G. 1685. De motu animalium. Leiden, The Netherlands: Lugduni. Vol. 1.
- Bruggemann, G-P., Arampatzis, A., Emrich, F., Potthast, W. 2008. Biomechanics of double transtibial amputee sprinting using dedicated sprinting prostheses. Sports Technology. No. 4–5, pp.220–227.
- Buckley, J. 1999. Sprint kinematics of athletes with lower-limb amputations. Archives of Physical Medicine and Rehabilitation. 80(5), pp.501–8.

- Buckley, J. 2000. Biomechanical adaptations of transtibial amputee sprinting in athletes using dedicated prostheses. *Clinical Biomechanics*. 15(5), pp.352–8.
- Bullimore, S.R., Burn, J.F. 2007. Ability of the planar spring-mass model to predict mechanical parameters in running humans. *Journal of Theoretical Biology*. 248(4), pp.686-695.
- Cavagna, G.A., Saibene, F.P., Margaria, R. 1964. Mechanical work in running. *Journal of Applied Physiology*. 19, pp.249-256.
- Cavagna, G.A., Heglund, N.C., Taylor, C.R. 1977. Mechanical work in terrestrial locomotion: two basic mechanisms for minimizing energy expenditure. *American Journal of Physiology*. 233, pp.243-261.
- Cavagna, G.A., Franzetti, P., Heglund, N.C., Willems, P. 1988. The determinants of step frequency in running, trotting, and hopping in man and other vertebrates. *Journal of Physiology*. 399, pp.81-92.
- Clark, K.P., Ryan, L.J., Weyand, P.G. 2014. Foot speed, foot strike and footwear: linking gait mechanics and running ground reaction forces. *Journal of Experimental Biology*. 217, pp.2037-2040.
- Collins, S.H., Kuo, A.D. 2005. Controlled energy storage and return prosthesis reduces metabolic cost of walking. ASB 29<sup>th</sup> Annual Meeting, pp.804
- Czerniecki, J.M., Gitter, A., Munro, C.J. 1991. Joint moment and muscle power output characteristics of below knee amputees during running: the influence of energy storing prosthetic feet. *Biomechanics*, 24(3-4), pp.271-2.
- Czerniecki, J.M. 2005. Research and Clinical Selection of Foot-Ankle Systems. *Journal Of Prosthetics And Orthotics*. 17(4S), pp.35.
- Dalleau, G., Nelli, B., Bourdin, M., Lacour, J-R. 1998. The spring-mass model and the energy cost of treadmill running. *European Journal of Applied Physiology*. 77, pp.257-263.

Dyer, B. 2013. How should we assess the mechanical properties of lower-limb prosthesis technology used in elite sport? - An initial investigation. *Journal of Biomedical Science and Engineering*. 6, pp.116-123.

Dutto, D. J., Smith, G. A. 2002. Changes in spring-mass characteristics during treadmill running to exhaustion. *Medicine & Science in Sports & Exercise*. pp. 1324-1331.

Endolite products catalogue. [www.endolite.co.uk](http://www.endolite.co.uk) (Accessed 20th February 2015).

Farley, C.T., Blickhan, R., Saito, J., Taylor, C. R. 1991. Hopping frequency in humans: a test of how springs set stride frequency in bouncing gaits. *Journal of Applied Physiology*. 716, pp.2127-2132.

Farley, C.T., González, O. 1996. Leg stiffness and stride frequency in human running. *Journal of Biomechanics*. 29(2), pp.181–186.

Farley, C.T., Glasheen, J., McMahon, T.A. 1993. Running springs: speed and animal size. *Journal of Experimental Biology*. 185, pp.71-86.

Farley, C.T., Morgenroth, D.C. 1999. Leg stiffness primarily depends on ankle stiffness during human hopping. *Journal of Biomechanics*. 32(3), pp.267-273.

Fey, N.P., Silverman, A.K., Neptune, R.R. 2010. The influence of increasing steady-state walking speed on muscle activity in below-knee amputees. *Journal of Electromyography and Kinesiology*. 20, pp.155-161.

Fey, N.P., Klute, G.K., Neptune, R.R. 2011. The influence of energy storage and return foot stiffness on walking mechanics and muscle activity in below-knee amputees. *Clinical Biomechanics*. 26, pp.1025-1032.

Fisher, R. A., 1935. *The Design of Experiments* (9th edition). Macmillan.

Freedom Innovations products catalogue. [www.freedom-innovations.com](http://www.freedom-innovations.com) (Accessed 20th February 2015).

Geil, M. 2001. Energy Loss and Stiffness Properties of Dynamic Elastic Response Prosthetic Feet. *Prosthetic and Orthotic Science*. 13(3), pp.70-73.

Geyer, H., Blickhan, R., Seyfarth, A. 2002. Natural dynamics of spring-like running: Emergence of selfstability. CLAWAR, Paris.

Geyer, H., Seyfarth, A., Blickhan, R. 2004. Spring-mass running : simple approximate solution and application to gait stability. *Journal of Theoretical Biology*. 232, pp.315–328.

Geyer, H., Seyfarth, A., Blickhan, R. 2006. Compliant leg behaviour explains basic dynamics of walking and running. *Proceedings of the Royal Society B*. 273, pp.2861-2867.

Gottschall, J.S., Kram, R. 2005. Ground reaction forces during downhill and uphill running. *Journal of Biomechanics*. 38(3), pp.445-452.

Grabowski, A.M., McGowan, C.P., McDermott, W.J., Beale, M.T., Kram, R., Herr, H.M. 2010. Running-specific prostheses limit ground-force during sprinting. *Biology Letters*. 6, pp.201–204.

Gunther, M., Blickhan, R. 2002. Joint stiffness of the ankle and knee in running. *Journal of Biomechanics*. 35, pp.1459-1474.

Hafner, B. 2005. Clinical Prescription and Use of Prosthetic Foot and Ankle Mechanisms: A Review of the Literature. *Journal of Prosthetics & Orthotics*. 17, pp.5–11.

Hafner, B., Sanders, J., Czerniecki, J., Fergason, J. 2002. Transtibial energy-storage-and-return prosthetic devices: A review of energy concepts and a proposed nomenclature. *Journal of Rehabilitation Research and Development*. 39(1), pp.1–11.

Hansen, A., Childress, D.S., Miff, S.C., Gard, S.A., Mesplay, K.P. 2004a. The human ankle during walking: implications for the design of biomimetic ankle prostheses. *Journal of Biomechanics*. 37, pp.1467-1474.

Hansen, A., Sam, M. & Childress, D. 2004b. The Effective Foot Length Ratio: A Potential Tool for Characterization and Evaluation of Prosthetic Feet. *American Academy of Orthotists & Prosthetists*. 16(2), pp.41-45.

He, J., Kram, R., McMahon, T.A. 1991. Mechanics of running under simulated reduced gravity. *Journal of Applied Physiology*. 71, pp.863-870.

Herr, H., Wilkenfeld, A., Blaya, J. 2002. Patient-Adaptive Prosthetic and Orthotic Leg Systems. *Proceedings of the 12th Nordic Baltic Conference on Biomedical Engineering and Medical Physics*. pp.123–128.

Hillery, S.C., Wallace, E.S., McIlhagger, R., Watson, P. 1997. The effect of changing the inertia of a trans-tibial dynamic elastic response prosthesis on the kinematics and ground reaction force patterns. *Prosthetics and Orthotics International*. 21, pp.114-123.

Holgate, M.A., Hitt, J.K., Bellman, R.D., Sugar, T.G., Hollander, K.W. 2008. The SPARKy (Spring Ankle with Regenerative Kinetics) Project: Choosing a DC motor based actuation method. *Proceedings of the 2<sup>nd</sup> Biennial IEEE/RAS-EMBS International Conference on Biomedical Robotics and Biomechatronics*. pp.163-168.

Hunter, J., Marshall, R. & McNair, P. 2005. Relationships between ground reaction force impulse and kinematics of sprint-running acceleration. *Journal of Applied Biomechanics*. 21(1), pp.31–43.

Ito, A., Komi, P.V., Sjodin, B., Bosco, C., Karlsson, J. 1983. Mechanical efficiency of positive work in running at different speeds. *Medical Science Sports Exert*. 15, pp.299-308.

Keller, T.S., Weisberger, A.M., Ray, J.L., Hasan, S.S., Shiavi, R.G., Spengler, D.M. 1996. Relationship between vertical ground reaction force and speed during walking, slow jogging, and running. *Clinical Biomechanics*. 11(5), pp.253-259.

Keogh, J.W.L. 2011. Paralympic sport: an emerging area for research and consultancy in sports biomechanics. *Sports Biomechanics*. 10(3), pp.234-253.

Kerdok, A.E., Biewener, A.A., McMahon, T.A., Weyand, P.G., Herr, H.M. 2002. Energetics and mechanics of human running on surfaces of different stiffnesses. *Journal of Applied Physiology*. 92, pp.469-478.

Lechler, K. 2005. Lower-Limb Prosthetics - Design Improvements of a Prosthetic Spring Foot. *American Journal of Physics*. 36, pp. 4-7.

Lechler, K. & Lilja, M. 2008. Lower extremity leg amputation: an advantage in running? *Sports Technology*. 1(4-5), pp.229–234.

Lehmann, J., Price, R., Boswell-Bessette, S., Dralle, A., Questad, K., 1993a. Comprehensive Analysis of Dynamic Elastic Response Feet: Seattle Ankle/Lite Foot Versus SACH Foot. *Archives of Physical Medicine & Rehabilitation*. 74(8), pp.853-861.

Lehmann, J., Price, R., Boswell-Bessette, S., Dralle, A., Questad, K., deLateur, BJ. 1993b. Comprehensive Analysis of Energy Storing Prosthetic Feet: Flex Foot and Seattle Foot Versus Standard SACH Foot. *Archives of Physical Medicine & Rehabilitation*. 74(11), pp.1225-1231.

Limbless Association website, 2012. [www.limbless-association.org](http://www.limbless-association.org) (Accessed 16th January 2015).

Limb Loss Information Centre website. [www.limblossinformationcentre.com](http://www.limblossinformationcentre.com) (Accessed 16th January 2015).

Liu, T., Inoue, Y., Shibata, K. 2009. Development of a wearable sensor system for quantitative gait analysis. *Measurement*. 42, pp.978-988.

Liu, W., Nigg, B.M. 2000. A mechanical model to determine the influence of masses and mass distribution on the impact force during running. *Journal of Biomechanics*. 33, pp.219-224.

Ly, Q.H., Alaoui, A., Erlicher, S., Baly, L. 2010. Towards a footwear design tool: influence of shoe midsole properties and ground stiffness on the impact force during running. *Journal of Biomechanics*. 43, pp.310-317.

Magness, S. 2014. *The Science of Running: How to find your limit and train to maximize your performance*. Origin Press 1<sup>st</sup> Edition.

- Mattes, S.J., Martin, P.E., Royer, T.D. 2000. Walking symmetry and energy cost in persons with unilateral transtibial amputations: patching prosthetic and intact limb inertial properties. *Archives of Physical Medicine & Rehabilitation*. 81, pp.561-568.
- McGeer, T. 1990. Passive bipedal running. *Proceedings of the Royal Society of London*. B240, pp.107-134.
- McGowan, C.P., Grabowski, A.M., McDermott, W.J., Herr, H.M., Kram, R. 2012. Leg stiffness of sprinters using running-specific prostheses. *Journal of the Royal Society Interface*. 9, pp.1975–1982.
- McMahon, T.A., Cheng, G.C. 1990. The mechanics of running: how does stiffness couple with speed? *Journal of Biomechanics*. 23(1), pp.65-78.
- Michael J.W. 1987. Energy Storing Feet: a clinical comparison. *Clinical Prosthetics and Orthotics*. 11(3), pp.154-168.
- Michael, J.W., Gailey, R.S., Bowker, J.H. 1990. New Developments in Recreational Prostheses and Adaptive Devices for the Amputee. *Clinical Orthopaedics & Related Research*. Section I.
- Morin, J.B., Jeannin, T., Chevalier, B., Belli, A. 2006. Spring-mass model characteristics during sprint running: correlation with performance and fatigue-induced changes. *International Journal of Sports Medicine*. 27(2), pp.158-165.
- Munro, C.F., Miller, D.I., Fuglevand, A.J. 1987. Ground reaction forces in running: a re-examination. *Journal of Biomechanics*. 20(2), pp. 147-155.
- NHS, 2015. <http://www.nhs.uk/conditions/amputation> (Accessed 16th January 2015).
- Nigg, B.M., Liu, W. 1999. The effect of muscle stiffness and damping on simulated impact force peaks during running. *Journal of Biomechanics*. 32, pp.849-856.
- Nikooyan, A.A., Zadpoor, A.A. 2011. Mass-spring damper modeling of the human body to study running and hopping – an overview. *Proceedings of the Institute of Mechanical Engineers*. H 225, pp.1121-1135.

- Nolan, L. 2008. Carbon fibre prostheses and running in amputees: a review. *Official Journal of the European Society of Foot and Ankle Surgeons*. 14(3), pp.125–9.
- Noroozi, S., Ghaffar Abdul Rahman, A., Khoo, S.Y., Zahedi, S., Sewell, P., Dyer, B., Chao, O.Z. 2014. The dynamic elastic response to impulse synchronisation of composite prosthetic energy storing and returning feet. *Journal of Sports Engineering and Technology*. 228(1), pp.24-32.
- Noroozi, S., Sewell, P., Ghaffar Abdul Rahman, A., Vinney, J., Chao, O.Z., Dyer, B. 2012a. Performance enhancement of bi-lateral lower-limb amputees in the latter phases of running events: an initial investigation. *Journal of Sports Engineering and Technology*. 227(2), pp.105-115.
- Noroozi, S., Sewell, P., Ghaffar Abdul Rahman, A., Vinney, J., Chao, O.Z., Dyer, B. 2012b. Modal Analysis of Composite Prosthetic Energy-Storing-and-Returning Feet: An Initial Investigation. *Journal of Sports Engineering and Technology*. 227(1), pp.39-48.
- Office for National Statistics, 2011. [www.ons.gov.uk/ons/dcp171778\\_292378.pdf](http://www.ons.gov.uk/ons/dcp171778_292378.pdf) (Accessed 16th January 2015).
- Ossur products catalogue, P161. [www.ossur.co.uk](http://www.ossur.co.uk) (Accessed 16th January 2015).
- Ossur Instructions for Use, 2012. [http://assets.ossur.com/library/25848/Flex-Run%20with%20Nike%20Sole\\_0153\\_IFU.pdf](http://assets.ossur.com/library/25848/Flex-Run%20with%20Nike%20Sole_0153_IFU.pdf) (Accessed 16th January 2015).
- Palermo, E., Rossi, S., Marini, F., Patane, F., Cappa, P. 2014. Experimental evaluation of accuracy and repeatability of a novel body-to-sensor calibration procedure for inertial sensor-based gait analysis. *Measurement*. 52, pp.145-155.
- Pasparakis, D., Darras, N. 2009. Normal walking principles, basic concepts, terminology 3-dimensional clinical gait analysis. *EEXOT*. 60(4), pp.183-194.
- Perry, J., Shanfield, S. 1993. Efficiency of dynamic elastic response feet. *Journal of Rehabilitation Research*. 30(1), pp.137-143.
- Riener, R., Rabuffetti, M., Frigo, C. 2002. Stair ascent and descent at different inclinations. *Gait and Posture*. 15, pp.32-44.

Science of Running blog. [www.scienceofrunning.com](http://www.scienceofrunning.com) (Accessed 16th January 2015).

Seyfarth, A., Geyer, H., Gunther, M., Blickhan, R. 2002. A movement criterion for running. *Journal of Biomechanics*. 35(5), pp.649-655.

Seyfarth, A., Geyer, H., Herr, H. 2003. Swing-leg retraction: a simple control model for stable running. *Journal of Experimental Biology*; 206, pp.2547-2555.

Stark, G. 2005. Perspectives on How and Why Feet are Prescribed. *Journal of Prosthetics and Orthotics*. 17(4), pp.18–22.

Strike, S., Hillery, M. 2000. The design and testing of a composite lower limb prosthesis. *Proceedings of the Institution of Mechanical Engineers. Part H, Journal of Engineering in Medicine*. 214(6), pp.603–14.

Thomas, S.S., Buckon, C.E., Helper, D., Turner, N., Moor, M., Krajbich, J.I. 2000. Comparison of the Seattle Lite foot and Genesis II prosthetic foot during walking and running. *Journal of Prosthetics and Orthotics*. 12(1), pp.9-14.

Thompson, C., Raibert, M. 1989. Passive dynamic running. *International Symposium of Experimental Robotics*. pp.74-83.

Tokuda, M., Li, C., Hashimoto, Y., Morimoto, S., Nakagawa, A, Akazawa, Y. 2006. Research and development of the intelligently-controlled prosthetic ankle joint. *Proceedings of the 2006 IEEE International Conference on Mechatronics and Automation*. pp.1114-1119.

Torburn, L., Perry, J., Ayyappa, E., Shanfield, S.L. 1990. Below-knee amputee gait with dynamic elastic response prosthetic feet: A pilot study. *The Journal of Rehabilitation Research and Development*. 27(4), pp.369-384.

Vinney, J., Noroozi, S., Ghaffar Abdul Rahman, A., Sewell, P., Chao, O.Z., Kuan K-K., Dupac, M. 2012. Analysis of Composite Prosthetic Energy-Storing-and-Returning (ESR) feet: A comparison between FEA and the experimental analysis. *International Journal of COMADEM*. 15(3), pp.19-28.

Versluys, R., Beyl, P., Van Damme, M., Desomer, A., Van Ham, R., Lefeber, D. 2009. Prosthetic feet: State-of-the-art review and the importance of mimicking human ankle-foot biomechanics. *Disability and Rehabilitation: Assistive Technology*. 4(2), pp.65-75.

Weyand, P.G., Sternlight, D.B., Bellizzi, M.J., Wright, S. 2000. Faster top running speeds are achieved with greater ground forces not more rapid leg movements. *Journal of Applied Physiology*. 89(5), pp.1991-1999.

Weyand, P.G., Sandell, R.F., Prime, D.N.L., Bundle, M.W. 2010. The biological limits to running speed are imposed from the ground up. *Journal of Applied Physiology*, 108, pp.950-961.

Weyand, P.G., Bundle, M.W., McGowan, C.P., Grabowski, A., Brown, M.B., Kram, R., Herr, H. 2009. The fastest runner on artificial legs: different limbs, similar function? *Journal of Applied Physiology*. 107, pp.903-911.

Wilson, J.R., Asfour, S., Abdelrahman, K.Z., Gailey, R. 2009. A new methodology to measure the running biomechanics of amputees. *Prosthetics and Orthotics International*. 33(3), pp.218–229.

Yack, H.J., Nielson, D.H., Shurr, D.G. 1999. Kinetic patterns during stair ascent in patients with transtibial amputations using three different prostheses. *Journal of Prosthetics and Orthotics*. 11 (3), pp. 57-62.

Zadpoor, A.A. and Nikooyan, A.A. 2010. Modeling muscle activity to study the effects of footwear on the impact forces and vibrations of the human body during running. *Journal of Biomechanics*. 43, pp.186-193.

# APPENDIX 1: FOOT INSTRUMENTATION

## A1.1 Displacement Sensor

The primary mode of operation of an ESR prosthetic running foot is bending in the sagittal plane. Therefore accurate logging of this mode is fundamental to understanding the dynamics of the system. A majority of the required variables can be

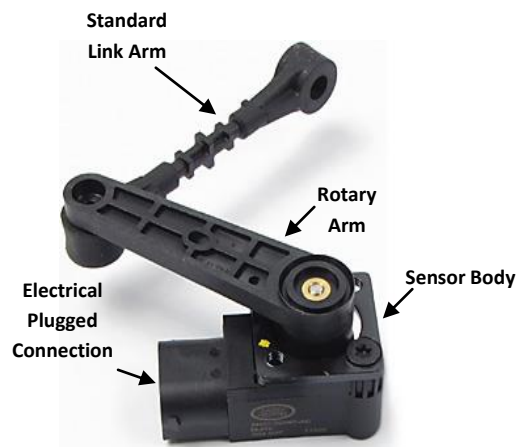


**Figure A1.1:** Rotary displacement transducer with standard link arm.  
*This arm was modified in order to suit a prosthetic foot.*

measured in this mode if logged at an adequate resolution (both in terms of numerical accuracy and logging frequency). For this reason an automotive suspension position sensor (height sensor) was used (figure A1.1). This is a resistive hall-effect device with a rotary input that emits a variable voltage output depending on arm position and supply voltage. Originally the purpose of such a sensor is for detecting suspension displacement and quality of road surface for the control of variable damping on the suspension systems of luxury automobiles. It has a specified manufacturing tolerance (across devices) of 2%.

The displacement sensor was attached to the proximal end of the prosthetic foot via a fabricated aluminium bracket. The bracket lightly clamped the carbon fibre section of the foot leaving it adjustable, easily detachable and non-invasive; as such it can be moved from one prosthetic foot to another without compromising the feet. The standard link arm of the sensor is specified for fitment to the original vehicle suspension system and as such was modified. It was lengthened in order to attach to

the distal end of the prosthetic foot via an adjustable threaded turnbuckle-style system allowing accurate tuning of the length (and therefore electrical output reading from the sensor) for different feet and set up conditions. As such the displacement sensor was able to measure any change in distance between the proximal and distal ends of the prosthetic device (and therefore a measure of strain energy). A picture of the setup of the equipment can be seen in figure 4.1.

## A1.2 Ground-Force Sensors

In order to build up a more accurate image of the dynamics of a prosthetic running device it was necessary to understand the ground contact point throughout a single stride. If the displacement of the foot is known then the force going through the foot can be easily derived as long as it is known where that force is being applied (i.e. what the ground contact point is).

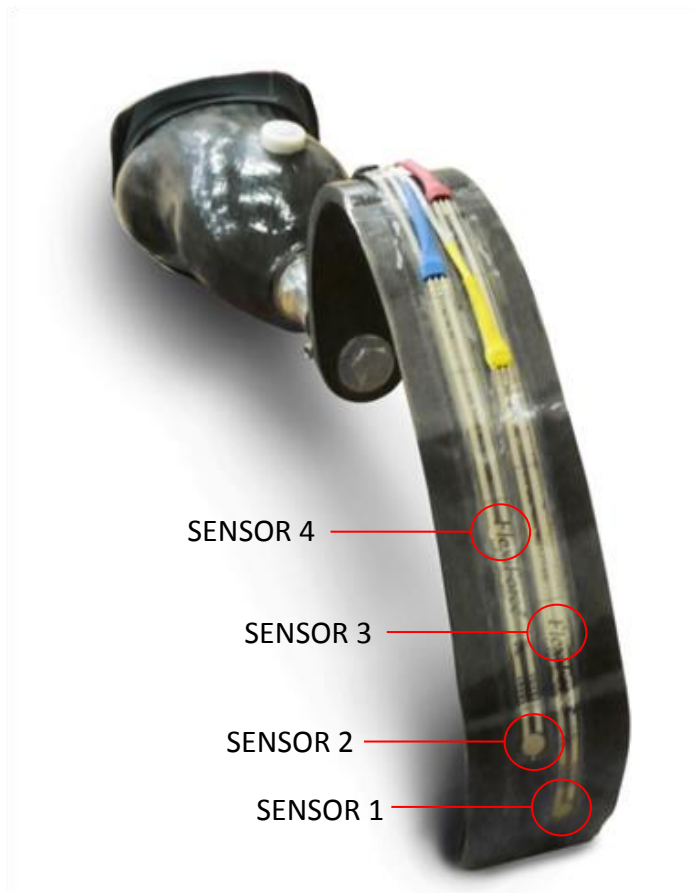


**Figure A1.2:** Piezo-resistive sensor array on metatarsal region of prosthetic foot.

The sensors chosen for this task were piezo-resistive devices of a printed construction from Tekscan Inc. These units are flexible and <0.2mm thick, and therefore can be inserted between the carbon fibre foot and the foam of the trainer sole used, thus protecting the sensors from direct contact with the ground. The sensing area of this sensor is 10mm diameter and cannot differentiate between forces applied at various points within this sensing area. Therefore a linear array of these sensors was used (four in total) along the metatarsal region of the prosthetic foot (figure A1.2) and their

results interpolated. A variety of these sensors are available from the manufacturer. The exact variant chosen for this investigation were the 100lb 9" models. It is anticipated that assuming the ground contact point does indeed progress along the base of the foot, the peak force of each sensor in turn will dictate the contact point at that specific moment. These points can then be plotted on a graph and interpolated meaning the contact point at any given time can be ascertained.

### **A1.3 Resistive Force Signal Conditioner**

This piece of apparatus was designed and built in-house for the specific application of converting the changing resistive function of the ground-force sensors to an analogue voltage signal that could then be logged. The circuit was designed and modelled using



**Figure A1.3:** In-house signal conditioner for piezo-resistive sensors providing a 0-5v output.

Proteus Isis and Ares software (Labcentre Electronics Ltd.) and fabricated using a CNC circuit cutter and a double-sided board blank. This circuit along with a battery was built into an aluminium case (figure A1.3) with plugged connections via two RS232 ports for the sensor inputs and the outputs to the logger. The device has four individual channels to allow the array of four separate sensors to be used simultaneously, is

powered from a single 9V alkaline battery and each output ranges from 0-5V depending on the load applied to each ground-force sensor.

The total size of this device was 140mm x 80mm x 30mm, weighing approximately 220 grams and throughout the course of the investigation it was stored in the pocket of the amputee athlete.

#### **A1.4 Analogue Data Logger**

In order to capture the data being generated by the respective sensing devices, a four channel analogue 0-5v data logger was used. The actual device chosen was a standalone 'MSR165' model from MSR Electronics GmbH (Modular Signal Recorders) of Switzerland (figure A1.4). It is capable of logging 4 analogue channels simultaneously at a selected frequency up to 1024Hz but is small and lightweight enough to be placed on the foot itself and not be noticed by the amputee (39mm x 23mm x 52mm, 70g).



*Figure A1.4: MSR165 Data logger (MSR Electronics GmbH)*

The logger was configured to start and stop data acquisition with the push of a button on the outer surface of the device. As an additional function the logger also contained a tri-axial accelerometer capable of recording +/-15g to an accuracy of +/-0.15g at a frequency of 1600Hz. The logger contains its own battery and can log for many hours at maximum frequency without running out of capacity. Once the data acquisition is

complete the logger can be attached to a PC via USB interface and data viewed in .csv format in Microsoft Excel.

## **A1.5 Battery Pack**

The data logger required an analogue input of 0-5v for each of the four channels. The Resistive Force Signal Conditioner unit (4.2.5) contained a 9v battery for the supply from the Ground Force Sensors (4.2.4) but as the displacement sensor (4.2.3) was not internally powered, an additional battery pack was required. The output of this displacement sensor was purely a function of angular condition of the input arm and the voltage supplied to it so to ensure a practical resolution a supply voltage of close to 5v was required. A common 3-cell AA alkaline battery case was chosen to provide an output voltage of up to 4.5v from the displacement sensor (subject to input arm angle). To ensure repeatability the state of charge of this pack was checked at the start of each test by measuring the output voltage.

## A1.6 Equipment Setup

The equipment was set up in a manner that could easily be repeated should further testing be required. A foot with all of the instrumentation can be seen in figure 4.1. It must be noted that the foot used in this series of measurements had been set up by a qualified and recognised prosthetist (as per ethics approval) specifically for the amputee volunteer and the adapter between the foot and shank adapter was not modified. All of the equipment was able to be fitted in a non-invasive manner so as not to affect or significantly influence the use of the foot.

### A1.6.1 Displacement Sensor

The setup started with the proximal end of the foot (the portion that attaches to the shank adapter) being aligned parallel to the ground surface. The displacement sensor was then arranged such that the pivot of the rotary arm was directly below the centreline of the shank adapter. Once this was done, the link arm (one end of which attaches to the distal end of the rotary arm) was attached with an adhesive pad to the toe portion of the foot such that it bridged the space between the toe and the

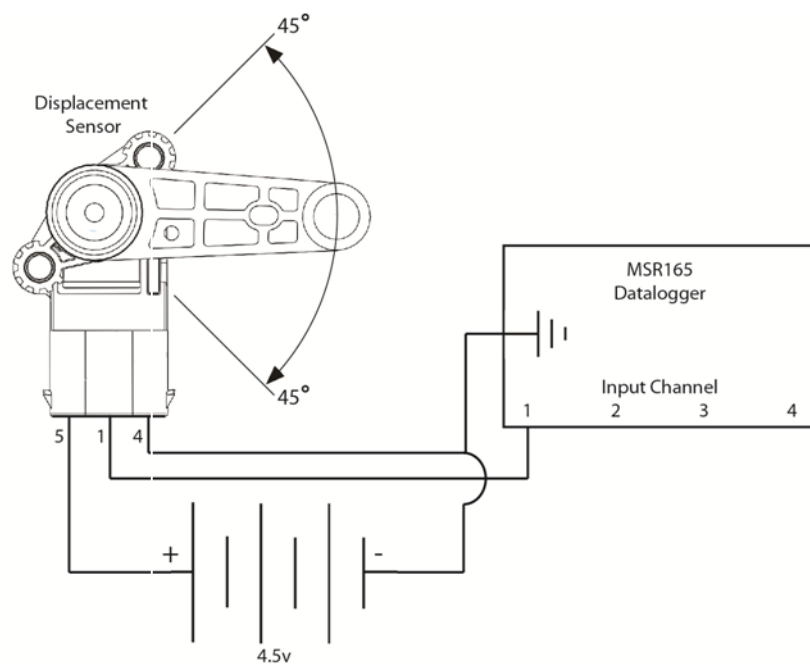


**Figure A1.5:** Circuit diagram of the rotary displacement sensor attached to the data logger and battery pack. Only a single channel is used.

displacement sensor. This link arm featured a turnbuckle-style thumbscrew allowing the length to be tuned for different foot geometries. The screw could therefore be used to align the radial arm of the displacement sensor with 0° on the angle indicator (an integral part of the displacement sensor bracket) and the output of the displacement sensor checked with a DVM (Digital Volt Meter) to confirm the sensor was at the extreme end of its sensing range. The logger could then be wired as shown in figure A1.5 to allow data acquisition from the displacement sensor.

### A1.6.2 Ground Force Sensors

Due to their fragile nature and to make their transference from one foot to another practical, the sensors were mounted on a sheet of acetate using tape to secure (figure A1.6). They were positioned into a near-linear array with equal spacing along what was anticipated to be the dynamic contact patch of the foot with the ground during running. The front edge of this acetate sheet could then be aligned with the distal edge of the toe region of the foot for repeatability.

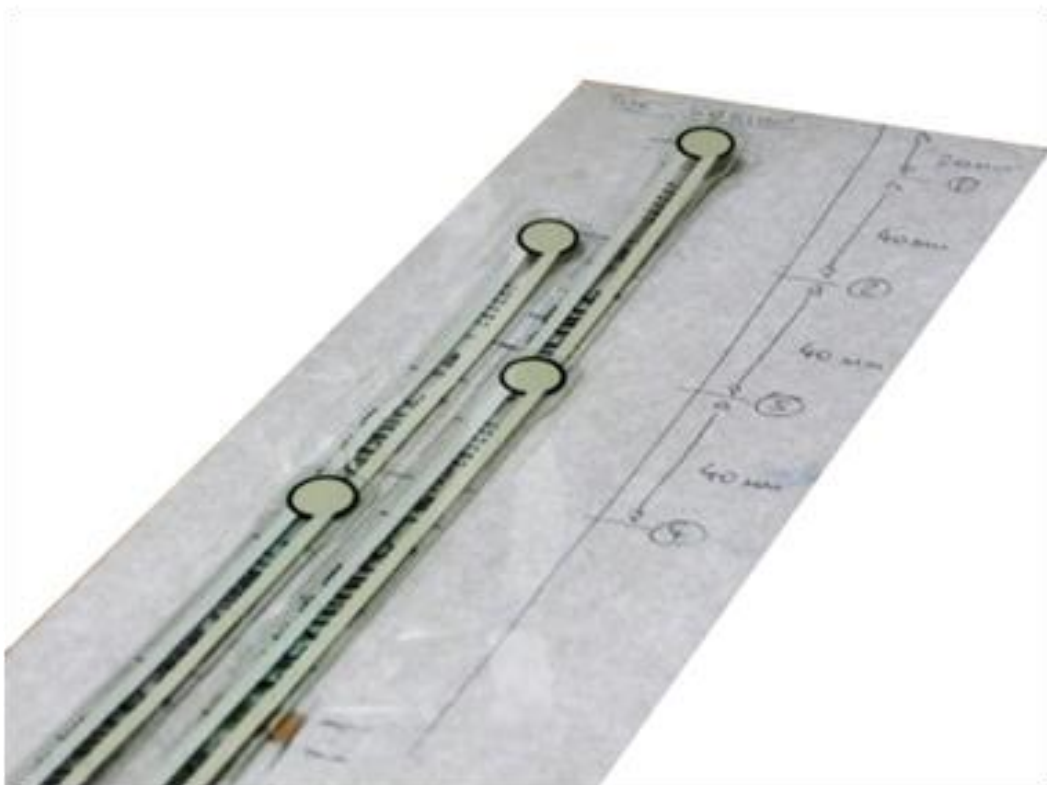


**Figure A1.6:** Layout of the piezo-resistive sensors on

Once the ground force sensors were attached to the base of the prosthetic foot they could be wired to the signal conditioner and in turn to the datalogger. This was done as described in figure A1.7. As such, the system could record the output of all four sensors simultaneously at a frequency of up to 1024Hz.

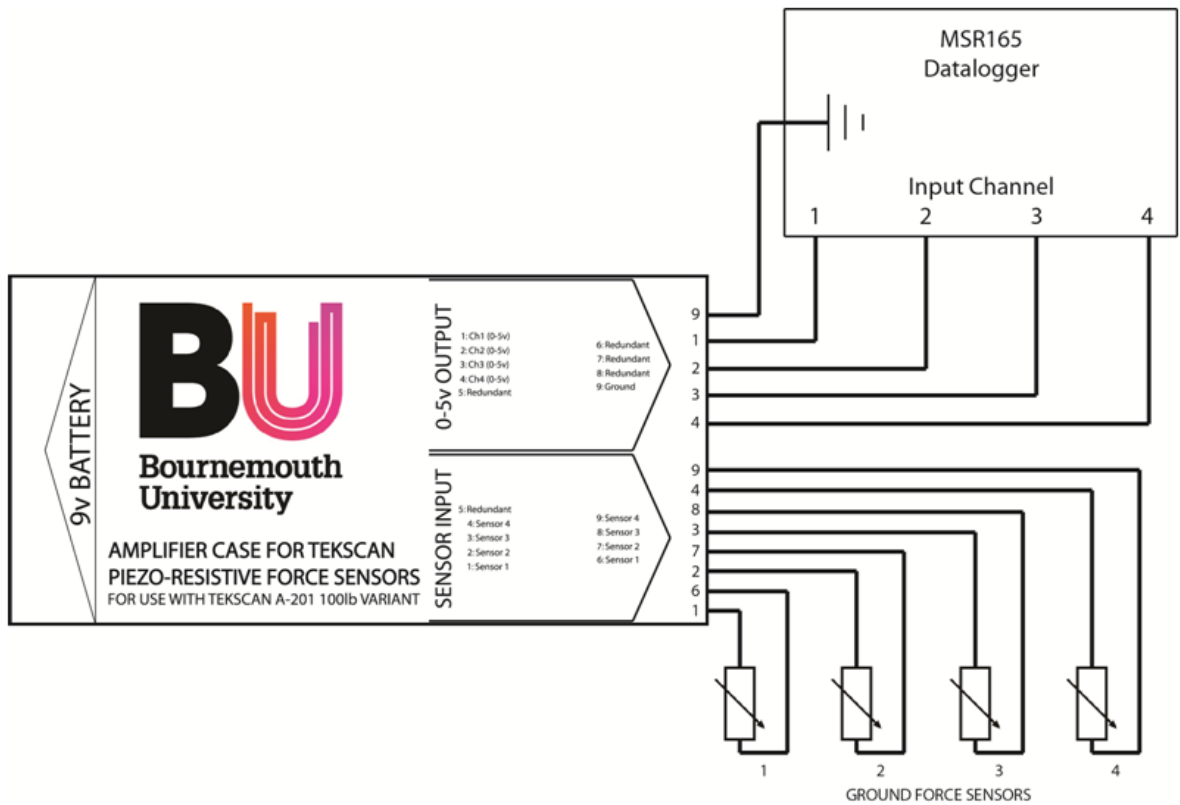


**Figure A1.7:** Circuit diagram of piezo-resistive force sensors connected to the signal conditioner and data logger. All four logger inputs are used.

## APPENDIX 2: RIG FABRICATION

### A2.1 Framework

The framework is of welded steel construction fabricated from 40mm x 40mm box section and 80mm x 40mm box section, triangulated to give an excessively stiff structure. All material has a wall thickness of 3mm.

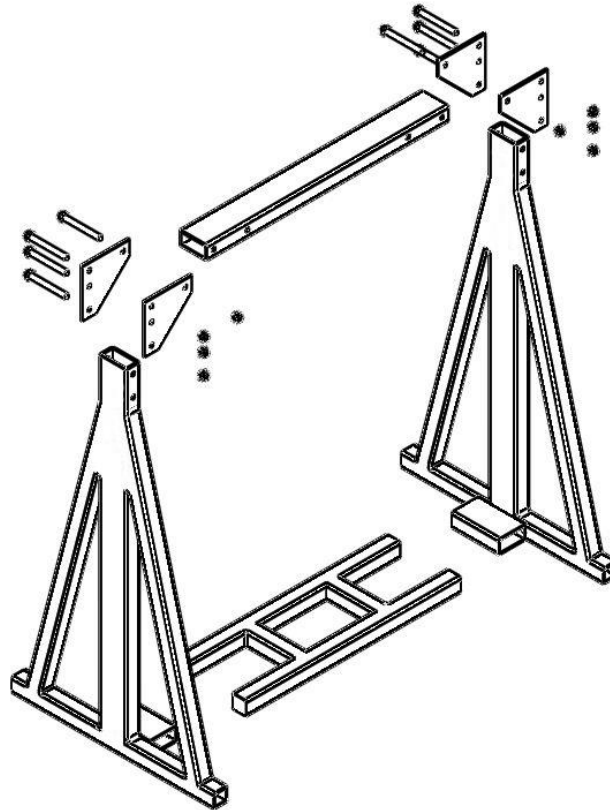


*Figure A2.1: Exploded diagram of the structural mainframe of the frequency response rig.*

The style of construction means that the rig can be dismantled. Each A-frame structure is bolted in place with the crossbar via two sandwiching plates of 6mm steel on each side. The distal end of the foot is held in a structure that locates in the centre of an 'H'-shaped fabrication.

In order to ensure stability, the rig was assembled and clamped onto a cast iron engineer's surface table weighing in excess of 300kg. The reason for this modular construction is to allow the carriage to be exercised through its range of motion to ensure correct alignment of all components before the fixings are fully tightened.

Figure A2.1 shows an exploded isometric view of the framework with the carriage and all linear motion components removed.

## A2.2 Carriage & Linear Motion Apparatus

The design requirements of the carriage are to allow smooth uninhibited vertical motion as dictated by the dynamic response of the prosthetic foot under test. In addition it must have the capacity to hold captive a range of masses (in this instance a selection of cast iron masses commonly used in gym equipment), although the masses must be easily interchangeable or removed to alter the mass applied to the foot.

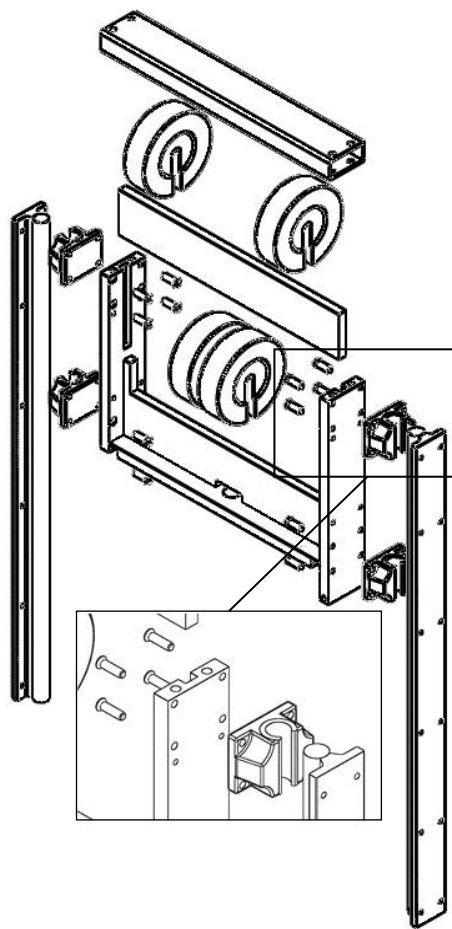


**Figure A2.2:** Exploded diagram of the weights carriage and linear motion

Smooth vertical motion was provided by two ground supported linear rails in combination with four matched 'pillow blocks' containing re-circulating ball bearings. These devices are designed to provide low-resistance linear motion under high load

applications and are commonly used in CNC or materials handling equipment. The supported rails were attached to the steel framework along their entire length via screws. This mounting method ensured a high structural stiffness with the aim of eradicating any low frequency harmonic modes that could have influenced the dynamic results of the testing.

The carriage is of an aluminium plate construction, machined such that each component mechanically locates with its neighbour. The structure is then fastened together with M8 screws. The cast iron masses feature a slot and two rails were provided onto which to mount the masses.

The prosthetic foot under test is mounted in the centre of the lower plate of the construction via an automotive ball joint. Information on this mounting interface can be found in section 3.3. Figure A2.2 shows an exploded isometric view of the carriage construction with detail view of the linear rail and pillow block arrangement.

### **A2.3            Securing the Mass**

Attaching the masses in a secure manner is essential so as not to influence the results of the dynamic response of the foot. The mass must act as a single unit and most importantly in a repeatable manner. Additionally all of the force must act through the centreline of the carriage (demonstrated in figure A2.3) and therefore through the centreline of the prosthetic foot attached for testing. If the masses were offset this would lead to additional forces in the linear bearings which could in turn lead to higher resistance in vertical motion, asymmetric loading of the foot and potentially failure of the linear components.

As such, the lateral placement of the masses was designed to be flexible meaning that the operator can effectively balance the loads on each side of the centreline of the carriage. The cast iron masses feature a slot for attaching them to a variety of equipment and a corresponding pair of rails were included in the carriage (a lower rail and upper rail). The lower rail formed a rigid and important structural member of the carriage chassis and bolted to the base and side plates as shown in figure A2.3. The

upper rail was free to move vertically in slots machined into the side plates of the chassis and as such could be dropped into place on top of the masses located on the lower rail. In doing this, the upper rail served to hold captive the masses on the lower rail, as well as providing additional space to locate more masses. Two decks of masses was an important step in reducing the overall dimensions of the test rig. A single array

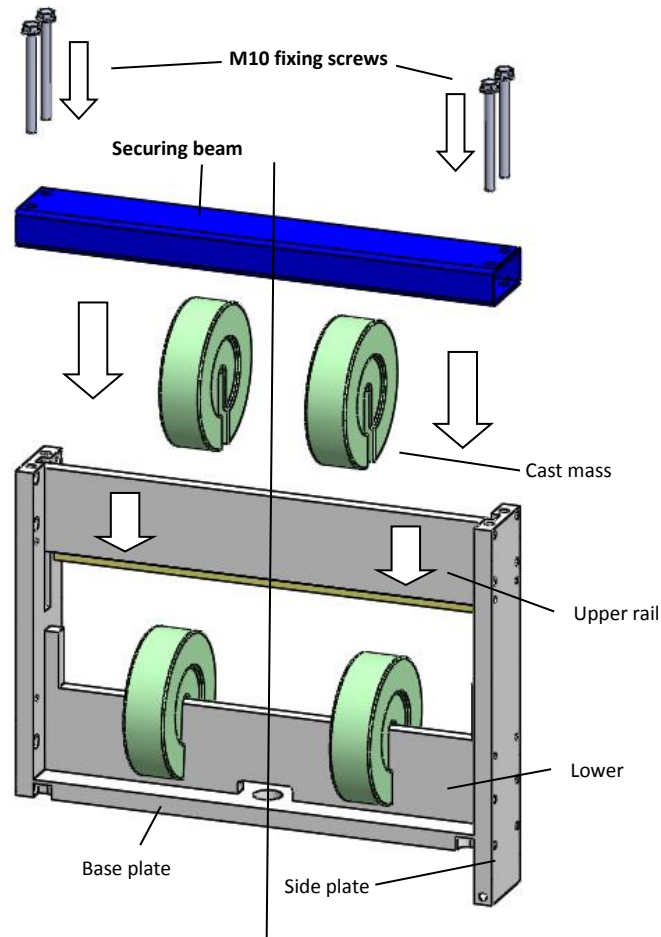


**Figure A2.3:** Exploded view of the weights carriage showing detail on how the individual masses are secured

of masses would result in either a very wide or very tall machine.

Once the masses and upper rail are in place, the entire assembly can be secured using the beam as shown in figure A2.3. This is bolted into place using four M10 screws into the side plates. However this was not sufficient to effectively clamp all of the masses. Due to their manufacturing process (casting), the dimensions of the masses are un-uniform. As such, if an accurately machined structure were used to clamp them in

place it would purely hold in place the mass with the largest vertical dimension. In order to combat this, cork strips of 12mm x 19mm cross section were attached to the lower edge of the upper rail and beam. These strips were soft enough to absorb any deviation in the dimensions of the masses and ensure the carriage formed a single homogenous mass for the purposes of testing. The action of the cork strips can be seen in figure A2.4.

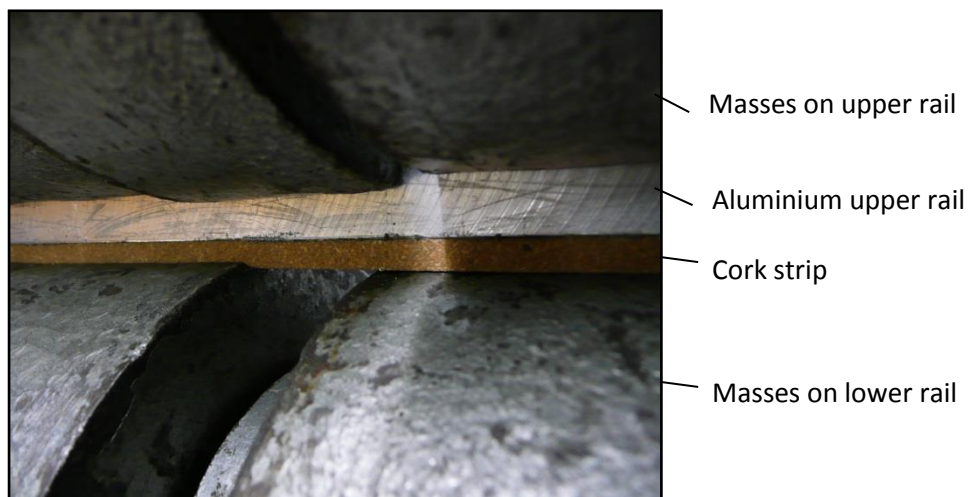


**Figure A2.4:** Detail of the cork strip employed on the lower edge of the upper rail and beam to secure the lower masses and prevent loose components

## APPENDIX 3: RIG INSTRUMENTATION

### A3.1 Processing Hardware

Before any calibration work could be conducted the processing circuitry had to be designed and fabricated. The load cells used were of a strain-gauge type with a Wheatstone Bridge contained in each. As such the output is in the order of millivolts (mv), but the desired output for logging using the already available MSR165 data

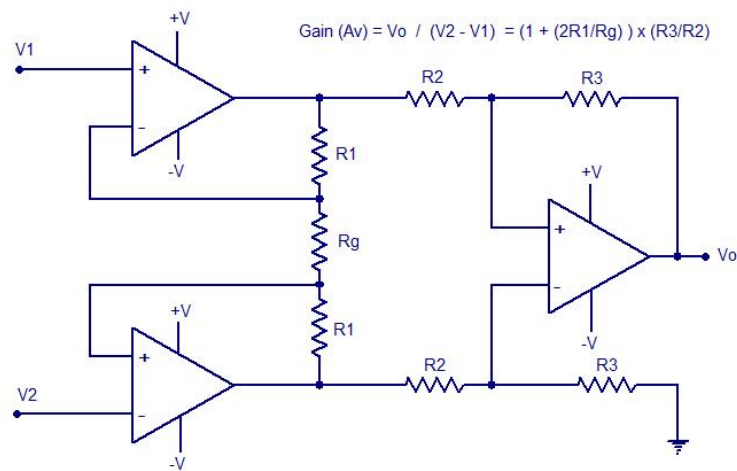


**Figure A3.1:** Example of a simple Operational Amplifier circuit (source: [www.circuitstoday.com](http://www.circuitstoday.com))

logger was 0-5 volts, meaning that a power source and amplifier circuit was required. A simple operational-amplifier circuit was used for each load cell, an example of which can be seen in figure A3.1.

The advantage of this style of amplifier is that the gain can be adjusted by changing resistor values. This means that the working range of the sensor could be manipulated to suit the specific application. For example the ground force load cell used was of a 10kN capacity. However the maximum force exerted by the rig is never likely to exceed 2.5kN. Therefore in order to improve the resolution of the readings, the 0-5v output from the amplifier circuit could be applied over this 2.5kN range instead of the full 10kN range of the load cell.



**Figure A3.2:** Amplifier case with output voltages displayed on the lid for each of the three channels requiring amplification.

The amplifier circuitry for each channel was then built into a case with a 12v power supply and a rectifier circuit to change the AC supply from the 12V transformer into a stable 12v DC supply. This case can be seen in figure A3.2. Additional circuitry for the linear resistive displacement transducer (to measure the distance travelled by the mass) was built into the case and this is discussed further in section A3.4. All three channels that required amplification (ground reaction force, excitement force and distance travelled by mass) were included in the case and each signal was manipulated to give an approximate 0-5v output across its working range. Digital volt meter displays

were built into the lid of the case meaning that each channel could be monitored without the need for a separate voltmeter (visible in figure A3.2).

### **A3.2 Ground Reaction Force Load Cell**

The purpose of this sensor was to define the force applied to the ground plane by the contact point of the foot (i.e. toe area). This could be when the system is static or when the mechanism is being exercised. Therefore this load cell would be able to record the mass applied to the carriage before testing as well as the progression of force into the ground plane up to the maximum value during dynamic loading. As mentioned previously this was a strain-gauge style load cell with a range of 10kN, manufactured by Applied Measurements Ltd. and can be seen in figure A3.3.



**Figure A3.3:** 10kN ground force load cell  
(Applied Measurements Ltd)

## Calibration

The calibration of the ground force load cell was conducted using an Instron 2280 hydraulic test machine. The load cell was placed under the cross-head and

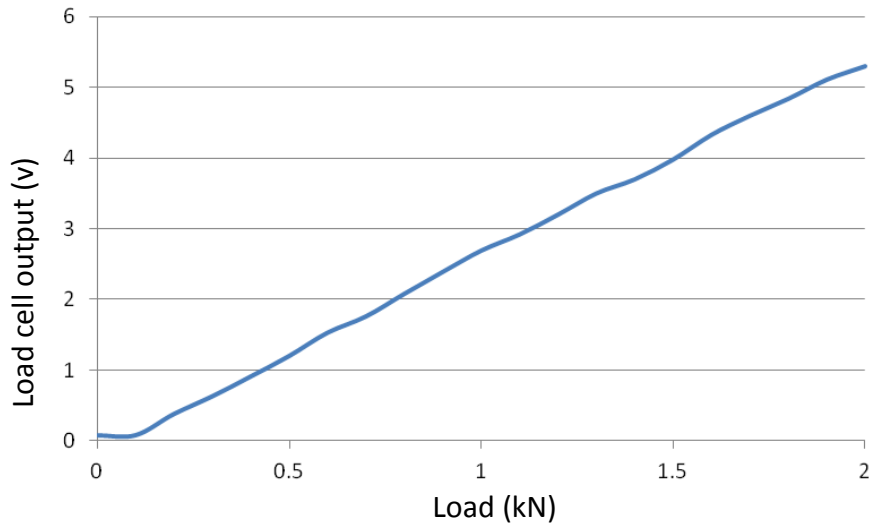


**Figure A3.4:** Calibration curve for ground force load cell

progressively loaded up to a maximum value of 2kN at 0.1kN intervals. The load measurements from the Instron load cell and the voltage output from the load cell under test (post amplification) were recorded and a calibration curve generated. This process was conducted three times and the results averaged. This data can be seen in figure A3.4. A line of best fit was applied to this curve and its equation derived so that any further voltage readings from the load cell could be converted into a value of force.

The load cell chosen uses a strain gauge to measure the ground reaction force. Therefore in terms of deflection, the difference between zero and a maximum load of 10kN is a fraction of 1mm. When attempting to calibrate the load cell using the Instron machine it was necessary to insert a strong spring between the load cell of the test machine and the unit under test (figure A3.5). This spring serves to improve the resolution of the test data dramatically by allowing the load to be progressively increased over a much larger deflection range. Without this spring it proved impossible to control the amplitude of load effectively.



*Figure A3.5: Spring fixture used to amplify the displacement of the Instron crosshead for a given load and therefore improve data resolution*

As can be seen from the curve in figure A3.4 the voltage output from the Applied Measurements Ltd. load cell (post amplification) is very linear. A simple linear line of best-fit was used to generate an equation for this curve, which was subsequently used for converting values of voltage output into that of force. However as is clear from the graph the load cell is inaccurate at low load values. The linearity stops at load values below 0.2kN and therefore any readings in this area should be ignored during the data analysis stages of this investigation.

### A3.3 Excitement Force Load Cell

In order to understand the true efficiency of the system under test the input energy should be defined. In this circumstance input energy means that energy applied to the system in order to build up or maintain the amplitude of the mass carriage and therefore deflection of the foot. As mentioned in section 5.1 the timing of this energy input is critical to the effective harmonic loading and unloading of the foot and therefore a handle was provided for the operator of the rig to use in order to build up the potential energy of the system. This can be seen in figure 5.5.

The amount of force applied to the handle was monitored and logged, again using a strain-gauge load cell and amplifier circuit as described previously. The load cell used was a beam-loading style component, model T66 (100kg variant) manufactured by Thames Side and can be seen in figure A3.6. This style of load cell is commonly found in industrial weighing applications.



**Figure A3.6:** 1kN input force load cell (Thames Side)

The load cell was fixed to the weights carriage of the rig. In order for the force applied to the input handle to be transferred into the load cell, a cantilever arrangement was fabricated as can be seen in figure A3.7. Two cantilever beams were attached to the weigh carriage chassis via bronze bushes at their midpoint. This ensured that no force was applied to the load cell as a result of the carriage accelerating or decelerating and exerting a moment on the cantilever beams. Two beams were used so that they could straddle the A-frame structure that formed the side of the rig. This meant that the input handle could be outside of the framework and therefore keeping the operator away from the moving components of the rig.

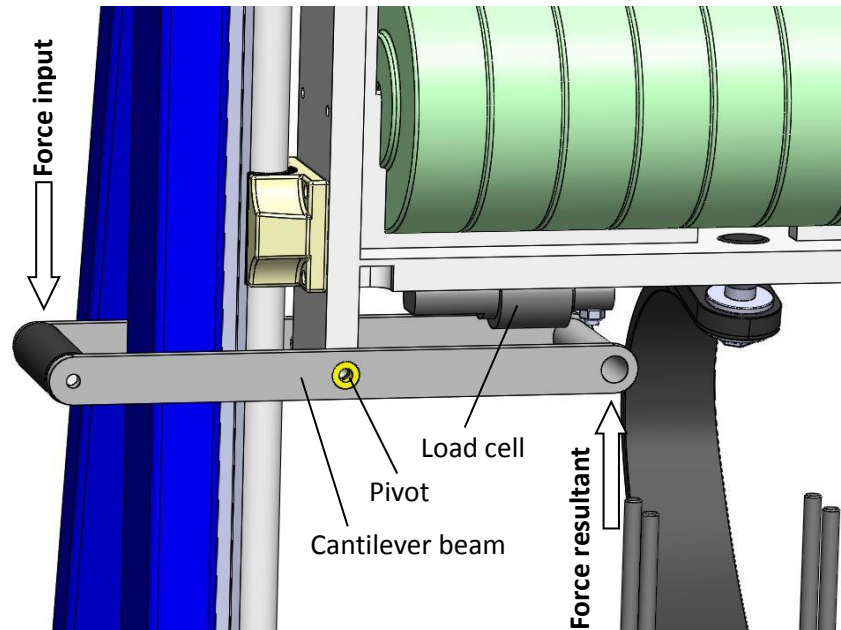


**Figure A3.7:** Detail of the cantilever arrangement that allowed the operator to apply an input force to the mass carriage whilst remaining at a safe distance.

Any force applied to the input handle would result in the same force being applied to the load cell attached to the carriage. In order to eradicate any 'slop' or play in the system, an adjustable stop was fabricated so that no knock would occur when first applying a load to the input handle, but the load cell was left in a completely unloaded state when no force was being applied.

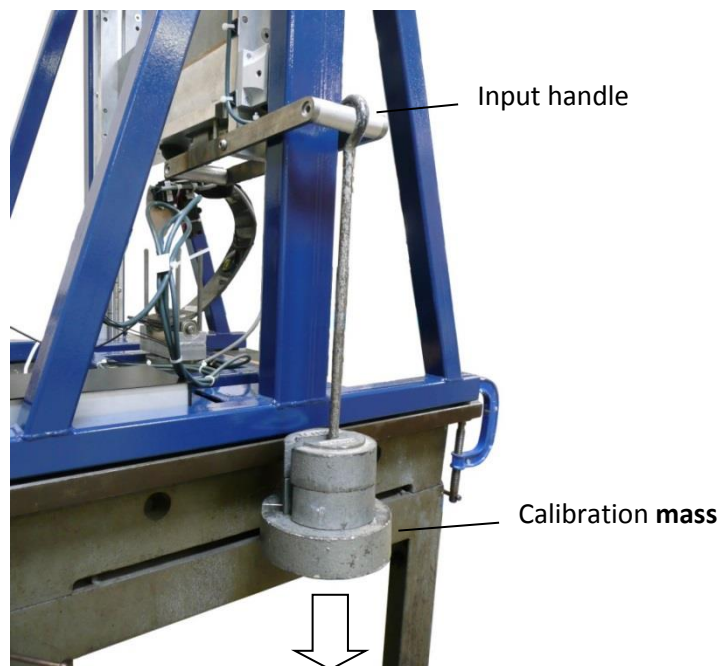


**Figure A3.8:** Illustration of the calibration process used for the excitement force load cell.

## Calibration

Calibration of this piece of instrumentation was conducted by hanging known masses to the input handle (as shown in figure A3.8). As conducted with the ground force load cell, a calibration curve was generated by incrementally increasing the load to the handle and recording the amplified output voltage being supplied to the data logger. In this instance the working range of the load cell was 100kg but it is unlikely that the operator would ever be able to (or need to) apply this much load to the handle. The intended design use of the rig requires only a small amount of effort from the operator in a repetitive harmonic manner to build up the energy stored in the rig, and as such the load cell was only calibrated up to a maximum value of 15kg. The resolution of the amplified output was also modified by adjusting the gain of the amplifier such that the 0 - 5 volt range occurred approximately between 0 - 15 kg. The resulting calibration curve can be seen in figure A3.9.

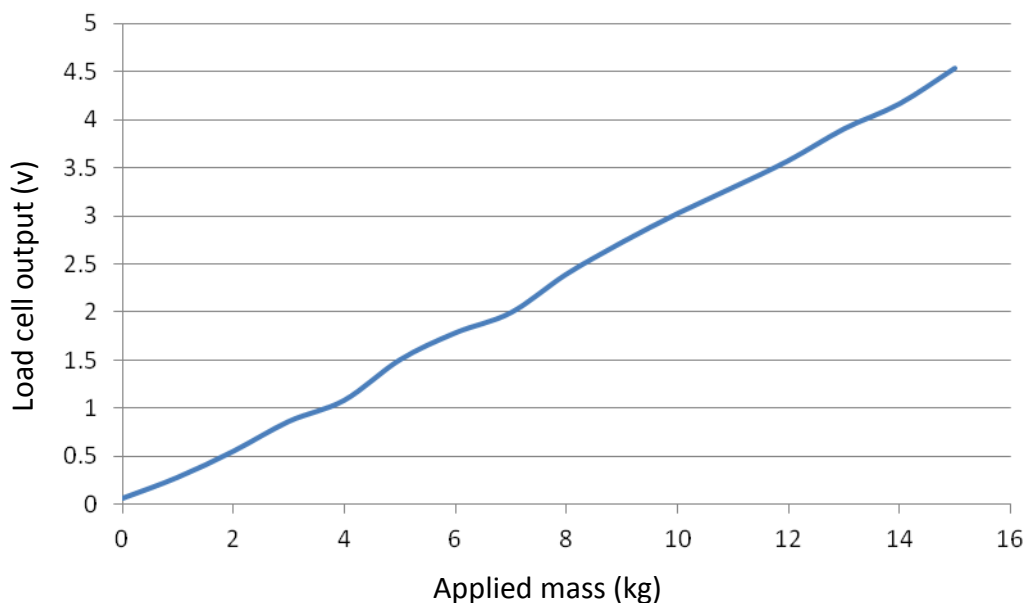


**Figure A3.9:** Calibration curve for input load cell

The output (post amplification) of the input handle load cell is once more quite linear in its characteristic. A line of best fit was applied to this curve and an equation generated that could be applied to any further voltage data collected from this sensor.

### A3.4 Linear Resistive Transducer

This piece of instrumentation was responsible for measuring the linear travel of the carriage and once more a 0-5 volt output was required for logging using the MSR165 data logger. This transducer was designed and built in-house and used the principle of voltage drop along a piece of resistance wire, therefore forming a slide resistor. The length of resistance wire was stretched vertically from the base of the rig to the top of the stanchion on one side with a sprung pickup located on the chassis of the carriage component. Therefore as the carriage moved up and down, the pickup also moved along the length of the resistance wire.

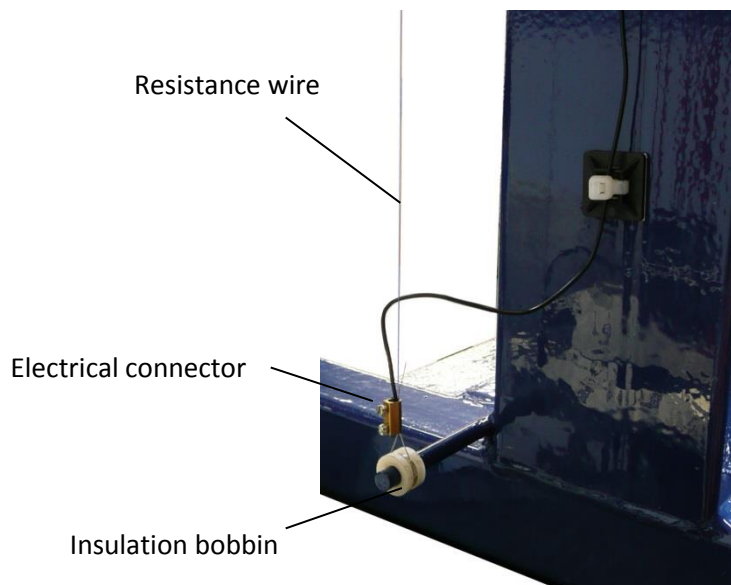


**Figure A3.10:** Illustration showing the length of the resistance wire and nylon insulation bobbin

The wire was tensioned using a spring mounted at the top end and ,as can be seen in figure A3.10, insulated from the framework of the rig using small machined nylon bobbins and connected electrically to the conditioning and amplifier circuits using electrical connector blocks.

Electrically the layout of the slide resistor circuit mimicked that of a Wheatstone Bridge as used in both of the load cells on the rig. However the slide resistor took place of one of the bridge resistors as can be seen in figure A3.11. In order to establish balance in the bridge it was essential that R3 exactly matched the resistance of the slide resistor. Therefore instead of using a proprietary resistor for this component, an identical length of resistance wire to that used in the slide resistor was wound around a nylon bobbin to take the place of R3. The output of this bridge circuit was connected to the input of a third Operational Amplifier circuit as also used with the load cell circuits and as described in section A3.1. The gain of the amplifier could then again be adjusted such that a 0-5 volt occurred across the length of the slide resistor in order to maximise resolution of the transducer.

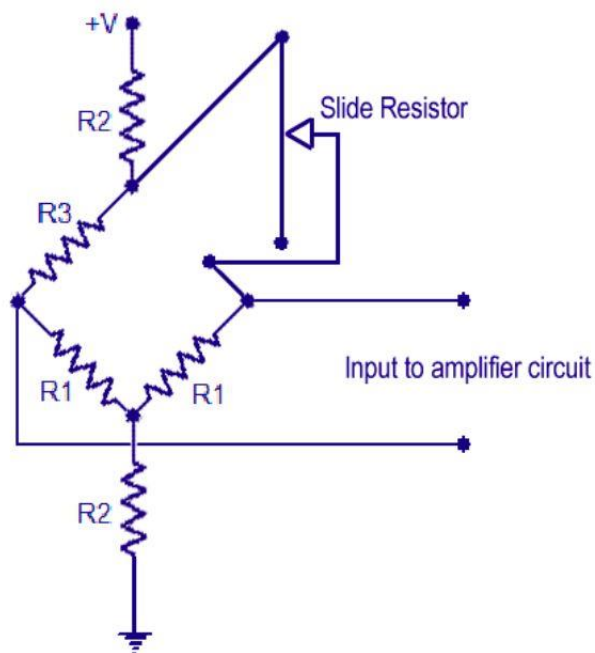


**Figure A3.11:** Slide resistor circuit diagram

## Calibration

Calibration of the linear resistive transducer was performed once the rig was completely assembled. The carriage was exercised along its path of travel and at intervals of 50mm post-amplifier voltage readings were recorded (the voltage that would be seen by the data logger). As previously mentioned the gain of the amplifier was adjusted such that at the extremity of travel the output voltage from the amplifier did not exceed 5 volts. The resulting calibration curve can be seen in figure A3.12.

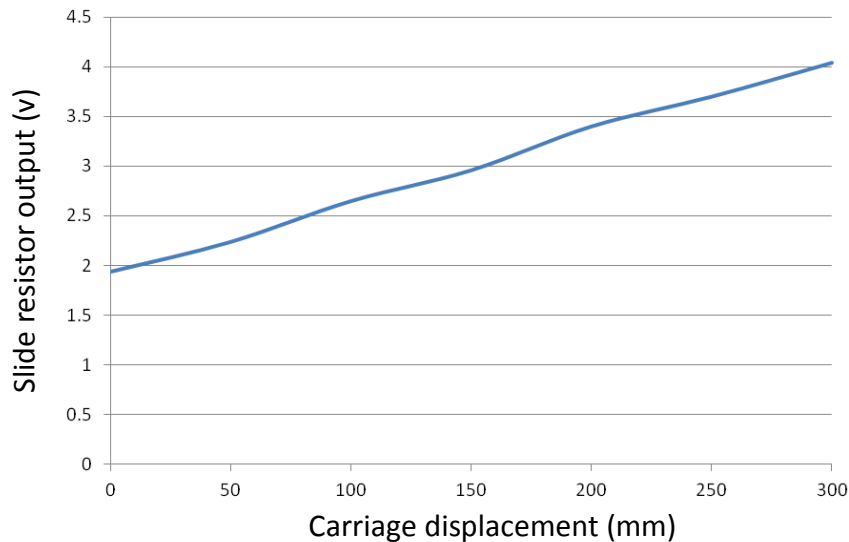


**Figure A3.12:** Calibration curve for slide resistor

As can be seen in figure A3.12, the voltage trace starts at circa 2volts despite the gain of the amplifier being optimised for the working travel of the carriage. This is because of the balance of resistors (R1 vs. R3 in figure A3.11) in the Wheatstone Bridge assembly. If the value of R1 were changed then this could be situation could be improved. However for the purposes of this investigation the calibration resolution was judged as acceptable.

### **A3.5 Displacement of Foot**

As measured previously during the amputee testing phase of this investigation the true displacement of the foot was recorded. This was conducted using the same instrumentation devices as before and details of the setup and calibration can be found in Chapter 4 & Appendix 1.

### **A3.6 Data Logger**

Logging of the data collected from each of the four channels was conducted using an MSR165 data logger from MSR Electronics GmbH. This is the same piece of equipment used to collect data during the amputee data acquisition phase as described in section 4.2.6 and is capable of recording analogue 0-5 volt information at a frequency of up to 1024Hz over four separate channels. As a result of the logger featuring four separate channels, each of the desired variables as set out in section 5.3.3 could be recorded simultaneously.

## **APPENDIX 4: RIG EFFICIENCY**

The efficiency of the rig is important to ascertain before any conclusions are drawn about the dynamic nature of the prosthetic foot on test. As described in Chapter 5 the rig was designed to replicate the mass of an amputee using a vertically sliding carriage with foot mounted on its underside. Rig components are restrained with various devices (for example linear slide rails with re-circulating ball bearings), all of which inevitably subtract from the overall efficiency by means of friction.

This section describes how the efficiency of the rig was measured using three different methods. These are detailed as follows:

**Method 1: Hysteresis curves**

**Method 2: Input energy vs. stored energy**

**Method 3: Carriage amplitude decay**

## **A4.1 Method 1: Hysteresis Curves**

### **Theory**

Using a similar technique to the forced oscillation testing (section 3.4) whereby the efficiency of the Ossur Flex Run foot was found by comparing the compression and rebound phases of a force-displacement curve, the hysteresis of the foot and rig assembly was found.

As described in section 5.3.3 the rig contained the relevant instrumentation to provide a ground reaction force and a value of both foot displacement and mass displacement (meaning the distance travelled by the mass once ground contact with the foot had occurred). Both of these figures were recorded in section 5.4.4 and shown to be nearly identical. Therefore a force-displacement curve can be generated for a typical displacement cycle and the compression and rebound phases overlaid. The area under each of the individual curves demonstrates the energy stored in the foot. The area between the curves (the disparity between the two curves) is a demonstration of energy difference and therefore inefficiency. The hysteresis value (displayed as a percentage) is defined by the following equation:

$$\text{Hysteresis} = \text{Energy input/energy output} \times 100\%$$

## Method

The foot under test (an Ossur Flex Run Cat6Hi) was mounted in the rig as described in section 5.3 and excited vertically using the input handle. The amplitude of displacement was gradually increased by rhythmically applying force to the input handle until the value of foot displacement measured that of a typical amputee (as ascertained in section 4.4). The data logger was activated and a series of 8 oscillation cycles were recorded. These cycles were then averaged into a single typical displacement cycle (shown in figure A4.1) and from this the individual compression and rebound phases were isolated.

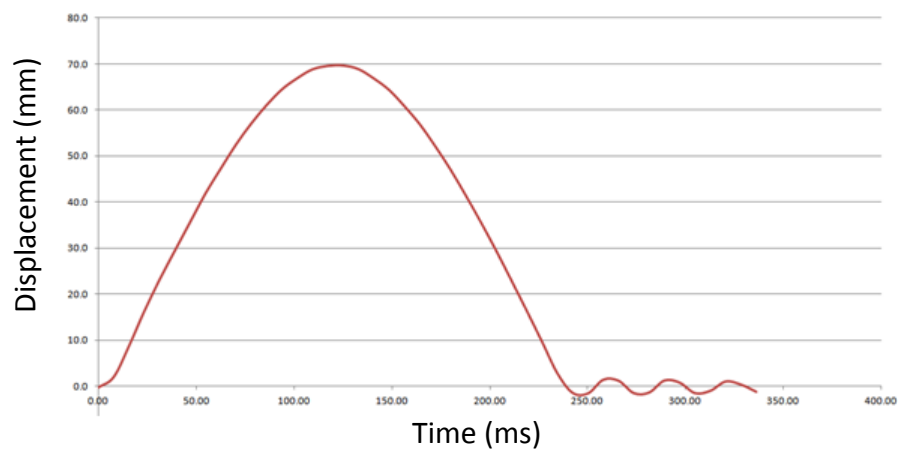


**Figure A4.1:** Averaged displacement data from a series of 8 oscillation cycles

Figure A4.2 show the resulting hysteresis loop when the compression and rebound phases are plotted together on the same force-displacement curve. The area under the curve represents the energy of the system and the shading represents this area for each isolated phase.

It can be seen that the force exerted to the ground plane by the foot on test during the rebound phase of the cycle was greater at any given point than during the compression cycle. Therefore the rig must exhibit an efficiency of <100%.

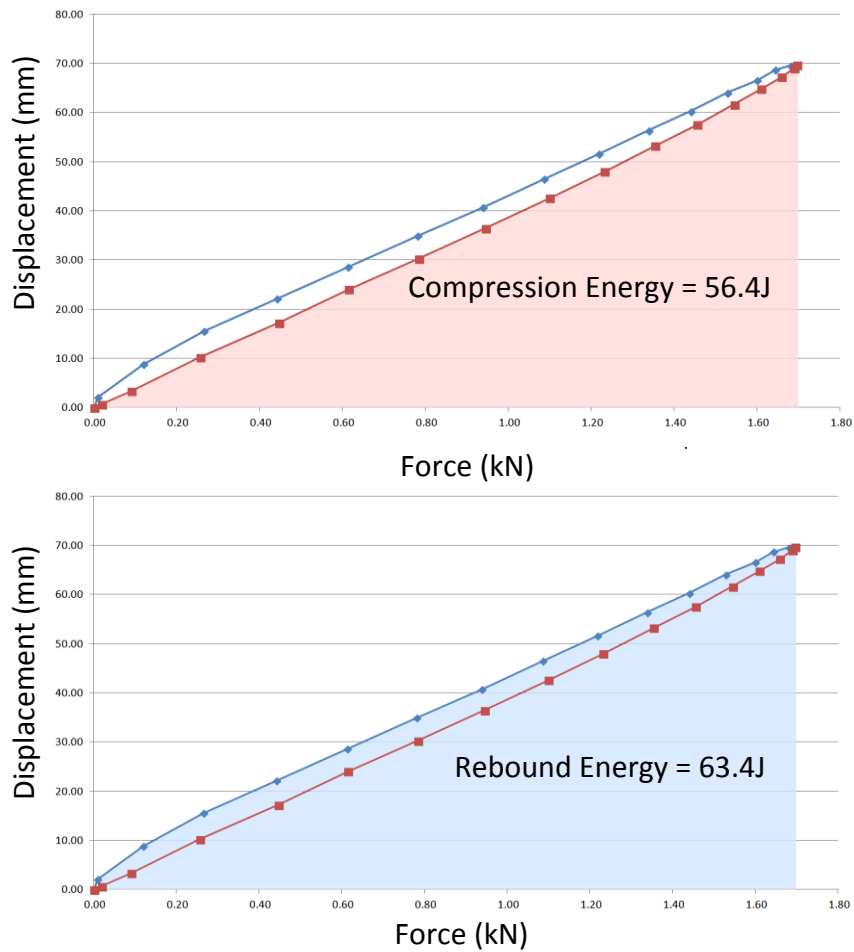


**Figure A4.2:** Rig hysteresis for a typical averaged displacement cycle (representing one single stance phase of an amputee).

The respective areas under the curves were calculated by dividing the curve into a number of segments and assuming a straight line between the associated points. Then using the equation described above, the efficiency of the rig using this method was ascertained.

**Results:**

Using this method, the efficiency of the rig can be defined as:

$$\text{Efficiency} = \frac{\text{compression energy}}{\text{rebound energy}} \times 100$$

Therefore:

$$\frac{56.4 \text{ J}}{63.4 \text{ J}} \times 100 = 88.9\%$$

## A4.2 Method 2: Input Energy vs. Stored Energy

### Theory

The rig as described in section 5.3 features an input handle with which the user can excite the mass vertically, building up the amplitude of oscillation. This handle is attached to a calibrated load cell and in turn a data logger, meaning that any force input applied to the handle can be recorded in Newtons. The recorded input force trace for a typical oscillation sequence of an Ossur Flex Run foot can be seen in figure A4.3, shown in red along with the amplitude of foot displacement in blue.

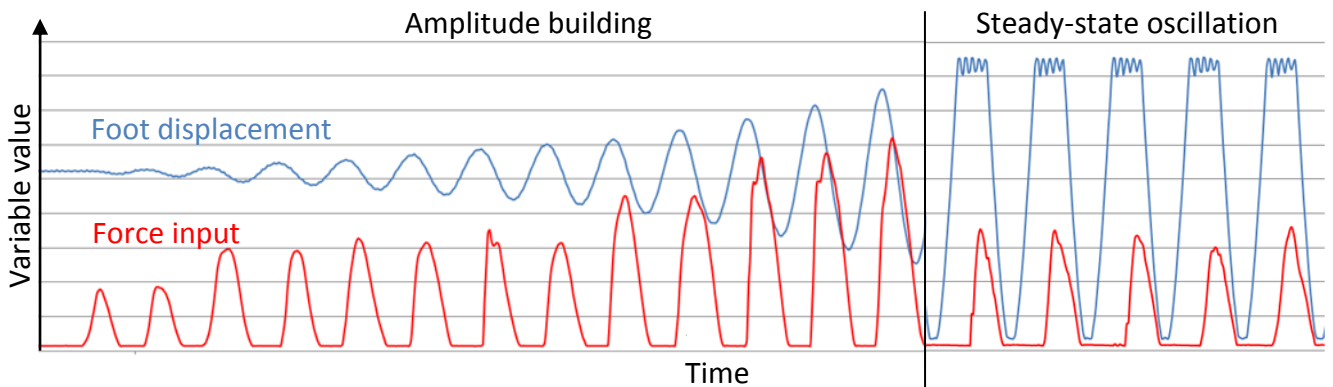


**Figure A4.3:** Graph demonstrating the input force required to build-up the amplitude of oscillation of a prosthetic foot mounted on the test rig, compared with that required to maintain steady-state amplitude oscillation.

If all losses were ignored, once the foot was excited to a certain value of displacement no additional energy input would be required to maintain the amplitude of oscillation and resonant steady-state motion would continue forever. However, because the rig exhibits losses (by the way of noise and heat generation) in order for steady-state oscillation to be maintained a certain amount of force must continue to be applied to the system in a resonant manner. Fundamentally if less force than this baseline level is applied, the amplitude of oscillation will reduce. Conversely if a greater force is applied the amplitude will increase. This is demonstrated in figure A4.3 where it can be seen that the energy input required to increase the amplitude of oscillation is greater than that required to maintain it.

During steady-state oscillation the system is known to possess stored energy, either in spring energy when at full compression, gravitational potential energy when at full rebound or kinetic energy during transition between these phases. If the energy required to maintain steady-state oscillation (through a force being applied to the input handle) is compared with this system energy the efficiency of the rig can be calculated.

**Method:**

Energy can be defined by the following equation:

$$\text{Energy (J)} = \text{Force (N)} \times \text{distance (m)}$$

Using this equation, both the energy stored in the system and that applied to the handle can be defined as follows:

$$\text{Energy in system} = \frac{(\text{max. GRF} - \text{nominal GRF}) \times (\text{max. displacement} - \text{nominal displacement})}{2}$$

Where:

**GRF** = Ground Reaction Force

**Nominal displacement** = Amplitude of displacement when the foot is statically loaded and no vertical motion is occurring.

**Nominal GRF** = Ground Reaction Force at nominal displacement. I.e.

The denominator is required because otherwise this equation assumes the maximum load is applied throughout the entire displacement of the foot. By halving the result, a straight line between nominal position and maximum load & deflection is assumed. This method therefore assumes a linear force-displacement curve of the foot and therefore a linear spring rate.

**It is important to subtract the nominal values for GRF and displacement because it is at this position that the foot on test finds equilibrium; that is when the force exerted by the mass is equally opposed by the reaction of the foot. To ignore this would be to count energy twice.**

Energy input through handle = handle force x displacement of foot during handle input

Where:

**Handle force** = force applied to the input handle

**Displacement of foot during handle input** = the effective distance travelled by this input force

In order to ensure comparable results, the data gathered during 'Method 1' above was used for this test. As described previously, 8 oscillation cycles were captured and averaged in order to provide a single 'typical' dataset for analysis. The logger used for this investigation was capable of capturing all four rig channels concurrently, namely Ground Reaction Force, Input Handle Force, Carriage Displacement and Foot Displacement. More information on the logger and rig equipment can be found in appendix 1.

**Results:**

Using this method, the efficiency of the rig can be defined as:

$$\text{Efficiency} = 100 - \left( \frac{\text{energy input through handle}}{\text{energy in system}} \times 100 \right)$$

Therefore:

$$\text{Efficiency} = 100 - \left( \frac{22.19 \text{ N} \times 0.08072 \text{ m}}{\frac{(1701 \text{ N} - 814 \text{ N}) \times (0.0697 \text{ m} - 0.028 \text{ m})}{2}} \times 100 \right)$$

Therefore:

$$\text{Efficiency} = 100 - \left( \frac{1.79 \text{ J}}{18.49 \text{ J}} \times 100 \right) = 90.3\%$$

### **A4.3 Method 3: Carriage Amplitude Decay**

#### **Theory:**

It is shown in figure A4.3 that a certain amount of energy is required to maintain the amplitude of displacement of the foot on the rig. Assuming constant amplitude of displacement, this amount of input energy must be equal to the energy lost in the system for each individual displacement cycle. If the input energy ceases, the losses in the system will result in a progressive and gradual decay in foot displacement, until the system once again returns to rest.

With each successive displacement cycle (once the input energy has been removed) the change in displacement amplitude can be quantified using the calibrated foot displacement sensor. Although this reduction of displacement is relatively unimportant when calculating the efficiency of the rig, the energy loss that it represents is fundamental.

If the energy lost as a result of the reduction in displacement for a single oscillation cycle were compared with the overall energy stored in the system at that time, this would allow the efficiency of the rig to be calculated.

#### **Method:**

The foot was excited in the manner described for methods 1 & 2 until the amplitude representative of the amputee testing (section 4.4) was replicated. Data logging was initiated and force input to the excitation handle was removed, allowing the amplitude of oscillation to decay until the weights carriage came to rest. Logging was then halted and the obtained traces could be examined.

**Results:**

Figure A4.4 shows the trace of foot displacement against time for the rig from the moment the input force was removed. As can be seen, the displacement progressively decays until the carriage comes to rest.

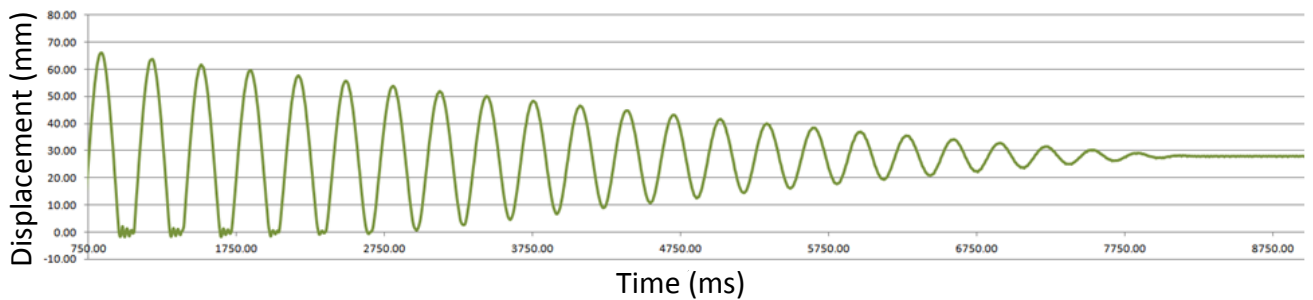


**Figure A4.4:** Graph showing the displacement amplitude of the prosthetic foot on test, demonstrating the progressive decay of foot displacement once the input force is removed

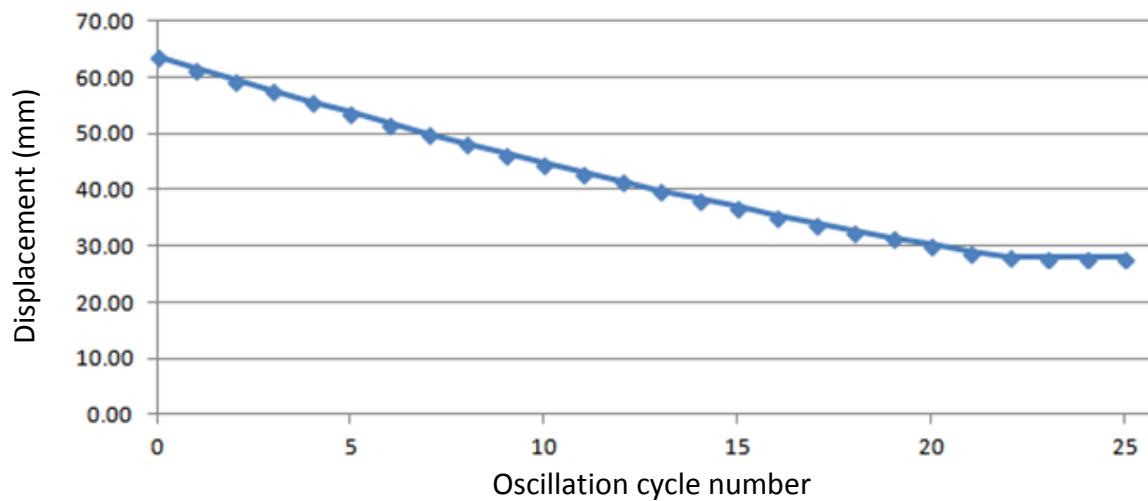


**Figure A4.5:** Graph showing the peak amplitude of successive oscillation cycles following the removal of input force to the rig.

The displacement value of each peak from this graph was extracted and plotted against the number of oscillations following the removal of the input force (figure A4.5).

The foot can be seen to come to rest at a displacement value of 28mm. This is the value of static deflection of the foot under the load of the carriage.

Knowing the total displacement (above nominal value as discussed during Method 2) and the maximum force at maximum displacement, the energy represented by these peaks of amplitude could also be plotted as shown in figure A4.6.

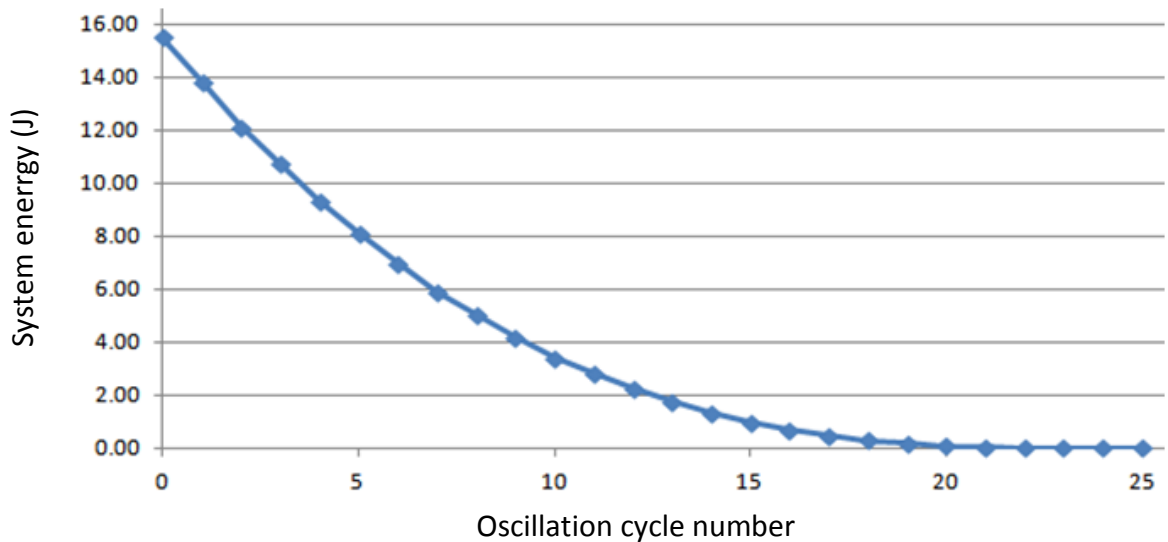


**Figure A4.6:** Graph showing the energy stored in the system, decaying with each successive oscillation cycle.

Following from this, the change in stored energy for each successive oscillation cycle was determined and expressed as a percentage of the remaining (residual) stored energy in the system (figure A4.7)

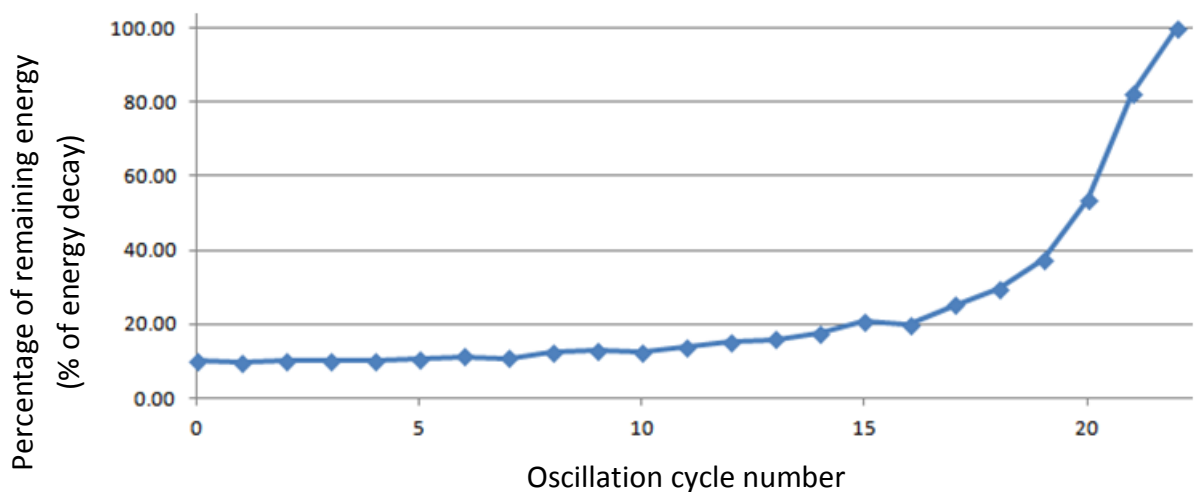


**Figure A4.7:** Graph showing the change in energy for successive oscillation cycles expressed as a percentage of the residual system energy

From this information it was then possible to produce a graph showing the percentage of energy lost (at each oscillation cycle) for a value of maximum displacement. This results in a measure of system inefficiency (importantly this is a value of inefficiency; to calculate efficiency this number should be subtracted from 100%) at any specific value of maximum deflection. This is illustrated in figure A4.8.

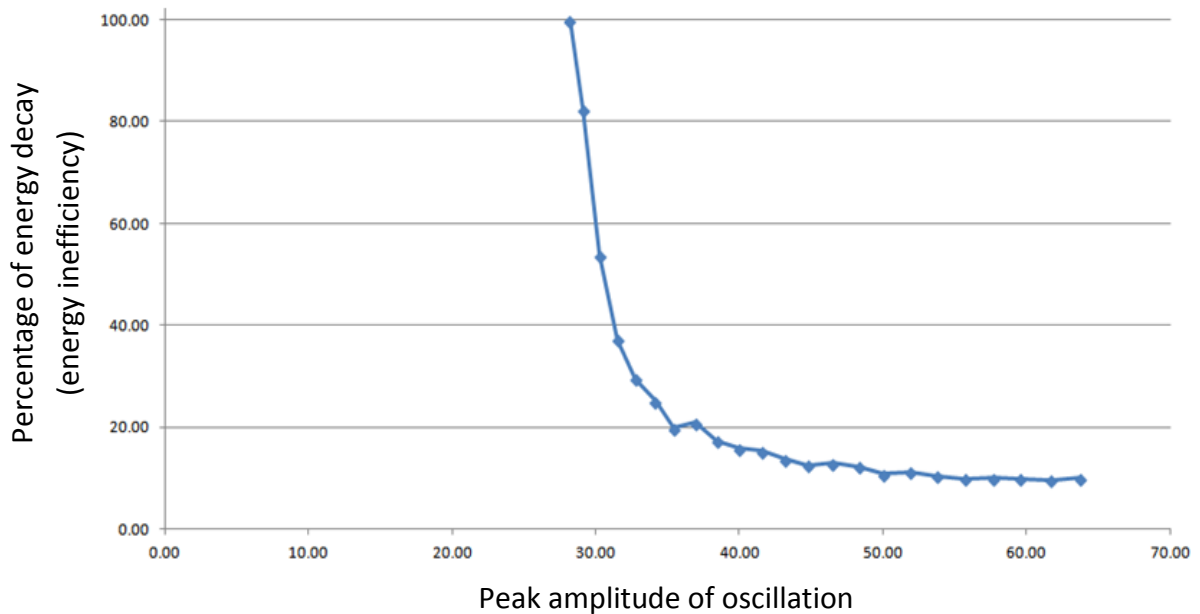


**Figure A4.8:** Graph showing the energy decay (expressed as a percentage of residual system energy) against the value of maximum displacement.

As can be seen in figure A4.8 the efficiency of the system decreases exponentially as the amplitude of oscillation approaches that of the nominal foot displacement. It is at nominal foot displacement that the force exerted by the mass and the force exerted by the reaction of the spring are equal and opposite. This occurs at a displacement of 28mm for this specific foot with 83kg mass (as were the set up conditions for this investigation). As the amplitude of displacement increases it can be seen that the efficiency of the system improves, levelling off at approximately 55mm. Above this displacement the inefficiency can be seen as constant, at a value of 10.1%. For the purpose of this investigation and to ensure comparable results with the previous two methods, it is at this maximum value of foot displacement that the efficiency should be defined.

#### A4.4 Rig Efficiency Conclusions

Despite using three different techniques to determine the efficiency of the rig system, the resulting figures are similar with a standard deviation of 0.8%. The three figures were averaged to provide a final value of efficiency (table A4.1).

Method 1: 88.9%	}	<b>Mean value = 89.4%</b>
Method 2: 90.3%		
Method 3: 88.9%		

**Table A4.1:** Results of the three separate methods for determining rig efficiency

It is important to remember throughout this investigation that the figures generated represent the efficiency of the system as a whole. This does not mean the efficiency of the foot or that of the rig, but both together when combined to make the 'system'. Inevitably if any aspect of this system were to change, this value of efficiency would be invalid. This includes using a different prosthetic foot or changing the mass applied to the carriage. Another example of how the changing conditions might affect the result is if a different displacement were achieved. It is demonstrated in figure A4.8 (under Method 3) that the maximum displacement alters the efficiency significantly, particularly at lower amplitudes. Above 55mm total displacement the trace can be seen to stabilise at 10.1%.

### **A note on energy storage**

Throughout this section, reference has been made to 'energy storage'. In Method 1, force-displacement graphs were generated for both the compression and rebound phases of the oscillation cycle with the areas under these graphs being calculated and compared to derive efficiency. In Method 2 the energy in the system was calculated and compared with the energy known to have been applied through the input handle, and Method 3 uses the principle of energy decay versus residual stored energy. If the figures for energy storage are compared however, they can be seen as an order of magnitude different.

**Energy storage in Method 1 = 56.4J (compression), 63.4J (rebound)**

**Energy storage in Method 2 = 18.49J**

**Energy storage in Method 3 = 15.5J**

The reason for this is that they are not measuring the same energy storage and therefore cannot be compared with one another. This is explained as follows:

**Method 1** relies on a value of energy storage to define the efficiency of the rig. Because this is undertaken using a force-displacement curve derived from foot displacement, the entire displacement cycle is used for both compression and rebound phases (i.e. the full displacement from 0mm up to a value of 70mm). The areas under the respective curves provide a value of energy storage, but this is energy storage in the foot, not the rig. If the foot were viewed as a standalone piece of apparatus, energy storage begins at 0mm displacement until it is fully loaded. However if the rig as a system is viewed, the mass under gravity exerts a force on the foot that is only equalled by the foot reaction at the 'nominal' height. This is shown to be at 28mm deflection and at this point, assuming no movement of the carriage, the rig is in equilibrium. No energy is stored within the rig system. However a significant amount of energy at this moment is stored in the foot when viewed alone. Because of this, the value of energy storage provided in Method 1 is inaccurate and artificially high if viewed as 'system energy storage'.

**Method 2** provides a more accurate account of true 'system' energy. The fundamental step taken to ensure this is to subtract the values of displacement and force found at the nominal position from those found at the maximum position. As explained above, useful energy storage does not begin to accumulate in the rig until the nominal displacement of 28mm has been surpassed. In doing this, the value for energy storage can be seen as significantly lower than that of Method 1 but this is a true value of system energy, not stored foot energy. This is illustrated in figure A4.9.

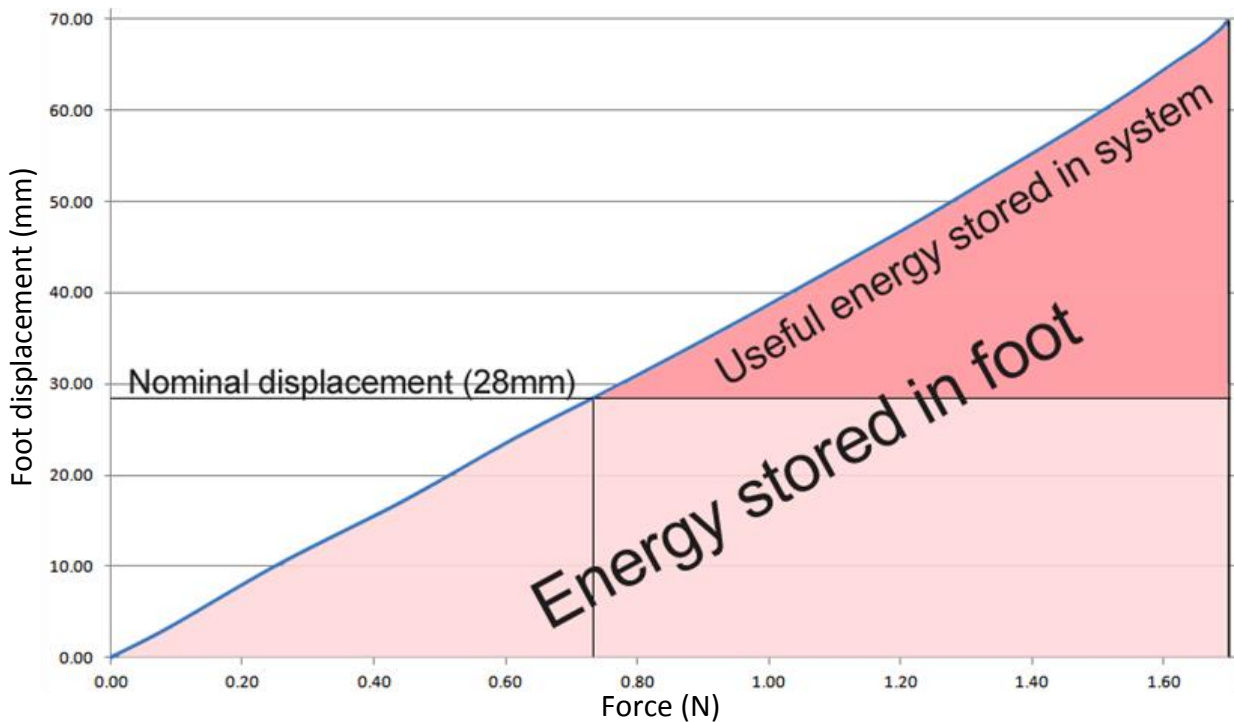


**Figure A4.9:** Graph illustrating the difference between energy stored in the foot and energy stored in the rig as a system

As can be seen in figure A4.9 if energy is considered to be stored (as it is by the standalone foot) from 0mm displacement up to the maximum displacement (in this case at 70mm), the value can be described as the area under the entire curve. However if the entire system is considered and equilibrium is achieved at a nominal height of 28mm (this is when the force exerted by the mass is equalled by the reaction force of the foot), useful energy storage only begins at this displacement value. This is represented by the darker shaded area of the graph and is a significantly smaller portion of the graph. This is the reason for the difference in measured energy storage between Method 1 and Method 2.

**Method 3** boasts a smaller value of stored energy purely because the first reading taken during this particular investigation was the first displacement cycle following the removal of the input force. This means the displacement of oscillation had already decayed for a single cycle before the measurements were considered. The maximum displacement used for Methods 1 & 2 was 70mm versus a value of 64mm for Method 3.

If a value of useful energy storage were to be defined by this investigation, the value obtained in Method 2 should be considered the most accurate and representative of the amputee testing of Chapter 4. This method uses the correct maximum displacement of 70mm but also considers the effect of the nominal height and nominal forcing levels.

## APPENDIX 5: VIDEO-BASED MEASUREMENT ACCURACY & REPEATABILITY

### A5.1 Stance length intra-rater reliability investigation

In order to generate stance length values for an amputee running at speed, high speed video was recorded in the sagittal plane at a variety of speeds on a treadmill. This required the interrogation of the video and specifically the positional relationship of visible markers to a matched pair of measuring reference tapes. Lines of effective heelstrike and toe-off positions are superimposed onto the video and the stance length can be read. This investigation is detailed in section 7.3.

In order to ensure accuracy and repeatability of this captured data an intra-rater reliability exercise was conducted. This involved making observations of a single running velocity ( $13\text{kph}^{-1}$ ) in an identical manner on ten independent occasions. The results gathered can then be compared and the variation objectively defined.

Table A5.1 displays the results of this comparison below.

Measurement #	Stance length observed (mm)	Rounded result to nearest whole cm (mm)
1	668	670
2	668	670
3	666	670
4	671	670
5	670	670
6	671	670
7	669	670
8	672	670
9	669	670
10	673	670
Mean	669.7	670
Standard Deviation	2.0	0

*Table A5.1: Intra-rater reliability data from ten independent stance length observations of the same single stride video.*

## A5.2 Deflection sensor vs. frame rate timing methods

During the amputee testing phase of this investigation both high speed video (1500fps) and foot deflection (at 512Hz) were recorded simultaneously. Both were deemed of a sufficiently high resolution to record the necessary data, and both were capable of providing timing information about the stride being recorded. For the purpose of defining stance and stride phase timing (as displayed in Table 7.1) the deflection transducer was used. However to ensure accuracy and rule out anomalies that might have occurred during interrogation of the data the same timing information was obtained using the video footage. At 1500fps each frame represents the passage of 0.667ms. Therefore by counting the number of frames between heel strike and toe-off events the stance phase timing can be ascertained and compared, as displayed in Table A5.2 (to the nearest ms).

<b>Velocity kmh</b>	<b>Velocity m/s</b>	<b>Stance timing (ms) Deflection sensor</b>	<b>Stance timing (ms) Video frames</b>
<b>8</b>	2.2	275	274
<b>9</b>	2.5	260	260
<b>10</b>	2.8	246	246
<b>11</b>	3.1	232	232
<b>12</b>	3.3	227	226
<b>13</b>	3.6	217	216
<b>14</b>	3.9	209	208
<b>15</b>	4.2	203	202
<b>16</b>	4.4	197	197
<b>17</b>	4.7	193	193
<b>18</b>	5.0	182	182
<b>Mean</b>	-	221.9	221.5
<b>Standard Deviation</b>	-	29.3	29.2

**Table A5.2:** Comparison of measured stance phase timing as recorded by the deflection sensor (512Hz) and high speed video (1500fps)

A logging frequency of 512Hz (deflection sensor) can provide timing accurate to approximately +/-1ms whereas the video is capable of defining an accuracy almost three times greater. As such there is an excellent correlation in the data. If an unpaired t-test statistical analysis is carried out on this data (using the mean and SD values as quoted in Table A5.2) a P-value of 0.9713 is generated. This is regarded as statistically insignificant.

## APPENDIX 6: ISPO JOURNAL PUBLICATION ABSTRACT

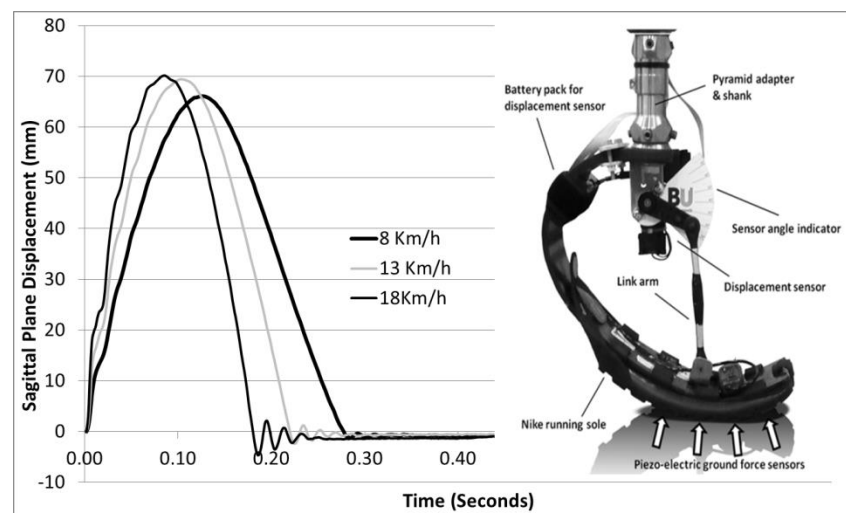
**Title:** An Investigation of the Ground Contact Point and Sagittal Plane Displacement of Energy Storage and Return (ESR) Composite Lower-Limb Prosthetic Feet during Running

**Background:** Energy storage and return (ESR) feet are designed for active amputees [1]. Their design appears to be carried out on a trial and error basis [2]. It has also been recognised there is little compelling scientific evidence to guide the clinical prescription of ESRs [3].

**Aim:** The aim of this study is to provide insight into the dynamic behaviour of ESR prosthetic feet by investigating the effect of increased velocity on the ground contact point and foot displacement.

**Method:** Sagittal plane displacement (utilising a displacement sensor attached between the proximal and distal end of the foot) and ground contact point (utilising a linear array of four piezo-electric ground force sensors on the metatarsal region) were recorded from an Ossur Flex-Run ESR foot attached to a highly active unilateral transtibial amputee while carrying out a series of running trials.

The data collected was analysed to provide information on and relationships between: stride cadence; ground contact time; swing phase time; timing and amplitude of maximum displacement; progression of the ground contact point.



**Results:** The figure shows the average sagittal plane displacement from ten full strides of the Flex-Run foot while the amputee ran at velocities of  $8\text{kmh}^{-1}$ ,  $13\text{kmh}^{-1}$  and  $18\text{kmh}^{-1}$  on a treadmill. These results show that maximum deflection of the foot increased minimally as the running velocity increased from 8 and  $18\text{kmh}^{-1}$ . In addition, ground contact time ( $280\text{ms}@8\text{kmh}^{-1}$  vs.  $180\text{ms}@18\text{kmh}^{-1}$ ) and stride time

(750ms@8kmh<sup>-1</sup> vs. 560ms@18kmh<sup>-1</sup>) were found to decrease. An increase of force at sensor 4 (the posterior sensor) was found as the running velocity increased; indicating that the ground contact point of the foot progressed towards the rear of the foot at increased velocity.

**Discussion & Conclusion:** Previous studies have assumed that a prosthetic foot and amputee forms a spring/mass system and therefore the ground contact duration at different running velocities should be comparable. This research concludes that ground contact duration decreases at increased velocity. This has been found to be due to the measured shift in ground contact point rearwards along the metatarsal region at heel-strike stiffening the foot spring rate, resulting in a shorter stride duration. Further research is now needed to generalise the relationship between the key variables to provide quantitative data to inform ESR foot prescription.

**References:**

- [1] Kobayashi, T. et al.; 2014; Clin. Biomech.
- [2] Strike, S. et al.; 2000; Proc. Inst. Mech. Eng. H J. Eng.
- [3] Hafner, B. et al.; 2011; J. Rehabil. Res. Dev.

# Research Ethics Checklist

Reference Id	4731
Status	Submitted

## Researcher Details

Name	James Hawkins
School	Faculty of Science & Technology
Status	Postgraduate Research (PhD, MPhil, DProf, DEng)
Course	Postgraduate Research
Have you received external funding to support this research project?	No

## Project Details

Title	Prosthetic ESR running foot observation
Proposed Start Date	20/08/2014
Proposed End Date	21/08/2014

Summary (including detail on background methodology, sample, outcomes, etc.)
--

A suite of testing is planned in a laboratory environment to characterise various prosthetic feet on dynamic test machines. No ethics approval is required for this stage. However in order to establish the test conditions, the action of one of these feet has to be measured using a human amputee volunteer. The foot under test is a standard proprietary 'off-the-shelf' item available from Ossur of Iceland and is the same model as is already used by the amputee volunteer. The testing shall require the foot that is already being used by the amputee to be replaced by a new item of the same model and variant for the duration of testing. This ensures that the foot is in a known condition and results are not affected by any use or misuse that the amputee's foot might have been subjected to in the past. Any work or adjustment/alignment on the prosthetic device of the amputee shall be carried out by a practicing, registered and qualified prosthetist who is familiar with this style of prosthetic device. Following testing the prosthetic device of the amputee shall be returned to an identical condition to that observed prior to testing commencing. Throughout the duration of the test work the amputee shall be asked to exercise as they would as part of their daily regime and no special activities are to be requested that the amputee would otherwise not already be doing. Some small and lightweight instrumentation is to be added to the prosthetic device for the purpose of monitoring the activity of the foot. This instrumentation has been designed to be unnoticed by the amputee during use and is purely for observation. It cannot significantly affect the operation of the prosthetic device in any way. The instrumentation will measure the deflection of the foot with a displacement transducer and the ground force with a series of paper-thin pressure sensors located under the toe of the foot. Once a short suite of testing with the amputee volunteer has been conducted, values obtained can be used as typical and representative data such that the testing machines in the laboratory can be programmed with reliable figures.

## External Ethics Review

<b>Does your research require external review through the NHS National Research Ethics Service (NRES) or through another external Ethics Committee?</b>	No
---	----

## Research Literature

<b>Is your research solely literature based?</b>	No
--	----

## Human Participants

<b>Will your research project involve interaction with human participants as primary sources of data (e.g. interview, observation, original survey)?</b>	Yes
<b>Does your research specifically involve participants who are considered vulnerable (i.e. children, those with cognitive impairment, those in unequal relationships—such as your own students, prison inmates, etc.)?</b>	No
<b>Does the study involve participants age 16 or over who are unable to give informed consent (i.e. people with learning disabilities)? NOTE: All research that falls under the auspices of the Mental Capacity Act 2005 must be reviewed by NHS NRES.</b>	No
<b>Will the study require the co-operation of a gatekeeper for initial access to the groups or individuals to be recruited? (i.e. students at school, members of self-help group, residents of Nursing home?)</b>	No

Will it be necessary for participants to take part in your study without their knowledge and consent at the time (i.e. covert observation of people in non-public places)?	No
Will the study involve discussion of sensitive topics (i.e. sexual activity, drug use, criminal activity)?	No

Are drugs, placebos or other substances (i.e. food substances, vitamins) to be administered to the study participants or will the study involve invasive, intrusive or potentially harmful procedures of any kind?	No
--	----

Will tissue samples (including blood) be obtained from participants? Note: If the answer to this question is 'yes' you will need to be aware of obligations under the Human Tissue Act 2004.	No
--	----

Could your research induce psychological stress or anxiety, cause harm or have negative consequences for the participant or researcher (beyond the risks encountered in normal life)?	No
Will your research involve prolonged or repetitive testing?	No
Will the research involve the collection of audio materials?	No
Will your research involve the collection of photographic or video materials?	Yes
Will financial or other inducements (other than reasonable expenses and compensation for time) be offered to participants?	No

<p>Please explain below why your research project involves the above mentioned criteria (be sure to explain why the sensitive criterion is essential to your project's success). Give a summary of the ethical issues and any action that will be taken to address these. Explain how you will obtain informed consent (and from whom) and how you will inform the participant(s) about the research project (i.e. participant information sheet). A sample consent form and participant information sheet can be found on the Research Ethics website.</p>
<p>Photographic evidence of the set-up conditions are required to ensure repeatability should the test have to be conducted again. Consent shall be obtained from the volunteer on the day and the identity of the volunteer shall be omitted from all material used.</p>

## Final Review

Will you have access to personal data that allows you to identify individuals OR access to confidential corporate or company data (that is not covered by confidentiality terms within an agreement or by a separate confidentiality agreement)?	No
Will your research involve experimentation on any of the following: animals, animal tissue, genetically modified organisms?	No

Will your research take place outside the UK (including any and all stages of research: collection, storage, analysis, etc.)?	No
---	----

Please use the below text box to highlight any other ethical concerns or risks that may arise during your research that have not been covered in this form.

# Research Ethics Checklist

Reference Id	5172
Status	Approved
Date Approved	17/10/2014

## Researcher Details

Name	James Hawkins
School	Faculty of Science & Technology
Status	Postgraduate Research (PhD, MPhil, DProf, DEng)
Course	Postgraduate Research
Have you received external funding to support this research project?	No

## Project Details

Title	Prosthetic ESR running foot observation (further work)
Proposed Start Date	20/10/2014
Proposed End Date	20/10/2014

Summary (including detail on background methodology, sample, outcomes, etc.)
--

A suite of testing is planned in a laboratory environment to characterise various prosthetic feet on dynamic test machines. No ethics approval is required for this stage. However in order to establish the test conditions, the action of one of these feet has to be measured using a human amputee volunteer. The foot under test is a standard proprietary 'off-the-shelf' item available from Ossur of Iceland and is the same model as is already used by the amputee volunteer. The testing shall require the foot that is already being used by the amputee to be replaced by a new item of the same model and variant for the duration of testing. This ensures that the foot is in a known condition and results are not affected by any use or misuse that the amputee's foot might have been subjected to in the past. Any work or adjustment/alignment on the prosthetic device of the amputee shall be carried out by a practicing, registered and qualified prosthetist who is familiar with this style of prosthetic device. Following testing the prosthetic device of the amputee shall be returned to an identical condition to that observed prior to testing commencing. Throughout the duration of the test work the amputee shall be asked to exercise as they would as part of their daily regime and no special activities are to be requested that the amputee would otherwise not already be doing. Some small and lightweight instrumentation is to be added to the prosthetic device for the purpose of monitoring the activity of the foot. This instrumentation has been designed to be unnoticed by the amputee during use and is purely for observation. It cannot significantly affect the operation of the prosthetic device in any way. The instrumentation will measure the deflection of the foot with a displacement transducer and the ground force with a series of paper-thin pressure sensors located under the toe of the foot. Once a short suite of testing with the amputee volunteer has been conducted, values obtained can be used as typical and representative data such that the testing machines in the laboratory can be programmed with reliable figures. This work forms an extension to testing that was carried out in September 2014. Some of the earlier work is to be repeated whilst being filmed with an ultra high-speed camera to observe some measured anomalies.

## External Ethics Review

<b>Does your research require external review through the NHS National Research Ethics Service (NRES) or through another external Ethics Committee?</b>	No
---	----

## Research Literature

<b>Is your research solely literature based?</b>	No
--	----

## Human Participants

<b>Will your research project involve interaction with human participants as primary sources of data (e.g. interview, observation, original survey)?</b>	Yes
<b>Does your research specifically involve participants who are considered vulnerable (i.e. children, those with cognitive impairment, those in unequal relationships—such as your own students, prison inmates, etc.)?</b>	No
<b>Does the study involve participants age 16 or over who are unable to give informed consent (i.e. people with learning disabilities)? NOTE: All research that falls under the auspices of the Mental Capacity Act 2005 must be reviewed by NHS NRES.</b>	No
<b>Will the study require the co-operation of a gatekeeper for initial access to the groups or individuals to be recruited? (i.e. students at school, members of self-help group, residents of Nursing home?)</b>	No

Will it be necessary for participants to take part in your study without their knowledge and consent at the time (i.e. covert observation of people in non-public places)?	No
Will the study involve discussion of sensitive topics (i.e. sexual activity, drug use, criminal activity)?	No

Are drugs, placebos or other substances (i.e. food substances, vitamins) to be administered to the study participants or will the study involve invasive, intrusive or potentially harmful procedures of any kind?	No
--	----

Will tissue samples (including blood) be obtained from participants? Note: If the answer to this question is 'yes' you will need to be aware of obligations under the Human Tissue Act 2004.	No
--	----

Could your research induce psychological stress or anxiety, cause harm or have negative consequences for the participant or researcher (beyond the risks encountered in normal life)?	No
Will your research involve prolonged or repetitive testing?	No
Will the research involve the collection of audio materials?	No
Will your research involve the collection of photographic or video materials?	Yes
Will financial or other inducements (other than reasonable expenses and compensation for time) be offered to participants?	No

<p>Please explain below why your research project involves the above mentioned criteria (be sure to explain why the sensitive criterion is essential to your project's success). Give a summary of the ethical issues and any action that will be taken to address these. Explain how you will obtain informed consent (and from whom) and how you will inform the participant(s) about the research project (i.e. participant information sheet). A sample consent form and participant information sheet can be found on the Research Ethics website.</p> <p>Photographic evidence of the set-up conditions are required to ensure repeatability should the test have to be conducted again. Further to this high-speed footage shall be obtained with a very limited and specifically framed shot of the affected leg during running. Consent shall be obtained from the volunteer on the day and the identity of the volunteer shall be omitted from all material used.</p>
---

## Final Review

Will you have access to personal data that allows you to identify individuals OR access to confidential corporate or company data (that is not covered by confidentiality terms within an agreement or by a separate confidentiality agreement)?	No
Will your research involve experimentation on any of the following: animals, animal tissue, genetically modified organisms?	No

<b>Will your research take place outside the UK (including any and all stages of research: collection, storage, analysis, etc.)?</b>	No
--	----

<b>Please use the below text box to highlight any other ethical concerns or risks that may arise during your research that have not been covered in this form.</b>